Published for SISSA by Springer

Received: *June 11, 2020*
Revised: *November 3, 2020*
Accepted: *November 4, 2020*
Published: *December 16, 2020*

JHEP12(2020)101

Complexity of mixed Gaussian states from Fisher information geometry

Giuseppe Di Giulio and Erik Tonni

SISSA and INFN — Sezione di Trieste,
via Bonomea 265, 34136, Trieste, Italy

E-mail: gdigiuli@sissa.it, erik.tonni@sissa.it

Abstract: We study the circuit complexity for mixed bosonic Gaussian states in harmonic lattices in any number of dimensions. By employing the Fisher information geometry for the covariance matrices, we consider the optimal circuit connecting two states with vanishing first moments, whose length is identified with the complexity to create a target state from a reference state through the optimal circuit. Explicit proposals to quantify the spectrum complexity and the basis complexity are discussed. The purification of the mixed states is also analysed. In the special case of harmonic chains on the circle or on the infinite line, we report numerical results for thermal states and reduced density matrices.

Keywords: AdS-CFT Correspondence, Black Holes, Lattice Quantum Field Theory

ArXiv ePrint: 2006.00921

Open Access, © The Authors.
Article funded by SCOAP[3].

https://doi.org/10.1007/JHEP12(2020)101

Contents

JHEP12(2020)101

JHEP12(2020)101

1 Introduction

The complexity of a quantum circuit is an insightful notion of quantum information theory [1–6]. During the last few years it has attracted increasing attention also because it has been proposed as a new quantity to explore within the (holographic) gauge/gravity correspondence between quantum (gauge) field theories and quantum gravity models from string theory. In this context, different proposals have been made to evaluate the complexity of a quantum state by considering different geometric constructions in the gravitational dual [7–16].

A quantum circuit constructs a target state by applying a specific sequence of gates to a reference state. The circuit complexity is given by the minimum number of allowed gates that is needed to construct the target state starting from the assigned reference state. This quantity depends on the target state, on the reference state, on the set of allowed gates

and, eventually, on the specified tolerance for the target state. Notice that this definition of complexity does not require the introduction of ancillary degrees of freedom.

Remarkable results have been obtained over the past few years in the attempt to evaluate complexity in quantum field theories [17–43]. Despite these advances, it remains an interesting open problem that deserves further investigations.

In order to understand the circuit complexity in continuum theories, it is worth exploring the complexity of a process that constructs a quantum state in lattice models whose continuum limit is well understood. The free scalar and the free fermion are the simplest models to consider. For these models, it is worth focussing on the Gaussian states because they provide an interesting arena that includes important states (e.g. the ground state and the thermal states) and that has been largely explored in the literature of quantum information [44–48]. The bosonic Gaussian states are particularly interesting because, despite the fact that the underlying Hilbert space is infinite dimensional, they can be studied through techniques of finite dimensional linear algebra.

Various studies have explored the complexity of quantum circuits made by pure Gaussian states in lattice models [17–27]. In these cases the gates implement only unitary transformations of the state. It is important to extend these analyses by considering quantum circuits that involve also mixed states; hence it is impossible to construct them by employing only unitary gates [6]. A natural way to construct mixed states consists in considering the system in a pure state and tracing out some degrees of freedom. This immediately leads to consider the entanglement entropy and other entanglement quantifiers (see [49–52] for reviews). The same consideration holds within the context of the holographic correspondence, where the gravitational dual of the entanglement entropy has been found in [53–55] (see [56–58] for recent reviews).

The notions of complexity are intimately related to the geometry of quantum states [59]. While for pure states a preferred geometry can be defined, when mixed states are involved, different metrics have been introduced in a consistent way [60]. Furthermore, for quantum circuits made also by mixed states, the notions of spectrum complexity and basis complexity can be introduced [29].

A method to quantify the complexity of circuits involving mixed states has been recently investigated in [23]. In this approach, the initial mixed state is purified by adding ancillary degrees of freedom and the resulting pure state is obtained by minimising the circuit complexity within the set of pure states. This procedure requires the choice of a fixed pure state to evaluated this circuit complexity for pure states.

In this manuscript we explore a way to evaluate the complexity of quantum circuits made by mixed states within the framework of the Information Geometry [61–63]. The method holds for bosonic Gaussian states and it does not require the introduction of ancillary degrees of freedom. It relies on the fact that, whenever the states provide a Riemannian manifold and the available gates allow to reach every point of the manifold, the standard tools of differential geometry can be employed to find the optimal circuit connecting two states. Since the pure states provide a submanifold of this manifold, this analysis also suggests natural quantum circuits to purify a given mixed state.

JHEP12(2020)101

We focus only on the bosonic Gaussian states occurring in the Hilbert space of harmonic lattices in any number of dimensions. These are prototypical examples of continuous variable quantum systems; indeed, they can be described by the positions and the momenta, which are continuous variables. The bosonic Gaussian states are completely characterised by their covariance matrix, whose elements can be written in terms of the two point correlators, and by their first moments. The covariance matrices associated to these quantum states are real symmetric and positive definite matrices constrained by the validity of the uncertainty principle [44–48]. We mainly explore the bosonic Gaussian mixed states with vanishing first moments. This set can be described by a proper subset of the Riemann manifold defined by the symmetric and positive definite matrices [64–68] equipped with the metric provided by the Fisher information matrix [61, 62, 69–71]. We remark that our analysis considers quantum circuits that are made by Gaussian states only. Despite this important simplifying assumption, the resulting quantum circuits are highly non trivial because non unitary states are involved in the circuit. In this setting, by exploiting the Williamson's theorem [72], we can consider circuits whose reference and target states have either the same spectrum or can be associated to the same basis. This allows us to propose some ways to quantify the spectrum and the basis complexity for bosonic Gaussian states with vanishing first moments.

The manuscript is organised as follows. In section 2 we introduce the quantities and the main results employed throughout the manuscript: the covariance matrix through the Gaussian Wigner function, the Fisher-Rao distance between covariance matrices and the corresponding geodesics, that provide the optimal circuits. The particular cases given by pure states, thermal states and coherent states (the latter ones need further results discussed in appendix B) are explicitly considered. In section 3 we provide explicit expressions to evaluate the spectrum complexity and the basis complexity, by employing also the first law of complexity [73, 74]. The purification of a mixed state is explored in section 4, where particular optimal circuits are mainly considered. In section 5 we discuss some lower and upper bounds on the complexity. In section 6 we focus on the circuits that do not contain pure states because they can be also parameterised through the entanglement hamiltonian matrices. The Gaussian channels underlying the optimal circuits are briefly discussed in section 7. In section 8 we describe the approach to the complexity of mixed states based on the purification of a mixed state through ancillary degrees of freedom. The last analysis reported in section 9 focuses on the periodic harmonic chain in one spatial dimension and on its limiting regime given by the harmonic chain on the infinite line. Numerical results are reported both for some quantities introduced in the other sections and for other quantities like the mutual complexity for the thermofield double states and for the reduced density matrices. Finally, in section 10 we summarise our results and discuss future directions.

Some appendices (A, E and D) contain the derivation of selected results reported in the main text and related technical details. Other appendices, instead, provide complementary analyses that expand the discussion of the main text, adding further results. In particular, in appendix B we explore Gaussian states with non vanishing first moments, in appendix C the Bures and the Hilbert-Schmidt distances are discussed, in appendix F the complexity of the thermofield double states is explored and in appendix G we describe the two particular bases employed in [23] to study the complexity of mixed states through the F_1 cost function.

JHEP12(2020)101

2 Complexity as Fisher-Rao distance and the optimal path

In section 2.1 we introduce Gaussian Wigner functions (defined in terms of the covariance matrix and of the first moment) to characterise a generic Gaussian state. The Fisher-Rao distance and other distances are defined in section 2.2. In section 2.3 we discuss the Williamson's decomposition of the covariance matrix, a crucial tool largely employed throughout the manuscript. The optimal circuit in the Fisher information geometry is analysed in section 2.4. The special cases given by pure states and thermal states are explored in section 2.5 and section 2.6 respectively. Finally, in section 2.7 some results about the complexity for the coherent states are discussed.

2.1 Gaussian states in harmonic lattices

The hamiltonian of a spatially homogeneous harmonic lattice made by N sites with nearest neighbour spring-like interaction with spring constant κ reads

$$\widehat{H} \,=\, \sum_{i=1}^{N} \left(\frac{1}{2m}\, \hat{p}_i^2 + \frac{m\omega^2}{2}\, \hat{q}_i^2 \right) + \sum_{\langle i,j \rangle} \frac{\kappa}{2} (\hat{q}_i - \hat{q}_j)^2 \,=\, \frac{1}{2}\, \hat{\boldsymbol{r}}^{\mathrm{t}} H^{\mathrm{phys}}\, \hat{\boldsymbol{r}} \tag{2.1}$$

where the second sum is performed over the nearest neighbour sites. The position and momentum operators $\hat{q}_i$ and $\hat{p}_i$ are hermitian and satisfy the canonical commutation relations $[\hat{q}_i, \hat{q}_j] = [\hat{p}_i, \hat{p}_j] = 0$ and $[\hat{q}_i, \hat{p}_j] = \mathrm{i}\delta_{ij}$ (we set $\hbar = 1$ throughout this manuscript). The boundary conditions do not change the following discussion, although they are crucial to determine the explicit expressions of the correlators. Collecting the position and momentum operators into the vector $\hat{\boldsymbol{r}} \equiv (\hat{q}_1, \dots, \hat{q}_N, \hat{p}_1, \dots, \hat{p}_N)^{\mathrm{t}}$, the canonical commutation relations can be written in the form $[\hat{r}_i, \hat{r}_j] = \mathrm{i} J_{ij}$, where J is the standard symplectic matrix

$$J \equiv \begin{pmatrix} \mathbf{0} & \mathbf{1} \\ -\mathbf{1} & \mathbf{0} \end{pmatrix} \tag{2.2}$$

and we have denoted byy $\mathbf{1}$ the $N \times N$ identity matrix and $\mathbf{0}$ the matrix with the proper size having all its elements equal to zero. Notice that $J^2 = -\mathbf{1}$ and $J^{\mathrm{t}} = J^{-1} = -J$.

The real symplectic group $\mathrm{Sp}(2N, \mathbb{R})$ is made by the real $2N \times 2N$ matrices S characterising the linear transformations $\hat{\boldsymbol{r}} \to \hat{\boldsymbol{r}}' = S\, \hat{\boldsymbol{r}}$ that preserve the canonical commutation relations [75–79]. This condition is equivalent to $SJS^{\mathrm{t}} = J$. Given $S \in \mathrm{Sp}(2N, \mathbb{R})$, it can be shown that $\det(S) = 1$, $S^{\mathrm{t}} \in \mathrm{Sp}(2N, \mathbb{R})$ and $S^{-1} = JS^{\mathrm{t}}J^{-1}$, hence $S^{-\mathrm{t}} = J^{\mathrm{t}} S J$ (we have adopted the notation $M^{-\mathrm{t}} \equiv (M^{\mathrm{t}})^{-1}$). The real dimension of $\mathrm{Sp}(2N, \mathbb{R})$ is $N(2N+1)$.

The density matrix $\hat{\rho}$, that characterises a state of the quantum system described by the hamiltonian (2.1), is a positive definite, hermitean operator whose trace is normalised to one. When the state is pure, the operator $\hat{\rho}$ is a projector.

A useful way to characterise a density matrix is based on the Wigner function $w(\boldsymbol{r})$, that depends on the vector $\boldsymbol{r}$ made by $2N$ real components. The Wigner function is defined through the Wigner characteristic function associated to $\hat{\rho}$, that is [46–48]

$$\chi(\boldsymbol{\xi}) \,\equiv\, \mathrm{Tr}(\hat{\rho}\, e^{\mathrm{i}\, \hat{\boldsymbol{r}}^{\mathrm{t}} J\, \boldsymbol{\xi}}) = \mathrm{Tr}(\hat{\rho}\, \widehat{D}_{\boldsymbol{\xi}}) \qquad\qquad \boldsymbol{\xi} \in \mathbb{R}^{2N} \tag{2.3}$$

where in the last step we have introduced the displacement operator as

$$\widehat{D}_{\boldsymbol{a}} \,\equiv\, e^{-\mathrm{i}\boldsymbol{a}^{\mathrm{t}} J\, \hat{\boldsymbol{r}}} \qquad\qquad \boldsymbol{a} \in \mathbb{R}^{2N}\,. \tag{2.4}$$

JHEP12(2020)101

The Fourier transform of the Wigner characteristic function provides the Wigner function

$$w(\boldsymbol{r}) \equiv \frac{1}{(2\pi)^{2N}} \int \chi(\boldsymbol{\xi})\, e^{-\mathrm{i}\, \boldsymbol{r}^{\mathrm{t}}\, J\, \boldsymbol{\xi}}\, d\boldsymbol{\xi} \tag{2.5}$$

where $d\boldsymbol{\xi} = \prod_{i=1}^{2N} d\xi_i$ denotes the integration over the $2N$ real components of $\boldsymbol{\xi}$.

In this manuscript we focus on the Gaussian states of the harmonic lattices, which are the states whose Wigner function is Gaussian [45, 46, 49, 80–83]

$$w_{\mathrm{G}}(\boldsymbol{r}; \gamma, \langle \hat{\boldsymbol{r}} \rangle) \equiv \frac{e^{-\frac{1}{2}(\boldsymbol{r}-\langle \hat{\boldsymbol{r}} \rangle)^{\mathrm{t}}\, \gamma^{-1}\, (\boldsymbol{r}-\langle \hat{\boldsymbol{r}} \rangle)}}{(2\pi)^N \sqrt{\det(\gamma)}}\,. \tag{2.6}$$

The $2N \times 2N$ real, symmetric and positive definite matrix γ is the covariance matrix of the Gaussian state, whose elements can be defined in terms of the anticommutator of the operators $\hat{r}_i$ as follows

$$\gamma_{i,j} = \frac{1}{2} \langle \{ \hat{r}_i - \langle \hat{r}_i \rangle\, , \hat{r}_j - \langle \hat{r}_j \rangle \} \rangle \;=\; \frac{1}{2} \langle \{ \hat{r}_i\, , \hat{r}_j \} \rangle - \langle \hat{r}_i \rangle\, \langle \hat{r}_j \rangle = \langle \hat{r}_i\, \hat{r}_j \rangle - \langle \hat{r}_i \rangle\, \langle \hat{r}_j \rangle - \frac{\mathrm{i}}{2}\, J_{i,j}\,. \tag{2.7}$$

The covariance matrix γ is determined by $N(2N+1)$ real parameters. The expressions (2.6) and (2.7) tell us that the Gaussian states are completely characterised by the one-point correlators (first moments) and by the two-points correlators (second moments) of the position and momentum operators collected into the vector $\hat{\boldsymbol{r}}$. It is important to remark that the validity of the uncertainty principle imposes the following condition on the covariance matrix [46, 76]

$$\gamma + \frac{\mathrm{i}}{2}\, J \;\geqslant\; 0\,. \tag{2.8}$$

In [68] a real, positive matrix with an even size and satisfying (2.8) is called Gaussian matrix. Thus, every symmetric Gaussian matrix provides the covariance matrix of a Gaussian state.

A change of base $\hat{\boldsymbol{r}} \to \hat{\boldsymbol{r}}' = S\, \hat{\boldsymbol{r}}$ characterised by $S \in \mathrm{Sp}(2N, \mathbb{R})$ induces the transformation $\gamma \to \gamma' = S\, \gamma\, S^{\mathrm{t}}$ on the covariance matrix.

In this manuscript we mainly consider Gaussian states with vanishing first moments, i.e. having $\langle \hat{r}_i \rangle = 0$ (pure states that do not fulfil this condition are discussed in section 2.7). In this case the generic element of covariance matrix (2.7) becomes

$$\gamma_{i,j} = \frac{1}{2} \langle \{ \hat{r}_i\, , \hat{r}_j \} \rangle = \mathrm{Re}\big[\langle \hat{r}_i\, \hat{r}_j \rangle \big] \tag{2.9}$$

and the Wigner function (2.6) slightly simplifies to

$$w_{\mathrm{G}}(\boldsymbol{r}; \gamma) = \frac{e^{-\frac{1}{2}\, \boldsymbol{r}^{\mathrm{t}}\, \gamma^{-1}\, \boldsymbol{r}}}{(2\pi)^N \sqrt{\det(\gamma)}}\,. \tag{2.10}$$

where we have lightened the notation with respect to (2.6) by setting $w_{\mathrm{G}}(\boldsymbol{r}; \gamma) \equiv w_{\mathrm{G}}(\boldsymbol{r}; \gamma, \boldsymbol{0})$. The quantities introduced above characterise generic mixed Gaussian states. The subclass made by the pure states is discussed in section 2.3.1.

The most familiar way to describe the Hilbert space is the Schrödinger representation, which employs the wave functions $\psi(\boldsymbol{q}) = \langle \boldsymbol{q} | \psi \rangle$ on $\mathbb{R}^N$ (elements of $L^2(\mathbb{R}^N)$ depending on

JHEP12(2020)101

$\boldsymbol{q} \equiv (q_1, \dots, q_N)^{\mathrm{t}}$) for the vectors of the Hilbert space and the kernels $O(\boldsymbol{q}, \tilde{\boldsymbol{q}}) = \langle \boldsymbol{q} | \, \widehat{O} \, | \tilde{\boldsymbol{q}} \rangle$ for the linear operators $\widehat{O}$ acting on the Hilbert space [75]. In the appendix A.1 we relate the kernel $\rho(\boldsymbol{q}, \tilde{\boldsymbol{q}}) = \langle \boldsymbol{q} | \, \hat{\rho} \, | \tilde{\boldsymbol{q}} \rangle$ of the density matrix to the corresponding Gaussian Wigner function (2.10). In the appendix A.2 we express the kernel $\rho_A(\boldsymbol{q}_A, \tilde{\boldsymbol{q}}_A)$ for the reduced density matrix of a spatial subsystem A in terms of the parameters defining the wave function of the pure state describing the entire bipartite system.

2.2 Fisher-Rao distance

The set made by the probability density functions (PDF's) parameterised by the quantities γ is a manifold. In information geometry, the distinguishability between PDF's characterised by two different sets of parameters γ_1 and γ_2 is described through a scalar quantity $D(\gamma_1, \gamma_2)$ called divergence [62, 63], a function such that $D(\gamma_1, \gamma_2) \geqslant 0$ and $D(\gamma_1, \gamma_2) = 0$ if and only if $\gamma_1 = \gamma_2$ and

$$D(\gamma, \gamma + d\gamma) = \frac{1}{2} \sum_{i,j} g_{ij} \, dy_i dy_j + O((dy)^3) \tag{2.11}$$

where g_{ij} is symmetric and positive definite and $\boldsymbol{y}$ denotes the vector collecting the independent parameters that determine $\gamma = \gamma(\boldsymbol{y})$. In general $D(\gamma_1, \gamma_2) \neq D(\gamma_2, \gamma_1)$; nonetheless, notice that the terms that could lead to the loss of this symmetry are subleading in the expansion (2.11). Thus, every divergence D introduces a metric tensor g_{ij} that makes $\mathcal{M}$ a Riemannian manifold.

A natural requirement for a measure of distinguishability between states is the information monotonicity [62, 63]. Let us denote by $\boldsymbol{s} = \boldsymbol{s}(\boldsymbol{r})$ a change of variables in the PDF's and by $\bar{D}(\gamma_1, \gamma_2)$ the result obtained from $D(\gamma_1, \gamma_2)$ after this change of variables. If $\boldsymbol{s}(\boldsymbol{r})$ is not invertible, a loss of information occurs because we cannot reconstruct $\boldsymbol{r}$ from $\boldsymbol{s}$. This information loss leads to a less distinguishability between PDF's, namely $\bar{D}(\gamma_1, \gamma_2) < D(\gamma_1, \gamma_2)$. Instead, when $\boldsymbol{s}(\boldsymbol{r})$ is invertible, information is not lost and the distinguishability of the two functions is preserved, i.e. $\bar{D}(\gamma_1, \gamma_2) = D(\gamma_1, \gamma_2)$. Thus, it is naturally to require that any change of variables must lead to [62, 63]

$$\bar{D}(\gamma_1, \gamma_2) \leqslant D(\gamma_1, \gamma_2) \, . \tag{2.12}$$

This property is called information monotonicity for the divergence D.

Let us consider a geometric structure on $\mathcal{M}$ induced by a metric tensor g_{ij} associated to a divergence satisfying (2.12). An important theorem in information geometry due to Chentsov claims that, considering any set of the PDF's, a unique metric satisfying (2.12) exists up to multiplicative constants [61, 62].

The Wigner functions of the bosonic Gaussian states (2.6) with vanishing first moments are PDF's that provide a manifold $\mathcal{M}_{\mathrm{G}}$ parameterised by the covariance matrices γ. The Chentsov's theorem for these PDF's leads to introduce the *Fisher information matrix* [61, 62, 69, 71, 84]

$$g_{ij} = \int w_{\mathrm{G}}(\boldsymbol{r}, \gamma) \, \frac{\partial \log[w_{\mathrm{G}}(\boldsymbol{r}; \gamma)]}{\partial y_i} \, \frac{\partial \log[w_{\mathrm{G}}(\boldsymbol{r}; \gamma)]}{\partial y_j} \, d\boldsymbol{r} \tag{2.13}$$

JHEP12(2020)101

which provides the *Fisher-Rao distance* between two bosonic Gaussian states with vanishing first moments. Denoting by γ_1 and γ_2 the covariance matrices of these states, their Fisher-Rao distance reads [65–68, 70, 85]

$$d(\gamma_1, \gamma_2) \equiv \sqrt{\mathrm{Tr}\big[(\log \Delta)^2\big]} \equiv \big\| \log(\gamma_1^{-1/2}\, \gamma_2\, \gamma_1^{-1/2}) \big\|_2 \qquad \Delta \equiv \gamma_2\, \gamma_1^{-1} \,. \tag{2.14}$$

This is the main formula employed throughout this manuscript to study the complexity of Gaussian mixed states.

In appendix B we report known results about the Fisher-Rao distance between Gaussian PDF's with non vanishing first moments [69, 70, 84, 86–88]. We remark that (2.14) is the Fisher-Rao distance also when the reference state and the target state have the same first moments, that can be non vanishing [70, 85, 89]. Although an explicit expression for the Fisher-Rao distance in the most general case of different covariance matrices and different first moments is not available in the literature, interesting classes of Gaussian PDF's have been identified where explicit expressions for this distance have been found [85, 89–91].

The distance between two states can be evaluated also through the distance between the corresponding density matrices. Various expressions for distances have been constructed and it is natural to ask whether they satisfy a property equivalent to the information monotonicity (2.12), that is known as contractivity [59, 92, 93]. A quantum operation Θ is realised by a completely positive operator which acts on the density matrix $\hat{\rho}$, providing another quantum state $\Theta(\hat{\rho})$ [46, 59, 92] (see also section 7). A distance d between two states characterised by their density matrices $\hat{\rho}_1$ and $\hat{\rho}_2$ is contractive when the action of a quantum operation Θ reduces the distance between any two given states [92, 93], namely[1]

$$d(\hat{\rho}_1, \hat{\rho}_2) \geqslant d\big(\Theta(\hat{\rho}_1), \Theta(\hat{\rho}_2)\big) \,. \tag{2.15}$$

This is a crucial property imposed to a distance in quantum information theory.

The main contractive distances are the Bures distance, defined in terms of the fidelity $\mathcal{F}$ as follows

$$d_{\mathrm{B}}^2(\hat{\rho}_1, \hat{\rho}_2) \equiv 2\,(1 - \mathcal{F}(\hat{\rho}_1, \hat{\rho}_2)) \qquad \mathcal{F}(\hat{\rho}_1, \hat{\rho}_2) \equiv \mathrm{Tr}\Big(\sqrt{\sqrt{\hat{\rho}_1}\, \hat{\rho}_2\, \sqrt{\hat{\rho}_1}}\,\Big) \tag{2.16}$$

the Hellinger distance

$$d_{\mathrm{H}}^2(\hat{\rho}_1, \hat{\rho}_2) = 2\left[1 - \mathrm{Tr}\Big(\sqrt{\hat{\rho}_1}\, \sqrt{\hat{\rho}_2}\Big)\right] \tag{2.17}$$

and the trace distance

$$d_{L^1}(\hat{\rho}_1, \hat{\rho}_2) \equiv \mathrm{Tr}|\hat{\rho}_1 - \hat{\rho}_2| \,. \tag{2.18}$$

The trace distance is the L^p-distance with $p = 1$ and it is the only contractive distance among the L^p-distances. For $p = 2$ we have the Hilbert-Schmidt distance [59]

$$d_{\mathrm{HS}}(\hat{\rho}_1, \hat{\rho}_2) = \sqrt{\mathrm{Tr}(\hat{\rho}_1 - \hat{\rho}_2)^2} \tag{2.19}$$

which is non contractive. In appendix C we further discuss the Bures distance and the Hilbert-Schmidt distance specialised to the bosonic Gaussian states.

[1] In [59] both the properties (2.12) and (2.15) are called monotonicity.

JHEP12(2020)101

The Bures distance and the Hellinger distance are Riemannian,[2] being induced by a metric tensor, while the trace distance is not. Another difference occurs when we restrict to the subset of the pure states. It is well known that the only Riemannian distance between pure states is the Fubini-Study distance $d^2_{\text{FS}} = 2\,(1 - |\langle\psi_1|\psi_2\rangle|)$, where $\hat{\rho}_1 = |\psi_1\rangle\langle\psi_1|$ and $\hat{\rho}_2 = |\psi_2\rangle\langle\psi_2|$. Restricting to pure states, the Bures distance becomes exactly the Fubini-Study distance, while the Hellinger distance and trace distance become $d^2_{\text{H}} = 2\,(1 - |\langle\psi_1|\psi_2\rangle|^2)$ and $d^2_{L^1} = 4\,(1 - |\langle\psi_1|\psi_2\rangle|^2)$ respectively, namely a function of the Fubini-Study distance [93].

2.3 Williamson's decomposition

The *Williamson's theorem* is a very important tool to study Gaussian states [72]: it provides a decomposition for the covariance matrix γ that is crucial throughout our analysis.

The Williamson's theorem holds for any real, symmetric and positive matrix with even size; hence also for the covariance matrices. Given a covariance matrix γ, the Williamson's theorem guarantees that a symplectic matrix $W \in \text{Sp}(2N, \mathbb{R})$ can be constructed such that

$$\gamma = W^{\text{t}}\, \mathcal{D}\, W \tag{2.20}$$

where $\mathcal{D} \equiv \text{diag}(\sigma_1, \dots, \sigma_N) \oplus \text{diag}(\sigma_1, \dots, \sigma_N)$ and $\sigma_k > 0$. The set $\{\sigma_k\}$ is the *symplectic spectrum* of γ and its elements are the symplectic eigenvalues (we often call $\mathcal{D}$ the symplectic spectrum throughout this manuscript, with a slight abuse of notation). The symplectic spectrum is uniquely determined up to permutations of the symplectic eigenvalues and it is invariant under symplectic transformations. Throughout this manuscript we refer to (2.20) as the Williamson's decomposition[3] of γ, choosing a decreasing ordering for the symplectic eigenvalues. The real dimension of the set made by the covariance matrices is $N(2N+1)$ [48].

Combining (2.8) and (2.20), it can be shown that $\sigma_k \geqslant \frac{1}{2}$ [46]. A diagonal matrix is symplectic when it has the form $\Upsilon \oplus \Upsilon^{-1}$. This implies that a generic covariance matrix is not symplectic because of the occurrence of the diagonal matrix $\mathcal{D}$ in the Williamson's decomposition (2.20).

Another important tool for our analysis is the *Euler decomposition* of a symplectic matrix S (also known as Bloch-Messiah decomposition) [77]. It reads

$$S = L\,\mathcal{X}\,R \qquad \mathcal{X} = e^{\Lambda} \oplus e^{-\Lambda} \qquad L, R \in K(N) \equiv \text{Sp}(2N, \mathbb{R}) \cap O(2N) \tag{2.21}$$

where $\Lambda = \text{diag}(\Lambda_1, \dots, \Lambda_N)$ with $\Lambda_j \geqslant 0$. The non-uniqueness of the decomposition (2.21) is due only to the freedom to order the elements along the diagonal of Λ. By employing the Euler decomposition (2.21) and that the real dimension of $K(N)$ is N^2, it is straightforward to realise that the real dimension of the symplectic group $\text{Sp}(2N, \mathbb{R})$ is $2N^2 + N$, as already mentioned in section 2.1. The simplest case corresponds to the one-mode case, i.e. $N = 1$, where a 2×2 real symplectic matrix can be parameterised by two rotation angles and a squeezing parameter Λ_1.

[2] In [64] Petz has classified all the contractive Riemannian metrics, finding a general formula that provides (2.16) and (2.17) as particular cases.

[3] It is often called normal modes decomposition [48].

JHEP12(2020)101

The quantities explored in this manuscript provide important tools to study the entanglement quantifiers in harmonic lattices. For instance, the symplectic spectrum in (2.20) for the reduced density matrix allows to evaluate the entanglement spectrum and therefore the entanglement entropies [52, 80–82, 94, 95] and the Euler decomposition (2.21) applied to the symplectic matrix occurring in the Williamson's decomposition of the covariance matrix of a subsystem has been employed in [96] to construct a contour function for the entanglement entropies [97, 98]. The Williamson's decomposition is also crucial to study the entanglement negativity [80, 99–102] a measure of the bipartite entanglement for mixed states.

2.3.1 Covariance matrix of a pure state

A Gaussian state is pure if and only if all the symplectic eigenvalues equal to $\frac{1}{2}$, i.e. $\mathcal{D} = \frac{1}{2}\,\mathbf{1}$. Thus, the Williamson's decomposition of the covariance matrix characterising a pure state reads

$$\gamma = \frac{1}{2}\, W^{\mathrm{t}}\, W = \frac{1}{2}\, R^{\mathrm{t}}\, \mathcal{X}^2 R \qquad\qquad W = L\, \mathcal{X}\, R\,. \tag{2.22}$$

The last expression, which has been found by employing the Euler decomposition (2.21) for the symplectic matrix W, tells us that the covariance matrix of a pure state can be determined by fixing $N^2 + N$ real parameters.

The covariance matrix of a pure state satisfies the following constraint [103]

$$\big(\mathrm{i} J \gamma\big)^2 = \frac{1}{4}\,\mathbf{1}\,. \tag{2.23}$$

After a change of basis characterised by the symplectic matrix S, the covariance matrix (2.22) becomes $\gamma' = \frac{1}{2}\, S\, W^{\mathrm{t}}\, W S^{\mathrm{t}}$. Choosing $S = K\, W^{-\mathrm{t}}$, where $K \in K(N)$, the covariance matrix drastically simplifies to $\gamma' = \frac{1}{2}\,\mathbf{1}$.

In the Schrödinger representation, the wave function of a pure Gaussian state reads [77]

$$\psi(\boldsymbol{q}) \;=\; \left(\frac{\det(E)}{\pi^N}\right)^{1/4} e^{-\frac{1}{2}\,\boldsymbol{q}^{\mathrm{t}}(E+\mathrm{i}F)\,\boldsymbol{q}} \tag{2.24}$$

where E and F are $N \times N$ real symmetric matrices and E is also positive definite; hence the pure state is parameterised by $N(N+1)$ real coefficients, in agreement with the counting of the real parameters discussed above. The L^2 norm of (2.24) is equal to one.

The covariance matrix corresponding to the pure state (2.24) can be written in terms of the matrices E and F introduced in the wave function (2.24) as follows [77]

$$\gamma \;=\; \frac{1}{2}\begin{pmatrix} E^{-1} & -\,E^{-1}F \\ -\,F\,E^{-1} & E + F\,E^{-1}F \end{pmatrix} = \frac{1}{2}\, W^{\mathrm{t}}\, W \tag{2.25}$$

where the symplectic matrix W and its inverse are given respectively by

$$W = \begin{pmatrix} E^{-1/2} & -\,E^{-1/2}F \\ \mathbf{0} & E^{1/2} \end{pmatrix} \qquad\qquad W^{-1} = \begin{pmatrix} E^{1/2} & F\,E^{-1/2} \\ \mathbf{0} & E^{-1/2} \end{pmatrix} \tag{2.26}$$

The expression (2.24) is employed in the appendix A.2 to provide the kernel of a reduced density matrix in the Schrödinger representation.

JHEP12(2020)101

2.4 Mixed states

Considering the set $\mathbb{P}(N)$ made by the $2N \times 2N$ real and positive definite matrices, the covariance matrices provide the proper subset of $\mathbb{P}(N)$ made by those matrices that also satisfy the inequality (2.8).

The set $\mathbb{P}(N)$ equipped with the Fisher-Rao distance is a Riemannian manifold where the length of a generic path $\gamma : [a, b] \to \mathbb{P}(N)$ is given by[4] [65–68, 71]

$$L[\gamma(\tau)] = \int_a^b \sqrt{\mathrm{Tr}\left\{ \left[\gamma(\tau)^{-1}\, \dot{\gamma}(\tau)\right]^2 \right\}}\, d\tau\,. \tag{2.27}$$

The unique geodesic connecting two matrices in the manifold $\mathbb{P}(N)$ has been constructed [67]. In our analysis we restrict to the subset made by the covariance matrices γ. Considering the covariance matrix γ_{R} and the covariance matrix γ_{T}, that correspond to the reference state and to the target state respectively, the unique geodesic that connects γ_{R} to γ_{T} is [67]

$$G_s(\gamma_{\mathrm{R}}\,, \gamma_{\mathrm{T}}) \equiv \gamma_{\mathrm{R}}^{1/2} \Big(\gamma_{\mathrm{R}}^{-1/2}\, \gamma_{\mathrm{T}}\, \gamma_{\mathrm{R}}^{-1/2} \Big)^s \gamma_{\mathrm{R}}^{1/2} \qquad\qquad 0 \leqslant s \leqslant 1 \tag{2.28}$$

where s parameterises the generic matrix along the geodesic (we always assume $0 \leqslant s \leqslant 1$ throughout this manuscript) and it is straightforward to verify that

$$G_0(\gamma_{\mathrm{R}}\,, \gamma_{\mathrm{T}}) = \gamma_{\mathrm{R}} \qquad\qquad G_1(\gamma_{\mathrm{R}}\,, \gamma_{\mathrm{T}}) = \gamma_{\mathrm{T}}\,. \tag{2.29}$$

The geodesic (2.28) provides the optimal circuit connecting γ_{R} to γ_{T}. In the mathematical literature, the matrix (2.28) is also known as the *s-geometric mean* of γ_{R} and γ_{T}. The matrix associated to $s = 1/2$ provides the *geometric mean* of γ_{R} and γ_{T}. We remark that since γ_{R} and γ_{T} are symmetric Gaussian matrices, it can be shown that also the matrices belonging to the geodesic (2.28) are symmetric and Gaussian [68].

By employing (D.1), we find that the geodesic (2.28) can be written in the following form

$$G_s(\gamma_{\mathrm{R}}\,, \gamma_{\mathrm{T}}) = \Big(\gamma_{\mathrm{T}}\, \gamma_{\mathrm{R}}^{-1} \Big)^s \gamma_{\mathrm{R}} = \gamma_{\mathrm{R}} \Big(\gamma_{\mathrm{R}}^{-1} \gamma_{\mathrm{T}} \Big)^s . \tag{2.30}$$

The Fisher-Rao distance between γ_{R} and γ_{T} is the length of the geodesic (2.28) evaluated through (2.27). It is given by

$$d(\gamma_{\mathrm{R}}, \gamma_{\mathrm{T}}) \equiv \sqrt{\mathrm{Tr}\big[(\log \Delta_{\mathrm{TR}})^2\big]} \equiv \big\| \log(\gamma_{\mathrm{R}}^{-1/2}\, \gamma_{\mathrm{T}}\, \gamma_{\mathrm{R}}^{-1/2}) \big\|_2 \tag{2.31}$$

where[5]

$$\Delta_{\mathrm{TR}} \equiv \gamma_{\mathrm{T}}\, \gamma_{\mathrm{R}}^{-1}\,. \tag{2.32}$$

This distance provides the following definition of complexity

$$\mathcal{C}_2 \;=\; \frac{1}{2\sqrt{2}}\, d(\gamma_{\mathrm{R}}\,, \gamma_{\mathrm{T}}) \tag{2.33}$$

[4] An explicit computation that relates (2.13) to (2.27) can be found e.g. in appendix A of [71].

[5] The expression (2.31) cannot be written as $\| \log(\gamma_{\mathrm{T}}\, \gamma_{\mathrm{R}}^{-1}) \|_2$ (see appendix D).

JHEP12(2020)101

It is straightforward to realise that, in the special case where both $\gamma_{\rm R}$ and $\gamma_{\rm T}$ correspond to pure states, the complexity (2.33) becomes the result obtained in [22] for the F_2 complexity, based on the F_2 cost function; hence we refer to (2.33) also as F_2 complexity in the following. The matching with [22] justifies the introduction of the numerical factor $\frac{1}{2\sqrt{2}}$ in (2.33) with respect to the distance (2.31). Equivalently, also the $\kappa = 2$ complexity given by $\mathcal{C}_{\kappa=2} \equiv \mathcal{C}_2^2$ can be considered.

We remark that the complexity (2.33) and the optimal circuit (2.28) can be applied also for circuits where the reference state and the target state have the same first moments [70, 85, 89].

The symmetry $d(\gamma_{\rm R}\,,\gamma_{\rm T}) = d(\gamma_{\rm T}\,,\gamma_{\rm R})$, imposed on any proper distance, can be verified for the Fisher-Rao distance (2.31) by observing that $\Delta_{\rm TR} \leftrightarrow \Delta_{\rm TR}^{-1}$ under the exchange $\gamma_{\rm R} \leftrightarrow \gamma_{\rm T}$.

Evaluating the distance (2.31) between γ and $\gamma + \delta\gamma$, which are infinitesimally close, one obtains [67, 104]

$$d(\gamma, \gamma+\delta\gamma)^2 = \mathrm{Tr}\left\{ \left[\log(\mathbf{1} + \delta\gamma\, \gamma^{-1}) \right]^2 \right\} = \mathrm{Tr}\left\{ \left[\, \delta\gamma\, \gamma^{-1} + \dots \, \right]^2 \right\} = \mathrm{Tr}[(\gamma^{-1}\delta\gamma)^2] + \dots \tag{2.34}$$

where the dots correspond to $O((\delta\gamma)^3)$ terms.

Performing a change of basis characterised by the symplectic matrix S, the matrix $\Delta_{\rm TR}$ changes as follows

$$\Delta'_{\rm TR} = \gamma'_{\rm T}(\gamma'_{\rm R})^{-1} = S\, \Delta_{\rm TR}\, S^{-1}\,. \tag{2.35}$$

From this expression it is straightforward to observe that the Fisher-Rao distance (2.31), and therefore the complexity (2.33) as well, is invariant under a change of basis. We remark that (2.33) is invariant under any transformation that induces on $\Delta_{\rm TR}$ the transformation (2.35) for any matrix S (even complex and not necessarily symplectic).

From the expression (2.28) of the geodesic connecting $\gamma_{\rm R}$ to $\gamma_{\rm T}$, one can show that the change $s \to 1-s$ provides the geodesic connecting $\gamma_{\rm T}$ to $\gamma_{\rm R}$; indeed, we have that[6]

$$G_{1-s}(\gamma_{\rm R}\,,\gamma_{\rm T}) \;=\; \gamma_{\rm T}^{1/2} \Big(\gamma_{\rm T}^{-1/2}\, \gamma_{\rm R}\, \gamma_{\rm T}^{-1/2} \Big)^s \gamma_{\rm T}^{1/2} \;=\; G_s(\gamma_{\rm T}\,,\gamma_{\rm R})\,. \tag{2.36}$$

Another interesting result is the Fisher-Rao distance between the initial matrix $\gamma_{\rm R}$ and the generic symmetric Gaussian matrix along the geodesic (2.28) reads [67]

$$d(\gamma_{\rm R}\,, G_s(\gamma_{\rm R}\,,\gamma_{\rm T})) \;=\; s\; d(\gamma_{\rm R}\,,\gamma_{\rm T})\,. \tag{2.37}$$

The derivation of some results reported in the forthcoming sections are based on the geodesic (2.28) written in the following form[7]

$$G_s(\gamma_{\rm R}\,,\gamma_{\rm T}) \;=\; U_s\, \gamma_{\rm R}\, U_s^{\rm t} \qquad\qquad U_s \equiv \Delta_{\rm TR}^{s/2}\,. \tag{2.39}$$

[6] This result can be found by considering e.g. the last expression in (2.30), that gives $G_{1-s}(\gamma_{\rm R}\,,\gamma_{\rm T}) = \gamma_{\rm T} \left(\gamma_{\rm T}^{-1}\gamma_{\rm R}\right)^s$ and becomes (2.36), once (D.1) with $M = \gamma_{\rm T}^{1/2}$ is employed.

[7] The expression (2.39) can be found by first writing (2.28) as

$$G_s(\gamma_{\rm R}\,,\gamma_{\rm T}) \;=\; \left[\gamma_{\rm R}^{1/2} \Big(\gamma_{\rm R}^{-1/2}\, \gamma_{\rm T}\, \gamma_{\rm R}^{-1/2} \Big)^{s/2} \right] \left[\Big(\gamma_{\rm R}^{-1/2}\, \gamma_{\rm T}\, \gamma_{\rm R}^{-1/2} \Big)^{s/2} \gamma_{\rm R}^{1/2} \right] \tag{2.38}$$

and then employing (D.1) in both the expressions within the square brackets of (2.38) with $f(x) = x^{s/2}$.

JHEP12(2020)101

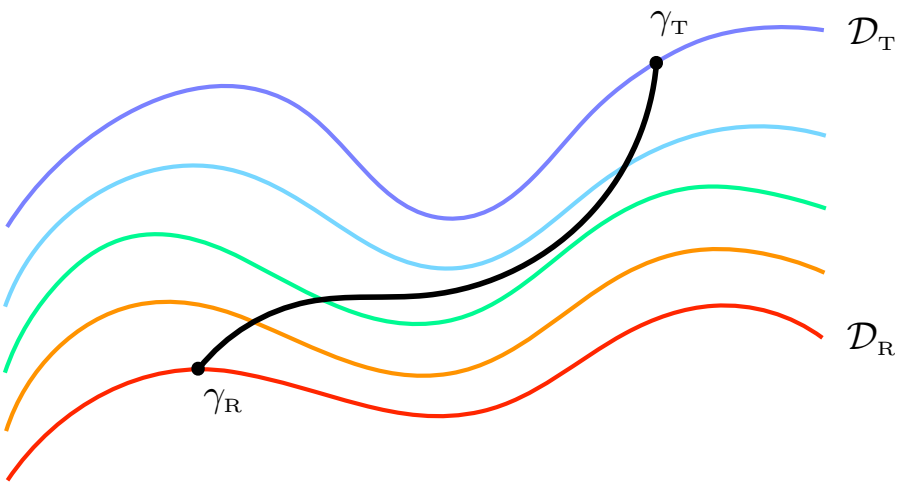

Figure 1. Pictorial representation of the optimal circuit (2.28) connecting $\gamma_{\rm R}$ to $\gamma_{\rm T}$ (solid black curve). Coloured solid curves represent the sets made by symmetric Gaussian matrices having the same symplectic spectrum. The red curve corresponds to $\mathcal{D}_{\rm R}$ and the blue curve to $\mathcal{D}_{\rm T}$.

This expression is interesting because the generic matrix of the optimal circuit is written in a form that reminds a symplectic transformation of $\gamma_{\rm R}$ through the U_s. Nonetheless, we remark that in general U_s is not symplectic because the covariance matrices are not symplectic matrices. The steps performed to obtain (2.39) lead to write (2.36) as follows

$$G_s(\gamma_{\rm T}\,,\gamma_{\rm R}) \,=\, U_s^{-1}\,\gamma_{\rm T}\,U_s^{-{\rm t}}. \tag{2.40}$$

It is enlightening to exploit the Williamson's decomposition of the covariance matrices discussed in section 2.3 in the expressions for the complexity and for the optimal circuit. The Williamson's decomposition (2.20) allows to write $\gamma_{\rm R}$ and $\gamma_{\rm T}$ as follows

$$\gamma_{\rm R} = W_{\rm R}^{\rm t}\,\mathcal{D}_{\rm R}\,W_{\rm R} \qquad \gamma_{\rm T} = W_{\rm T}^{\rm t}\,\mathcal{D}_{\rm T}\,W_{\rm T} \qquad W_{\rm R}\,,W_{\rm T}\in{\rm Sp}(2N,\mathbb{R}) \tag{2.41}$$

where $\mathcal{D}_{\rm R}$ and $\mathcal{D}_{\rm T}$ contain the symplectic spectra of $\gamma_{\rm R}$ and $\gamma_{\rm T}$ respectively. Let us introduce also the Williamson's decomposition of the generic matrix along the geodesic (2.28), namely

$$G_s(\gamma_{\rm R}\,,\gamma_{\rm T}) = W_s^{\rm t}\,\mathcal{D}_s\,W_s \qquad W_s\in{\rm Sp}(2N,\mathbb{R})\,. \tag{2.42}$$

It would be insightful to find analytic expressions for W_s and $\mathcal{D}_s$ in terms of $\gamma_{\rm R}$ and $\gamma_{\rm T}$. This has been done later in the manuscript for some particular optimal circuits.

In figure 1 we show a pictorial representation of the optimal circuit (2.28), which corresponds to the solid black curve. The figure displays that the symplectic spectrum changes along the geodesic because the black curve crosses solid curves having different colours, which correspond to the sets of matrices having the same symplectic spectrum.

In order to write the complexity (2.33) in a convenient form depending on the symplectic spectra and on the symplectic matrices $W_{\rm R}$ and $W_{\rm T}$, let us employ that, after a canonical

JHEP12(2020)101

transformation characterised by the symplectic matrix S, the covariance matrices in (2.41) become

$$\gamma'_{\rm R} = S\, W_{\rm R}^{\rm t}\, \mathcal{D}_{\rm R}\, W_{\rm R} S^{\rm t} \qquad \gamma'_{\rm T} = S\, W_{\rm T}^{\rm t}\, \mathcal{D}_{\rm T}\, W_{\rm T} S^{\rm t}\,. \tag{2.43}$$

By choosing $S = K_{\mathcal{D}_{\rm R}} W_{\rm R}^{-{\rm t}}$ where $K_{\mathcal{D}_{\rm R}}$ is symplectic and such that $K_{\mathcal{D}_{\rm R}} \mathcal{D}_{\rm R}\, K_{\mathcal{D}_{\rm R}}^{\rm t} = \mathcal{D}_{\rm R}$ (the set of matrices made by $K_{\mathcal{D}_{\rm R}}$ is a subgroup of $\mathrm{Sp}(2N,\mathbb{R})$ called stabilizer [22]), we have that (2.43) become respectively

$$\gamma'_{\rm R} = \mathcal{D}_{\rm R} \qquad \gamma'_{\rm T} = (W_{\rm TR}\, K_{\mathcal{D}_{\rm R}}^{\rm t})^{\rm t}\, \mathcal{D}_{\rm T} (W_{\rm TR}\, K_{\mathcal{D}_{\rm R}}^{\rm t}) \tag{2.44}$$

where we have introduced the symplectic matrix $W_{\rm TR}$ defined as follows

$$W_{\rm TR} \equiv W_{\rm T}\, W_{\rm R}^{-1}. \tag{2.45}$$

For later convenience, let us consider the Euler decomposition (defined in section 2.3) of the symplectic matrix $W_{\rm TR}$, namely

$$W_{\rm TR} = L_{\rm TR}\, \mathcal{X}_{\rm TR}\, R_{\rm TR} \tag{2.46}$$

where

$$L_{\rm TR}\,, R_{\rm TR} \in K(N) \qquad \mathcal{X}_{\rm TR} = e^{\Lambda_{\rm TR}} \oplus e^{-\Lambda_{\rm TR}} \in \mathrm{Sp}(2N,\mathbb{R}) \tag{2.47}$$

and $\Lambda_{\rm TR}$ is a diagonal matrix with positive entries. By specifying (2.35) to (2.44), we find that

$$\Delta'_{\rm TR} = K_{\mathcal{D}_{\rm R}} W_{\rm TR}^{\rm t}\, \mathcal{D}_{\rm T}\, W_{\rm TR}\, \mathcal{D}_{\rm R}^{-1} K_{\mathcal{D}_{\rm R}}^{-1} \tag{2.48}$$

which allows to write the F_2 complexity (2.33) as[8]

$$\mathcal{C}_2 = \frac{1}{2\sqrt{2}} \sqrt{\mathrm{Tr}\left\{ \left[\log(\mathcal{D}_{\rm T}\, W_{\rm TR}\, \mathcal{D}_{\rm R}^{-1}\, W_{\rm TR}^{\rm t}) \right]^2 \right\}}\,. \tag{2.49}$$

This expression is independent of $K_{\mathcal{D}_{\rm R}}$ and tells us that, in order to evaluate the F_2 complexity (2.33) we need the symplectic spectra $\mathcal{D}_{\rm R}$ and $\mathcal{D}_{\rm T}$ and the symplectic matrix (2.45).

By employing the Euler decomposition (2.46), the second covariance matrix in (2.44) can be decomposed as follows

$$\gamma'_{\rm T} = K_{\mathcal{D}_{\rm R}} R_{\rm TR}^{\rm t}\, \mathcal{X}_{\rm TR}\, L_{\rm TR}^{\rm t}\, \mathcal{D}_{\rm T}\, L_{\rm TR}\, \mathcal{X}_{\rm TR}\, R_{\rm TR} K_{\mathcal{D}_{\rm R}}^{\rm t} \tag{2.50}$$

which cannot be further simplified in the general case. Similarly, the Euler decomposition (2.46) does not simplify (2.49) in a significant way.

From (2.28), one finds that the geodesic $G_s(\gamma'_{\rm R}, \gamma'_{\rm T})$ connecting $\gamma'_{\rm R}$ to $\gamma'_{\rm T}$ defined in (2.44) reads

$$\begin{aligned} G_s(\gamma'_{\rm R}\,, \gamma'_{\rm T}) &= \mathcal{D}_{\rm R}^{1/2} \left(\mathcal{D}_{\rm R}^{-1/2}\, K_{\mathcal{D}_{\rm R}} W_{\rm TR}^{\rm t}\, \mathcal{D}_{\rm T}\, W_{\rm TR}\, K_{\mathcal{D}_{\rm R}}^{\rm t}\, \mathcal{D}_{\rm R}^{-1/2} \right)^s \mathcal{D}_{\rm R}^{1/2} \\ &= \left(K_{\mathcal{D}_{\rm R}} W_{\rm TR}^{\rm t}\, \mathcal{D}_{\rm T}\, W_{\rm TR}\, K_{\mathcal{D}_{\rm R}}^{\rm t}\, \mathcal{D}_{\rm R}^{-1} \right)^s \mathcal{D}_{\rm R} \end{aligned} \tag{2.51}$$

[8] The expression (2.49) can be obtained also by first plugging (2.41) into (2.33) and then employing the cyclic property of the trace.

JHEP12(2020)101

which is simpler to compute than (2.28) because $\gamma'_{\rm R}$ is diagonal. Let us remark that $G_s(\gamma'_{\rm R}, \gamma'_{\rm T})$ is different from $G_s(\gamma_{\rm R}, \gamma_{\rm T})$ but they have the same length given by (2.49). Furthermore, while the optimal circuit (2.51) depends on the matrix $K_{\mathcal{D}_{\rm R}}$, its length (2.49) does not.

For pure states, both (2.49) and (2.51) simplify in a significant way, as discussed in section 2.5.

2.4.1 One-mode mixed states

For mixed states defined by a single mode (i.e. $N = 1$), the results discussed above significantly simplify because the diagonal matrices $\mathcal{D}_{\rm R}$ and $\mathcal{D}_{\rm T}$ are proportional to the 2×2 identity matrix; hence the covariance matrices of the reference state and of the target state become respectively

$$\gamma_{\rm R} = \sigma_{\rm R}\, W_{\rm R}^{\rm t}\, W_{\rm R} \qquad \gamma_{\rm T} = \sigma_{\rm T}\, W_{\rm T}^{\rm t}\, W_{\rm T} \qquad W_{\rm R}\,, W_{\rm T} \in {\rm Sp}(2, \mathbb{R}) \tag{2.52}$$

where $\sigma_{\rm R} \geqslant 1/2$ and $\sigma_{\rm T} \geqslant 1/2$.

In this case the Williamson's decomposition for the optimal circuit (2.28) can be explicitly written. Indeed, from (2.52) one finds that $\Delta_{\rm TR} = \sigma_{\rm T}\, \sigma_{\rm R}^{-1}\, W_{\rm T}^{\rm t}\, W_{\rm TR}\, W_{\rm R}^{-{\rm t}}$ and this leads to write the expression (2.39) for the optimal circuit as follows

$$G_s(\gamma_{\rm R}\,, \gamma_{\rm T}) \;=\; \sigma_s\, W_s^{\rm t}\, W_s \tag{2.53}$$

where

$$\sigma_s = \sigma_{\rm T}^s\, \sigma_{\rm R}^{1-s} \qquad\qquad W_s \;=\; W_{\rm R} \Big[(W_{\rm T}^{\rm t}\, W_{\rm TR}\, W_{\rm R}^{-{\rm t}})^{s/2} \Big]^{\rm t} \tag{2.54}$$

which provide the Williamson's decomposition of the generic matrix along the optimal circuit.

By specialising the complexity (2.49) to the one-mode mixed states in (2.52) we get

$$\mathcal{C}_2 = \frac{1}{2\sqrt{2}} \sqrt{{\rm Tr} \Big\{ \big[\log(\sigma_{\rm T}\, \sigma_{\rm R}^{-1}\, W_{\rm TR}\, W_{\rm TR}^{\rm t}) \big]^2 \Big\}}\,. \tag{2.55}$$

Thus, the formal expression for the complexity does not simplify significantly for the one-mode mixed states with respect to the general case with $N \geqslant 1$.

2.5 Pure states

It is very insightful to specialise the results presented in section 2.4 to pure states.

When both the reference state $|\psi_{\rm R}\rangle$ and the target state $|\psi_{\rm T}\rangle$ are pure states, the corresponding density matrices are the projectors $\hat{\rho}_{\rm R} = |\psi_{\rm R}\rangle\langle\psi_{\rm R}|$ and $\hat{\rho}_{\rm T} = |\psi_{\rm T}\rangle\langle\psi_{\rm T}|$ respectively. In this case the symplectic spectra drastically simplify to

$$\mathcal{D}_{\rm R} = \mathcal{D}_{\rm T} = \frac{1}{2}\, \mathbf{1} \tag{2.56}$$

where $\mathbf{1}$ is the $2N \times 2N$ identity matrix. This implies that the Williamson's decompositions in (2.41) become respectively

$$\gamma_{\rm R} = \frac{1}{2}\, W_{\rm R}^{\rm t}\, W_{\rm R} \qquad\qquad \gamma_{\rm T} = \frac{1}{2}\, W_{\rm T}^{\rm t}\, W_{\rm T}\,. \tag{2.57}$$

JHEP12(2020)101

The complexity of pure states can be easily found by specialising (2.49) to (2.56). The resulting expression can be further simplified by employing (2.46), (2.47) and the cyclic property of the trace. This gives the result obtained in [22]

$$\mathcal{C}_2 = \frac{1}{2\sqrt{2}} \sqrt{\mathrm{Tr}\left\{ \left[\log(W_{\mathrm{TR}}\, W_{\mathrm{TR}}^{\mathrm{t}}) \right]^2 \right\}} = \frac{1}{2\sqrt{2}} \sqrt{\mathrm{Tr}\left\{ \left[\log(\mathcal{X}_{\mathrm{TR}}^2) \right]^2 \right\}} = \sqrt{\sum_i (\Lambda_{\mathrm{TR}})_i^2} \quad (2.58)$$

which can be also obtained through the proper choice of the base described below.

Since we are considering pure states, (2.26) can be employed to write W_{R} and W_{T} in terms of the pairs of symmetric matrices $(E_{\mathrm{R}}, F_{\mathrm{R}})$ and $(E_{\mathrm{T}}, F_{\mathrm{T}})$ occurring in the wave functions (2.24) of the reference state and of the target state respectively. The matrix W_{TR} in (2.45), that provides the complexity (2.58), can be written as follows

$$W_{\mathrm{TR}} = \begin{pmatrix} E_{\mathrm{T}}^{-1/2} E_{\mathrm{R}}^{1/2} & E_{\mathrm{T}}^{-1/2} F_{\mathrm{R}}\, E_{\mathrm{R}}^{-1/2} - E_{\mathrm{T}}^{-1/2} F_{\mathrm{T}}\, E_{\mathrm{R}}^{-1/2} \\ \mathbf{0} & E_{\mathrm{T}}^{1/2} E_{\mathrm{R}}^{-1/2} \end{pmatrix} \quad (2.59)$$

which becomes block diagonal for real wave functions (i.e. when $F_{\mathrm{R}} = F_{\mathrm{T}} = \mathbf{0}$).

As for the optimal circuit (2.28), by specialising the form (2.30) to the covariance matrices of pure states in (2.57), we obtain

$$G_s(\gamma_{\mathrm{R}}\,, \gamma_{\mathrm{T}}) \;=\; \frac{1}{2}\, W_{\mathrm{R}}^{\mathrm{t}} \left(W_{\mathrm{TR}}^{\mathrm{t}}\, W_{\mathrm{TR}} \right)^s W_{\mathrm{R}}\,. \quad (2.60)$$

We find it instructive also to specialise the expression (2.39) for the optimal circuit to pure states. Indeed, in this case Δ_{TR} is symplectic and the result reads

$$G_s(\gamma_{\mathrm{R}}\,, \gamma_{\mathrm{T}}) = \frac{1}{2}\, W_s^{\mathrm{t}}\, W_s \qquad W_s = W_{\mathrm{R}}\, U_s^{\mathrm{t}} \quad (2.61)$$

This expression provides the Williamson's decomposition of the optimal circuit made by pure states, given that $W_s \in \mathrm{Sp}(2N, \mathbb{R})$.

A proper choice of the basis leads to a simple expression for the optimal circuit. Since $\mathcal{D}_{\mathrm{R}} = \frac{1}{2}\,\mathbf{1}$, we have that $K_{\mathcal{D}_{\mathrm{R}}}$ introduced in the text below (2.43) is an orthogonal matrix. For pure states the convenient choice is $K_{\mathcal{D}_{\mathrm{R}}} = R_{\mathrm{TR}}$. Indeed, by specifying (2.44) to this case we obtain that in this basis the covariance matrices γ_{R} and γ_{T} become the following diagonal matrices

$$\gamma'_{\mathrm{R}} = \frac{1}{2}\,\mathbf{1} \qquad \gamma'_{\mathrm{T}} = \frac{1}{2}\,\mathcal{X}_{\mathrm{TR}}^2\,. \quad (2.62)$$

We remark that this result has been obtained by exploiting the peculiarity of the pure states mentioned in section 2.3, namely that, after a change of basis that brings the covariance matrix into the diagonal form $\frac{1}{2}\mathbf{1}$, another change of basis characterised by a symplectic matrix that is also orthogonal leaves the covariance matrix invariant. The occurrence of non trivial symplectic spectra considerably complicates this analysis (see (2.49) and (2.51)).

Specialising the form (2.30) of the optimal circuit to the covariance matrices in (2.62), the following simple expression is obtained [22]

$$G_s(\gamma'_{\mathrm{R}}\,, \gamma'_{\mathrm{T}}) = \frac{1}{2}\,\mathcal{X}_{\mathrm{TR}}^{2s}\,. \quad (2.63)$$

This expression tells us that, for pure states, this basis is very convenient because the optimal circuit is determined by the diagonal matrix $\mathcal{X}_{\mathrm{TR}}$.

JHEP12(2020)101

2.6 Thermal states

The thermal states provide an important class of Gaussian mixed states. The density matrix of a thermal state at temperature $T \equiv 1/\beta$ is $\hat{\rho}_{\rm th} = e^{-\beta \widehat{H}}/\mathcal{Z}$, where $\widehat{H}$ is the hamiltonian (2.1) for the harmonic lattices that we are considering and the constant $\mathcal{Z} = \mathrm{Tr}\big(e^{-\beta \widehat{H}}\big)$ guarantees the normalisation condition $\mathrm{Tr}\hat{\rho}_{\rm th} = 1$.

In order to study the Williamson's decomposition of the covariance matrix associated to a thermal state, let us observe the matrix $H^{\rm phys}$ in (2.1) can be written as

$$H^{\rm phys} = Q^{\rm phys} \oplus P^{\rm phys} \tag{2.64}$$

where $P^{\rm phys} = \frac{1}{m}\mathbf{1}$ and $Q^{\rm phys}$ is a $N \times N$ real, symmetric and positive definite matrix whose explicit expression is not important for the subsequent discussion.

Denoting by $\widetilde{V}$ the real orthogonal matrix that diagonalises $Q^{\rm phys}$ (for the special case of the harmonic chain with periodic boundary conditions, $\widetilde{V}$ has been written in (9.6) e (9.7)), it is straightforward to notice that (2.64) can be diagonalised as follows

$$H^{\rm phys} = V \left[\frac{1}{m}\, \mathrm{diag}\big((m\Omega)_1^2, \dots, (m\Omega_N)^2, 1, \dots, 1\big) \right] V^{\rm t} \qquad\qquad V \equiv \widetilde{V} \oplus \widetilde{V} \tag{2.65}$$

where Ω_k^2 are the real eigenvalues of $Q^{\rm phys}/m$. It is worth remarking that the $2N \times 2N$ matrix V is symplectic and orthogonal, given that $\widetilde{V}$ is orthogonal. By employing the argument that leads to (D.10), the r.h.s. of (2.65) can be written as

$$H^{\rm phys} = V\, \mathcal{X}_{\rm phys} \Big[\mathrm{diag}\big(\Omega_1, \dots, \Omega_N, \Omega_1, \dots, \Omega_N\big) \Big]\, \mathcal{X}_{\rm phys}\, V^{\rm t} \tag{2.66}$$

where we have introduced the following symplectic and diagonal matrix

$$\mathcal{X}_{\rm phys} = \mathrm{diag}\Big((m\Omega_1)^{1/2}, \dots, (m\Omega_N)^{1/2}, (m\Omega_1)^{-1/2}, \dots, (m\Omega_N)^{-1/2} \Big)\,. \tag{2.67}$$

The expression (2.66) provides the Williamson's decomposition of the matrix $H^{\rm phys}$ entering in the hamiltonian (2.1). It reads

$$H^{\rm phys} = W_{\rm phys}^{\rm t}\, \mathcal{D}_{\rm phys}\, W_{\rm phys} \tag{2.68}$$

where

$$\mathcal{D}_{\rm phys} = \mathrm{diag}\big(\Omega_1, \dots, \Omega_N, \Omega_1, \dots, \Omega_N\big) \qquad\qquad W_{\rm phys} = \mathcal{X}_{\rm phys}\, V^{\rm t}\,. \tag{2.69}$$

The Williamson's decomposition (2.68) suggests to write the physical hamiltonian (2.1) in terms of the canonical variables defined through $W_{\rm phys}$. The result is

$$\widehat{H} = \frac{1}{2}\, \hat{\boldsymbol{s}}^{\rm t}\, \mathcal{D}_{\rm phys}\, \hat{\boldsymbol{s}} \qquad\qquad \hat{\boldsymbol{s}} \equiv W_{\rm phys}\, \hat{\boldsymbol{r}} \equiv \begin{pmatrix} \hat{\mathbf{q}} \\ \hat{\mathbf{p}} \end{pmatrix}. \tag{2.70}$$

Following the standard quantisation procedure, one introduces the annihilation operators $\hat{\mathfrak{b}}_k$ and the creation operators $\hat{\mathfrak{b}}_k^\dagger$ as

$$\hat{\boldsymbol{b}} \equiv \big(\, \hat{\mathfrak{b}}_1, \dots, \hat{\mathfrak{b}}_N,\, \hat{\mathfrak{b}}_1^\dagger, \dots, \hat{\mathfrak{b}}_N^\dagger \,\big)^{\rm t} \equiv \Theta^{-1} \hat{\boldsymbol{s}} \qquad \hat{\mathfrak{b}}_k \equiv \frac{\hat{\mathfrak{q}}_k + \mathrm{i}\, \hat{\mathfrak{p}}_k}{\sqrt{2}} \qquad \Theta \equiv \frac{1}{\sqrt{2}} \begin{pmatrix} \mathbf{1} & \mathbf{1} \\ -\mathrm{i}\mathbf{1} & \mathrm{i}\mathbf{1} \end{pmatrix} \tag{2.71}$$

JHEP12(2020)101

which satisfy the well known algebra given by $[\hat{\boldsymbol{b}}_i, \hat{\boldsymbol{b}}_j] = J_{ij}$. In terms of these operators, the hamiltonian (2.70) assumes the standard form

$$\widehat{H} = \sum_{k=1}^{N} \Omega_k \left(\hat{\mathfrak{b}}_k^\dagger \, \hat{\mathfrak{b}}_k + \frac{1}{2} \right) . \tag{2.72}$$

Thus, the symplectic spectrum in (2.69) provides the dispersion relation of the model.

The operator (2.72) leads us to introduce the eigenstates $|n_k\rangle$ of the occupation number operator $\hat{\mathfrak{b}}_k^\dagger \hat{\mathfrak{b}}_k$, whose eigenvalues are given by non negative integers n_k, and the states $|\boldsymbol{n}\rangle \equiv \bigotimes_{k=1}^{N} |n_k\rangle$. The expectation value of an operator $\widehat{O}$ on the thermal state reads

$$\langle \hat{O} \rangle = \mathrm{Tr}(\hat{\rho}_{\mathrm{th}} \widehat{O}) = \frac{1}{\mathcal{Z}} \sum_{\boldsymbol{n}} \langle \boldsymbol{n} | \widehat{O} | \boldsymbol{n} \rangle \, e^{-\beta \sum_{k=1}^{N} \Omega_k (n_k + 1/2)} \, . \tag{2.73}$$

Considering the covariance matrix of a Gaussian state defined in (2.9), by employing (2.70), where W_{phys} is a real matrix, one finds that the covariance matrix of the thermal state can be written as

$$\gamma_{\mathrm{th}} = W_{\mathrm{phys}}^{-1} \, \mathrm{Re} \, \langle \hat{\boldsymbol{s}} \, \hat{\boldsymbol{s}}^{\mathrm{t}} \rangle \, W_{\mathrm{phys}}^{-\mathrm{t}} \tag{2.74}$$

in terms of the covariance matrix in the canonical variables collected into $\hat{\boldsymbol{s}}$, whose elements are given by the correlators $\langle \hat{\mathfrak{q}}_k \, \hat{\mathfrak{q}}_{k'} \rangle$, $\langle \hat{\mathfrak{p}}_k \, \hat{\mathfrak{p}}_{k'} \rangle$ and $\langle \hat{\mathfrak{q}}_k \, \hat{\mathfrak{p}}_{k'} \rangle$. These correlators can be evaluated by first using (2.71) to write $\mathrm{Re} \, \langle \hat{\boldsymbol{s}} \, \hat{\boldsymbol{s}}^{\mathrm{t}} \rangle = \mathrm{Re} \, (\Theta \langle \hat{\boldsymbol{b}} \, \hat{\boldsymbol{b}}^{\mathrm{t}} \rangle \Theta^{\mathrm{t}})$, where we remark that Θ is not a symplectic matrix because it does not preserve the canonical commutation relations. Then, by exploiting (2.73) and the action of $\hat{\mathfrak{b}}_k$ and $\hat{\mathfrak{b}}_k^\dagger$ onto the Fock states, one computes $\langle \hat{\boldsymbol{b}} \, \hat{\boldsymbol{b}}^{\mathrm{t}} \rangle$. This leads to a diagonal matrix $\mathrm{Re} \, \langle \hat{\boldsymbol{s}} \, \hat{\boldsymbol{s}}^{\mathrm{t}} \rangle$ whose non vanishing elements are given by [46, 48]

$$\mathrm{Re} \langle \hat{\mathfrak{q}}_k \hat{\mathfrak{q}}_k \rangle = \mathrm{Re} \langle \hat{\mathfrak{p}}_k \hat{\mathfrak{p}}_k \rangle = \frac{1}{2} \coth(\beta \Omega_k / 2) \qquad \mathrm{Re} \langle \hat{\mathfrak{q}}_k \hat{\mathfrak{p}}_k \rangle = 0 \, . \tag{2.75}$$

Combining these results with (2.74), for the Williamson's decomposition of the covariance matrix of the thermal state one obtains

$$\gamma_{\mathrm{th}} = W_{\mathrm{th}}^{\mathrm{t}} \, \mathcal{D}_{\mathrm{th}} \, W_{\mathrm{th}} \tag{2.76}$$

where the symplectic eigenvalues entering in the diagonal matrix $\mathcal{D}_{\mathrm{th}}$ and the symplectic matrix W_{th} are given respectively by

$$\sigma_{\mathrm{th},k} = \frac{1}{2} \coth(\beta \Omega_k / 2) \qquad W_{\mathrm{th}} = W_{\mathrm{phys}}^{-\mathrm{t}} \, . \tag{2.77}$$

We remark that W_{th} is independent of the temperature.

Taking the zero temperature limit $\beta \to +\infty$ of (2.76), one obtains the Williamson's decomposition of the covariance matrix of the ground state. This limit gives $\sigma_{\mathrm{th},k} \to 1/2$, as expected from the fact that the ground state is a pure state, while W_{th} does not change, being independent of the temperature. Thus, the Williamson's decomposition of the covariance matrix of the ground state reads

$$\gamma_{\mathrm{gs}} = \frac{1}{2} \, W_{\mathrm{phys}}^{-1} \, W_{\mathrm{phys}}^{-\mathrm{t}} \tag{2.78}$$

where W_{phys} has been defined in (2.69).

JHEP12(2020)101

It is worth considering the complexity when the reference state and the target state are thermal states having the same physical hamiltonian $\widehat{H}$ but different temperatures (we denote respectively by $\beta_{\rm R}$ and $\beta_{\rm T}$ their inverse temperatures). From (2.76), we have that the Williamson's decomposition of the covariance matrices of the reference state and the target state read respectively

$$\gamma_{\rm th,R} = W_{\rm th}^{\rm t}\, \mathcal{D}_{\rm th,R}\, W_{\rm th} \qquad\qquad \gamma_{\rm th,T} = W_{\rm th}^{\rm t}\, \mathcal{D}_{\rm th,T}\, W_{\rm th} \tag{2.79}$$

where $W_{\rm th}$ is independent of the temperature; hence $W_{\rm R} = W_{\rm T}$. This means that $W_{\rm TR} = \mathbf{1}$ in this case (see (2.45)); hence the expression (2.49) for the complexity significantly simplifies to

$$\mathcal{C}_2 = \frac{1}{2\sqrt{2}} \sqrt{\mathrm{Tr}\left\{\left[\log(\mathcal{D}_{\rm th,T}\, \mathcal{D}_{\rm th,R}^{-1})\right]^2\right\}} = \frac{1}{2} \sqrt{\sum_{k=1}^{N} \left\{\left[\log\left(\frac{\coth(\beta_{\rm T}\Omega_k/2)}{\coth(\beta_{\rm R}\Omega_k/2)}\right)\right]^2\right\}}\,. \tag{2.80}$$

The optimal path connecting these particular thermal states is obtained by plugging (2.79) into (2.39). Furthermore, by exploiting (D.1) and some straightforward matrix manipulations, we find that the Williamson's decomposition of the generic covariance matrix belonging to this optimal path reads

$$G_s(\gamma_{\rm th,R}\,, \gamma_{\rm th,T}) = W_{\rm th}^{\rm t}\, \mathcal{D}_s\, W_{\rm th} \qquad \mathcal{D}_s = \mathcal{D}_{\rm th,T}^{s}\, \mathcal{D}_{\rm th,R}^{1-s} \qquad 0 \leqslant s \leqslant 1 \tag{2.81}$$

where the same symplectic matrix $W_{\rm th}$ of the reference state and of the target state occurs and only the symplectic spectrum depends on the parameter s labelling the covariance matrices along the optimal path.

It is worth asking whether, for any given value of s, the covariance matrix $G_s(\gamma_{\rm th,R}\,, \gamma_{\rm th,T})$ in (2.81) can be associated to a thermal state of the system characterised by the same physical hamiltonian underlying the reference and the target states. Denoting by $\sigma_{s,k}$ the symplectic eigenvalues of (2.81) this means to find a temperature $T_s \equiv \beta_s^{-1}$ such that $\sigma_{s,k} = \frac{1}{2}\coth(\beta_s \Omega_k/2)$. This equation can be written more explicitly as follows

$$\coth(\beta_s\, \Omega_k/2) = \left[\frac{\coth(\beta_{\rm T}\, \Omega_k/2)}{\coth(\beta_{\rm R}\, \Omega_k/2)}\right]^s \coth(\beta_{\rm R}\, \Omega_k/2)\,. \tag{2.82}$$

We checked numerically that a solution $T_s = T_s(T_{\rm R}, T_{\rm T})$ for any $1 \leqslant k \leqslant N$ does not exist.

The quantities discussed above are further explored in section 9.3, where the thermal states of the harmonic chain are considered.

2.7 Coherent states

The coherent states are pure states with non vanishing first moments [48]. They can be introduced through the displacement operator defined in (2.4), where the real vector $\boldsymbol{a} \in \mathbb{R}^{2N}$ can be parameterised in terms of the complex vector $\boldsymbol{\alpha} \in \mathbb{C}^N$ as $\boldsymbol{a}^{\rm t} = \sqrt{2}\,(\mathrm{Re}(\boldsymbol{\alpha})^{\rm t}, \mathrm{Im}(\boldsymbol{\alpha})^{\rm t})$.

The displacement operator (2.4), which is unitary and satisfies $\widehat{D}_{\boldsymbol{a}}^{-1} = \widehat{D}_{-\boldsymbol{a}}$, shifts the position and the momentum operators as follows

$$\widehat{D}_{-\boldsymbol{a}}\, \hat{\boldsymbol{r}}\, \widehat{D}_{\boldsymbol{a}} = \hat{\boldsymbol{r}} + \boldsymbol{a}\,. \tag{2.83}$$

JHEP12(2020)101

The coherent state $|\boldsymbol{\alpha}\rangle$ is the pure state obtained by applying the displacement operator to the ground state

$$|\boldsymbol{\alpha}\rangle \equiv \widehat{D}_{\boldsymbol{a}}|0\rangle\,. \tag{2.84}$$

This state is Gaussian and, from (2.4), we have that the ground state corresponds to the coherent state with vanishing $\boldsymbol{\alpha}$ [48]. From (2.83), (2.84) and the fact that $\langle 0|\hat{\boldsymbol{r}}|0\rangle = 0$, for the first moments of the coherent state (2.84) one finds

$$\langle\boldsymbol{\alpha}|\hat{\boldsymbol{r}}|\boldsymbol{\alpha}\rangle = \langle 0|\widehat{D}_{-\boldsymbol{a}}\,\hat{\boldsymbol{r}}\,\widehat{D}_{\boldsymbol{a}}|0\rangle = \langle 0|\hat{\boldsymbol{r}}+\boldsymbol{a}|0\rangle = \boldsymbol{a}\,. \tag{2.85}$$

By employing this property, from the definition (2.7) for the covariance matrix γ_{cs} of a coherent state we find that

$$\gamma_{\text{cs}} + \frac{\mathrm{i}}{2}\,J \;=\; \langle\boldsymbol{\alpha}|(\hat{\boldsymbol{r}}-\boldsymbol{a})\,(\hat{\boldsymbol{r}}-\boldsymbol{a})^{\mathrm{t}}|\boldsymbol{\alpha}\rangle \;=\; \langle 0|\widehat{D}_{-\boldsymbol{a}}(\hat{\boldsymbol{r}}-\boldsymbol{a})\widehat{D}_{\boldsymbol{a}}\,\widehat{D}_{-\boldsymbol{a}}(\hat{\boldsymbol{r}}-\boldsymbol{a})^{\mathrm{t}}\widehat{D}_{\boldsymbol{a}}|0\rangle \;=\; \langle 0|\hat{\boldsymbol{r}}\,\hat{\boldsymbol{r}}^{\mathrm{t}}|0\rangle \tag{2.86}$$

where (2.83) has been used in the last step. Thus, the coherent states have the same covariance matrix of the ground state, but their first moments (2.85) are non vanishing. Combining this observation with (2.78), for γ_{cs} we find

$$\gamma_{\text{cs}} = \frac{1}{2}\,W_{\text{phys}}^{-1}\,W_{\text{phys}}^{-\text{t}}\,. \tag{2.87}$$

The distance (2.31), that is mainly used throughout this manuscript to study the circuit complexity of mixed states, is valid for states having the same first moments [67, 70, 85], as reported in the appendix B.

In the appendix B it is also mentioned that an explicit expression for the complexity between coherent states is available in the literature if we restrict to the coherent states having a diagonal covariance matrix and $\boldsymbol{a} = (\sqrt{2}\,\alpha, 0, \dots, 0)$ [85, 90, 91]. These states provide a manifold parametrised by $(\alpha, v_1, \dots, v_{2N})$, where v_k^2 is the k-th entry of the diagonal covariance matrix, and whose metric is given by (B.10) with $n = 2N$ and $\mu = \sqrt{2}\alpha$, namely

$$ds^2 = \frac{2\,d\alpha^2 + 2\,dv_1^2}{v_1^2} + 2\sum_{k=2}^{2N}\frac{dv_k^2}{v_k^2}\,. \tag{2.88}$$

Let us remind that the covariance matrices that we are considering must satisfy the constraint (2.8), which is equivalent $\sigma_k \geqslant 1/2$ for the symplectic eigenvalues, where $k = 1, \dots, N$. By using (D.10), one finds that the symplectic eigenvalues of the diagonal covariance matrix $\text{diag}(v_1^2, \dots, v_{2N}^2)$ are $\sigma_k = v_k\,v_{k+N}$ for $k = 1, \dots, N$. Thus, in our case the manifold equipped with the metric (2.88) must be constrained by the conditions $v_k\,v_{k+N} \geqslant 1/2$ for $k = 1, \dots, N$.

The coherent states are pure states, hence their covariance matrices must satisfy the condition (2.23), which holds also when the first moments are non vanishing [48, 103]. For the class of coherent states that we are considering, the constraint (2.23) leads to

$$v_{k+N}^2 = \frac{1}{4v_k^2} \qquad k = 1, \dots, N \tag{2.89}$$

JHEP12(2020)101

which saturate the constraints $v_k\, v_{k+N} \geqslant 1/2$ introduced above. By imposing the conditions (2.89), the metric (2.88) becomes

$$ds^2 = \frac{2\, d\alpha^2 + 4\, dv_1^2}{v_1^2} + 4 \sum_{k=2}^{N} \frac{dv_k^2}{v_k^2} = 2 \left(\frac{d\alpha^2 + 2\, dv_1^2}{v_1^2} + 2 \sum_{k=2}^{N} \frac{dv_k^2}{v_k^2} \right) \tag{2.90}$$

which is twice (B.10) with $n = N$ and $\mu = \alpha$. The geometry given by (2.90) has been found also in [18]. The constraint (2.89) tells us that the metric (2.90) is defined on a set of pure states, but we are not guaranteed that the resulting manifold is totally geodesic. This is further discussed in the final part of this subsection.

Given a reference state and a target state parametrised[9] by $\boldsymbol{\phi}_{\mathrm{R}} = (\alpha_{\mathrm{R}}, v_{\mathrm{R},1}, \ldots, v_{\mathrm{R},N})$ and $\boldsymbol{\phi}_{\mathrm{T}} = (\alpha_{\mathrm{T}}, v_{\mathrm{T},1}, \ldots, v_{\mathrm{T},N})$ respectively, the square of the complexity of the circuit corresponding to the geodesic connecting these states in the manifold equipped with (2.90) is easily obtained from (B.11). The result reads

$$d_{\mathrm{cs}}(\boldsymbol{\phi}_{\mathrm{R}}, \boldsymbol{\phi}_{\mathrm{T}}) = 2\sqrt{2} \sqrt{ \left[\operatorname{arccosh}\left(1 + \frac{(\alpha_{\mathrm{R}} - \alpha_{\mathrm{T}})^2/2 + (v_{\mathrm{R},1} - v_{\mathrm{T},1})^2}{2\, v_{\mathrm{R},1} v_{\mathrm{T},1}} \right) \right]^2 + \sum_{k=2}^{N} \left[\log\left(\frac{v_{\mathrm{T},k}}{v_{\mathrm{R},k}} \right) \right]^2 } \,. \tag{2.91}$$

By adopting the normalisation in (2.33), which is consistent with [17, 18], one can introduce the complexity between coherent states as follows

$$\mathcal{C}_2 \,=\, \frac{1}{2\sqrt{2}}\, d_{\mathrm{cs}}(\boldsymbol{\phi}_{\mathrm{R}}, \boldsymbol{\phi}_{\mathrm{T}}) \,. \tag{2.92}$$

Setting $\alpha_{\mathrm{R}} = 0$ (or $\alpha_{\mathrm{T}} = 0$, equivalently) in (2.92), one obtains the complexity between a coherent state in the particular set introduced above and the ground state. As consistency check, we observe that, by setting $\alpha_{\mathrm{R}} = \alpha_{\mathrm{T}}$ in (2.92), the complexity (2.58) between pure states is recovered.

It is instructive to compare (2.92) with the results reported in [18], where the complexity $\mathcal{C}_{\kappa=2} = \mathcal{C}_2^2$ between the ground state and a bosonic coherent state has been studied through the Nielsen's approach [1–3]. The analytic expression for the complexity in [18] has been obtained for reference and target states with diagonal covariance matrices and first moments with at most one non vanishing component. Since these are the assumptions under which (2.92) has been obtained, we can compare the two final results for the complexity. The analysis of [18] allows to write the complexity $\mathcal{C}_{\kappa=2}$ in terms of a free parameter x_0 which does not occur neither in the reference state nor in the target state. We observe that the square of (2.92) with $\alpha_{\mathrm{R}} = 0$ coincides with the result in [18][10] with $x_0 = 2v_{\mathrm{R},1}$.

In the following we consider circuits in the space of the Gaussian states with non vanishing first moments such that the reference and the target states are given by two coherent states (2.84) originating from the same ground state, denoting their first moments by $\boldsymbol{a}_{\mathrm{R}}$ and $\boldsymbol{a}_{\mathrm{T}}$ respectively. These states have the same covariance matrix γ_0 (see (2.86)), whose symplectic eigenvalues are equal to 1/2, given that the coherent states are pure states.

[9] The vector $\boldsymbol{\phi}$ corresponds to the vector $\boldsymbol{\theta}$ used in appendix B restricted by the condition (2.89).

[10] In eqs. (4.23) and (4.24) of [18], set $i = 1$, $\sqrt{2}\,\omega_{\mathrm{R,there}} = 1/v_{\mathrm{R},k}$, $\sqrt{2\, m_{\mathrm{there}}\, \omega_{k,\mathrm{there}}} = 1/v_{\mathrm{T},k}$ and $\mathfrak{a}_{i,\mathrm{there}} = a_{\mathrm{there}}/x_0 = \alpha_{\mathrm{T}}/(\sqrt{2}\, v_{\mathrm{R},1})$.

JHEP12(2020)101

Parametrising the reference state by $\boldsymbol{\theta}_{\rm R} = (\boldsymbol{a}_{\rm R}, \gamma_0)$ and the target state by $\boldsymbol{\theta}_{\rm T} = (\boldsymbol{a}_{\rm T}, \gamma_0)$, a recent result obtained in [89] and discussed in appendix B allows us to write the circuit complexity as follows

$$\mathcal{C}_2 \,=\, \frac{1}{2\sqrt{2}}\, d_{\rm FR}(\boldsymbol{\theta}_{\rm R}, \boldsymbol{\theta}_{\rm T}) \tag{2.93}$$

where $d_{\rm FR}$ has been defined in (B.13). We are not able to prove that $\sigma_k \geqslant 1/2$ for the symplectic eigenvalues of the symmetric and positive matrices making the geodesic whose length is (2.93).

It is worth remarking that the expressions (2.92) and (2.93) for the complexity are defined for different sets of Gaussian Wigner functions with a non vanishing intersection. Indeed, (2.93) holds between PDF's with the same covariance matrix (that can be also non diagonal), while (2.92) is valid for diagonal covariance matrices that can be different. Moreover in (2.92), $\boldsymbol{a}_{\rm R}$ and $\boldsymbol{a}_{\rm T}$ can have only one non vanishing components, while in (2.93) they are generic. Thus, in order to compare (2.92) and (2.93) we have to consider reference and target states which have the same diagonal covariance matrix and whose first moments have only one non vanishing component. Setting $v_{{\rm R},k} = v_{{\rm T},k} \equiv v_k$ with $k = 1, \dots, N$ in (2.92), we obtain

$$\mathcal{C}_2 \,=\, \operatorname{arccosh}\!\left(1 + \frac{(\alpha_{\rm R} - \alpha_{\rm T})^2}{4\, v_1^2}\right). \tag{2.94}$$

Plugging $\gamma_0 = \operatorname{diag}(v_1^2, \dots, v_N^2, (2v_1)^{-2}, \dots, (2v_N)^{-2})$ and $\boldsymbol{a}_{\rm S} = (\sqrt{2}\,\alpha_{\rm S}, 0, \dots, 0)$ for ${\rm S} = {\rm R}$ and ${\rm S} = {\rm T}$ in (2.93), one finds

$$\mathcal{C}_2 \,=\, \frac{1}{\sqrt{2}} \operatorname{arccosh}\!\left(1 + \frac{(\alpha_{\rm R} - \alpha_{\rm T})^2}{2\, v_1^2}\right). \tag{2.95}$$

A simple numerical inspection shows that (2.95) is always smaller than (2.94). This example allows to conclude that the submanifold of pure states with diagonal covariance matrix equipped with the metric (2.90) is not totally geodesics.

3 Spectrum complexity and basis complexity

In this section we discuss the spectrum complexity and the basis complexity for mixed Gaussian states in harmonic lattices.

By exploiting the Williamson's decomposition we introduce the W *path* as the optimal circuit connecting two covariance matrices with $W_{\rm R} = W_{\rm T} \equiv W$ and the $\mathcal{D}$ *path* as the optimal circuit connecting two covariance matrices having $\mathcal{D}_{\rm R} = \mathcal{D}_{\rm T} \equiv \mathcal{D}$. In order to study these circuits, in section 3.1 we discuss the first law of complexity for the Gaussian states that we are considering. The lengths of a W path and of a $\mathcal{D}$ path are employed to study the spectrum complexity (section 3.3) and the basis complexity (section 3.4) respectively. In figure 2 the dashed curves correspond to W paths (see (3.18)).

3.1 First law of complexity

It is worth investigating the first law of complexity [73, 74] for the states described in section 2. The derivations of the results reported below are given in the appendix E.

JHEP12(2020)101

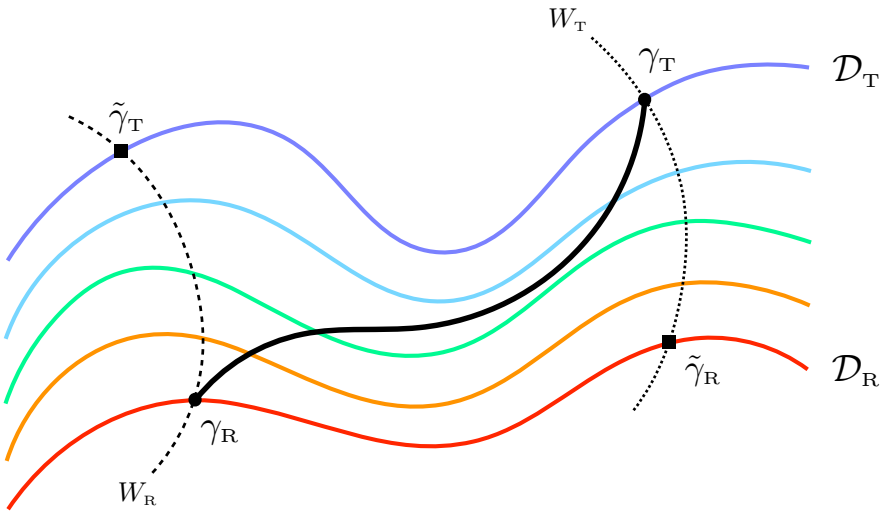

Figure 2. The solid black curve and the solid coloured curves have been defined in figure 1. Eq. (3.18) tells us that the dashed black curves represent the $W_{\rm R}$ path and the $W_{\rm T}$ path that pass through $\gamma_{\rm R}$ and $\gamma_{\rm T}$ respectively (the auxiliary covariance matrices $\tilde{\gamma}_{\rm R}$ and $\tilde{\gamma}_{\rm T}$ have been defined in (5.1)). The arcs of the dashed curves that connect the blue curve to the red curve have the same length given by (3.19).

Let us consider the following functional

$$S[q(t)] = \int_{t_0}^{t_1} \mathcal{L}[q(t), \dot{q}(t), t]\, dt \tag{3.1}$$

where $q_0 = q(t_0)$ and $q_1 = q(t_1)$ are the initial and final configurations respectively.

It is well known that the first variation of (3.1) under an infinitesimal change of the boundary conditions $q_i \to q_i + \delta q_i$ for $i = 0, 1$ evaluated on a solution of the equations of motion is

$$\delta S[q(t)] \;=\; \frac{\partial \mathcal{L}}{\partial \dot{q}}\, \delta q \Big|_{t_1} - \frac{\partial \mathcal{L}}{\partial \dot{q}}\, \delta q \Big|_{t_0} . \tag{3.2}$$

The functional we are interested in is the length functional (2.27) and the solution of its equations of motion is given by the optimal circuit (2.28), that satisfies the boundary conditions (2.29). In order to apply (3.2), one considers the infinitesimal variations $\gamma_{\rm T} \to \gamma_{\rm T} + \delta\gamma_{\rm T}$ and $\gamma_{\rm R} \to \gamma_{\rm R} + \delta\gamma_{\rm R}$ of the covariance matrices of the reference and of the target states that preserve the properties of these matrices. In other words, these variations are such that also the resulting matrices are covariance matrices.

The length functional (2.27) leads to introduce the following cost function

$$F(\gamma, \dot{\gamma}) \;=\; \sqrt{\mathrm{Tr}\big[\,(\gamma^{-1}\,\dot{\gamma})^2\,\big]}\,. \tag{3.3}$$

By applying (3.2) to the length functional (2.27), one obtains the first law of complexity

$$\delta d = \sum_{ij} \frac{\partial F}{\partial \dot{\gamma}_{ij}}\, \delta\gamma_{ij} \Big|_{s=0}^{s=1} \tag{3.4}$$

where the r.h.s. is evaluated on the geodesic (2.28).

JHEP12(2020)101

Equivalent expressions for the variation (3.4) have been derived in appendix E. For instance, it can be written as

$$\delta d \,=\, \frac{1}{d}\Big(\mathrm{Tr}\left\{ \partial_s G_s^{-1}|_{s=0}\, \delta\gamma_{\mathrm{R}} \right\} - \mathrm{Tr}\left\{ \partial_s G_s^{-1}|_{s=1}\, \delta\gamma_{\mathrm{T}} \right\} \Big) \tag{3.5}$$

where G_s is the geodesic (2.28). Another useful expression for (3.4), which is simpler to evaluate than (3.5), reads

$$\delta d \,=\, \frac{1}{d}\, \mathrm{Tr}\left\{ (\delta\gamma_{\mathrm{T}}\, \gamma_{\mathrm{T}}^{-1} - \delta\gamma_{\mathrm{R}}\, \gamma_{\mathrm{R}}^{-1})\, \log(\Delta_{\mathrm{TR}}) \right\} \tag{3.6}$$

where Δ_{TR} has been defined in (2.32).

We find it worth providing also an expression for the variation (3.4) that is based on the Williamson's decompositions (2.41). It is given by

$$\begin{aligned} \delta d = \frac{1}{d} \Big[& 2\, \mathrm{Tr}\left\{ \log(\gamma_{\mathrm{T}}^{-1}\gamma_{\mathrm{R}})\, (W_{\mathrm{R}}^{-1}\, \delta W_{\mathrm{R}} - W_{\mathrm{T}}^{-1}\, \delta W_{\mathrm{T}}) \right\} \\ & + \mathrm{Tr}\left\{ [\, W_{\mathrm{T}} \log(\gamma_{\mathrm{R}}^{-1}\gamma_{\mathrm{T}}) W_{\mathrm{T}}^{-1}\,]\, \mathcal{D}_{\mathrm{T}}^{-1}\, \delta\mathcal{D}_{\mathrm{T}} - [\, W_{\mathrm{R}} \log(\gamma_{\mathrm{R}}^{-1}\gamma_{\mathrm{T}}) W_{\mathrm{R}}^{-1}\,]\, \mathcal{D}_{\mathrm{R}}^{-1}\, \delta\mathcal{D}_{\mathrm{R}} \right\} \Big] \end{aligned} \tag{3.7}$$

where, by using (D.1), one can write the matrices within the square brackets in terms of the matrix W_{TR} introduced in (2.45) as follows

$$W_{\mathrm{T}} \log(\gamma_{\mathrm{R}}^{-1}\gamma_{\mathrm{T}}) W_{\mathrm{T}}^{-1} = \log(W_{\mathrm{TR}}\, \mathcal{D}_{\mathrm{R}}^{-1}\, W_{\mathrm{TR}}^{\mathrm{t}}\, \mathcal{D}_{\mathrm{T}}) \tag{3.8}$$

$$W_{\mathrm{R}} \log(\gamma_{\mathrm{R}}^{-1}\gamma_{\mathrm{T}}) W_{\mathrm{R}}^{-1} = \log(\mathcal{D}_{\mathrm{R}}^{-1}\, W_{\mathrm{TR}}^{\mathrm{t}}\, \mathcal{D}_{\mathrm{T}}\, W_{\mathrm{TR}})\,. \tag{3.9}$$

The form (3.7) for δd tells us that this variation can be written as the sum of four contributions: two terms from the variations δW_{R} and δW_{T} of the symplectic matrices in (2.41) and two terms from the diagonal and non negative variations $\delta\mathcal{D}_{\mathrm{R}}$ and $\delta\mathcal{D}_{\mathrm{T}}$ of the symplectic spectra.

3.2 Solving $\delta d = 0$

It is natural to look for relations between γ_{R} and γ_{T} that lead to $\delta d = 0$ and, in order to find them, let us consider the first law of complexity written in the form (3.7).

First we focus on the variations of W_{R} and W_{T}. When $\delta\mathcal{D}_{\mathrm{R}} = \delta\mathcal{D}_{\mathrm{T}} = \mathbf{0}$ in (3.7), the equation $\delta d = 0$ becomes

$$\mathrm{Tr}\left\{ \log(\gamma_{\mathrm{T}}^{-1}\gamma_{\mathrm{R}})\, (W_{\mathrm{R}}^{-1}\, \delta W_{\mathrm{R}} - W_{\mathrm{T}}^{-1}\, \delta W_{\mathrm{T}}) \right\} = 0\,. \tag{3.10}$$

A trivial solution of this equation is given by

$$W_{\mathrm{R}} = W_{\mathrm{T}}\,. \tag{3.11}$$

Another solution of (3.10) is $W_{\mathrm{R}} = M\, W_{\mathrm{T}}$, where M is a constant symplectic matrix whose elements are just real numbers, i.e. it does not contain parameters to vary. Notice that these two simple solutions require that both W_{R} and W_{T} are allowed to vary.

JHEP12(2020)101

In order to find solutions to (3.10) for any choice of the independent variations $\delta W_{\rm R}$ and $\delta W_{\rm T}$, let us first observe that, by taking the first variation of the relation $W^{\rm t} J\, W = J$, that characterises a symplectic matrix $W^{\rm t}$, it is not difficult to realise that $\delta X \equiv W^{\rm t} J\, \delta W$ must be a symmetric matrix. By using that $W^{-1} = J^{-1}\, W^{\rm t} J$, for the two terms in the r.h.s. of (3.10) one obtains $\mathrm{Tr}[A\, W^{-1}\, \delta W] = \mathrm{Tr}(Y \delta X)$, where $Y \equiv A\, J^{-1}$. Since δX corresponds to a generic infinitesimal real and symmetric matrix, $\mathrm{Tr}(Y \delta X) = 0$ is satisfied for every δX e.g. when Y is a real antisymmetric matrix. These observations lead us to write (3.10) as

$$\mathrm{Tr}\left\{ \log(\gamma_{\rm T}^{-1}\gamma_{\rm R})\, J^{-1} \left[\delta X_{\rm R} - \delta X_{\rm T}\right] \right\} = 0 \tag{3.12}$$

where $\delta X_{\rm R} \equiv W_{\rm R}^{\rm t}\, J\, \delta W_{\rm R}$ and $\delta X_{\rm T} \equiv W_{\rm T}^{\rm t}\, J\, \delta W_{\rm T}$ are real and symmetric matrices. Thus, from (3.12), we have that (3.10) is satisfied for $\gamma_{\rm T}^{-1}\gamma_{\rm R} = e^{YJ}$, i.e.

$$\gamma_{\rm T} \,=\, \gamma_{\rm R}\, e^{-YJ} \tag{3.13}$$

where Y is a real antisymmetric matrix that can depend on $\gamma_{\rm R}$ or $\gamma_{\rm T}$. We remark that (3.13) solves (3.10) for any choice of the independent variations $\delta W_{\rm R}$ and $\delta W_{\rm T}$.

It is worth asking when the case $W_{\rm R} = M\, W_{\rm T}$ mentioned above, where M is a symplectic matrix made of real numbers, becomes a special case of (3.13). The Williamson's decompositions (2.41) and $W_{\rm R} = M\, W_{\rm T}$ lead to $\log(\gamma_{\rm T}^{-1}\gamma_{\rm R})J^{-1} = \log(W_{\rm T}^{-1}\mathcal{D}_{\rm T}^{-1}M^{\rm t}\mathcal{D}_{\rm R}MW_{\rm T})J^{-1}$. Then, (D.1) allows us to write the transpose of this matrix as $J\log(W_{\rm T}^{\rm t}M^{\rm t}\mathcal{D}_{\rm R}M\mathcal{D}_{\rm T}^{-1}W_{\rm T}^{-{\rm t}})$. By inserting the identity $\mathbf{1} = J^{-1}J$ between all the factors within the argument of the logarithm occurring in this matrix, using (D.1) again and exploiting the properties of the symplectic matrices, one arrives to $\left[\log(\gamma_{\rm T}^{-1}\gamma_{\rm R})J^{-1}\right]^{\rm t} = -\log(W_{\rm T}^{-1}M^{-1}\mathcal{D}_{\rm R}M^{-{\rm t}}\mathcal{D}_{\rm T}^{-1}W_{\rm T})J^{-1}$. Comparing this expression with the one reported above, we conclude that the matrix $\log(\gamma_{\rm T}^{-1}\gamma_{\rm R})J^{-1}$ is antisymmetric when $W_{\rm R} = M\, W_{\rm T}$ and $M^{-1}\mathcal{D}_{\rm R}M^{-{\rm t}} = M^{\rm t}\mathcal{D}_{\rm R}M$. This is the case for a symplectic matrix that is also orthogonal, i.e. $M \in K(N)$. In particular, the special case given by $M = \mathbf{1} \in K(N)$ corresponds to (3.11). Summarising, in the special case given by $W_{\rm R} = M\, W_{\rm T}$, the matrix Y introduced in (3.13) can be written as $Y = \log(W_{\rm T}^{-1}\mathcal{D}_{\rm T}^{-1}M^{\rm t}\mathcal{D}_{\rm R}MW_{\rm T})J^{-1}$ with $M^{-1}\mathcal{D}_{\rm R}M^{-{\rm t}} = M^{\rm t}\mathcal{D}_{\rm R}M$.

As for the terms corresponding to the variations of $\mathcal{D}_{\rm R}$ and $\mathcal{D}_{\rm T}$ in (3.7), let us observe that, for a diagonal matrix $\Lambda > 0$, we have that $\Lambda^{-1}\delta\Lambda = \delta \log\Lambda$ and that $\mathrm{Tr}(H\, \delta \log\Lambda) = 0$ holds for a generic $\delta\Lambda$ when all the elements along the diagonal of H vanish. The matrices having vanishing elements on their main diagonal are called hollow matrices. By employing these observations in the equation $\delta d = 0$ with δd given by (3.7), where the variations of $\mathcal{D}_{\rm R}$ and $\mathcal{D}_{\rm T}$ are independent, we conclude that the main diagonals of the matrices within the square brackets in (3.7) must vanish. By introducing two non vanishing hollow matrices Z and $\widetilde{Z}$, this gives

$$\log(\gamma_{\rm R}^{-1}\gamma_{\rm T}) = W_{\rm T}^{-1}\, Z\, W_{\rm T} \qquad\qquad \log(\gamma_{\rm R}^{-1}\gamma_{\rm T}) = W_{\rm R}^{-1}\, \widetilde{Z}\, W_{\rm R} \tag{3.14}$$

which correspond to the terms containing $\delta\mathcal{D}_{\rm T}$ and $\delta\mathcal{D}_{\rm R}$ respectively in (3.7). By employing (3.8) and (3.9), one finds that the relations in (3.14) can be written respectively as

$$W_{\rm TR}\, \mathcal{D}_{\rm R}^{-1}\, W_{\rm TR}^{\rm t}\, \mathcal{D}_{\rm T} = e^{Z} \qquad\qquad \mathcal{D}_{\rm R}^{-1}\, W_{\rm TR}^{\rm t}\, \mathcal{D}_{\rm T}\, W_{\rm TR} = e^{\widetilde{Z}}\,. \tag{3.15}$$

JHEP12(2020)101

These observations tell us that $\delta d = 0$ for generic variations of $\gamma_{\rm R}$ and $\gamma_{\rm T}$ when these covariance matrices are related by (3.13) with Y constrained by the conditions that the elements on the diagonals of $W_{\rm T}\, Y J\, W_{\rm T}^{-1}$ and $W_{\rm R}\, Y J\, W_{\rm R}^{-1}$ vanish.

A rough analysis shows that this problem is too constrained for $N = 1$ and $N = 2$. Indeed, the antisymmetric matrix Y depends on $N(2N-1)$ parameters and imposing that the diagonals of Z and $\widetilde{Z}$ vanish provides $4N$ constraints. In particular, when $N = 1$ the 2×2 antisymmetric matrix Y has only one non vanishing off diagonal element a in the top right position and it is straightforward to check that $YJ = -a\,\mathbf{1}$. By using also (3.13) and (3.14) specialised to this case, we obtain that the above procedure leads to impose that $W_{\rm S}\, Y J\, W_{\rm S}^{-1}$, with ${\rm S} = \{{\rm R}, {\rm T}\}$, must have vanishing elements along the diagonal. This is possible only for $a = 0$, i.e. $Y = \mathbf{0}$. Thus, when $N = 1$ we cannot find a solution of the form (3.13) for the equation $\delta d = 0$ with δd given by (3.7).

3.3 Spectrum complexity

It is worth exploring the possibility to define the circuit complexity associated to the change of the symplectic spectrum.

Let us consider a reference state and a target state such that in the Williamson's decompositions of their covariance matrices $\gamma_{\rm R}$ and $\gamma_{\rm T}$ (see (2.41)) the same symplectic matrix occurs, namely

$$\gamma_{\rm R} = W^{\rm t}\, \mathcal{D}_{\rm R}\, W \qquad \gamma_{\rm T} = W^{\rm t}\, \mathcal{D}_{\rm T}\, W \qquad W \in {\rm Sp}(2N, \mathbb{R})\,. \tag{3.16}$$

We call W *path* the optimal circuit (2.28) connecting these two covariance matrices.

In order to study the Williamson's decomposition of a matrix belonging to a W path, we consider the expression (2.39) for the optimal circuit. When (3.16) holds, from (2.32) it is straightforward to find that $\Delta_{\rm TR} = W^{\rm t}\, \mathcal{D}_{\rm T}\, \mathcal{D}_{\rm R}^{-1}\, W^{-{\rm t}}$. Then, by employing (D.1) both in U_s and in $U_s^{\rm t}$ occurring in (2.39), we obtain

$$G_s(\gamma_{\rm R}\,, \gamma_{\rm T}) = W^{\rm t} (\, \mathcal{D}_{\rm R}^{1-s}\, \mathcal{D}_{\rm T}^{s}\,) W \tag{3.17}$$

which tells us that the Williamson's decomposition of the matrix along the W path is (2.42) with

$$\mathcal{D}_s \;=\; \mathcal{D}_{\rm R}^{1-s}\, \mathcal{D}_{\rm T}^{s} \qquad W_s = W\,. \tag{3.18}$$

It is remarkable that the symplectic matrix W_s is independent of s. This means that in the Williamson's decomposition of a matrix belonging to a W path the same symplectic matrix W occurs. In figure 2 the dashed curves correspond to the $W_{\rm R}$ path and to the $W_{\rm T}$ path. Considering e.g. the $W_{\rm R}$ path in figure 2, from (3.18) we have that the Williamson's decomposition of a generic matrix γ belonging to this $W_{\rm R}$ path is given by the symplectic matrix $W_{\rm R}$ and by the symplectic spectrum corresponding to the coloured line intersecting the dashed line of the $W_{\rm R}$ path at γ.

An interesting example of W path is given by the thermal states of a given model at different temperatures (see section 2.6). Indeed, in the Williamson's decomposition (2.76), the symplectic matrix $W_{\rm th}$ is independent of the temperature.

JHEP12(2020)101

For a W path we have $\delta d = 0$ (see (3.11)); hence the W paths provide a preferred way to connect the set of covariance matrices with symplectic spectrum $\mathcal{D}_{\rm R}$ to the set of covariance matrices with symplectic spectrum $\mathcal{D}_{\rm T}$.

We find it natural to define the spectrum complexity as the length of a W path because this quantity is independent of the choice of W. In particular, from (3.16), we have that $W_{\rm TR} = \mathbf{1}$, hence (2.49) simplifies to

$$d_{\rm spectrum}(\gamma_{\rm R}\,,\gamma_{\rm T}) \equiv \sqrt{{\rm Tr}\Big\{\big[\log(\mathcal{D}_{\rm T}\,\mathcal{D}_{\rm R}^{-1})\big]^2\Big\}} = \sqrt{2\sum_{k=1}^{N}\left[\log\left(\frac{\sigma_{{\rm T},k}}{\sigma_{{\rm R},k}}\right)\right]^2} \tag{3.19}$$

which is independent of W. This implies that $d_{\rm spectrum}(\gamma_{\rm R}\,,\gamma_{\rm T}) = d_{\rm spectrum}(\mathcal{D}_{\rm R}\,,\mathcal{D}_{\rm T})$. Thus, in figure 2 the arcs of the dashed curves that connect the blue curve to the red curve have the same length given by (3.19).

Another natural definition for the spectrum complexity is the distance between the set of covariance matrices whose symplectic spectrum is $\mathcal{D}_{\rm R}$ (red curve in figure 2) and the set of covariance matrices whose symplectic spectrum is $\mathcal{D}_{\rm T}$ (blue curve in figure 2). It reads

$$\tilde{d}_{\rm spectrum}(\mathcal{D}_{\rm R}\,,\mathcal{D}_{\rm T}) \equiv \min\big[\,d(W^{\rm t}\,\mathcal{D}_{\rm R}\,W\,,\widetilde{W}^{\rm t}\,\mathcal{D}_{\rm T}\,\widetilde{W})\,\big] \qquad W,\,\widetilde{W} \in {\rm Sp}(2N,\mathbb{R}) \tag{3.20}$$

where the minimisation over the symplectic matrices W and $\widetilde{W}$ is difficult to perform. It is straightforward to realise that $\tilde{d}_{\rm spectrum}(\mathcal{D}_{\rm R}\,,\mathcal{D}_{\rm T}) \leqslant d_{\rm spectrum}(\mathcal{D}_{\rm R}\,,\mathcal{D}_{\rm T})$.

In the simplest case of one-mode mixed states (i.e. when $N = 1$), the optimal circuit (3.17) simplifies to

$$G_s(\gamma_{\rm R}\,,\gamma_{\rm T}) \,=\, \sigma_{\rm R}^{1-s}\sigma_{\rm T}^{s}\,W^{\rm t}\,W \,=\, \left(\frac{\sigma_{\rm T}}{\sigma_{\rm R}}\right)^{s}\gamma_{\rm R} \tag{3.21}$$

which tells us that the 2×2 matrix belonging to the W path is a proper rescaling of the covariance matrix of the reference state.

3.4 Basis complexity

In order to study the circuit complexity associated to a change of basis, let us consider the Williamson's decompositions of two covariance matrices $\gamma_{\rm R}$ and $\gamma_{\rm T}$ having the same symplectic spectrum, i.e.

$$\gamma_{\rm R} = W_{\rm R}^{\rm t}\,\mathcal{D}\,W_{\rm R} \qquad\qquad \gamma_{\rm T} = W_{\rm T}^{\rm t}\,\mathcal{D}\,W_{\rm T} \tag{3.22}$$

that have been obtained by setting $\mathcal{D}_{\rm R} = \mathcal{D}_{\rm T} = \mathcal{D}$ in (2.41). An important example is given by states whose density matrices $\hat{\rho}_{\rm T}$ and $\hat{\rho}_{\rm R}$ are related through a unitary transformation U, namely $\hat{\rho}_{\rm T} = U\hat{\rho}_{\rm R}U^{\dagger}$. Indeed, this means that the corresponding covariance matrices are related through a symplectic matrix (that does not change the symplectic spectrum) [46, 48].

We denote as $\mathcal{D}$ *path* the optimal circuit connecting the covariance matrices having the same symplectic spectrum, identifying its length as a basis complexity. This basis

JHEP12(2020)101

complexity can be found by specifying (2.49) to (3.22) and the result is[11]

$$d_{\text{basis}}(\gamma_{\text{R}}\,,\gamma_{\text{T}}) \,=\, \sqrt{\text{Tr}\left\{\left[\log(\mathcal{D}\,W_{\text{TR}}\,\mathcal{D}^{-1}\,W_{\text{TR}}^{\text{t}})\right]^2\right\}} \tag{3.23}$$

where W_{TR} has been defined in (2.45). Notice that we have not required that all the matrices along a $\mathcal{D}$ path have the same symplectic spectrum.

We find it reasonable to introduce also another definition of basis complexity as the minimal length of an optimal circuit that connects a covariance matrix whose Williamson's decomposition contains the symplectic matrix W_{R} (i.e. that lies on the dashed curve on the left in figure 2) to a covariance matrix having the symplectic matrix W_{T} in its Williamson's decomposition (i.e. that belongs to the dashed curve on the right in figure 2). This basis complexity is defined as follows

$$\tilde{d}_{\text{basis}}(W_{\text{R}}\,,W_{\text{T}}) \equiv \min\left[\, d(W_{\text{R}}^{\text{t}}\,\mathcal{D}\,W_{\text{R}}\,,\, W_{\text{T}}^{\text{t}}\,\widetilde{\mathcal{D}}\,W_{\text{T}})\,\right] \qquad \mathcal{D},\,\widetilde{\mathcal{D}} \in \text{Diag}(N,\mathbb{R}) \tag{3.24}$$

where the minimisation is performed over the set $\text{Diag}(2N,\mathbb{R})$ made by the diagonal matrices of the form $\text{diag}(\boldsymbol{\sigma})\oplus\text{diag}(\boldsymbol{\sigma})$, with $\boldsymbol{\sigma}$ vector of N real numbers $\sigma_i \geqslant 1/2$. It is immediate to notice that (3.24) is a lower bound for (3.23), i.e. $\tilde{d}_{\text{basis}}(W_{\text{R}}\,,W_{\text{T}}) \leqslant d_{\text{basis}}(\gamma_{\text{R}}\,,\gamma_{\text{T}})$.

Specifying the form (2.39) for the optimal circuit to (3.22), it is straightforward to find that the $\mathcal{D}$ path is given by

$$G_s(\gamma_{\text{R}}\,,\gamma_{\text{T}}) \,=\, \widetilde{W}_s^{\text{t}}\,\mathcal{D}\,\widetilde{W}_s \qquad\qquad \widetilde{W}_s \equiv W_{\text{R}}\,U_s^{\text{t}} \tag{3.25}$$

where we remark that $\widetilde{W}_s$ is not symplectic in general.

It is worth asking when $\widetilde{W}_s$ is symplectic because in these cases (3.25) provides the Williamson's decomposition of the $\mathcal{D}$ path. The requirement $U_s \in \text{Sp}(2N,\mathbb{R})$ leads to

$$\left[\, W_{\text{TR}}\,,\mathcal{D}\,\right] \,=\, 0\,. \tag{3.26}$$

When this condition holds, (3.23) simplifies to the following expression

$$d_{\text{basis}}(\gamma_{\text{R}}\,,\gamma_{\text{T}}) \,=\, \sqrt{\text{Tr}\left\{\left[\log(W_{\text{TR}}\,W_{\text{TR}}^{\text{t}})\right]^2\right\}} \tag{3.27}$$

which is independent of $\mathcal{D}$.

For pure states, which have $\mathcal{D} = \frac{1}{2}\,\mathbf{1}$, the condition (3.26) is trivially verified. Another interesting example where (3.26) holds is given by the one-mode states, where $\mathcal{D}$ is proportional to the 2×2 identity matrix. In this case we can always connect two covariance matrices with the same symplectic spectrum through the optimal circuit (2.53), that can be written as

$$G_s(\gamma_{\text{R}}\,,\gamma_{\text{T}}) \,=\, \sigma\; W_s^{\text{t}}\,W_s \tag{3.28}$$

where $\sigma_{\text{R}} = \sigma_{\text{T}} \equiv \sigma$ and W_s is defined in (2.54); hence from (3.25) we have that $W_s = \widetilde{W}_s$.

When $N > 1$ the condition (3.26) is a non trivial requirement. For instance, when W_{TR} is diagonal, (3.26) is verified and (3.25) holds with $\widetilde{W}_s = \mathcal{X}_{\text{TR}}^s W_{\text{R}}$. The basis complexity (3.23) simplifies to $d^2_{\text{basis}}(\gamma_{\text{R}}\,,\gamma_{\text{T}}) = \text{Tr}\{[\log(\mathcal{X}^2_{\text{TR}})]^2\}$, that is independent of $\mathcal{D}$.

[11] The result (3.23) can be obtained also by employing (2.48) with $\mathcal{D}_{\text{R}} = \mathcal{D}_{\text{T}}$.

JHEP12(2020)101

Writing $W_{\rm TR}$ as a block matrix made by four $N \times N$ matrices, it is straightforward to find that the condition (3.26) holds whenever every block of $W_{\rm TR}$ commutes with $\mathrm{diag}(\sigma_1, \dots, \sigma_N)$. Then, we can exploit the fact that a diagonal matrix with distinct elements commutes with another matrix only when the latter one is diagonal.[12] Thus, if the symplectic spectrum is non degenerate, all the blocks of $W_{\rm TR}$ must be diagonal to fulfil the condition (3.26). We remark that the non-degeneracy condition for the symplectic spectrum is not guaranteed; indeed, the symplectic spectrum has some degeneracy in several interesting cases. For instance, for pure states all the symplectic eigenvalues are equal to $\frac{1}{2}$. Another important example is the reduced covariance matrix of an interval in an infinite harmonic chain with non vanishing mass [94].

We find it worth discussing the relation between the optimal circuits considered above to study the basis complexity and the solutions of the equation $\delta d = 0$ described in section 3.2. For the set of paths occurring in (3.24), which includes the $\mathcal{D}$ paths, we have $\delta W_{\rm R} = \delta W_{\rm T} = 0$ in (3.7). In this case, in section 3.2 we found that a solution of $\delta d = 0$ is given by (3.15), where Z and $\widetilde{Z}$ are non vanishing hollow matrices. Restricting to the cases of $\mathcal{D}$ paths that satisfy also (3.26), these relations simplify respectively to $W_{\rm TR}\, W_{\rm TR}^{\rm t} = e^{Z}$ and $W_{\rm TR}^{\rm t}\, W_{\rm TR} = e^{\widetilde{Z}}$, whose solution is non trivial because a matrix does not commute with its transpose in general (the matrices satisfying this property are called normal matrices). Notice that $W_{\rm TR} \in K(N)$ are not admissible solutions because Z and $\widetilde{Z}$ are non vanishing.

A slightly more general solution can be obtained by restricting to the $\mathcal{D}$ paths (see (3.22)). In this case, from (3.24) with $\delta W_{\rm R} = \delta W_{\rm T} = 0$ and $\delta \mathcal{D}_{\rm R} = \delta \mathcal{D}_{\rm T} \equiv \delta \mathcal{D}$, we have that $\delta d = 0$ becomes

$$\mathrm{Tr}\left\{ \left[W_{\rm T} \log(\gamma_{\rm R}^{-1}\gamma_{\rm T}) W_{\rm T}^{-1} - W_{\rm R} \log(\gamma_{\rm R}^{-1}\gamma_{\rm T}) W_{\rm R}^{-1} \right] \mathcal{D}^{-1}\, \delta\mathcal{D} \right\} = 0\,. \tag{3.29}$$

By using (3.8), (3.9) and the discussion made in section 3.2, one finds that (3.29) is solved when $\log(W_{\rm TR}\, \mathcal{D}^{-1}\, W_{\rm TR}^{\rm t}\, \mathcal{D}) - \log(\mathcal{D}^{-1}\, W_{\rm TR}^{\rm t}\, \mathcal{D}\, W_{\rm TR})$ is a non vanishing hollow matrix. When (3.26) also holds, this condition simplifies to the requirement that $\log(W_{\rm TR}\, W_{\rm TR}^{\rm t}) - \log(W_{\rm TR}^{\rm t} W_{\rm TR})$ is a non vanishing hollow matrix, which is independent of $\mathcal{D}$.

4 Purification through the W path

The purification of a mixed state is a process that provides a pure state starting from a mixed state. This procedure is not unique. Considering the context of the bosonic Gaussian states that we are exploring, in this section we discuss the purification of a mixed state by employing the results reported in section 3.

Given a mixed state that is not pure and that is characterised by the covariance matrix $\gamma_{\rm R}$, any circuit connecting $\gamma_{\rm R}$ to a pure state provides a *purification path*. A purification path connects the covariance matrices $\gamma_{\rm R}$ to $\gamma_{\rm T}$ whose Williamson's decompositions are given respectively by

$$\gamma_{\rm R} = W_{\rm R}^{\rm t}\, \mathcal{D}\, W_{\rm R} \qquad\qquad \gamma_{\rm T} = \frac{1}{2}\, W_{\rm T}^{\rm t}\, W_{\rm T} \tag{4.1}$$

[12] Consider the diagonal matrix $\Lambda = \mathrm{diag}(\lambda_1, \dots, \lambda_N)$ with $\lambda_i \neq \lambda_j$ and a matrix M such that $[\Lambda, M] = 0$. The generic element of this relation reads $M_{i,j}\lambda_j = \lambda_i M_{i,j}$, i.e. $M_{i,j}(\lambda_i - \lambda_j) = 0$. Since $\lambda_i \neq \lambda_j$ when $i \neq j$, we have $M_{i,j} = 0$ for $i \neq j$.

JHEP12(2020)101

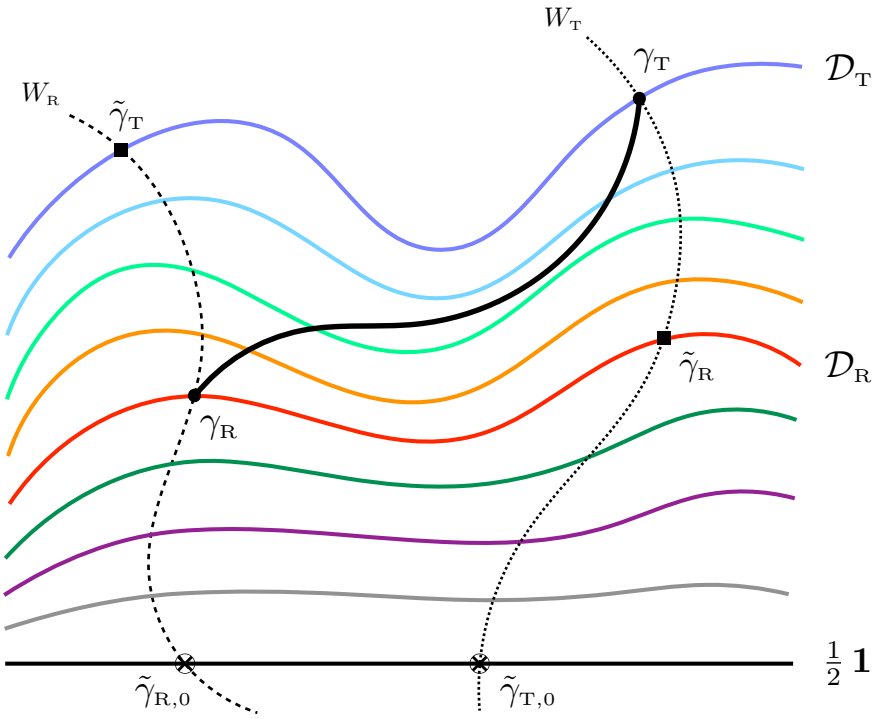

Figure 3. The optimal purification paths for $\gamma_{\rm R}$ and $\gamma_{\rm T}$ correspond respectively to the $W_{\rm R}$ path and to the $W_{\rm T}$ path, that are represented through dashed lines. The straight black solid line represent the set of the pure states, whose symplectic spectrum is given by $\mathcal{D} = \frac{1}{2}\mathbf{1}$.

where $W_{\rm R} \in {\rm Sp}(2N,\mathbb{R})$ and $\mathcal{D} \neq \frac{1}{2}\,\mathbf{1}$ are assigned, while $W_{\rm T} \in {\rm Sp}(2N,\mathbb{R})$ is not. Among all the possible paths, the optimal circuit is obtained by specifying (2.28) to (4.1). The result is

$$G_s^{(0)}(\gamma_{\rm R}, W_{\rm T}) \equiv \frac{1}{2^s}\,\gamma_{\rm R}^{1/2}\Big(\gamma_{\rm R}^{-1/2}\,W_{\rm T}^{\rm t}\,W_{\rm T}\,\gamma_{\rm R}^{-1/2}\Big)^s\,\gamma_{\rm R}^{1/2} \tag{4.2}$$

which depends on the symplectic matrix $W_{\rm T}$ that determines the final pure state. The length of the purification path (4.2) can be found by evaluating (2.31) for the special case described by (4.1). It reads

$$d_0(\gamma_{\rm R}, W_{\rm T}) \equiv \sqrt{{\rm Tr}\left\{\left[\log(2\,\gamma_{\rm R}\,W_{\rm T}^{-1}W_{\rm T}^{-{\rm t}})\right]^2\right\}}\,. \tag{4.3}$$

The *optimal purification path* is the purification path with minimal length, which can be found by minimising (4.3) as $W_{\rm T} \in {\rm Sp}(2N,\mathbb{R})$ varies within the symplectic group. This extremization procedure selects a symplectic matrix W_0 that determines the pure state through its covariance matrix $\frac{1}{2}\,W_0^{\rm t}\,W_0$. The matrix W_0 is obtained by solving $\delta d_0 = 0$, where d_0 is defined in (4.3). This is a special case of the analysis performed in section 3.2 corresponding to $\delta\mathcal{D}_{\rm R} = \delta\mathcal{D}_{\rm T} = \delta W_{\rm R} = \mathbf{0}$.

In section 3.2 we have shown that a W path provides a solution to this equation, namely

$$W_0 = W_{\rm R} \tag{4.4}$$

JHEP12(2020)101

which is the trivial solution corresponding to $\delta W_{\rm R} = \mathbf{0}$. In the following we focus on the purification process based on the W paths. We cannot prove that, among all the solution of $\delta d_0 = 0$ (see section 3.2), the W path corresponds to the one having minimal length.

The $W_{\rm R}$ path connects the mixed state $\gamma_{\rm R} = W_{\rm R}^{\rm t}\, \mathcal{D}\, W_{\rm R}$ to the pure state $\gamma_0 = \frac{1}{2}\, W_{\rm R}^{\rm t}\, W_{\rm R}$. By specialising (3.17) to $\mathcal{D}_{\rm T} = \frac{1}{2}\,\mathbf{1}$, we find that this $W_{\rm R}$ path is given by

$$G_s(\gamma_{\rm R}\,,\gamma_0) = G_s^{(0)}(\gamma_{\rm R}, W_{\rm R}) = \frac{1}{2^s}\; W_{\rm R}^{\rm t}\, \mathcal{D}^{1-s}\, W_{\rm R} \tag{4.5}$$

and its length can be easily obtained by setting $\mathcal{D}_{\rm T} = \frac{1}{2}\,\mathbf{1}$ in (3.19), finding an expression that depends only on $\mathcal{D}$

$$d_0(\gamma_{\rm R}, W_{\rm R}) \equiv d_{\rm spectrum}(\gamma_{\rm R}\,,\gamma_0) = \sqrt{\mathrm{Tr}\Big\{\big[\log(2\,\mathcal{D})\big]^2\Big\}} = \sqrt{2\sum_{k=1}^{N}\big[\log(2\,\sigma_k)\big]^2}\,. \tag{4.6}$$

It is instructive to focus on the one-mode mixed states, when the covariance matrices (4.1) become $\gamma_{\rm R} = \sigma\, W_{\rm R}^{\rm t}\, W_{\rm R}$ and $\gamma_{\rm T} = \frac{1}{2}\, W_{\rm T}^{\rm t}\, W_{\rm T}$. Any purification path corresponding to a geodesic can be written as in (2.53) with $\sigma_s = \frac{1}{2}\,(2\sigma)^{1-s}$ and W_s defined in (2.54). In particular, for the $W_{\rm R}$ path we have $W_s = W_{\rm R}$ and its length is given by $d_0(\gamma_{\rm R}, W_{\rm R}) = \sqrt{2}\,|\log(2\sigma)\,|$.

The thermal states are interesting examples of mixed states to explore. The Williamson's decomposition of the covariance matrix of a thermal state is given by (2.76). By specialising (4.5) to this case, we obtain the W path that purifies a thermal state. It reads

$$G_s(\gamma_{\rm th}\,,\gamma_0) = \frac{1}{2^s}\; W_{\rm th}^{\rm t}\, \mathcal{D}_{\rm th}^{1-s}\, W_{\rm th} \tag{4.7}$$

where it is worth reminding that the symplectic matrix $W_{\rm th}$, given in (2.77), does not depend on the temperature of the thermal state, but only on the parameters occurring in the hamiltonian.

It is natural to ask whether the $W_{\rm th}$ path (4.7) is made by thermal states. This is the case if, for any given $s \in [0,1]$, the symplectic spectrum of (4.7) is thermal at some inverse temperature β_s determined by the inverse temperature β of the thermal state that plays the role of the reference state in this purification path. Using (2.77), this requirement leads to the following condition

$$\big[\coth(\beta\Omega_k/2)\,\big]^{1-s} = \coth(\beta_s\Omega_k/2) \tag{4.8}$$

which corresponds to (2.82) when $\beta_{\rm T} \to \infty$, as expected. This condition depends on the dispersion relation of the model. A straightforward numerical inspection for the periodic chains (see section 9.1) shows that (4.8) cannot be solved by $\beta_s = \beta_s(\beta)$ for any $1 \leqslant k \leqslant N$; hence we conclude that the purification path (4.7) is not entirely made by thermal states.

The W paths provide a natural alternative way to connect two generic mixed states $\gamma_{\rm R}$ and $\gamma_{\rm T}$ by using a path that passes through the set of pure states. In particular, by exploiting the Williamson's decompositions given in (2.41), one first considers the $W_{\rm R}$ path

JHEP12(2020)101

that connects $\gamma_{\rm R}$ to the pure state $\tilde{\gamma}_{\rm R,0}$ and the $W_{\rm T}$ path that connects $\gamma_{\rm T}$ to the pure state $\tilde{\gamma}_{\rm T,0}$. From (4.5), these W paths are given respectively by

$$G_s(\gamma_{\rm R}\,,\tilde{\gamma}_{\rm R,0}) = \frac{1}{2^s}\, W_{\rm R}^{\rm t}\, \mathcal{D}_{\rm R}^{1-s}\, W_{\rm R} \qquad\qquad G_s(\gamma_{\rm T}\,,\tilde{\gamma}_{\rm T,0}) = \frac{1}{2^s}\, W_{\rm T}^{\rm t}\, \mathcal{D}_{\rm T}^{1-s}\, W_{\rm T} \tag{4.9}$$

where

$$\tilde{\gamma}_{\rm R,0} \equiv \frac{1}{2}\, W_{\rm R}^{\rm t}\, W_{\rm R} \qquad\qquad \tilde{\gamma}_{\rm T,0} \equiv \frac{1}{2}\, W_{\rm T}^{\rm t}\, W_{\rm T}\,. \tag{4.10}$$

Then, within the set of the pure states, we consider the geodesic connecting $\tilde{\gamma}_{\rm R,0}$ to $\tilde{\gamma}_{\rm T,0}$. Our preferred path to connect $\gamma_{\rm R}$ and $\gamma_{\rm T}$ passing through the set of pure states is obtained by combining these three paths as follows

$$\gamma_{\rm R} \longrightarrow \tilde{\gamma}_{\rm R,0} \longrightarrow \tilde{\gamma}_{\rm T,0} \longrightarrow \gamma_{\rm T} \tag{4.11}$$

The length $d_{\rm pur}(\gamma_{\rm R}\,,\gamma_{\rm T})$ of this path can be found by summing the lengths of its three components. From (3.23) and (4.6), we get

$$d_{\rm pur}(\gamma_{\rm R}\,,\gamma_{\rm T}) \equiv d_0(\gamma_{\rm R}, W_{\rm R}) + d_{\rm basis}(\tilde{\gamma}_{\rm R,0}\,,\tilde{\gamma}_{\rm T,0}) + d_0(\gamma_{\rm T}, W_{\rm T}) \tag{4.12}$$

which can be written more explicitly as follows

$$d_{\rm pur}(\gamma_{\rm R}\,,\gamma_{\rm T}) \;=\; \sqrt{{\rm Tr}\Big\{\big[\log(2\,\mathcal{D}_{\rm R})\big]^2\Big\}} + \sqrt{{\rm Tr}\Big\{\big[\log(2\,\mathcal{D}_{\rm T})\big]^2\Big\}} + \sqrt{{\rm Tr}\Big\{\big[\log(W_{\rm TR}\,W_{\rm TR}^{\rm t})\big]^2\Big\}}\,. \tag{4.13}$$

This expression provides an upper bound $d(\gamma_{\rm R}\,,\gamma_{\rm T}) \leqslant d_{\rm pur}(\gamma_{\rm R}\,,\gamma_{\rm T})$ on (2.31).

5 Bounding complexity

Explicit formulas to evaluate the circuit complexity for mixed states are difficult to obtain; hence it is worth finding calculable expressions which provide either higher or lower bounds to this quantity. In this section we construct some bounds in the setup of the bosonic Gaussian states that we are exploring. In section 5.1 we focus on the states with vanishing first moments, while in section 5.2 the most general case of states with non vanishing first moments is considered.

5.1 States with vanishing first moments

The complexity (2.33), which holds for states with vanishing first moments, is proportional to the length of the optimal circuit (2.28) connecting $\gamma_{\rm R}$ to $\gamma_{\rm T}$; hence it is straightforward to observe that the length of any other path connecting these two covariance matrices provides an upper bound on the complexity. The analysis reported in section 3 and in section 4 naturally leads to consider some particular paths.

The simplest choice is a path made by two geodesics that connect $\gamma_{\rm R}$ and $\gamma_{\rm T}$ to an auxiliary covariance matrix $\gamma_{\rm aux}$ that does not belong to the optimal circuit (2.28) (i.e. that does not lie on the black solid curve in figure 2). Natural candidates for $\gamma_{\rm aux}$ are the covariance matrices whose Williamson's decompositions contain either $\mathcal{D}_{\rm R}$ or $\mathcal{D}_{\rm T}$ or $W_{\rm R}$ or $W_{\rm T}$. For instance, we can choose for $\gamma_{\rm aux}$ a covariance matrix whose symplectic spectrum

JHEP12(2020)101

is $\mathcal{D}_{\rm R}$ or a covariance matrix whose symplectic spectrum is $\mathcal{D}_{\rm T}$ (that lie respectively on the red solid curve and on the blue solid curve in figure 2). Different choices for $\gamma_{\rm aux}$ lead to different bounds; hence it is worth asking whether a particular choice provides the best bound. The answer depends on the set where $\gamma_{\rm aux}$ is allowed to vary.

Let us consider some natural paths where only a single auxiliary covariance matrix $\gamma_{\rm aux}$ is involved. In section 3.2 we have shown that the W paths satisfy the first law of complexity with $\delta d = 0$. Thus, natural candidates to consider for $\gamma_{\rm aux}$ are

$$\tilde{\gamma}_{\rm R} \equiv W_{\rm T}^{\rm t}\, \mathcal{D}_{\rm R} W_{\rm T} \qquad\qquad \tilde{\gamma}_{\rm T} \equiv W_{\rm R}^{\rm t}\, \mathcal{D}_{\rm T} W_{\rm R} \tag{5.1}$$

that have been represented by black squares in figure 2 and figure 3.

By first applying the triangle inequality for the paths $\gamma_{\rm R} \to \tilde{\gamma}_{\rm R} \to \gamma_{\rm T}$ and $\gamma_{\rm R} \to \tilde{\gamma}_{\rm T} \to \gamma_{\rm T}$, and then picking the one that provides the best constraint between the $\mathcal{D}$ paths, we obtain

$$d(\gamma_{\rm R}\,,\gamma_{\rm T}) \,\leqslant\, d_{\rm spectrum}(\gamma_{\rm R}\,,\gamma_{\rm T}) + \min\big[d_{\rm basis}(\gamma_{\rm R}\,,\tilde{\gamma}_{\rm R})\,,\, d_{\rm basis}(\tilde{\gamma}_{\rm T}\,,\gamma_{\rm T})\big]\,. \tag{5.2}$$

Denoting by $\tilde{d}(\gamma_{\rm R}\,,\gamma_{\rm T})$ the r.h.s. of this inequality, by using (3.19) and (3.23) we find that

$$\begin{aligned}\tilde{d}(\gamma_{\rm R}\,,\gamma_{\rm T}) \,=\, & \sqrt{\mathrm{Tr}\Big\{\big[\log(\mathcal{D}_{\rm T}\,\mathcal{D}_{\rm R}^{-1})\big]^2\Big\}} \\ & + \min\left[\sqrt{\mathrm{Tr}\Big\{\big[\log(\mathcal{D}_{\rm R}\,W_{\rm TR}\,\mathcal{D}_{\rm R}^{-1}\,W_{\rm TR}^{\rm t})\big]^2\Big\}}\,,\, \sqrt{\mathrm{Tr}\Big\{\big[\log(\mathcal{D}_{\rm T}\,W_{\rm TR}\,\mathcal{D}_{\rm T}^{-1}\,W_{\rm TR}^{\rm t})\big]^2\Big\}}\right].\end{aligned} \tag{5.3}$$

The path $\gamma_{\rm R} \to \tilde{\gamma}_{\rm T} \to \gamma_{\rm T}$ corresponds to an explicit realisation of the proposal made in figure 6 of [29] within the approach that we are considering, that does not require the addition of ancillary degrees of freedom.

Better bounds could be obtained by constructing paths that involve more auxiliary covariance matrices $\gamma_{\rm aux}$. For instance, one can consider paths $\gamma_{\rm R} \to \gamma_{\rm aux,1} \to \gamma_{\rm aux,2} \to \gamma_{\rm T}$ that involve two auxiliary covariance matrices $\gamma_{\rm aux,1}$ and $\gamma_{\rm aux,2}$. Referring to figure 2, natural paths to consider within this class are the ones where $\gamma_{\rm aux,1}$ belongs to the $W_{\rm R}$ path and $\gamma_{\rm aux,2}$ to the $W_{\rm T}$ path, or the ones where $\gamma_{\rm aux,1}$ belongs to the red curve (i.e. its symplectic spectrum is $\mathcal{D}_{\rm R}$) and $\gamma_{\rm aux,2}$ belongs to the blue curve (i.e. its symplectic spectrum is $\mathcal{D}_{\rm T}$).

Another interesting path to consider is the one constructed in (4.11): it involves the two auxiliary matrices $\gamma_{\rm aux,1} = \tilde{\gamma}_{\rm R,0}$ and $\gamma_{\rm aux,2} = \tilde{\gamma}_{\rm T,0}$ and its length is (4.12) (see figure 3). It is straightforward to observe that $d(\gamma_{\rm R}\,,\gamma_{\rm T}) \leqslant d_{\rm pur}(\gamma_{\rm R}\,,\gamma_{\rm T})$, but it is non trivial to find the best bound between $\tilde{d}(\gamma_{\rm R}\,,\gamma_{\rm T})$ and $d_{\rm pur}(\gamma_{\rm R}\,,\gamma_{\rm T})$. Since we cannot provide a general solution to this problem, in the following we focus on simple special cases where we can show that $d(\gamma_{\rm R}\,,\gamma_{\rm T}) \leqslant \tilde{d}(\gamma_{\rm R}\,,\gamma_{\rm T}) \leqslant d_{\rm pur}(\gamma_{\rm R}\,,\gamma_{\rm T})$.

When $\gamma_{\rm T}$ is pure, from (5.3) it is straightforward to observe that $\tilde{d}(\gamma_{\rm R}\,,\gamma_{\rm T}) \leqslant d_{\rm pur}(\gamma_{\rm R}\,,\gamma_{\rm T})$. Another class of special cases that we find interesting to consider is given by the pairs $(\gamma_{\rm R},\gamma_{\rm T})$ such that all the matrices along the $\mathcal{D}_{\rm R}$ path connecting $\gamma_{\rm R}$ to $\tilde{\gamma}_{\rm R}$ have the same symplectic spectrum $\mathcal{D}_{\rm R}$ and, similarly, all the matrices along the $\mathcal{D}_{\rm T}$ path connecting $\gamma_{\rm T}$ to $\tilde{\gamma}_{\rm T}$ have the same symplectic spectrum $\mathcal{D}_{\rm T}$. This means that (3.26) holds

JHEP12(2020)101

for both $\mathcal{D} = \mathcal{D}_{\rm R}$ and $\mathcal{D} = \mathcal{D}_{\rm T}$; hence (5.3) simplifies to

$$\tilde{d}(\gamma_{\rm R}\,,\gamma_{\rm T}) = \sqrt{{\rm Tr}\Big\{\big[\log(\mathcal{D}_{\rm T}\,\mathcal{D}_{\rm R}^{-1})\big]^2\Big\}} + \sqrt{{\rm Tr}\,\Big\{\big[\log(W_{\rm TR}\,W_{\rm TR}^{\rm t})\big]^2\Big\}}\,. \tag{5.4}$$

The first square root in the r.h.s. can be bounded as follows

$$\begin{aligned}\sqrt{{\rm Tr}\Big\{\big[\log(\mathcal{D}_{\rm T}\,\mathcal{D}_{\rm R}^{-1})\big]^2\Big\}} &= \sqrt{{\rm Tr}\Big\{\big[\log(2\mathcal{D}_{\rm T}) - \log(2\mathcal{D}_{\rm R})\big]^2\Big\}} \\ &\leqslant \sqrt{{\rm Tr}\Big\{\big[\log(2\,\mathcal{D}_{\rm R})\big]^2\Big\}} + \sqrt{{\rm Tr}\Big\{\big[\log(2\,\mathcal{D}_{\rm T})\big]^2\Big\}}\end{aligned} \tag{5.5}$$

where we have employed first that all the elements of $2\mathcal{D}$ are larger than or equal to 1 (in order to discard a positive term under the square root) and then the inequality $\sqrt{a+b} \leqslant \sqrt{a} + \sqrt{b}$, that holds for any a and b. By employing (5.5) in (5.4) and comparing the result against (4.13), we can conclude that $\tilde{d}(\gamma_{\rm R}\,,\gamma_{\rm T}) \leqslant d_{\rm pur}(\gamma_{\rm R}\,,\gamma_{\rm T})$.

5.2 States with non vanishing first moments

In the most general case where the first moments are non vanishing $\langle \hat{\boldsymbol{r}} \rangle \equiv \boldsymbol{a} \neq \boldsymbol{0}$, a closed expression for the Fisher-Rao distance is not known, as also remarked in the appendix B, where the notation $\boldsymbol{\mu} = \boldsymbol{a}$ and $\Sigma = \gamma$ has been adopted. Nonetheless, lower and upper bounds on the complexity can be written by employing some known results about the Gaussian PDF's [85, 89, 91, 105, 106].

Given a reference state and a target state, that can be parameterised by $\boldsymbol{\theta}_{\rm R} = (\boldsymbol{a}_{\rm R}, \gamma_{\rm R})$ and $\boldsymbol{\theta}_{\rm T} = (\boldsymbol{a}_{\rm T}, \gamma_{\rm T})$ respectively, let us introduce the following $(2N+1) \times (2N+1)$ matrix

$$\Gamma_{\rm S} = \begin{pmatrix} \gamma_{\rm S} + \boldsymbol{a}_{\rm S}\,\boldsymbol{a}_{\rm S}^{\rm t} & \boldsymbol{a}_{\rm S} \\ \boldsymbol{a}_{\rm S}^{\rm t} & 1 \end{pmatrix} \qquad {\rm S} \in \{{\rm R}, {\rm T}\}\,. \tag{5.6}$$

A lower bound for the Fisher-Rao distance, first obtained in [105], is given by

$$d_{\rm lower}(\boldsymbol{\theta}_{\rm R}, \boldsymbol{\theta}_{\rm T}) \equiv \sqrt{{\rm Tr}\,[(\log \Delta_{\Gamma,{\rm TR}})^2]} = \big\| \log\Big(\Gamma_{\rm R}^{-1/2}\,\Gamma_{\rm T}\,\Gamma_{\rm R}^{-1/2}\Big)\big\|_2 = \left[\sum_{i=1}^{2N+1} \big(\log(\tilde{\lambda}_i)\big)^2\right]^{1/2} \tag{5.7}$$

where $\Delta_{\Gamma,{\rm TR}} \equiv \Gamma_{\rm T}\,\Gamma_{\rm R}^{-1}$ and $\tilde{\lambda}_i$ are the eigenvalues of $\Gamma_{\rm R}^{-1/2}\,\Gamma_{\rm T}\,\Gamma_{\rm R}^{-1/2}$.

Upper bounds for the Fisher-Rao distance have been also found for non vanishing first moments [85, 89, 91, 106]. An upper bound can be written through $d_{\rm FR}^{(1)}$ defined in (B.4) as follows [106]

$$d_{\rm upper,1}(\boldsymbol{\theta}_{\rm R}, \boldsymbol{\theta}_{\rm T}) \equiv \left[\sum_{i=1}^{2N} d_{\rm FR}^{(1)}((0,1),(\tilde{a}_i,\lambda_i))^2\right]^{1/2} \tag{5.8}$$

where λ_i is the i-th eigenvalue of $\gamma_{\rm R}^{-1/2}\gamma_{\rm T}\,\gamma_{\rm R}^{-1/2}$, $\tilde{a}_i$ is the i-th component of $\tilde{\boldsymbol{a}}_{\rm T,R} \equiv \widetilde{O}^{\rm t}\,\boldsymbol{a}_{\rm T,R}$, being $\boldsymbol{a}_{\rm T,R} \equiv \gamma_{\rm R}^{-1/2}(\boldsymbol{a}_{\rm T} - \boldsymbol{a}_{\rm R})$, and $\widetilde{O}$ is the orthogonal matrix whose columns are the eigenvectors of $\gamma_{\rm R}^{-1/2}\gamma_{\rm T}\,\gamma_{\rm R}^{-1/2}$.

JHEP12(2020)101

Another upper bound has been found in [91]. It has been written by introducing the $2N \times 2N$ orthogonal matrix O such that $O\,\boldsymbol{a}_{\mathrm{T,R}} = (|\boldsymbol{a}_{\mathrm{T,R}}|, 0, \dots, 0)$ and the following $2N \times 2N$ matrices

$$D_{\mathrm{T,R}} \equiv \mathrm{diag}(\sqrt{(|\boldsymbol{a}_{\mathrm{T,R}}|+2)/2}\,, 1, \dots, 1) \qquad \gamma_{\mathrm{T,R}} \equiv O^{-1} D_{\mathrm{T,R}}\, O^{-\mathrm{t}}\,. \tag{5.9}$$

These matrices are employed to identify the states corresponding to the following vectors

$$\boldsymbol{\theta}_0 \equiv (0, \mathbf{1}) \qquad \boldsymbol{\theta}_O \equiv (O\,\boldsymbol{a}_{\mathrm{T,R}}\,, D_{\mathrm{T,R}}) \qquad \boldsymbol{\theta}_* \equiv (\boldsymbol{a}_{\mathrm{T,R}}\,, \gamma_{\mathrm{R}}^{-1/2} \gamma_{\mathrm{T}}\, \gamma_{\mathrm{R}}^{-1/2}) \qquad \boldsymbol{\theta}_\gamma \equiv (\boldsymbol{a}_{\mathrm{T,R}}\,, \gamma_{\mathrm{T,R}})\,. \tag{5.10}$$

The upper bound reads

$$d_{\mathrm{upper},2}(\boldsymbol{\theta}_{\mathrm{R}}, \boldsymbol{\theta}_{\mathrm{T}}) \equiv d_{\mathrm{diag}}(\boldsymbol{\theta}_0, \boldsymbol{\theta}_O) + d_{\boldsymbol{a}_{\mathrm{T,R}}}(\boldsymbol{\theta}_*, \boldsymbol{\theta}_\gamma) \tag{5.11}$$

where $d_{\boldsymbol{a}_{\mathrm{T,R}}}$ is defined in (B.6) and d_{diag} in (B.9). Since an inequality between the two upper bounds in (5.8) and (5.11) cannot be found for any value of $\boldsymbol{\theta}_{\mathrm{R}}$ and $\boldsymbol{\theta}_{\mathrm{T}}$ [89], we pick the minimum between them.

Combining the above results, one obtains

$$d_{\mathrm{lower}}(\boldsymbol{\theta}_{\mathrm{R}}, \boldsymbol{\theta}_{\mathrm{T}}) \leqslant d(\boldsymbol{\theta}_{\mathrm{R}}, \boldsymbol{\theta}_{\mathrm{T}}) \leqslant \min\big[d_{\mathrm{upper},1}(\boldsymbol{\theta}_{\mathrm{R}}, \boldsymbol{\theta}_{\mathrm{T}}), d_{\mathrm{upper},2}(\boldsymbol{\theta}_{\mathrm{R}}, \boldsymbol{\theta}_{\mathrm{T}})\big] \tag{5.12}$$

In order to provide a consistency check for these bounds, let us consider the case $\boldsymbol{a}_{\mathrm{R}} = \boldsymbol{a}_{\mathrm{T}} = \boldsymbol{a}$. From (5.6) we obtain

$$\Gamma_{\mathrm{T}}\, \Gamma_{\mathrm{R}}^{-1} = \begin{pmatrix} \gamma_{\mathrm{T}}\, \gamma_{\mathrm{R}}^{-1} & (\mathbf{1} - \gamma_{\mathrm{T}}\, \gamma_{\mathrm{R}}^{-1})\boldsymbol{a} \\ \mathbf{0} & 1 \end{pmatrix}. \tag{5.13}$$

By employing a formula for the determinant of a block matrix reported below (see (8.14)), one finds that the first $2N$ eigenvalues of (5.13) are the eigenvalues of $\gamma_{\mathrm{T}}\gamma_{\mathrm{R}}^{-1}$, while the last eigenvalue is equal to 1. Thus, d_{lower} in (5.7) becomes (2.31) in this case, saturating the lower bound. As for the upper bound in (5.12), we have (5.10) simplify to $\boldsymbol{\theta}_0 = \boldsymbol{\theta}_O = \boldsymbol{\theta}_\gamma = (0, \mathbf{1})$ in this case. This implies that $d_{\mathrm{upper},2}$ in (5.11) becomes (2.31); hence also the upper bound is saturated.

6 Optimal path for entanglement hamiltonians

The density matrix of a mixed state can be written as follows

$$\hat{\rho} \propto e^{-\widehat{K}} \tag{6.1}$$

where the proportionality constant determines the normalisation of $\hat{\rho}$. We denote the operator $\widehat{K}$ as *entanglement hamiltonian*, with a slight abuse of notation. Indeed, the operator $\widehat{K}$ is the entanglement hamiltonian when $\hat{\rho} = \hat{\rho}_A = \mathrm{Tr}_{\mathcal{H}_B}\hat{\rho}_0$ is the reduced density matrix obtained by tracing out the part $\mathcal{H}_B$ of a bipartite Hilbert space $\mathcal{H} = \mathcal{H}_A \otimes \mathcal{H}_B$. Instead, for instance, the thermal states are mixed states that do not correspond to a bipartition of the Hilbert space. For these states $\widehat{K} = \beta\,\widehat{H}$, where $\widehat{H}$ is the hamiltonian of the system and β the inverse temperature.

JHEP12(2020)101

The entanglement hamiltonians associated to some particular reduced density matrices have been largely studied for simple models, both in quantum field theories [50, 107–114] and on the lattice [52, 95, 115–121]. The spectrum of the entanglement hamiltonian, that is usually called entanglement spectrum [122], is rich in information. For instance, in conformal field theories the entanglement spectrum provides both the central charge [123] and the conformal spectrum of the underlying model [110, 113, 114, 120, 121, 124–126].

For the bosonic Gaussian states that we are considering, the entanglement hamiltonians are quadratic operators in terms of the position and momentum operators; hence they can be written as follows

$$\widehat{K} = \frac{1}{2}\,\hat{\boldsymbol{r}}^{\mathrm{t}} H\,\hat{\boldsymbol{r}} \qquad\qquad \hat{\boldsymbol{r}} = \begin{pmatrix} \hat{\boldsymbol{q}} \\ \hat{\boldsymbol{p}} \end{pmatrix} \tag{6.2}$$

where H is a $2N \times 2N$ symmetric and positive definite matrix that characterises the underlying mixed state. We denote H as the entanglement hamiltonian matrix. It can be written in terms of the corresponding covariance matrix γ as follows [50, 95, 115–117, 121]

$$H = 2\,\mathrm{i}\,J\,\mathrm{arccoth}(2\,\mathrm{i}\gamma\,J) \equiv h(\gamma) \tag{6.3}$$

where J is the standard symplectic matrix (2.2). The expression (6.3) holds for covariance matrices that are not associated to pure states. Thus, in particular, the purification procedure reported in section 4 cannot be described through the entanglement hamiltonian matrices H defined by (6.2).

Since the matrix H is symmetric and positive definite, we can adapt to the entanglement hamiltonian matrices many results reported in the previous discussions for the covariance matrices.

Given the matrices H_{R} and H_{T} corresponding to the reference state γ_{R} and to the target state γ_{T} respectively, we can consider the optimal path connecting H_{R} to H_{T}, namely

$$\widetilde{G}_s(H_{\mathrm{R}}\,,H_{\mathrm{T}}) \;\equiv\; H_{\mathrm{R}}^{1/2}\Big(H_{\mathrm{R}}^{-1/2}\,H_{\mathrm{T}}\,H_{\mathrm{R}}^{-1/2}\Big)^{s} H_{\mathrm{R}}^{1/2} \qquad\qquad 0 \leqslant s \leqslant 1 \tag{6.4}$$

whose boundary conditions are given by $\widetilde{G}_0(H_{\mathrm{R}}\,,H_{\mathrm{T}}) = H_{\mathrm{R}}$ and $\widetilde{G}_1(H_{\mathrm{R}}\,,H_{\mathrm{T}}) = H_{\mathrm{T}}$. The length of the geodesic (6.4) measured through the Fisher-Rao metric reads

$$d(H_{\mathrm{R}}, H_{\mathrm{T}}) \equiv \sqrt{\mathrm{Tr}\left\{\left[\log(H_{\mathrm{T}}\,H_{\mathrm{R}}^{-1})\right]^2\right\}}\,. \tag{6.5}$$

The Williamson's decomposition of the entanglement hamiltonian matrix H is given by

$$H = \widetilde{W}^{\mathrm{t}}\,\mathcal{E}\,\widetilde{W} \tag{6.6}$$

where $\mathcal{E} \equiv \mathrm{diag}(\varepsilon_1, \ldots, \varepsilon_N) \oplus \mathrm{diag}(\varepsilon_1, \ldots, \varepsilon_N)$ with $\varepsilon_k > 0$. The symplectic spectrum of H can be determined from the symplectic spectrum of γ as follows [95, 115, 116]

$$\mathcal{E} = 2\,\mathrm{arccoth}(2\,\mathcal{D}) = \log\!\left(\frac{\mathcal{D}+1/2}{\mathcal{D}-1/2}\right). \tag{6.7}$$

This formula cannot be applied for pure states, which have $\mathcal{D} = \frac{1}{2}\mathbf{1}$. The symplectic matrices W and $\widetilde{W}$, introduced in (2.20) and (6.6) respectively, are related as follows [117, 121]

$$\widetilde{W} \equiv J^{\mathrm{t}}\,W\,J = W^{-\mathrm{t}}\,. \tag{6.8}$$

JHEP12(2020)101

We find it worth expressing the distance (6.5) in terms of the matrices occurring in the Williamson's decompositions of $H_{\rm R}$ and $H_{\rm T}$, as done in section 2.4 for the covariance matrices. These decompositions read

$$H_{\rm R} = \widetilde{W}_{\rm R}^{\rm t}\, \mathcal{E}_{\rm R}\, \widetilde{W}_{\rm R} \qquad\qquad H_{\rm T} = \widetilde{W}_{\rm T}^{\rm t}\, \mathcal{E}_{\rm T}\, \widetilde{W}_{\rm T} \tag{6.9}$$

where $\widetilde{W}_{\rm R}$ and $\widetilde{W}_{\rm T}$ are related respectively to $W_{\rm R}$ and $W_{\rm T}$ through (6.8). By using (2.49) and the following relation

$$\widetilde{W}_{\rm TR} \equiv \widetilde{W}_{\rm T}\, \widetilde{W}_{\rm R}^{-1} = J^{\rm t}\, W_{\rm TR}\, J \tag{6.10}$$

we can write the distance (6.5) as

$$d(H_{\rm R}, H_{\rm T}) = \sqrt{{\rm Tr}\left\{ \left[\log\left(\mathcal{E}_{\rm T}\, W_{\rm TR}\, \mathcal{E}_{\rm R}^{-1}\, W_{\rm TR}^{\rm t} \right) \right]^2 \right\}}\,. \tag{6.11}$$

The expression (6.3) (or equivalently (6.7) and (6.8)) provides a highly non trivial relation between the set made by the covariance matrices γ that are associated to the mixed states that are not pure states and the set of the entanglement hamiltonian matrices H. The map h in (6.3) is not an isometry, hence the distances are not preserved and geodesics are not sent into geodesics. Thus, we find it worth comparing the distance $d(\gamma_{\rm R}, \gamma_{\rm T}) = d(h^{-1}(H_{\rm R}), h^{-1}(H_{\rm T}))$ from (2.49) and the distance $d(H_{\rm R}, H_{\rm T})$ in (6.11).

For the sake of simplicity, let us explore the case of one-mode mixed states, where $\mathcal{D} = \sigma\, \mathbf{1}$ and $\mathcal{E} = \varepsilon\, \mathbf{1}$ are proportional to the 2×2 identity matrix. In this simple case the expressions for $d(\gamma_{\rm R}, \gamma_{\rm T})^2$ from (2.49) and for $d(H_{\rm R}, H_{\rm T})^2$ from (6.11) take the form[13]

$${\rm Tr}\left\{ \left[a\, \mathbf{1} + \log(W_{\rm TR}\, W_{\rm TR}^{\rm t}) \right]^2 \right\} \;=\; 2\, a \left(a + {\rm Tr}\big[\log(W_{\rm TR}\, W_{\rm TR}^{\rm t}) \big] \right) + {\rm Tr}\Big\{ \big[\log(W_{\rm TR}\, W_{\rm TR}^{\rm t}) \big]^2 \Big\} \tag{6.12}$$

with $a = \log(\sigma_{\rm T}/\sigma_{\rm R}) \equiv a_\sigma$ and $a = \log(\varepsilon_{\rm T}/\varepsilon_{\rm R}) \equiv a_\varepsilon$ respectively, which can take any real value. Since $d(\gamma_{\rm R}, \gamma_{\rm T})$ is symmetric under the exchange $\gamma_{\rm R} \leftrightarrow \gamma_{\rm T}$, we can assume $\sigma_{\rm R} \geqslant \sigma_{\rm T}$ without loss of generality. Then, since the function $\frac{2{\rm arccoth}(2x)}{x}$ is a properly decreasing function when $x > 0$, we have that $\frac{2{\rm arccoth}(2\sigma_{\rm R})}{\sigma_{\rm R}} \leqslant \frac{2{\rm arccoth}(2\sigma_{\rm T})}{\sigma_{\rm T}}$, i.e. $\sigma_{\rm T}/\sigma_{\rm R} \leqslant \varepsilon_{\rm T}/\varepsilon_{\rm R}$, once (6.7) has been used; hence $a_\sigma \leqslant a_\varepsilon$. This does not provide a relation between $d(\gamma_{\rm R}, \gamma_{\rm T})$ and $d(H_{\rm R}, H_{\rm T})$ because the r.h.s. of (6.12) does not have a well defined monotonicity as function of a, given that $\log(W_{\rm TR}\, W_{\rm TR}^{\rm t})$ is non vanishing in general. Thus, the one-mode case teaches us that $W_{\rm TR}$ plays a major role in finding a possible relation between $d(H_{\rm R}, H_{\rm T})$ and $d(\gamma_{\rm R}, \gamma_{\rm T})$. In order to find this relation in some simple cases, the expression (6.12) naturally leads us to consider the special cases of one-mode mixed states such that $\log(W_{\rm TR}\, W_{\rm TR}^{\rm t}) = \mathbf{0}$. In this cases (6.12) tells us that $d(\gamma_{\rm R}, \gamma_{\rm T}) = \sqrt{2}\, |a_\sigma|$ and $d(H_{\rm R}, H_{\rm T}) = \sqrt{2}\, |a_\varepsilon|$. Since $a_\sigma^2 \leqslant a_\varepsilon^2$ is equivalent to $(a_\sigma - a_\varepsilon)(a_\sigma + a_\varepsilon) \leqslant 0$, we observe that the latter inequality is satisfied because $a_\sigma \leqslant a_\varepsilon$ and[14] $a_\sigma + a_\varepsilon = \log\left(\frac{\sigma_{\rm T} {\rm arccoth}(2\sigma_{\rm T})}{\sigma_{\rm R} {\rm arccoth}(2\sigma_{\rm R})} \right) \geqslant 0$. Thus, for one-mode states such that $W_{\rm TR}\, W_{\rm TR}^{\rm t} = \mathbf{1}$ we have that $d(\gamma_{\rm R}, \gamma_{\rm T}) \leqslant d(H_{\rm R}, H_{\rm T})$.

[13] The l.h.s. of (6.12) comes from Baker-Campbell-Hausdorff formula [127].

[14] This inequality comes from the fact that the function $x\, {\rm arccoth}(2x)$ is properly decreasing for $x > 0$ and that $\sigma_{\rm R} \geqslant \sigma_{\rm T}$ has been assumed.

JHEP12(2020)101

When $N \geqslant 1$ and $W_{\mathrm{T}} = W_{\mathrm{R}}$, i.e. $W_{\mathrm{TR}} = \mathbf{1}$ (this includes the thermal states originating from the same physical hamiltonian), the distance (6.11) simplifies to

$$d(H_{\mathrm{R}}, H_{\mathrm{T}}) = \sqrt{\mathrm{Tr}\left\{\left[\log\left(\mathcal{E}_{\mathrm{T}}\,\mathcal{E}_{\mathrm{R}}^{-1}\right)\right]^2\right\}} = \sqrt{2\sum_{k=1}^{N}\left[\log\left(\frac{\varepsilon_{\mathrm{T},k}}{\varepsilon_{\mathrm{R},k}}\right)\right]^2} \tag{6.13}$$

while $d(\gamma_{\mathrm{R}}, \gamma_{\mathrm{T}})$ is given by (3.19). By applying the above analysis made for the one-mode case to the k-th mode, we can conclude that $[\log(\sigma_{\mathrm{T},k}/\sigma_{\mathrm{R},k})]^2 \leqslant [\log(\varepsilon_{\mathrm{T},k}/\varepsilon_{\mathrm{R},k})]^2$ for any given k; hence $d(\gamma_{\mathrm{R}}, \gamma_{\mathrm{T}})^2 \leqslant d(H_{\mathrm{R}}, H_{\mathrm{T}})^2$ is obtained after summing over the modes.

By using the decompositions (6.9), one can draw a pictorial representation similar to figure 1 and figure 2 also for the entanglement hamiltonian matrices H, just by replacing each γ with the corresponding H, each W with the corresponding $\widetilde{W}$ and where the solid coloured lines are labelled by the corresponding symplectic spectra $\mathcal{E}$.

We find it worth discussing further the set of thermal states through the approach based on the entanglement hamiltonian matrices because the simplicity of these matrices in this case allows to write analytic results. For a thermal state $H = \beta H^{\mathrm{phys}}$, where H^{phys} is the matrix characterising the physical hamiltonian (2.1) and β is the inverse temperature. This implies that the symplectic eigenvalues of H are $\varepsilon_{\mathrm{th},k} = \beta\,\sigma_{\mathrm{phys},k}$, where $\sigma_{\mathrm{phys},k}$ are the symplectic eigenvalues of H^{phys}.

We denote by β_{R} and β_{T} the inverse temperatures of the reference state and of the target state respectively. An interesting special case is given by thermal states of the same system, which have the same H^{phys}. In this case $H_{\mathrm{T}} H_{\mathrm{R}}^{-1} = (\beta_{\mathrm{T}}/\beta_{\mathrm{R}})\,\mathbf{1}$; hence (6.5) simplifies to

$$d(H_{\mathrm{R}}, H_{\mathrm{T}}) = \left|\log(\beta_{\mathrm{T}}/\beta_{\mathrm{R}})\right| \sqrt{2V} = \sqrt{\mathrm{Tr}\left\{\left[\log\left(\mathcal{E}_{\mathrm{T}}\,\mathcal{E}_{\mathrm{R}}^{-1}\right)\right]^2\right\}} \tag{6.14}$$

where V is the number of sites in the harmonic lattice and the last expression has been obtained by specialising (6.11) to this case, where $\widetilde{W}_{\mathrm{TR}} = \mathbf{1}$. Furthermore, from (6.4) it is straightforward to observe that in this case the entire optimal circuit is made by thermal states having the same H^{phys}. The optimal circuit (6.4) significantly simplifies to

$$\widetilde{G}_s(H_{\mathrm{R}}\,, H_{\mathrm{T}}) = \beta_s\, H^{\mathrm{phys}} \qquad \beta_s \equiv \beta_{\mathrm{R}}\left(\frac{\beta_{\mathrm{T}}}{\beta_{\mathrm{R}}}\right)^s \qquad 0 \leqslant s \leqslant 1\,. \tag{6.15}$$

By employing (2.68), one finds that the Williamson's decomposition of this optimal circuit reads

$$\widetilde{G}_s(H_{\mathrm{R}}\,, H_{\mathrm{T}}) \;=\; W_{\mathrm{phys}}^{\mathrm{t}}\,\mathcal{D}_s\,W_{\mathrm{phys}} \qquad \mathcal{D}_s = \beta_s\,\mathcal{D}_{\mathrm{phys}} \qquad 0 \leqslant s \leqslant 1 \tag{6.16}$$

where W_{phys} is independent of s. Thus, (6.15) tells us that β_s is the inverse temperature of the thermal state labelled by s along this optimal circuit.

In section 9.3.3 the above results are applied to the thermal states of the harmonic chain with periodic boundary conditions.

7 Gaussian channels

Quantum operations are described by completely positive operators acting on a quantum state, which can be either pure or mixed, and they are classified in *quantum channels* and

JHEP12(2020)101

quantum measurements [59, 128]. The quantum channels are trace preserving quantum operations, while quantum measurements are not trace preserving [129].

The output $\Theta(\hat{\rho})$ of a quantum channel applied to the density matrix $\hat{\rho}$ of a system is obtained by first extending the system through an ancillary system (the environment) in a pure state $|\Phi_E\rangle$, then by allowing an interaction characterised by a unitary transformation U and finally by tracing out the degrees of freedom of the environment [46, 92, 130], namely

$$\Theta(\hat{\rho}) = \mathrm{Tr}_E\big[\, U^\dagger (\hat{\rho} \otimes |\Phi_E\rangle\langle\Phi_E|)\, U \,\big] \,. \tag{7.1}$$

While within the set of the pure states the unitary transformations are the only operations that allow to pass from a state to another, within the general set of mixed states also non unitary operations must be taken into account.

In this manuscript we consider circuits in the space made by quantum Gaussian states; hence only quantum operations between Gaussian states (also called Gaussian operations) can be considered [129]. The quantum channels and the quantum measurements restricted to the set of the Gaussian states are often called Gaussian channels [46, 103] and Gaussian measurements [47] respectively.

In the following we focus only on the Gaussian channels. A Gaussian state with vanishing first moments is completely described by its covariance matrix; hence the action of a Gaussian channel on a Gaussian state can be defined through its effect on the covariance matrix of the Gaussian state. This effect can be studied by introducing two real matrices T and N as [103]

$$\gamma \,\to\, T\,\gamma\,T^{\mathrm{t}} + N \qquad\qquad N = N^{\mathrm{t}} \qquad\qquad N + \mathrm{i}\,\frac{J}{2} - \mathrm{i}\,T\,\frac{J}{2}\,T^{\mathrm{t}} \geqslant 0 \tag{7.2}$$

where T is unconstrained and the last inequality corresponds to the complete positivity condition. The Gaussian unitary transformations are the Gaussian channels with $N = 0$ and symplectic T. In this case the inequality in (7.2) is saturated. Further interesting results for Gaussian operations have been reported e.g. in [47, 131].

We find it worth asking whether a matrix along the optimal circuit (2.28) can be obtained by acting with a Gaussian channel on the reference state. This means finding T_s and N_s that fulfil (7.2) for any $0 \leqslant s \leqslant 1$ and such that

$$G_s(\gamma_{\mathrm{R}}\,,\gamma_{\mathrm{T}}) \;=\; U_s\,\gamma_{\mathrm{R}}\,U_s^{\mathrm{t}} \;=\; T_s\,\gamma_{\mathrm{R}}\,T_s^{\mathrm{t}} + N_s \qquad\qquad 0 \leqslant s \leqslant 1 \tag{7.3}$$

where U_s is defined in (2.39). Unfortunately, we are not able to determine T_s and N_s as functions of U_s in full generality. In the following we provide some simple particular solutions.

A simple possibility reads

$$T_s = 0 \qquad\qquad N_s = G_s \tag{7.4}$$

which satisfies the inequality in (7.2), since G_s is a symmetric Gaussian matrix (see section 2.4).

Another, less trivial, solution is given by

$$T_s = U_s \qquad\qquad N_s = \mathbf{0} \tag{7.5}$$

JHEP12(2020)101

where the complete positivity condition in (7.2) becomes $\mathrm{i}\,\frac{J}{2} - \mathrm{i}\,T_s\,\frac{J}{2}\,T_s^{\mathrm{t}} \geqslant 0$. We have considered numerically some cases, finding that U_s satisfies the complete positivity condition only when it is symplectic (in this case the complete positivity inequality is saturated).

An explicit example belonging to the class identified by (7.5) can be constructed by considering a particular $\mathcal{D}$ path where $W_{\mathrm{T}} = \mathcal{X}_{\mathrm{TR}} W_{\mathrm{R}}$ (see section 3.4). In this case (3.25) holds, hence (7.5) is realised with[15]

$$T_s = U_s = W_{\mathrm{R}}^{\mathrm{t}}\, \mathcal{X}_{\mathrm{TR}}^{s}\, W_{\mathrm{R}}^{-\mathrm{t}}\,. \tag{7.6}$$

A more general solution where both T_s and N_s can be non vanishing is obtained by imposing the following relation

$$T_s \;=\; \Big[(G_s - N_s)\,\gamma_{\mathrm{R}}^{-1}\Big]^{1/2} \tag{7.7}$$

which solves (7.3) for any symmetric N_s. The solution (7.4) is recovered from (7.7) with $T_s = 0$. When $N_s = 0$, the relation (7.7) gives $T_s = \big(G_s\gamma_{\mathrm{R}}^{-1}\big)^{1/2} = U_s$, where the last equality is obtained from (2.30) and (2.39). Plugging (7.7) into the complete positivity condition in (7.2), we obtain

$$N_s + \mathrm{i}\,\frac{J}{2} - \mathrm{i}\,\big[(G_s - N_s)\,\gamma_{\mathrm{R}}^{-1}\big]^{1/2}\,\frac{J}{2}\,\big[\gamma_{\mathrm{R}}^{-1}\,(G_s - N_s)\big]^{1/2} \;\geqslant\; 0 \tag{7.8}$$

Thus, for any N_s fulfilling this inequality, by using (7.7) we can implement our optimal circuit (2.28) through Gaussian channels.

An interesting class of N_s that saturates (7.8) has been constructed in [132]. It is given by

$$N_s = \sqrt{K_s^{\mathrm{t}}\,K_s} \qquad\qquad K_s = T_s^{\mathrm{t}}\,\frac{J}{2}\,T_s - \frac{J}{2}\,. \tag{7.9}$$

By plugging (7.9) into (7.7) first and then employing (2.30), we find the following equation for T_s

$$T_s^2 = \Delta_{\mathrm{TR}}^{s} - \sqrt{K_s^{\mathrm{t}} K_s}\;\gamma_{\mathrm{R}}^{-1} \tag{7.10}$$

whose solutions provide realisations of the optimal circuit (2.28) through Gaussian channels.

Plugging the definition of K_s given in (7.9) into (7.10) we find

$$T_s^2 + \mathrm{i}\,T_s^{\mathrm{t}}\,\frac{J}{2}\,T_s\gamma_{\mathrm{R}}^{-1} = \Delta_{\mathrm{TR}}^{s} + \mathrm{i}\,\frac{J}{2}\,\gamma_{\mathrm{R}}^{-1}\,. \tag{7.11}$$

The real part of this relation tells us that $T_s = \Delta_{\mathrm{TR}}^{s/2} = U_s$, while from the imaginary part we find that $T_s^{\mathrm{t}}\,J\,T_s = J$, i.e. that T_s is symplectic. The latter result and (7.9) lead to $K_s = N_s = 0$.

Let us conclude by emphasising that all the explicit expressions for the Gaussian channels given above saturate the complete positivity condition in (7.2) (more details can be found in [132]). It would be interesting to explore also Gaussian channels where this inequality is not saturated, as done e.g. in (7.7) and (7.8).

[15] The last expression in (7.6) is obtained by observing that $W_{\mathrm{T}} = \mathcal{X}_{\mathrm{TR}} W_{\mathrm{R}}$ and $\mathcal{D}_{\mathrm{T}} = \mathcal{D}_{\mathrm{R}}$ into (2.39) give $U_s = (W_{\mathrm{R}}^{\mathrm{t}}\,\mathcal{X}_{\mathrm{TR}}^2 W_{\mathrm{R}}^{-\mathrm{t}})^{s/2}$, that becomes (7.6) once (D.1) is employed with $M = W_{\mathrm{R}}^{\mathrm{t}}\,\mathcal{X}_{\mathrm{TR}}^2$ and $N = W_{\mathrm{R}}^{-\mathrm{t}}$.

JHEP12(2020)101

8 Complexity of mixed states through ancillae

In this section we discuss the approach to the complexity of mixed states explored in [23], which is based on the introduction of ancillary degrees of freedom.

Consider a quantum system in a mixed state characterised by the density matrix $\hat{\rho}$. A pure state can be always constructed from $\hat{\rho}$ by adding ancillary degrees of freedom. This purification procedure consists in first extending the Hilbert space of the system to a larger Hilbert space $\mathcal{H}_{\text{extended}} \equiv \mathcal{H} \otimes \mathcal{H}_{\text{anc}}$ through an auxiliary Hilbert space $\mathcal{H}_{\text{anc}}$, and then finding a pure state $|\Omega\rangle \in \mathcal{H}_{\text{extended}}$ such that the original mixed state is obtained as the reduced density matrix given by

$$\hat{\rho} \,=\, \text{Tr}_{\mathcal{H}_{\text{anc}}} |\Omega\rangle\langle\Omega| \tag{8.1}$$

where the ancillary degrees of freedom have been traced out. We remark that the purifications discussed in section 4 do not involve ancillary degrees of freedom.

There are infinitely many ways to construct $\mathcal{H}_{\text{extended}}$ and $|\Omega\rangle$ such that (8.1) is satisfied; hence a purification criterion must be introduced. Different purtification criteria have been considered in the literature to study different quantities. An important example is the entanglement of purification [133–136]. In this manuscript we are interested in the purification complexity [29], that has been employed in [23] to study the complexity of mixed states.

8.1 Covariance matrix of the extended system

We are interested in a generic harmonic lattice made by N sites in the Gaussian mixed state characterised by the covariance matrix γ and by vanishing first moments. The covariance matrix γ can be decomposed in blocks as follows

$$\gamma \equiv \begin{pmatrix} Q & M \\ M^{\text{t}} & P \end{pmatrix} \tag{8.2}$$

where Q and P are $N \times N$ symmetric matrices, while M is a generic $N \times N$ real matrix; hence $N(2N+1)$ real parameters must be fixed to determine γ.

We consider a simplification of the purification process by focussing only on Gaussian purifications. This means that a mixed state characterised by the covariance matrix (8.2) is purified by introducing ancillary degrees of freedom and constrcuing a $2N_{\text{ext}} \times 2N_{\text{ext}}$ covariance matrix γ_{ext} that corresponds to a Gaussian pure state $|\Omega\rangle$ for the extended lattice having $N_{\text{ext}} \equiv N + N_{\text{anc}}$ sites. For the sake of simplicity, we assume also that $|\Omega\rangle$ has vanishing first moments, i.e. $\langle\Omega|\hat{\boldsymbol{r}}_{\text{ext}}|\Omega\rangle = 0$, where $\hat{\boldsymbol{r}}^{\text{t}}_{\text{ext}} \equiv (\hat{\boldsymbol{q}}^{\text{t}}$, $\hat{\boldsymbol{q}}^{\text{t}}_{\text{anc}}$ and $\hat{\boldsymbol{p}}^{\text{t}}, \hat{\boldsymbol{p}}^{\text{t}}_{\text{anc}})$, where we have separated the ancillary degrees of freedom from the ones associated to the physical system.

By writing also γ_{ext} through the block decomposition (8.2) we have

$$\gamma_{\text{ext}} \equiv \begin{pmatrix} Q_{\text{ext}} & M_{\text{ext}} \\ M^{\text{t}}_{\text{ext}} & P_{\text{ext}} \end{pmatrix} \tag{8.3}$$

JHEP12(2020)101

where $Q_{\rm ext}$ and $P_{\rm ext}$ are $N_{\rm ext} \times N_{\rm ext}$ symmetric matrices. Since the covariance matrix (8.3) corresponds to a pure state, the condition (2.23) must hold. This tells us that the blocks occurring in (8.3) are related by the following constraints

$$Q_{\rm ext}\, P_{\rm ext} - M_{\rm ext}^2 = \frac{1}{4}\,\mathbf{1} \qquad M_{\rm ext}\, Q_{\rm ext} = Q_{\rm ext}\, M_{\rm ext}^{\rm t} \qquad P_{\rm ext}\, M_{\rm ext} = M_{\rm ext}^{\rm t}\, P_{\rm ext}\,. \tag{8.4}$$

The first relation tells us that $M_{\rm ext}$ is determined by the product $Q_{\rm ext}\, P_{\rm ext}$, while the remaining two relations mean that $M_{\rm ext}\, Q_{\rm ext}$ and $P_{\rm ext}\, M_{\rm ext}$ are symmetric. Thus, (8.3) is determined by the symmetric matrices $Q_{\rm ext}$ and $P_{\rm ext}$, that depend on $2\,\frac{N_{\rm ext}(N_{\rm ext}+1)}{2}$ real parameters, as expected also from section 2.3.1 (see (2.24)).

We can impose that $\gamma_{\rm ext}$ is the covariance matrix of a pure state also by using (2.22), i.e. by requiring that the Williamson's decomposition of (8.3) reads

$$\gamma_{\rm ext} = \frac{1}{2}\, W_{\rm ext}^{\rm t} W_{\rm ext} = \frac{1}{2}\, R_{\rm ext}^{\rm t}\, \mathcal{X}_{\rm ext}^2\, R_{\rm ext} \tag{8.5}$$

where $W_{\rm ext} \in {\rm Sp}(2N_{\rm ext}, \mathbb{R})$ and the last expression has been obtained from the Euler decomposition of $W_{\rm ext}$, that includes $R_{\rm ext} \in K(N_{\rm ext})$. The symplectic matrix $W_{\rm ext}$ can be partitioned through $N_{\rm ext} \times N_{\rm ext}$ matrices as follows

$$W_{\rm ext} = \begin{pmatrix} U_{\rm ext} & Y_{\rm ext} \\ Z_{\rm ext} & V_{\rm ext} \end{pmatrix} \qquad \begin{cases} U_{\rm ext} Y_{\rm ext}^{\rm t} \text{ and } V_{\rm ext} Z_{\rm ext}^{\rm t} \text{ are symmetric} \\ U_{\rm ext} V_{\rm ext}^{\rm t} - Y_{\rm ext} Z_{\rm ext}^{\rm t} = \mathbf{1}\,. \end{cases} \tag{8.6}$$

The relation (8.5) provides the blocks in (8.3) through to the ones in (8.6). The result reads

$$Q_{\rm ext} = \frac{1}{2}(U_{\rm ext}^{\rm t} U_{\rm ext} + Z_{\rm ext}^{\rm t} Z_{\rm ext}) \quad P_{\rm ext} = \frac{1}{2}(V_{\rm ext}^{\rm t} V_{\rm ext} + Y_{\rm ext}^{\rm t} Y_{\rm ext}) \quad M_{\rm ext} = \frac{1}{2}(U_{\rm ext}^{\rm t} Y_{\rm ext} + Z_{\rm ext}^{\rm t} V_{\rm ext})\,. \tag{8.7}$$

Another useful way to impose the purity condition on the final state of this purification process exploits the general form (2.24) for the wave function of a pure state and the corresponding covariance matrix (2.25). This allows us to write the covariance matrix of the extended system as[16]

$$\gamma_{\rm ext} = \frac{1}{2} \begin{pmatrix} E_{\rm ext}^{-1} & -E_{\rm ext}^{-1} F_{\rm ext} \\ -F_{\rm ext} E_{\rm ext}^{-1} & E_{\rm ext} + F_{\rm ext} E_{\rm ext}^{-1} F_{\rm ext} \end{pmatrix} \tag{8.8}$$

where the $N_{\rm ext} \times N_{\rm ext}$ symmetric matrices $E_{\rm ext}$ and $F_{\rm ext}$ are related to the blocks occurring in (8.3) as follows

$$E_{\rm ext} = \frac{1}{2}\, Q_{\rm ext}^{-1} \qquad F_{\rm ext} = -\, Q_{\rm ext}^{-1}\, M_{\rm ext}\,. \tag{8.9}$$

The second relation in (8.4) ensures that $F_{\rm ext}$ is symmetric. We remark that (8.9) also tell us that the relation $P_{\rm ext} = \frac{1}{2}(E_{\rm ext} + F_{\rm ext}\, E_{\rm ext}^{-1}\, F_{\rm ext})$ coming from the second block on the diagonal in (8.3) becomes the first relation in (8.4).

In order to relate γ in (8.2) to $\gamma_{\rm ext}$ in (8.3), one observes that, since $\hat{\boldsymbol{r}}_{\rm ext}^{\rm t} \equiv (\hat{\boldsymbol{q}}^{\rm t}, \hat{\boldsymbol{q}}_{\rm anc}^{\rm t}, \hat{\boldsymbol{p}}^{\rm t}, \hat{\boldsymbol{p}}_{\rm anc}^{\rm t})$, we have that the $N_{\rm ext} \times N_{\rm ext}$ blocks occurring in (8.3) can be partitioned in blocks as follows

$$Q_{\rm ext} \equiv \begin{pmatrix} Q & \Gamma_Q \\ \Gamma_Q^{\rm t} & Q_{\rm anc} \end{pmatrix} \qquad P_{\rm ext} \equiv \begin{pmatrix} P & \Gamma_P \\ \Gamma_P^{\rm t} & P_{\rm anc} \end{pmatrix} \qquad M_{\rm ext} \equiv \begin{pmatrix} M & \Gamma_M \\ \widetilde{\Gamma}_M^{\rm t} & M_{\rm anc} \end{pmatrix} \tag{8.10}$$

[16] The special case $F_{\rm ext} = \mathbf{0}$ has been considered e.g. in [23, 136].

JHEP12(2020)101

where Q, P and M are the $N \times N$ blocks of γ in (8.2), while $Q_{\rm anc}$ and $P_{\rm anc}$ are $N_{\rm anc} \times N_{\rm anc}$ symmetric matrices. Instead, $M_{\rm anc}$ is a generic $N_{\rm anc} \times N_{\rm anc}$ real matrix. Indeed, by plugging (8.10) into (8.3), it is straightforward to observe that the covariance matrix (8.2) is obtained by restricting $\gamma_{\rm ext}$ to the sites corresponding to the original degrees of freedom. Instead, by restricting $\gamma_{\rm ext}$ to the ancillary sites, one gets the following $2N_{\rm anc} \times 2N_{\rm anc}$ symmetric matrix

$$\gamma_{\rm anc} \equiv \begin{pmatrix} Q_{\rm anc} & M_{\rm anc} \\ M_{\rm anc}^{\rm t} & P_{\rm anc} \end{pmatrix} . \tag{8.11}$$

By changing the order of the rows and the columns, the matrix in (8.3) becomes

$$\begin{pmatrix} \gamma & \Gamma \\ \Gamma^{\rm t} & \gamma_{\rm anc} \end{pmatrix} \tag{8.12}$$

where γ is the covariance matrix (8.2), $\gamma_{\rm anc}$ is the symmetric matrix defined in (8.11) and

$$\Gamma \equiv \begin{pmatrix} \Gamma_Q & \Gamma_M \\ \widetilde{\Gamma}_M & \Gamma_P \end{pmatrix} \tag{8.13}$$

By using that (8.12) is positive definite, it can be shown that also $\gamma_{\rm anc}$ is positive definite;[17] hence $\gamma_{\rm anc}$ can be interpreted as the covariance matrix of the ancillary system made by $N_{\rm anc}$ sites.

An alternative approach exploits the expressions in the Schrödinger representation discussed in appendix A. In particular, given the covariance matrix γ in the block matrix form (8.2), we can construct the $N \times N$ complex matrices Θ and Φ by using (A.11) and (A.12). Then, (A.19) provide the constraints for the blocks of $E_{\rm ext}$ and $F_{\rm ext}$ in terms of the complex matrices Θ and Φ.

There are many ways to construct the pure state $|\Omega\rangle$. They correspond to the freedom to fix $N_{\rm anc}$ first and then to choose e.g. the blocks in (8.10) that are different from Q, P and M, provided that the constraints (8.4) are satisfied.

8.1.1 One-mode mixed states

We find it instructive to consider explicitly the simplest case of a one-mode mixed state, i.e. $N = 1$. The minimal choice for the number of ancillae is $N_{\rm anc} = 1$.

When $N = 1$, only a non trivial symplectic eigenvalue σ occurs; hence the Williamson's decomposition (2.20) and the Euler decomposition (2.21) of a symplectic matrix provide the 2×2 covariance matrix given by

$$\gamma = \sigma\, W^{\rm t}\, W = \sigma\, R^{\rm t} \eta^2 R = R^{\rm t}\, {\rm diag}(\sigma e^{2\lambda}, \sigma e^{-2\lambda}) R = \begin{pmatrix} Q & M \\ M & P \end{pmatrix} \tag{8.15}$$

[17] By employing the following formula for the determinant of a block matrix

$$\det \begin{pmatrix} A & B \\ C & D \end{pmatrix} = \det(A - B\, D^{-1} C)\, \det(D) \tag{8.14}$$

where it is assumed that D is invertible, one finds that the eigenvalues of $\gamma_{\rm anc}$ are also eigenvalues of $\gamma_{\rm ext}$. If A is invertible, a formula similar to (8.14) can be written where $\det(A)$ is factorised and this result can be used to show that the eigenvalues of γ are eigenvalues of $\gamma_{\rm ext}$ as well.

JHEP12(2020)101

where λ is the squeezing parameter and R is a 2×2 rotation matrix, which is completely fixed by the rotation angle θ. Notice that Q, P and M are real parameters in (8.15). Le us remark that the pure state condition (2.23) for (8.15) gives $1-4d_\gamma=0$, where we have introduced $d_\gamma \equiv \det(\gamma) = QP - M^2$. This implies that $1-4d_\gamma \neq 0$ for the covariance matrices (8.15) that correspond to the mixed states that are not pure.

When $N_{\rm anc}=1$, the covariance matrix (8.5) of the pure state for the extended system reads

$$\gamma_{\rm ext} = \frac{1}{2}\, W_{\rm ext}^{\rm t} W_{\rm ext} = \frac{1}{2}\, R_{\rm ext}^{\rm t}\, \eta_{\rm ext}^2\, R_{\rm ext} = \frac{1}{2}\, R_{\rm ext}^{\rm t}\, {\rm diag}(e^{2\lambda_1}, e^{2\lambda_2}, e^{-2\lambda_1}, e^{-2\lambda_2}) R_{\rm ext}\,. \tag{8.16}$$

This 4×4 covariance matrix corresponds to a pure state, hence it depends on $N_{\rm ext}(N_{\rm ext}+1) = 6$ real parameters (2^2 from $R_{\rm ext}$ and two squeezing parameters λ_i), since $N_{\rm ext}=2$. Writing the 4×4 covariance matrix $\gamma_{\rm ext}$ in the form (8.3), it is straightforward to realise that 3 elements are given by the real parameters Q, P and M. Thus, we are left with three real parameters to construct the pure state for the extended system.

We find it instructive to write explicit expressions for the elements of the covariance matrix $\gamma_{\rm ext}$. The constraints (8.4) for the 2×2 matrices $Q_{\rm ext}$, $P_{\rm ext}$ and $M_{\rm ext}$ provide six equations: four from the first relation and one from each one of the other two relations (that can be written in the form $X=0$, where X is a 2×2 antisymmetric matrix).

When $\Gamma_M \neq 0$, the solution of this system can be written in terms of Γ_Q, Γ_P and Γ_M as

$$\begin{aligned}
Q_{\rm anc} &= -\frac{1-4d_\gamma}{4\Gamma_M^2}\left(Q + \frac{8\Gamma_Q(M\,\Gamma_M - Q\,\Gamma_P)}{1-4d_\gamma} + \frac{16\Gamma_Q^2\big[P\,\Gamma_M^2 - \Gamma_P(2M\,\Gamma_M - Q\,\Gamma_P)\big]}{(1-4d_\gamma)^2}\right)\\
M_{\rm anc} &= -\frac{1}{\Gamma_M}\left(M\,\Gamma_M - Q\,\Gamma_P + \frac{4\Gamma_Q\big[P\,\Gamma_M^2 - \Gamma_P(2M\,\Gamma_M - Q\,\Gamma_P)\big]}{1-4d_\gamma}\right)\\
P_{\rm anc} &= -\frac{4\big[P\,\Gamma_M^2 - \Gamma_P(2M\,\Gamma_M - Q\,\Gamma_P)\big]}{1-4d_\gamma}\\
\widetilde{\Gamma}_M &= \frac{4\Gamma_Q\,\Gamma_P + 4d_\gamma - 1}{4\Gamma_M}\,.
\end{aligned} \tag{8.17}$$

When $\Gamma_M=0$ and $\Gamma_P\neq0$, we find

$$\begin{aligned}
Q_{\rm anc} &= \frac{P(4d_\gamma-1)}{4\Gamma_P^2} + \frac{2M\,\widetilde{\Gamma}_M}{\Gamma_P} - \frac{4Q\,\widetilde{\Gamma}_M^2}{1-4d_\gamma} \qquad & \Gamma_Q &= \frac{1-4d_\gamma}{4\Gamma_P}\\
P_{\rm anc} &= -\frac{4Q\,\Gamma_P^2}{1-4d_\gamma} & M_{\rm anc} &= M - \frac{4Q\,\Gamma_P\,\widetilde{\Gamma}_M}{1-4d_\gamma}
\end{aligned} \tag{8.18}$$

while a solution does not exist for $\Gamma_M=\Gamma_P=0$. Notice that $1-4d_\gamma\neq0$ in these expressions because γ does not corresponds to a pure state.

We remark that also the analysis based on the Schrödinger representation reported in the appendix A.2 allows to conclude that the purification of a one-mode mixed state can be realised through a pure state in an extended lattice with $N_{\rm ext}=2$ that depends on three real parameters.

JHEP12(2020)101

8.1.2 Block diagonal covariance matrices

Many interesting mixed states are described by a block diagonal covariance matrix $\gamma = Q \oplus P$. In this cases $M = \mathbf{0}$ in (8.2).

It is worth considering a pure state for the extended system such that $M_{\rm ext} = \mathbf{0}$ in the corresponding covariance matrix (8.3). In this case (8.4) reduce to

$$Q_{\rm ext}\, P_{\rm ext} = \frac{1}{4}\,\mathbf{1} \qquad \Longleftrightarrow \qquad \begin{cases} Q\,P = \dfrac{1}{4}\,\mathbf{1} - \Gamma_Q\,\Gamma_P^{\rm t} \\ Q_{\rm anc}\,P_{\rm anc} = \dfrac{1}{4}\,\mathbf{1} - \Gamma_Q^{\rm t}\,\Gamma_P \\ Q\,\Gamma_P + \Gamma_Q\,P_{\rm anc} = \mathbf{0} \\ P\,\Gamma_Q + \Gamma_P\,Q_{\rm anc} = \mathbf{0} \end{cases} \tag{8.19}$$

where $\Gamma_Q\,\Gamma_P^{\rm t} \neq \mathbf{0}$, and $\gamma = Q \oplus P$ is the covariance matrix of a state that is not pure.

A common choice consists in considering purifications where the extended system has twice the degrees of freedom occurring in the original one, namely $N_{\rm anc} = N$. In these cases Γ_Q, Γ_P and Γ_M are $N \times N$ matrices.

Considering the purifications with $N_{\rm anc} = N$, a drastic simplification corresponds to require that $\gamma = \gamma_{\rm anc}$, which is equivalent to impose that $Q = Q_{\rm anc}$ and $P = P_{\rm anc}$. In this case, a solution is given by symmetric and commuting matrices Γ_Q and Γ_P that can be related through the last two equations in (8.19), which give

$$Q = -\,\Gamma_Q\,P\,\Gamma_P^{-1} \qquad\qquad \Gamma_Q\,P\,\Gamma_P^{-1} = \Gamma_P^{-1}\,P\,\Gamma_Q\,. \tag{8.20}$$

Setting $\Gamma_P = \alpha\,\Gamma_Q^{-1}$ with $\alpha \in \mathbb{R}$, the last equality is solved while the remaining relation $Q = -\,\frac{1}{\alpha}\,\Gamma_Q\,P\,\Gamma_Q$, whose validity is not guaranteed, provides Γ_Q.

A different solution for the matrix equations in (8.20) can be written when Q and P can be decomposed through three real matrices A, B and Λ as follows

$$Q = A\,\Lambda\,B^{-1} \qquad\qquad P = B\,\Lambda\,A^{-1}\,. \tag{8.21}$$

In this case, we can construct Γ_Q and Γ_P as

$$\Gamma_Q = A\,\tilde{\Lambda}\,B^{-1} \qquad\qquad \Gamma_P = -\,B\,\tilde{\Lambda}\,A^{-1} \qquad\qquad \big[\,\tilde{\Lambda}\,,\Lambda\,\big] = 0 \tag{8.22}$$

where a new matrix $\tilde{\Lambda}$ that commutes with Λ has been introduced.

It is straightforward to check that (8.21) and (8.22) satisfy the matrix equations in (8.20). Notice that Γ_P is not proportional to Γ_Q^{-1} in (8.22).

An important example where $N_{\rm anc} = N$ and $\gamma = \gamma_{\rm anc}$ is the thermofield double state (TFD). In appendix F a detailed analysis for this pure state for harmonic lattices is reported. The relations (F.25) and (F.26) tell us that the TFD corresponds to a special case[18] of (8.21) and (8.22).

[18] In particular, Λ and $\tilde{\Lambda}$ are the diagonal matrices in (F.13), while $A = \widetilde{V}\,\mathcal{S}^{-1}$ and $B = \widetilde{V}\,\mathcal{S}$, in terms of the matrices $\widetilde{V}$ and $\mathcal{S}$ introduced in the appendix F.

JHEP12(2020)101

The simplest case corresponds to $N = N_{\rm anc} = 1$, which has been discussed in section 8.1.1 in the most general setting. Solving the system (8.19) for this case, one finds

$$Q_{\rm anc} = -\frac{(1-4QP)P}{4\Gamma_P^2} \qquad P_{\rm anc} = \frac{4Q\Gamma_P^2}{4QP-1} \qquad \Gamma_Q = \frac{1-4QP}{4\Gamma_P}\,. \tag{8.23}$$

When $M = 0$, the observation in the text below (8.15) tells us that $4QP - 1 \neq 0$ in order to have a mixed state that is not pure to purify. Notice also that, by setting $M = \widetilde{\Gamma}_M = 0$ in (8.18), that holds for $\Gamma_M = 0$, one finds (8.23) and $M_{\rm anc} = 0$. Thus, when $M_{\rm ext} = \mathbf{0}$ and $N = N_{\rm anc} = 1$ we can parameterise the pure state of the extended system through a single parameter. This is consistent with the analysis reported in [23]. As final remark about the purifications having $N = N_{\rm anc} = 1$, let us observe that the second equation in (8.20) is trivially satisfied, while the first one is obtained by setting $Q = Q_{\rm anc}$ and $P = P_{\rm anc}$ in (8.23).

8.2 Selection criterion for the pure state

In the previous discussion we have explored the constraints guaranteeing that the covariance matrix $\gamma_{\rm ext}$ corresponds to a pure state under the condition that $\gamma_{\rm ext}$ provides the covariance matrix γ of the given mixed state once the ancillary degrees of freedom have been traced out.

These constraints identify the parameter space of the pure states allowed by γ for a given value of $N_{\rm anc}$. Within this space of parameters, it is natural to introduce a quantity $\mathcal{F}$ whose minimisation provides a particular pure state with certain properties. Thus, $\mathcal{F}$ characterises the criterion to select the pure state provided by the purification procedure as follows

$$\widetilde{\mathcal{F}}(\gamma) \equiv \min_{\gamma_{\rm ext}} [\mathcal{F}(\gamma_{\rm ext})] \tag{8.24}$$

where $\gamma_{\rm ext}$ is the covariance matrix for the extended system, that is constrained as described in section 8.1, and $\widetilde{\mathcal{F}}$ denotes the minimal value of $\mathcal{F}$ as $\gamma_{\rm ext}$ spans all the pure states allowed by γ. For the bosonic Gaussian states that we are considering, the calculations can be performed by employing either the wave functions or the covariance matrices.

For instance, the entanglement of purification for a bipartite mixed state [133–136] is (8.24), with $\mathcal{F}$ given by the entanglement entropy of a particular bipartition of $\mathcal{H}_{\rm extended}$.

In [23, 29], the purification complexity has been introduced to quantify the complexity of a mixed state. The definition of purification complexity is given by (8.24) in the special case where $\mathcal{F}$ is the complexity of the pure state corresponding to $\gamma_{\rm ext}$ with respect to a given fixed pure state in $\mathcal{H}_{\rm extended}$, whose covariance matrix is denoted by $\gamma_{\rm ext,0}$. This definition of purification complexity requires the choice of a cost function. The purification complexity explored in [23] reads

$$\widetilde{\mathcal{C}}_r(\gamma) \equiv \min_{\gamma_{\rm ext}} \big[\, \mathcal{C}_r(\gamma_{\rm ext}, \gamma_{\rm ext,0})\big] \tag{8.25}$$

where either $r = 1$ or $r = 2$, depending on whether the F_1 cost function or the F_2 cost function is adopted. In [23] the purification complexity based on the F_1 cost function has been mainly studied because, for the pure states, the divergence structure of the complexity evaluated through the F_1 cost function is closer to the one obtained from holographic calculations [17, 33]. The complexity defined through the F_1 cost function depends on the

JHEP12(2020)101

choice of the underlying basis, while the F_2 cost function leads to a complexity that is independent of this choice.

This approach to the complexity of mixed states is different from the one considered in this manuscript. The main difference is due to the fact that in the purification procedure described in section 4 ancillary degrees of freedom have not been introduced. Moreover, the purification complexity defined in (8.25) depends on the choice of the pure state corresponding to $\gamma_{\text{ext},0}$ (in [23] this pure state has been fixed to the one whose wave function (2.24) has $E_{\text{ext}} \propto \mathbf{1}$ and $F_{\text{ext}} = \mathbf{0}$). Furthermore, in the evaluation of the complexity of a mixed state through (8.25), no cost is assigned to the purification process of extending the system through ancillary degrees of freedom, given that the circuit considered in (8.25) is entirely made by pure states in $\mathcal{H}_{\text{extended}}$.

Explicit computations through (8.25) are technically involved and discussing them is beyond the scope of this manuscript. We refer the interested reader to the detailed analysis performed in [23]. Focussing on the simple case of one-mode thermal states, in section 9.7 we compare the complexity evaluated through the Fisher-Rao distance with the results found in [23] for the $\mathcal{C}_1$ complexity of mixed states based on the purification complexity. The latter quantity depends on the basis: in appendix G we discuss the diagonal basis and the physical basis, that have been introduced in [23] to evaluate this $\mathcal{C}_1$ complexity.

9 Harmonic chains

In this section we further study some of the quantities discussed in the previous sections by focussing on the one-dimensional case of the harmonic chain, either on the circle (i.e. with periodic boundary conditions) or on the infinite line. In this case we obtain analytic expressions in terms of the parameters of the circuit for some quantities and provide numerical results for the quantities that are more difficult to address analytically. After a brief discussion of the model in section 9.1, circuits whose reference and target states are either pure or thermal are considered in section 9.2 and section 9.3 respectively. In section 9.4 we study the mutual complexity for the thermofield double states (TFD's). Numerical results for the complexity and the mutual complexity associated to subregions are presented in section 9.5 and section 9.6. Finally, in section 9.7 we consider a simple comparison between the complexity for mixed states discussed in this manuscript and the one based on the purification complexity recently proposed in [23].

For the sake of simplicity, in this section we consider only examples that involve states whose covariance matrices are block diagonal. We remark that the results discussed in the previous sections hold also for states characterised by covariance matrices that are not block diagonal. For instance, these states typically occur in the out-of-equilibrium dynamics of the harmonic lattices [121, 137–139].

9.1 Hamiltonian

The hamiltonian of the periodic harmonic chain made by L sites, with frequency ω, mass m and elastic constant κ reads

$$\widehat{H} = \sum_{i=1}^{L} \left(\frac{1}{2m}\, \hat{p}_i^2 + \frac{m\omega^2}{2}\, \hat{q}_i^2 + \frac{\kappa}{2}(\hat{q}_{i+1} - \hat{q}_i)^2 \right) \tag{9.1}$$

JHEP12(2020)101

where $\hat{\boldsymbol{r}} \equiv (\hat{q}_1, \dots, \hat{q}_L, \hat{p}_1, \dots, \hat{p}_L)^{\mathrm{t}}$ collects the position and momentum operators and the periodic boundary condition $\hat{q}_{L+1} = \hat{q}_1$ is imposed.

Assuming that both κ and m are non-vanishing, the canonical transformation given by $\hat{q}_i \to \hat{q}_i / \sqrt[4]{m\kappa}$ and $\hat{p}_i \to \sqrt[4]{m\kappa}\, \hat{p}_i$ allows to write (9.1) as follows

$$\widehat{H} = \frac{\sqrt{\kappa/m}}{2} \sum_{i=1}^{L} \left(\hat{p}_i^2 + \frac{\omega^2}{\kappa/m}\, \hat{q}_i^2 + (\hat{q}_{i+1} - \hat{q}_i)^2 \right) \equiv \frac{1}{2}\, \hat{\boldsymbol{r}}^{\mathrm{t}} H^{\mathrm{phys}}\, \hat{\boldsymbol{r}} \tag{9.2}$$

where

$$H^{\mathrm{phys}} = \sqrt{\kappa/m} \left([(\tilde{\omega}^2 + 2)\mathbf{1} - T] \oplus \mathbf{1} \right) \tag{9.3}$$

and we are naturally led to introduce the dimensionless parameter

$$\tilde{\omega}^2 = \frac{\omega^2}{\kappa/m}\,. \tag{9.4}$$

The non vanishing elements of the symmetric matrix T in (9.3) are $T_{i,i+1} = T_{i+1,i} = 1$ with $1 \leqslant i \leqslant L-1$ and $T_{1,L} = T_{L,1} = 1$.

In order to find the Williamson's decomposition (2.68) for (9.3), first one observes that the matrix T in (9.3) is diagonalised by the following unitary matrix

$$\widetilde{U}_{r,s} \equiv \frac{e^{2\pi \mathrm{i}\, r\, s/L}}{\sqrt{L}} \tag{9.5}$$

that implements the discrete Fourier transform and it is independent of the parameters ω, m and κ. This implies that H^{phys} in (9.3) is diagonalised by $U \equiv \widetilde{U} \oplus \widetilde{U}$.

Since the symplectic matrix entering in the Williamson's decomposition (2.68) is real, let us consider the proper combinations of the eigenvectors entering in (9.5) that correspond to the same eigenvalue. This leads to introduce the $L \times L$ real and orthogonal matrix $\widetilde{V}$, whose generic element for even L is given by

$$\widetilde{V}_{i,k} \equiv \begin{cases} \sqrt{2/L}\, \cos(2\pi i\, k/L) & 1 \leqslant k < L/2 \\ (-1)^i/\sqrt{L} & k = L/2 \\ \sqrt{2/L}\, \sin(2\pi i\, k/L) & L/2 + 1 \leqslant k < L-1 \\ 1/\sqrt{L} & k = L \end{cases} \tag{9.6}$$

and for odd L by

$$\widetilde{V}_{i,k} \equiv \begin{cases} \sqrt{2/L}\, \cos(2\pi i\, k/L) & 1 \leqslant k < (L-1)/2 \\ \sqrt{2/L}\, \sin(2\pi i\, k/L) & (L-1)/2 + 1 \leqslant k < L-1 \\ 1/\sqrt{L} & k = L\,. \end{cases} \tag{9.7}$$

The matrix $\widetilde{V}$ diagonalises both T and $\mathbf{1}$ in (9.3); hence, by introducing the orthogonal matrix $V \equiv \widetilde{V} \oplus \widetilde{V}$, that is also symplectic, we have [48]

$$H^{\mathrm{phys}} = V \left[\sqrt{\kappa/m}\, \mathrm{diag}(\Omega_1^2, \dots, \Omega_L^2, 1, \dots, 1) \right] V^{-1} \tag{9.8}$$

JHEP12(2020)101

where Ω_k provides the dispersion relation, which depends on the parameter $\tilde{\omega}$ defined in (9.4) as follows

$$\Omega_k \equiv \sqrt{\tilde{\omega}^2 + 4\,(\sin[\pi k/L])^2} \qquad k = 1, \dots, L\,. \tag{9.9}$$

By applying the observation made in the final part of the appendix D to (9.8), one obtains the Williamson's decomposition (2.68) with the symplectic eigenvalues given by

$$\sigma_{\text{phys},k} = \sqrt{\kappa/m}\;\Omega_k \tag{9.10}$$

and the symplectic matrix W_{phys} by

$$W_{\text{phys}} = \mathcal{X}_{\text{phys}}\, V^t \qquad \mathcal{X}_{\text{phys}} \equiv \text{diag}(\sqrt{\Omega_1}, \dots, \sqrt{\Omega_L}, 1/\sqrt{\Omega_1}, \dots, 1/\sqrt{\Omega_L})\,. \tag{9.11}$$

In these expressions the zero mode corresponds to $k = L$ and its occurrence is due to the invariance of the system under translations. The comparison between the expressions reported throughout this section and the corresponding ones in section 2.6 can be done once the canonical transformation above (9.2) has been taken into account.[19]

It is worth remarking that the canonical transformation that brings (9.1) into (9.2) cannot be defined when $\kappa = 0$. This implies, for instance, that, in order to employ the unentangled product state of the harmonic chain as reference state (this is often the case in the recent literature on the circuit complexity [17, 18, 22, 23, 36]), our analysis must be adapted to the hamiltonian (9.1).

9.2 Pure states

In this subsection we study the circuit complexity for pure states that are the ground states of periodic harmonic chains having different frequencies [17].

9.2.1 Covariance matrix

The two-point correlators in the ground state of the hamiltonian (9.2), where periodic boundary conditions are imposed, read

$$\langle \hat{q}_i \hat{q}_j \rangle = \frac{1}{2L} \sum_{k=1}^{L} \frac{1}{\Omega_k} \cos[2\pi k\,(i-j)/L] \qquad \langle \hat{p}_i \hat{p}_j \rangle = \frac{1}{2L} \sum_{k=1}^{L} \Omega_k \cos[2\pi k\,(i-j)/L] \tag{9.12}$$

where Ω_k is the dispersion relation (9.9). The periodic boundary conditions make this system invariant under translations. The expressions in (9.12) define the elements of the correlation matrices Q_{gs} and P_{gs} respectively. These matrices provide the block diagonal covariance matrix $\gamma_{\text{gs}} = Q_{\text{gs}} \oplus P_{\text{gs}}$.

By introducing the discrete Fourier transform of the operators $\hat{q}_j$ and $\hat{p}_j$ in the standard way [140], the matrices Q_{gs} and P_{gs} can be written as follows

$$Q_{\text{gs}} = \widetilde{U}\, \mathcal{Q}_{\text{gs}}\, \widetilde{U}^{-1} \qquad P_{\text{gs}} = \widetilde{U}\, \mathcal{P}_{\text{gs}}\, \widetilde{U}^{-1} \tag{9.13}$$

[19] This canonical transformation is responsible e.g. for the different definitions of Ω_k in (9.9) and in section 2.6 and also for the factor between (9.10) and (2.69), which is the same prefactor occurring in the hamiltonian (9.2).

JHEP12(2020)101

where the matrix $\widetilde{U}$ have been defined in (9.3), while $\mathcal{Q}_{\rm gs}$ and $\mathcal{P}_{\rm gs}$ are diagonal matrices whose elements read

$$(\mathcal{Q}_{\rm gs})_{k,k} = \frac{1}{2\,\Omega_k} \qquad (\mathcal{P}_{\rm gs})_{k,k} = \frac{1}{2}\,\Omega_k \qquad k = 1, \dots, L\,. \tag{9.14}$$

In order to find the Williamson's decomposition of $\gamma_{\rm gs}$, we have to consider the symplectic matrix V introduced in section 9.1. Then, the observation made in the final part of the appendix D specified to $\gamma_{\rm gs}$ leads us to introduce the following symplectic and diagonal matrix

$$\mathcal{X}_{\rm C} \equiv \text{diag}(1/\sqrt{\Omega_1}, \dots, 1/\sqrt{\Omega_L}, \sqrt{\Omega_1}, \dots, \sqrt{\Omega_L}) = J^{\rm t}\,\mathcal{X}_{\rm phys}\,J \tag{9.15}$$

where $\mathcal{X}_{\rm phys}$ has been introduced in (9.11). This matrix is related to (9.14) as follows

$$\mathcal{Q}_{\rm gs} \oplus \mathcal{P}_{\rm gs} = \frac{1}{2}\,\mathcal{X}_{\rm C}^2\,. \tag{9.16}$$

By introducing the symplectic matrix

$$W_{\rm C} \equiv \mathcal{X}_{\rm C}\,V^{\rm t} \tag{9.17}$$

we have that the Williamson's decomposition of $\gamma_{\rm gs}$ reads

$$\gamma_{\rm gs} = \frac{1}{2}\,W_{\rm C}^{\rm t}\,W_{\rm C}\,. \tag{9.18}$$

Notice that the symplectic matrices $W_{\rm phys}$ and $W_{\rm C}$, defined in (9.11) and (9.17) respectively, are related as follows

$$W_{\rm C} = J^{\rm t}\,\mathcal{X}_{\rm phys}\,(J\,V^{\rm t}\,J^{\rm t})J = J^{\rm t}\,\mathcal{X}_{\rm phys}\,V^{\rm t}J = J^{\rm t}\,W_{\rm phys}J = W_{\rm phys}^{-{\rm t}} \tag{9.19}$$

where we have also used (9.15), (9.17), the property $S^{-{\rm t}} = J^{\rm t}SJ$ of the symplectic matrices S and the fact that symplectic V is also orthogonal (see also (2.77)).

As consistency check, we can plug (9.17) into (9.18) first and then use (9.16), finding that

$$\gamma_{\rm gs} = V\,(\mathcal{Q}_{\rm gs} \oplus \mathcal{P}_{\rm gs})\,V^{\rm t} = V\,(\mathcal{Q}_{\rm gs} \oplus \mathcal{P}_{\rm gs})\,V^{-1}\,. \tag{9.20}$$

This tells us that V is also the orthogonal matrix that diagonalises the symmetric matrix $\gamma_{\rm gs}$. Let us remark that V depends only on the number of sites L of the harmonic chain.

9.2.2 Complexity

We consider the circuit complexity where the reference state and the target state are the ground states of periodic harmonic chains whose hamiltonians are characterised by the parameters $(\omega_{\rm R}, \kappa_{\rm R}, m_{\rm R})$ and $(\omega_{\rm T}, \kappa_{\rm T}, m_{\rm T})$ respectively.

For the sake of simplicity, in our analysis we set $\kappa_{\rm R} = \kappa_{\rm T} \equiv \kappa$ and $m_{\rm R} = m_{\rm T} \equiv m$; hence only the parameter $\tilde{\omega}$ distinguishes the reference and the target states.

In this case, from (9.20) and the fact that V is independent of the parameters ω, κ and m, it is straightforward to find that (2.32) becomes

$$\Delta_{\rm TR} = V\,(\mathcal{Q}_{\rm gs,T}\,\mathcal{Q}_{\rm gs,R}^{-1} \oplus \mathcal{P}_{\rm gs,T}\,\mathcal{P}_{\rm gs,R}^{-1})\,V^{-1} \tag{9.21}$$

JHEP12(2020)101

where the diagonal matrices $\mathcal{Q}_{\rm gs,R}$, $\mathcal{Q}_{\rm gs,T}$, $\mathcal{P}_{\rm gs,R}$ and $\mathcal{P}_{\rm gs,T}$ can be easily obtained by writing (9.14) for the reference and for the target state. By employing (9.21) and (9.14), it is straightforward to find that, in this case, the complexity given by (2.31) and (2.33) simplifies to [17]

$$\mathcal{C}_2 = \frac{1}{2\sqrt{2}} \sqrt{\mathrm{Tr}\left\{ \left[\log(\mathcal{Q}_{\rm gs,T}\, \mathcal{Q}_{\rm gs,R}^{-1} \oplus \mathcal{P}_{\rm gs,T}\, \mathcal{P}_{\rm gs,R}^{-1}) \right]^2 \right\}} = \frac{1}{2} \sqrt{\sum_{k=1}^{L} \Big(\log \left[\Omega_{{\rm T},k} / \Omega_{{\rm R},k} \right] \Big)^2} \tag{9.22}$$

where

$$\Omega_{{\rm S},k} \equiv \sqrt{\tilde{\omega}_{\rm S}^2 + 4\,(\sin[\pi k/L])^2} \qquad\qquad k = 1, \dots, L \qquad\qquad {\rm S} \in \{{\rm R}, {\rm T}\}\,. \tag{9.23}$$

Notice that the complexity (9.22) depends on m and κ only through the dimensionless parameters $\tilde{\omega}_{\rm R}$ and $\tilde{\omega}_{\rm T}$.

We remark that, if $\kappa_{\rm R} \neq \kappa_{\rm T}$, the canonical transformation reported in the text between (9.1) and (9.2) is not the same for reference and target states. This is crucial in the evaluation of the circuit complexity between the ground state of the harmonic chain with $\kappa \neq 0$ and the unentangled product state, where $\kappa = 0$. In these cases we have to consider the hamiltonian (9.1) instead of (9.2). Adapting our analyses to this hamiltonian is a straightforward exercise whose details will not be reported here. For instance, considering $m_{\rm R} = m_{\rm T} = m$ but keeping $\kappa_{\rm R} \neq \kappa_{\rm T}$, we obtain

$$\mathcal{C}_2 \;=\; \frac{1}{2} \sqrt{\sum_{k=1}^{L} \left(\log \left[\frac{\sigma_{{\rm phys,T},k}}{\sigma_{{\rm phys,R},k}} \right] \right)^2} \tag{9.24}$$

where $\sigma_{{\rm phys,S},k}$ with ${\rm S} \in \{{\rm R}, {\rm T}\}$ are the symplectic spectra corresponding to the reference and the target states, evaluated through the hamiltonian (9.10). Ref [17] mainly considered the case where the reference state is the unentangled product state and the target state is the ground state of a harmonic chain (with periodic boundary conditions). The circuit complexity in this case can be found by taking the limit $\kappa_{\rm R} \to 0$ in (9.24). The result is [17]

$$\mathcal{C}_2 \;=\; \frac{1}{2} \sqrt{\sum_{k=1}^{L} \left(\log \left[\frac{\sigma_{{\rm phys,T},k}}{\omega_{\rm R}} \right] \right)^2} \tag{9.25}$$

It is instructive to obtain (9.22) also as a special case of (2.58), that is written in terms of the matrix $W_{\rm TR}$ introduced in (2.45). For the pure states that have been chosen, whose covariance matrices have the form (9.18), $W_{\rm R}$ and $W_{\rm T}$ can be obtained by specialising (9.17) to the reference and the target states considered. Since the matrix V is the same for both of them, (2.45) simplifies to

$$W_{\rm TR} = \mathcal{X}_{\rm C,T}\, \mathcal{X}_{\rm C,R}^{-1} = {\rm diag}\left[\left(\frac{\Omega_{{\rm T},1}}{\Omega_{{\rm R},1}} \right)^{-1/2}, \dots, \left(\frac{\Omega_{{\rm T},L}}{\Omega_{{\rm R},L}} \right)^{-1/2} \right] \oplus {\rm diag}\left[\left(\frac{\Omega_{{\rm T},1}}{\Omega_{{\rm R},1}} \right)^{1/2}, \dots, \left(\frac{\Omega_{{\rm T},L}}{\Omega_{{\rm R},L}} \right)^{1/2} \right] \tag{9.26}$$

JHEP12(2020)101

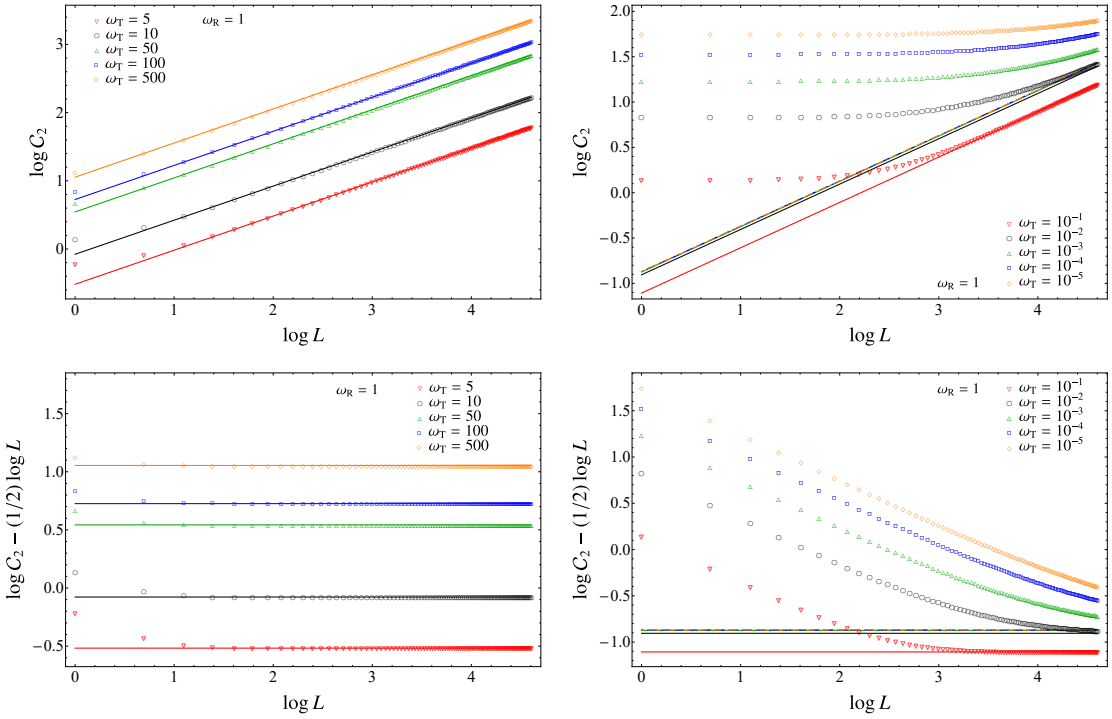

Figure 4. The complexity $\mathcal{C}_2$ in terms of the size L of the periodic harmonic chain. The reference and the target states are the ground states with $\omega = \omega_R$ and $\omega = \omega_T$ respectively (here $\kappa = m = 1$). The data reported correspond to $\omega_R = 1$ and different ω_T. The solid lines in the top panels represent (9.27), while the horizontal solid lines in the bottom panels correspond to the constant values of $a(\tilde{\omega}_T, \tilde{\omega}_R)$ obtained from (9.28).

where the last expression has been found by using (9.15). Thus, in this case $W_{TR} = \mathcal{X}_{TR} = \mathcal{X}_{C,T}\, \mathcal{X}_{C,R}^{-1}$ and this leads to obtain (9.22) from (2.58).

In the thermodynamic limit $L \to \infty$, the expression (9.22) for the complexity becomes [17]

$$\mathcal{C}_2 = a(\tilde{\omega}_T, \tilde{\omega}_R)\, \sqrt{L} + \dots \qquad \tilde{\omega}_R \neq \tilde{\omega}_T \qquad L \to \infty \tag{9.27}$$

where the subleading terms have been neglected and the coefficient of the leading term reads

$$a(\tilde{\omega}_T, \tilde{\omega}_R) \equiv \frac{1}{2} \sqrt{\frac{1}{\pi} \int_0^\pi \Big(\log \left[\Omega_{T,\theta} / \Omega_{R,\theta} \right] \Big)^2 d\theta} \qquad \Omega_R \neq \Omega_T \tag{9.28}$$

with

$$\Omega_{S,\theta} \equiv \sqrt{\tilde{\omega}_S^2 + 4\, (\sin\theta)^2} \qquad \theta \in (0, \pi) \tag{9.29}$$

which can be easily obtained from (9.23). As consistency check, notice that $a(\tilde{\omega}_R, \tilde{\omega}_R) = 0$, as expected. For large ω_T, the leading term of (9.28) is

$$a(\tilde{\omega}_T, \tilde{\omega}_R) = \frac{1}{2} \log \tilde{\omega}_T + \dots \qquad \tilde{\omega}_T \to \infty\,. \tag{9.30}$$

We find it interesting to observe that, once the limit $L \to \infty$ has been taken, either $\tilde{\omega}_R$ or $\tilde{\omega}_T$ can be set to zero. For instance, setting $\tilde{\omega}_T = 0$ in (9.28) gives the following

JHEP12(2020)101

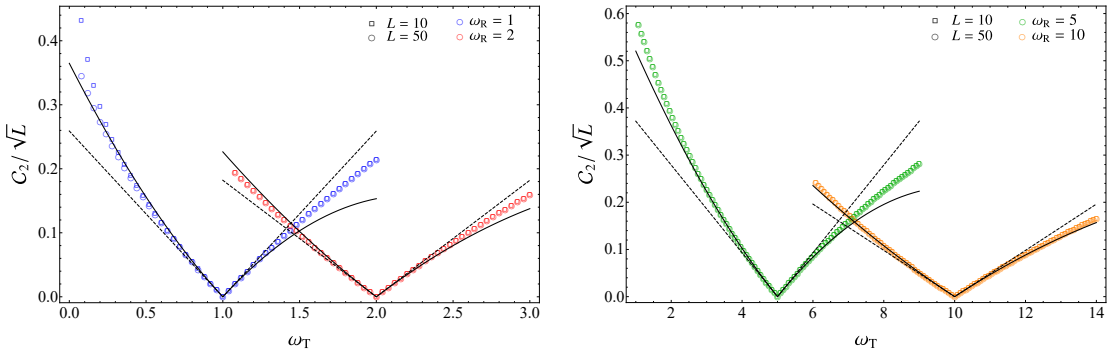

Figure 5. The complexity $\mathcal{C}_2$ between the ground states of harmonic chains with $\kappa = m = 1$ and different frequencies, for a given ω_R and as function of ω_T. The data points come from (9.22). The dashed lines correspond to the first order approximation (9.32) and the solid lines to the second order approximation (9.33), in the thermodynamic limit and in the expansion where $\tilde{\omega}_T = \tilde{\omega}_R + \delta\tilde{\omega}$.

finite result

$$a(\tilde{\omega}_R, \tilde{\omega}_T = 0)^2 = \frac{1}{16\pi}\int_0^\pi \left(2\log[\sin\theta] - \log\left[\frac{\tilde{\omega}_R^2}{4} + (\sin\theta)^2\right]\right)^2 d\theta\,. \tag{9.31}$$

On the other hand, it is well known that the correlators $\langle \hat{q}_i \hat{q}_j \rangle$ in (9.12) diverge when the frequency of the chain vanishes because of the occurrence of the zero mode; hence we cannot evaluate $\mathcal{C}_2$ for a finite chain when either $\tilde{\omega}_T = 0$ or $\tilde{\omega}_R = 0$. This tells us that the limits $L \to \infty$ and $\tilde{\omega}_T \to 0$ do not commute.

In figure 4 we show the complexity $\mathcal{C}_2$ as function of the size L of the periodic chain. The numerical results discussed in this manuscript have been obtained for $\kappa = 1$ and $m = 1$, unless otherwise specified; hence $\tilde{\omega}_R = \omega_R$ and $\tilde{\omega}_T = \omega_T$. In the left and right panels of figure 4 we have $\omega_T > \omega_R$ and $\omega_T < \omega_R$ respectively (notice that $\omega_R = 1$ for all the panels). In the top panels the numerical data are compared against the expression (9.27) (solid lines) obtained in the thermodynamic limit: while in the top left panel the agreement is very good at large L, from the top right panel we conclude that larger values of L are needed to observe a reasonable agreement as $\tilde{\omega}_T \to 0$. In the bottom panels of figure 4 we consider the subleading term in (9.27): while in the bottom left panel the data agree with the horizontal lines corresponding to $a(\tilde{\omega}_T, \tilde{\omega}_R)$ given by (9.28), in the bottom right panel the agreement gets worse as $\tilde{\omega}_T \to 0$. Notice that the solid lines in the right panels of figure 4 accumulate on a limiting line as $\omega_T \to 0$. This line can be found by plugging (9.31) with $\omega_R = 1$ into (9.27).

We find it worth considering a perturbative expansion of the complexity of these pure states when the target state is infinitesimally close to the reference state. This means that $\tilde{\omega}_T = \tilde{\omega}_R + \delta\tilde{\omega}$ with $|\delta\tilde{\omega}| \ll \tilde{\omega}_R$. Assuming $\tilde{\omega}_R \neq 0$, we expand (9.28) as $\delta\tilde{\omega}/\tilde{\omega}_R \to 0$. The first order of this expansion gives

$$\mathcal{C}_2 = \frac{\sqrt{L}\,|\delta\tilde{\omega}|}{2\tilde{\omega}_R}\sqrt{\frac{1}{\pi}\int_0^\pi \left[1 + \frac{4}{\tilde{\omega}_R^2}(\sin\theta)^2\right]^2 d\theta} = \frac{|\delta\tilde{\omega}|}{2\,\tilde{\omega}_R}\sqrt{\frac{1 + 2/\tilde{\omega}_R^2}{(1 + 4/\tilde{\omega}_R^2)^{3/2}}}\,\sqrt{L}\,. \tag{9.32}$$

JHEP12(2020)101

Including also the $O((\delta\tilde{\omega})^2)$ term in the expansion of (9.28), we find

$$\mathcal{C}_2 = \frac{|\delta\tilde{\omega}|}{2\,\tilde{\omega}_{\rm R}} \sqrt{\frac{1+2/\tilde{\omega}_{\rm R}^2}{(1+4/\tilde{\omega}_{\rm R}^2\,)^{3/2}}} \left[1 + \frac{\delta\tilde{\omega}}{2\tilde{\omega}_{\rm R}}\left(1 - \frac{\tilde{\omega}_{\rm R}^4 + 4\tilde{\omega}_{\rm R}^2 + 6}{4\tilde{\omega}_{\rm R}^3(\tilde{\omega}_{\rm R}^2+2)(\tilde{\omega}_{\rm R}^2+4)}\right)\right] \sqrt{L} \tag{9.33}$$

In figure 5 we compare the exact formula (9.22) for finite L against the first order result (9.32) (dashed lines) and against (9.33), that includes also the second order correction (solid lines).

9.3 Thermal states

The thermal states are the most natural mixed states to consider. In the following we evaluate the complexity (2.33) when both the reference and the target states are thermal states of the harmonic chain.

9.3.1 Covariance matrix

The two-point correlators of a periodic chain in a thermal state at temperature T read

$$\langle \hat{q}_i \hat{q}_j \rangle = \frac{1}{2L} \sum_{k=1}^{L} \frac{\coth[\Omega_k/(2\widetilde{T})]}{\Omega_k} \cos[2\pi k\,(i-j)/L] \tag{9.34}$$

$$\langle \hat{p}_i \hat{p}_j \rangle = \frac{1}{2L} \sum_{k=1}^{L} \Omega_k \coth[\Omega_k/(2\widetilde{T})] \cos[2\pi k\,(i-j)/L] \tag{9.35}$$

where Ω_k is given by (9.9) and we have introduced the dimensionless parameter

$$\widetilde{T} \equiv \frac{T}{\sqrt{\kappa/m}}\,. \tag{9.36}$$

The correlators (9.34) and (9.35) provide the generic elements of the correlation matrices $Q_{\rm th}$ and $P_{\rm th}$ respectively, which are the non vanishing blocks of the covariance matrix $\gamma_{\rm th} = Q_{\rm th} \oplus P_{\rm th}$ of the thermal state.

Following the standard procedure, also for the thermal state one first performs the discrete Fourier transform through the matrix $\widetilde{U}$ in (9.5), finding that (9.13) can be written also for the correlation matrices $Q_{\rm th}$ and $P_{\rm th}$, i.e.

$$Q_{\rm th} = \widetilde{U}\,\mathcal{Q}_{\rm th}\,\widetilde{U}^{-1} \qquad P_{\rm th} = \widetilde{U}\,\mathcal{P}_{\rm th}\,\widetilde{U}^{-1} \tag{9.37}$$

with the proper diagonal matrices $\mathcal{Q}_{\rm th}$ and $\mathcal{P}_{\rm th}$, whose elements are given respectively by [140]

$$(\mathcal{Q}_{\rm th})_{k,k} = \frac{\coth\left[\Omega_k/(2\widetilde{T})\right]}{2\,\Omega_k} \qquad (\mathcal{P}_{\rm th})_{k,k} = \frac{1}{2}\,\Omega_k \coth\left[\Omega_k/(2\widetilde{T})\right] \qquad k = 1, \dots, L \tag{9.38}$$

which reduce to (9.14) when $\widetilde{T} \to 0$, as expected.

By employing the results obtained in section 9.2 for the covariance matrix of the ground state, it is not difficult to find that the Williamson's decomposition of the covariance matrix $\gamma_{\rm th}$ of the thermal state reads

$$\gamma_{\rm th} = W_{\rm C}^{\rm t}\,\mathcal{D}_{\rm th}\,W_{\rm C}\,. \tag{9.39}$$

JHEP12(2020)101

The matrix $W_{\rm C}$ is the symplectic matrix (9.17) occurring in the Williamson's decomposition (9.18) of the ground state and $\mathcal{D}_{\rm th} \equiv \mathrm{diag}(\sigma_{{\rm th},1},\dots,\sigma_{{\rm th},L}) \oplus \mathrm{diag}(\sigma_{{\rm th},1},\dots,\sigma_{{\rm th},L})$, with the symplectic eigenvalues given by [47]

$$\sigma_{{\rm th},k} = \frac{1}{2}\,\coth[\Omega_k/(2\widetilde{T})] = \frac{1}{2}\,\coth[\sigma_{{\rm phys},k}/(2T)] \qquad\qquad k = 1,\dots,L\,. \tag{9.40}$$

From these observations, we find that

$$\gamma_{\rm th} = V\,(\mathcal{Q}_{\rm th} \oplus \mathcal{P}_{\rm th})\,V^{\rm t} = V\,(\mathcal{Q}_{\rm th} \oplus \mathcal{P}_{\rm th})\,V^{-1} \tag{9.41}$$

where V is the same symplectic and orthogonal matrix introduced through (9.6) and (9.7) for the ground state. It is straightforward to check that (9.41) becomes (9.20) as $T \to 0$, as expected.

9.3.2 Complexity

In order to explore the complexity of two thermal states of a periodic chain, let us consider a reference state characterised by frequency $\omega_{\rm R}$ and temperature $T_{\rm R}$ and a target state characterised by frequency $\omega_{\rm T}$ and temperature $T_{\rm T}$, assuming again that $\kappa_{\rm R} = \kappa_{\rm T} = \kappa$ and $m_{\rm R} = m_{\rm T} = m$. Like (9.20), we have that also (9.21) can be adapted to this case, simply by replacing $\mathcal{Q}_{{\rm gs},{\rm M}}$ with $\mathcal{Q}_{{\rm th},{\rm M}}$ and $\mathcal{P}_{{\rm gs},{\rm M}}$ with $\mathcal{P}_{{\rm th},{\rm M}}$ taken from (9.38), with ${\rm M} \in \{{\rm R},{\rm T}\}$. Thus, the complexity given by (2.33) and (2.31) for these thermals states becomes

$$\mathcal{C}_2 = \frac{1}{2\sqrt{2}}\,\sqrt{\mathrm{Tr}\left\{\left[\log(\mathcal{Q}_{{\rm th},{\rm T}}\,\mathcal{Q}_{{\rm th},{\rm R}}^{-1} \oplus \mathcal{P}_{{\rm th},{\rm T}}\,\mathcal{P}_{{\rm th},{\rm R}}^{-1})\right]^2\right\}} \tag{9.42}$$

$$= \frac{1}{2\sqrt{2}}\,\sqrt{\sum_{k=1}^{L}\left\{\left[\log\left(\frac{\Omega_{{\rm R},{\rm T},k}}{\Omega_{{\rm T},{\rm R},k}}\right)\right]^2 + \left[\log\left(\frac{\Omega_{{\rm T},{\rm T},k}}{\Omega_{{\rm R},{\rm R},k}}\right)\right]^2\right\}} \tag{9.43}$$

where we have introduced

$$\Omega_{{\rm M},{\rm N},k} \equiv \Omega_{{\rm M},k}\,\coth(\Omega_{{\rm N},k}/(2\widetilde{T}_{\rm N})) \qquad\qquad {\rm M},{\rm N} \in \{{\rm R}\,,{\rm T}\} \tag{9.44}$$

with $\Omega_{{\rm S},k}$ given in (9.23). Notice that $\Omega_{{\rm M},{\rm N},k} \to \Omega_{{\rm M},k}$ as $T_{\rm N} \to 0$; hence in the limit given by $\widetilde{T}_{\rm R} \to 0$ and $\widetilde{T}_{\rm T} \to 0$, the expected expression (9.22) for pure states is recovered. Notice that the complexity (9.43) depends on the dimensionless parameters $\tilde{\omega}_{\rm R}$, $\tilde{\omega}_{\rm T}$, $\tilde{T}_{\rm R}$ and $\tilde{T}_{\rm T}$.

As briefly discussed in section 9.1, in order to consider the unentangled product state as reference state, we have to keep the hamiltonian in the form (9.1) and generalise the above analyses by setting $m_{\rm R} = m_{\rm T} = m$ and $\kappa_{\rm R} \neq \kappa_{\rm T}$. For thermal states, this slight generalisation leads to

$$\mathcal{C}_2 = \frac{1}{2\sqrt{2}}\,\sqrt{\sum_{k=1}^{L}\left\{\left[\log\left(\frac{\sigma_{{\rm phys},{\rm R},{\rm T},k}}{\sigma_{{\rm phys},{\rm T},{\rm R},k}}\right)\right]^2 + \left[\log\left(\frac{\sigma_{{\rm phys},{\rm T},{\rm T},k}}{\sigma_{{\rm phys},{\rm R},{\rm R},k}}\right)\right]^2\right\}} \tag{9.45}$$

where $\sigma_{{\rm phys},{\rm M},{\rm N},k}$ is defined in terms of $\sigma_{{\rm phys},{\rm S},k}$ given in (9.10) as follows

$$\sigma_{{\rm phys},{\rm M},{\rm N},k} \equiv \sigma_{{\rm phys},{\rm M},k}\,\coth(\sigma_{{\rm phys},{\rm N},k}/(2T_{\rm N})) \qquad\qquad {\rm M},{\rm N} \in \{{\rm R}\,,{\rm T}\} \tag{9.46}$$

JHEP12(2020)101

The complexity between a thermal state at temperature $T_{\rm T}$ and the unentangled product state can be found by taking $\kappa_{\rm R} \to 0$ and $T_{\rm R} \to 0$ in (9.45).

In the special case where $\tilde{\omega}_{\rm R} = \tilde{\omega}_{\rm T} \equiv \tilde{\omega}$, the expression (9.43) simplifies to

$$\mathcal{C}_2 \,=\, \frac{1}{2}\sqrt{\sum_{k=1}^{L}\left[\log\left(\frac{\coth(\Omega_k/(2\widetilde{T}_{\rm T}))}{\coth(\Omega_k/(2\widetilde{T}_{\rm R}))}\right)\right]^2} = \frac{1}{2\sqrt{2}}\sqrt{{\rm Tr}\left\{\left[\log\left(\mathcal{D}_{\rm th,T}\,\mathcal{D}_{\rm th,R}^{-1}\right)\right]^2\right\}}\,. \tag{9.47}$$

This result is consistent with the general expression (2.49) for the complexity in the special case where $W_{\rm TR} = \mathbf{1}$. This relation can be verified by setting $\tilde{\omega}_{\rm R} = \tilde{\omega}_{\rm T}$ in (9.26).

In the special case of $\tilde{\omega}_{\rm R} = \tilde{\omega}_{\rm T}$, from (9.39) and (9.17) we have that $W_{\rm T} = W_{\rm R}$, hence (9.47) provides the length of the W path connecting the reference and the target state that we are considering (see section 3.3). Indeed it is proportional to the proposal (3.19) for the spectrum complexity.

As for the basis complexity, from (9.40), one observes that, for a generic number of modes larger than one, the requirement $\mathcal{D}_{\rm R} = \mathcal{D}_{\rm T}$ leads to $\tilde{\omega}_{\rm R} = \tilde{\omega}_{\rm T}$ and $\tilde{T}_{\rm R} = \tilde{T}_{\rm T}$. This implies $W_{\rm R} = W_{\rm T}$, as just remarked above, hence $\gamma_{\rm R} = \gamma_{\rm T}$ and the basis complexity (3.23) vanishes for the thermal states. Also the corresponding basis complexity (3.24) vanishes because it is bounded from above by (3.23). We expect that this is a peculiar feature due to the simplicity of the model. Notice that, for pure states or one-mode mixed states, the constraint $\mathcal{D}_{\rm R} = \mathcal{D}_{\rm T}$ does not imply that $\gamma_{\rm R} = \gamma_{\rm T}$, hence a non vanishing basis complexity is obtained.

Another interesting special case to explore is given by a pure reference state, i.e. $\widetilde{T}_{\rm R} = 0$. In this limit (9.43) becomes

$$\mathcal{C}_2 \,=\, \frac{1}{2\sqrt{2}}\sqrt{\sum_{k=1}^{L}\left[\log\left(\frac{\Omega_{{\rm R},k}}{\Omega_{{\rm T},k}}\,\coth(\Omega_{{\rm T},k}/(2\widetilde{T}_{\rm T}))\right)\right]^2 + \left[\log\left(\frac{\Omega_{{\rm T},k}}{\Omega_{{\rm R},k}}\,\coth(\Omega_{{\rm T},k}/(2\widetilde{T}_{\rm T}))\right)\right]^2}\,. \tag{9.48}$$

In the low temperature limit (i.e. when $\widetilde{T}_{\rm T} \ll \tilde{\omega}_{\rm R}, \tilde{\omega}_{\rm T}$), by using that $\coth x \simeq 1 + 2e^{-2x} + \dots$ as $x \to \infty$ and that $\log(1+x) \simeq x + \dots$ as $x \to 0$, we find that (9.48) simplifies to

$$\mathcal{C}_2 \,=\, \frac{1}{2}\sqrt{\sum_{k=1}^{L}\left\{\left[\log\left(\Omega_{{\rm R},k}/\Omega_{{\rm T},k}\right)\right]^2 + 4\,e^{-2\,\Omega_{{\rm T},k}/\widetilde{T}_{\rm T}}\right\}} + \dots \tag{9.49}$$

where the dots denote subleading terms. This expansion tells us that the first correction to the pure state result (9.22) as $\widetilde{T}_{\rm T} \to 0$ is exponentially small. The high temperature regime corresponds to $\widetilde{T}_{\rm R} \gg \tilde{\omega}_{\rm R}$ and $\widetilde{T}_{\rm T} \gg \tilde{\omega}_{\rm T}$. In this limit, by using that $\coth x \simeq 1/x$ when $x \to 0$, we find that (9.43) becomes

$$\mathcal{C}_2 \,=\, \frac{1}{2}\sqrt{\sum_{k=1}^{L}\left\{\left[\log(\widetilde{T}_{\rm T}/\widetilde{T}_{\rm R})\right]^2 + 2\left[\log(\Omega_{{\rm R},k}/\Omega_{{\rm T},k})\right]^2\right\}}\,. \tag{9.50}$$

In the thermodynamic limit $L \to \infty$, for the complexity (9.43) we find

$$\mathcal{C}_2 = \sqrt{L}\; a(\tilde{\omega}_{\rm R}, \tilde{\omega}_{\rm T}, \widetilde{T}_{\rm R}, \widetilde{T}_{\rm T}) + \dots \tag{9.51}$$

JHEP12(2020)101

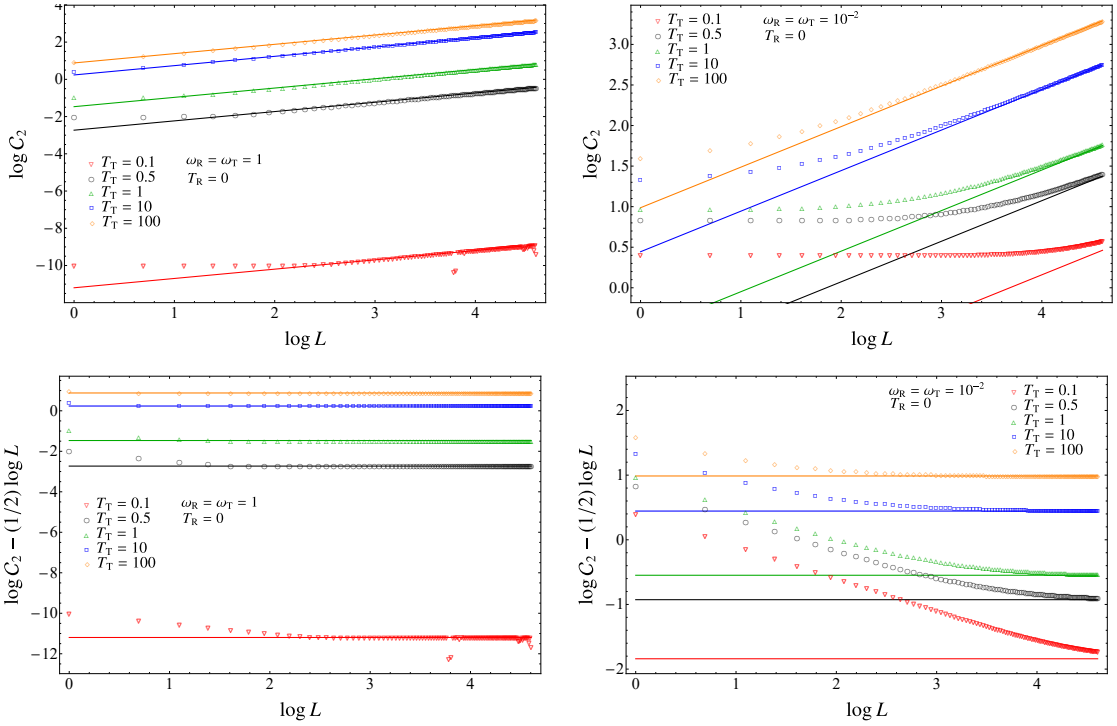

Figure 6. The complexity $\mathcal{C}_2$ for thermal states as function of the size L of the periodic harmonic chain. Here $\kappa = 1$ and $m = 1$; hence $\tilde{\omega}_R = \omega_R$, $\tilde{\omega}_T = \omega_T$, $\widetilde{T}_R = T_R$ and $\widetilde{T}_T = T_T$. In all the panels $T_R = 0$ and various values of T_T are considered. Top panels: $\omega_R = \omega_T = 1$ (left) and $\omega_R = \omega_T = 10^{-2}$ (right). The solid lines correspond to (9.51). Bottom panels: subleading term $\log \mathcal{C}_2 - \frac{1}{2}\log L$ as function of $\log L$, for $T_R = 0$ and various values of T_T. In the left panel $\omega_R = \omega_T = 1$ and $\omega_R = \omega_T = 10^{-2}$ in the right panel. The horizontal solid lines correspond to the constant values obtained from (9.52).

where

$$a(\tilde{\omega}_R, \tilde{\omega}_T, \widetilde{T}_R, \widetilde{T}_T) \equiv \frac{1}{2\sqrt{2}} \sqrt{\int_0^\pi \left\{ \left[\log\left(\frac{\Omega_{R,T,\theta}}{\Omega_{T,R,\theta}} \right) \right]^2 + \left[\log\left(\frac{\Omega_{T,T,\theta}}{\Omega_{R,R,\theta}} \right) \right]^2 \right\} \frac{d\theta}{\pi}} \tag{9.52}$$

and $\Omega_{M,N,\theta} \equiv \Omega_{M,\theta} \coth(\Omega_{N,\theta}/(2\widetilde{T}_N))$, with $M, N \in \{R, T\}$ (see (9.44)), written in terms of the dispersion relation $\Omega_{S,\theta}$ given by (9.29). Notice that $a(\tilde{\omega}_R, \tilde{\omega}_T, \widetilde{T}_R, \widetilde{T}_T) \to a(\tilde{\omega}_R, \tilde{\omega}_T)$ when $\widetilde{T}_R \to 0$ and $\widetilde{T}_T \to 0$, where $a(\tilde{\omega}_R, \tilde{\omega}_T)$ has been defined in (9.28).

In section 9.2 we have observed that the massless limit of the coefficient of the leading term of the complexity of pure states is finite (see (9.31)). This happens also for thermal states. Indeed, by setting $\tilde{\omega}_R = \tilde{\omega}_T = 0$ in (9.52), we find

$$a(\tilde{\omega}_R = 0, \tilde{\omega}_T = 0, \widetilde{T}_R, \widetilde{T}_T) = \frac{1}{2} \sqrt{\int_0^\pi \left[\log\left(\frac{\coth((\sin\theta)/\widetilde{T}_T)}{\coth((\sin\theta)/\widetilde{T}_R)} \right) \right]^2 \frac{d\theta}{\pi}} \,. \tag{9.53}$$

In figure 6 and figure 7 we report some numerical results for the complexity (2.33) between thermal states with different temperatures and $\omega_R = \omega_T \equiv \omega$. The data have been

JHEP12(2020)101

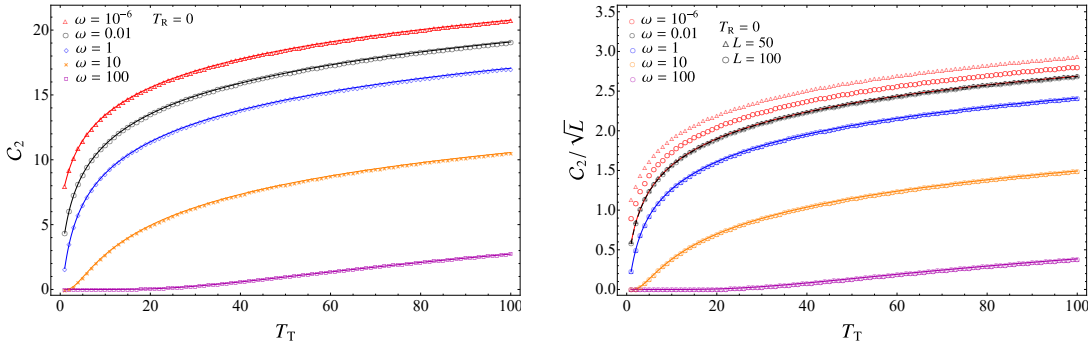

Figure 7. The complexity $\mathcal{C}_2$ for thermal states when $T_R = 0$. Left panel: $\mathcal{C}_2$ for a chain of length $L = 50$ as function of T_T, reported for different values of $\omega_R = \omega_T = \omega$. The solid lines correspond to (9.43). Right panel: $\mathcal{C}_2/\sqrt{L}$ as function of T_T for different values of $\omega_R = \omega_T = \omega$ and two values of L. The solid lines correspond to (9.52). The dashed black line and the solid red line are collapsed on the curve (9.53).

taken for $\kappa = m = 1$, hence $\widetilde{T}_R = T_R$ and $\widetilde{T}_T = T_T$. Notice that these numerical results display an example of spectrum complexity for thermal states, as discussed in the text below (9.47).

In figure 6 we consider the complexity as function of the length L of the periodic harmonic chain. For the sake of simplicity, the reference state is the ground state (i.e. $T_R = 0$) and the target state is a thermal state with temperature T_T. In the left panels $\omega = 1$, while in the right panels $\omega = 10^{-2}$. In the top panels the data are compared against the expression (9.51) (solid lines), while in the bottom panels the subleading term of the same expression is considered (horizontal solid lines). The data having $\omega = 1$ agree very well with the predictions, while for the ones with $\omega \ll 1$ the agreement is worse because in these cases the values of L considered are not large enough.

In figure 7 the same quantity considered in figure 6 is shown as function of T_T. The increasing behaviour of the curves tells us that the distance between the states increases with T_T, as expected. In the left panel we test numerically the analytic expression (9.43) for $L = 50$ and different values of ω. Instead, in the right panel we test numerically the formula (9.52), obtained in the thermodynamic limit $L \to \infty$: the agreement is very good when $\omega \gtrsim 1$, while it gets worse when $\omega \ll 1$. Thus, when ω is very small, larger values of L should be explored to observe the expected agreement between the numerical data and the curve (9.52). When $T_R = 0$, in the latter case the curves for (9.52) collapse onto the limiting curve (9.53), obtained by setting $\omega_R = \omega_T = 0$.

9.3.3 Optimal path for entanglement hamiltonians and its complexity

In section 6 we have discussed the map that provides the entanglement hamiltonian in terms of the covariance matrix of a mixed state. In the following we explore further the optimal path of entanglement hamiltonian matrices for the periodic harmonic chain in the special case where both the reference and the target states are thermal states.

JHEP12(2020)101

The entanglement hamiltonian matrices $H_{\rm R}$ and $H_{\rm T}$ of a reference state and of a target state that are both thermal can be obtained by applying the map (6.3) to the covariance matrix $\gamma_{\rm th} = Q_{\rm th} \oplus P_{\rm th}$ introduced in section 9.3.1, whose Williamson's decomposition is (9.39). The symplectic spectrum of the entanglement hamiltonian matrix of a thermal state can be easily obtained by plugging (9.40) into (6.7), finding

$$\varepsilon_{{\rm th},k} = \frac{\Omega_k}{\widetilde{T}} \qquad\qquad k = 1, \dots, L\,. \tag{9.54}$$

This provides the elements of the diagonal matrix $\mathcal{E}_{\rm th}$ entering in the Williamson's decomposition (6.6) for the thermal state. Comparing (9.54) with (9.36) and (9.40), we get $\varepsilon_{{\rm th},k} = \beta\sigma_{{\rm phys},k}$, as discussed in section 6 for the thermal states in any number of dimensions.

The distance (6.11) between $H_{\rm R}$ and $H_{\rm T}$ can be evaluated by employing (9.26) and (9.54). The result reads

$$d(H_{\rm R}, H_{\rm T}) = \sqrt{\sum_{k=1}^{L} \left\{ \left[\log\left(\frac{T_{\rm R}}{T_{\rm T}}\right) \right]^2 + \left[\log\left(\frac{T_{\rm R}\,\Omega_{{\rm T},k}}{T_{\rm T}\,\Omega_{{\rm R},k}}\right) \right]^2 \right\}} \tag{9.55}$$

which can be obtained also by replacing $\mathcal{D}_{\rm th}$ with $\mathcal{E}_{\rm th}$ in (9.47).

In the special case of $\widetilde{\omega}_{\rm R} = \widetilde{\omega}_{\rm T}$, the summation in (9.55) can be easily performed, finding

$$d(H_{\rm R}, H_{\rm T}) = \sqrt{2L}\,\big|\log(\beta_{\rm T}/\beta_{\rm R})\big| \tag{9.56}$$

which corresponds to (6.14) specified to the one-dimensional harmonic chain. In this case we can employ the discussion made in section 6 for the cases where $W_{\rm TR} = \mathbf{1}$ (see (9.26)) to conclude that $d(\gamma_{\rm R}, \gamma_{\rm T}) \leqslant d(H_{\rm R}, H_{\rm T})$.

In the periodic harmonic chain the Williamson's decomposition of the optimal circuit connecting $H_{\rm R}$ and $H_{\rm T}$ is given by (6.16), with the symplectic eigenvalues (9.10) and the symplectic matrix (9.11). Thus, the symplectic eigenvalues for the matrix labeled by $s \in [0, 1]$ along this optimal circuit are

$$\sigma_{k,s} = \beta_{\rm T}^{s}\,\beta_{\rm R}^{1-s}\,\sqrt{\kappa/m}\,\Omega_k \tag{9.57}$$

where Ω_k is the dispersion relation (9.9). This means that the optimal circuit is made by the entanglement hamiltonian matrices of thermal states, as also discussed in section 6. This is not a feature of the optimal circuit connecting the covariance matrices of two thermal states, as discussed in section 2.6. This discrepancy is consistent with the fact that the map (6.3) does not send geodesics into geodesics.

9.4 Mutual complexity of TFD's

The thermofield double state (TFD) is a pure state obtained by entangling two equal copies of the harmonic lattice and such that a thermal state of the original system is obtained after the partial trace over one of the two copies. A detailed analysis of the TFD and of the circuit complexity between two TFD's is reported in the appendix F.

JHEP12(2020)101

It is worth comparing the circuit complexity of two thermal states with the one obtained from the corresponding TFD's. Following [23], we introduce the mutual complexity for the TFD's as

$$\mathcal{M}_{\rm TFD}(\tilde{\omega}_{\rm R},\tilde{\omega}_{\rm T},\tilde{\beta}_{\rm R},\tilde{\beta}_{\rm T}) = 2\,\mathcal{C}^2_{\rm th}(\tilde{\omega}_{\rm R},\tilde{\omega}_{\rm T},\tilde{\beta}_{\rm R},\tilde{\beta}_{\rm T}) - \mathcal{C}^2_{\rm TFD}(\tilde{\omega}_{\rm R},\tilde{\omega}_{\rm T},\tilde{\beta}_{\rm R},\tilde{\beta}_{\rm T}) \tag{9.58}$$

where $\mathcal{C}_{\rm th}$ and $\mathcal{C}_{\rm TFD}$ are given by (9.43) and (F.38) respectively. More explicitly, (9.58) reads

$$\begin{aligned}
&\mathcal{M}_{\rm TFD}(\tilde{\omega}_{\rm R},\tilde{\omega}_{\rm T},\tilde{\beta}_{\rm R},\tilde{\beta}_{\rm T}) \qquad (9.59)\\
&= \frac{1}{4}\sum_{k=1}^{L}\Bigg\{\left[\log\left(\frac{\Omega_{{\rm R},k}\coth\left(\tilde{\beta}_{\rm R}\Omega_{{\rm R},k}/2\right)}{\Omega_{{\rm T},k}\coth\left(\tilde{\beta}_{\rm T}\Omega_{{\rm T},k}/2\right)}\right)\right]^2 - \left[\log\left(\frac{\Omega_{{\rm R},k}\coth\left(\tilde{\beta}_{\rm R}\Omega_{{\rm R},k}/4\right)}{\Omega_{{\rm T},k}\coth\left(\tilde{\beta}_{\rm T}\Omega_{{\rm T},k}/4\right)}\right)\right]^2\\
&\quad + \left[\log\left(\frac{\Omega_{{\rm R},k}\coth\left(\tilde{\beta}_{\rm T}\Omega_{{\rm T},k}/2\right)}{\Omega_{{\rm T},k}\coth\left(\tilde{\beta}_{\rm R}\Omega_{{\rm R},k}/2\right)}\right)\right]^2 - \left[\log\left(\frac{\Omega_{{\rm R},k}\coth\left(\tilde{\beta}_{\rm T}\Omega_{{\rm T},k}/4\right)}{\Omega_{{\rm T},k}\coth\left(\tilde{\beta}_{\rm R}\Omega_{{\rm R},k}/4\right)}\right)\right]^2\Bigg\}
\end{aligned}$$

which can be written also in terms of $\Omega_{{\rm M,N},k}$ defined in (9.44) as follows

$$\begin{aligned}
&\mathcal{M}_{\rm TFD}(\tilde{\omega}_{\rm R},\tilde{\omega}_{\rm T},\tilde{\beta}_{\rm R},\tilde{\beta}_{\rm T})\\
&= \frac{1}{4}\sum_{k=1}^{L}\Bigg\{\left[\log\left(\frac{\Omega_{{\rm R,R},k}}{\Omega_{{\rm T,T},k}}\right)\right]^2 + \left[\log\left(\frac{\Omega_{{\rm R,T},k}}{\Omega_{{\rm T,R},k}}\right)\right]^2 \qquad (9.60)\\
&\quad - \left[\log\left(\frac{\Omega_{{\rm R,R},k}}{\Omega_{{\rm T,T},k}}\right) + \log\left(\frac{\cosh\left(\tilde{\beta}_{\rm T}\Omega_{{\rm T},k}/2\right)\left(\cosh\left(\tilde{\beta}_{\rm R}\Omega_{{\rm R},k}/2\right)-1\right)}{\cosh\left(\tilde{\beta}_{\rm R}\Omega_{{\rm R},k}/2\right)\left(\cosh\left(\tilde{\beta}_{\rm T}\Omega_{{\rm T},k}/2\right)-1\right)}\right)\right]^2\\
&\quad - \left[\log\left(\frac{\Omega_{{\rm R,T},k}}{\Omega_{{\rm T,R},k}}\right) + \log\left(\frac{\cosh\left(\tilde{\beta}_{\rm R}\Omega_{{\rm R},k}/2\right)\left(\cosh\left(\tilde{\beta}_{\rm T}\Omega_{{\rm T},k}/2\right)-1\right)}{\cosh\left(\tilde{\beta}_{\rm T}\Omega_{{\rm T},k}/2\right)\left(\cosh\left(\tilde{\beta}_{\rm R}\Omega_{{\rm R},k}/2\right)-1\right)}\right)\right]^2\Bigg\}.
\end{aligned}$$

After expanding the squares and a bit of manipulation, one obtains

$$\begin{aligned}
&\mathcal{M}_{\rm TFD}(\tilde{\omega}_{\rm R},\tilde{\omega}_{\rm T},\tilde{\beta}_{\rm R},\tilde{\beta}_{\rm T}) \qquad (9.61)\\
&= \frac{1}{2}\sum_{k=1}^{L} F_{{\rm TR},k}\left\{2\log\left[\frac{\coth\left(\tilde{\beta}_{\rm T}\Omega_{{\rm T},k}/2\right)}{\coth\left(\tilde{\beta}_{\rm R}\Omega_{{\rm R},k}/2\right)}\right] - F_{{\rm TR},k}\right\} \qquad (9.62)\\
&= \frac{1}{2}\sum_{k=1}^{L} F_{{\rm TR},k}\left\{\log\left[\frac{\coth^2\left(\tilde{\beta}_{\rm T}\Omega_{{\rm T},k}/2\right)\cosh\left(\tilde{\beta}_{\rm R}\Omega_{{\rm R},k}/2\right)\left(\cosh\left(\tilde{\beta}_{\rm T}\Omega_{{\rm T},k}/2\right)-1\right)}{\coth^2\left(\tilde{\beta}_{\rm R}\Omega_{{\rm R},k}/2\right)\cosh\left(\tilde{\beta}_{\rm T}\Omega_{{\rm T},k}/2\right)\left(\cosh\left(\tilde{\beta}_{\rm R}\Omega_{{\rm R},k}/2\right)-1\right)}\right]\right\}
\end{aligned}$$

where

$$F_{{\rm TR},k} = \log\left(\frac{\cosh\left(\tilde{\beta}_{\rm T}\Omega_{{\rm T},k}/2\right)\left(\cosh\left(\tilde{\beta}_{\rm R}\Omega_{{\rm R},k}/2\right)-1\right)}{\cosh\left(\tilde{\beta}_{\rm R}\Omega_{{\rm R},k}/2\right)\left(\cosh\left(\tilde{\beta}_{\rm T}\Omega_{{\rm T},k}/2\right)-1\right)}\right). \tag{9.63}$$

For fixed k, the argument of the sum in (9.61) only depends on $\tilde{\beta}_{\rm T}\Omega_{{\rm T},k}$ and $\tilde{\beta}_{\rm R}\Omega_{{\rm R},k}$ and it is symmetric under the exchange of T and R; hence we can fix $\tilde{\beta}_{\rm T}\Omega_{{\rm T},k} > \tilde{\beta}_{\rm R}\Omega_{{\rm R},k}$ for every k without loss of generality. This allows to show that every term of the sum (9.61) is negative[20] and therefore $\mathcal{M}_{\rm TFD}(\tilde{\omega}_{\rm R},\tilde{\omega}_{\rm T},\tilde{\beta}_{\rm R},\tilde{\beta}_{\rm T})$ is always negative.

[20] We use that $\frac{\cosh(x/2)}{\cosh(x/2)-1}$ is a monotonically decreasing function and that $\frac{\coth^2(x/2)(\cosh(x/2)-1)}{\cosh(x/2)}$ is a monotonically increasing function when $x>0$. This implies that $F_{{\rm TR},k}<0$, while the function within the curly brackets in the last sum of (9.61) is positive for any value of k.

JHEP12(2020)101

The formula (9.59) can be generalised to the case where $\kappa_{\rm R} \neq \kappa_{\rm T}$ as discussed in the final part of section 9.1. This leads to

$$\begin{aligned}
&\mathcal{M}_{\rm TFD}(\omega_{\rm R},\omega_{\rm T},\kappa_{\rm R},\kappa_{\rm T},\beta_{\rm R},\beta_{\rm T}) \qquad (9.64)\\
&= \frac{1}{4}\sum_{k=1}^{L}\Bigg\{\Bigg[\log\left(\frac{\sigma_{{\rm phys,R},k}\coth\left(\beta_{\rm R}\sigma_{{\rm phys,R},k}/2\right)}{\sigma_{{\rm phys,T},k}\coth\left(\beta_{\rm T}\sigma_{{\rm phys,T},k}/2\right)}\right)\Bigg]^2\\
&-\Bigg[\log\left(\frac{\sigma_{{\rm phys,R},k}\coth\left(\beta_{\rm R}\sigma_{{\rm phys,R},k}/4\right)}{\sigma_{{\rm phys,T},k}\coth\left(\beta_{\rm T}\sigma_{{\rm phys,T},k}/4\right)}\right)\Bigg]^2+\Bigg[\log\left(\frac{\sigma_{{\rm phys,R},k}\coth\left(\beta_{\rm T}\sigma_{{\rm phys,T},k}/2\right)}{\sigma_{{\rm phys,T},k}\coth\left(\beta_{\rm R}\sigma_{{\rm phys,R},k}/2\right)}\right)\Bigg]^2\\
&-\Bigg[\log\left(\frac{\sigma_{{\rm phys,R},k}\coth\left(\beta_{\rm T}\sigma_{{\rm phys,T},k}/4\right)}{\sigma_{{\rm phys,T},k}\coth\left(\beta_{\rm R}\sigma_{{\rm phys,R},k}/4\right)}\right)\Bigg]^2\Bigg\}
\end{aligned}$$

where $\sigma_{{\rm phys,S},k}$ with ${\rm S}=\{{\rm R},{\rm T}\}$ has been defined in (9.10). In the special case where the reference state is the unentangled product ground state, i.e. $\kappa_{\rm R}=0$ and $\beta_{\rm R}\to\infty$, we find that (9.64) in this limit becomes

$$\begin{aligned}
&\mathcal{M}_{\rm TFD}(\omega_{\rm R},\omega_{\rm T},\kappa_{\rm R}=0,\kappa_{\rm T},\beta_{\rm R}\to\infty,\beta_{\rm T}) \qquad (9.65)\\
&= \frac{1}{4}\sum_{k=1}^{L}\Bigg\{\Bigg[\log\left(\frac{\omega_{\rm R}}{\sigma_{{\rm phys,T},k}\coth\left(\beta_{\rm T}\sigma_{{\rm phys,T},k}/2\right)}\right)\Bigg]^2\\
&-\Bigg[\log\left(\frac{\omega_{\rm R}}{\sigma_{{\rm phys,T},k}\coth\left(\beta_{\rm T}\sigma_{{\rm phys,T},k}/4\right)}\right)\Bigg]^2+\Bigg[\log\left(\frac{\omega_{\rm R}\coth\left(\beta_{\rm T}\sigma_{{\rm phys,T},k}/2\right)}{\sigma_{{\rm phys,T},k}}\right)\Bigg]^2\\
&-\Bigg[\log\left(\frac{\omega_{\rm R}\coth\left(\beta_{\rm T}\sigma_{{\rm phys,T},k}/4\right)}{\sigma_{{\rm phys,T},k}}\right)\Bigg]^2\Bigg\}
\end{aligned}$$

The thermodynamic limit $L\to\infty$ of (9.59) gives

$$\mathcal{M}_{\rm TFD}(\tilde\omega_{\rm R},\tilde\omega_{\rm T},\tilde\beta_{\rm R},\tilde\beta_{\rm T}) \;=\; a_{\rm TFD}(\tilde\omega_{\rm R},\tilde\omega_{\rm T},\tilde\beta_{\rm R},\tilde\beta_{\rm T})\,L+\ldots \qquad (9.66)$$

where the coefficient of the linear divergence can be written in terms $\Omega_{{\rm S},\theta}$ in (9.29) as

$$\begin{aligned}
&a_{\rm TFD}(\tilde\omega_{\rm R},\tilde\omega_{\rm T},\tilde\beta_{\rm R},\tilde\beta_{\rm T}) \qquad (9.67)\\
&= \frac{1}{4\pi}\int_0^\pi\Bigg\{\Bigg[\log\left(\frac{\Omega_{{\rm R},\theta}\coth\left(\tilde\beta_{\rm R}\Omega_{{\rm R},\theta}/2\right)}{\Omega_{{\rm T},\theta}\coth\left(\tilde\beta_{\rm T}\Omega_{{\rm T},\theta}/2\right)}\right)\Bigg]^2-\Bigg[\log\left(\frac{\Omega_{{\rm R},\theta}\coth\left(\tilde\beta_{\rm R}\Omega_{{\rm R},\theta}/4\right)}{\Omega_{{\rm T},\theta}\coth\left(\tilde\beta_{\rm T}\Omega_{{\rm T},\theta}/4\right)}\right)\Bigg]^2\\
&+\Bigg[\log\left(\frac{\Omega_{{\rm R},\theta}\coth\left(\tilde\beta_{\rm T}\Omega_{{\rm T},\theta}/2\right)}{\Omega_{{\rm T},\theta}\coth\left(\tilde\beta_{\rm R}\Omega_{{\rm R},\theta}/2\right)}\right)\Bigg]^2-\Bigg[\log\left(\frac{\Omega_{{\rm R},\theta}\coth\left(\tilde\beta_{\rm T}\Omega_{{\rm T},\theta}/4\right)}{\Omega_{{\rm T},\theta}\coth\left(\tilde\beta_{\rm R}\Omega_{{\rm R},\theta}/4\right)}\right)\Bigg]^2\Bigg\}\,d\theta\,.
\end{aligned}$$

We remark that the massless limit of $\mathcal{M}_{\rm TFD}/L$ diverges when $L<\infty$, while it is finite once $L\to\infty$ is considered. Indeed, by setting $\tilde\omega_{\rm R}=\tilde\omega_{\rm T}=0$ in (9.67) we find

$$\begin{aligned}
&a_{\rm TFD}(\tilde\omega_{\rm R}=0,\tilde\omega_{\rm T}=0,\tilde\beta_{\rm R},\tilde\beta_{\rm T}) \qquad (9.68)\\
&\qquad=\int_0^\pi\Bigg\{\Bigg[\log\left(\frac{\coth\left(\tilde\beta_{\rm R}\sin\theta\right)}{\coth\left(\tilde\beta_{\rm T}\sin\theta\right)}\right)\Bigg]^2-\Bigg[\log\left(\frac{\coth\left(\tilde\beta_{\rm R}\sin\theta/2\right)}{\coth\left(\tilde\beta_{\rm T}\sin\theta/2\right)}\right)\Bigg]^2\Bigg\}\,\frac{d\theta}{2\pi}\,.
\end{aligned}$$

This feature has been observed also for the complexity of pure states (section 9.2) and for the complexity of thermal states (section 9.3).

JHEP12(2020)101

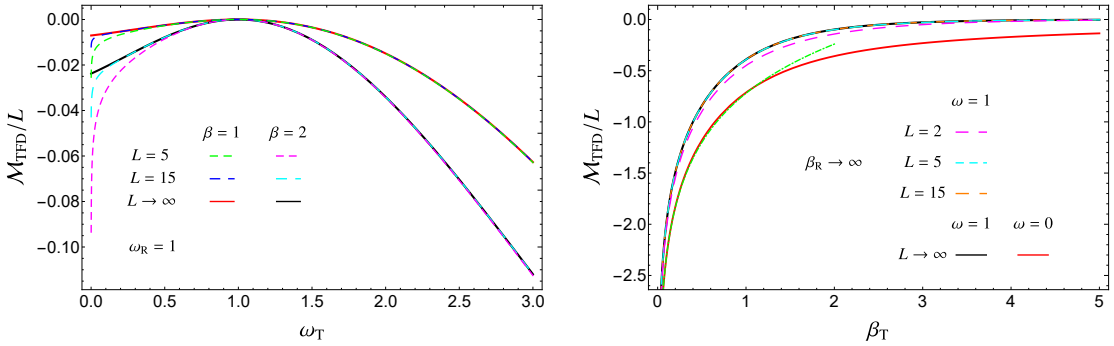

Figure 8. Comparison between the mutual complexity for the TFD state (9.59) and its thermodynamic limit in the periodic harmonic chain (here $\kappa = m = 1$). In the left panel we show $\mathcal{M}_{\rm TFD}/L$ as function of $\omega_{\rm T}$ setting $\omega_{\rm R} = 1$ and considering two values of $\beta_{\rm R} = \beta_{\rm T} \equiv \beta$ and two values of L (dashed curves). We also report $a_{\rm TFD}$ in (9.67) for the same values of the parameters (solid curves). In the right panel the dependence on $\beta_{\rm T}$ is investigated by plotting (9.59) for three different values of L (dashed curves) and (9.67) (black solid curve) both for $\beta_{\rm R} \to \infty$ and $\omega_{\rm R} = \omega_{\rm T} \equiv \omega = 1$. The massless limit in (9.69) is also reported (red solid curve) and its small $\beta_{\rm T}$ behaviour in (9.70) is checked (green dot-dashed curve).

In the limit $\tilde{\beta}_{\rm R} \to \infty$ both the TFD in (F.8) and the thermal reference state become the product of two ground states. In this regime, (9.68) slightly simplifies to

$$a_{\rm TFD}(\tilde{\omega}_{\rm R} = 0, \tilde{\omega}_{\rm T} = 0, \tilde{\beta}_{\rm R} \to \infty, \tilde{\beta}_{\rm T}) \qquad (9.69)$$
$$= \int_0^\pi \left\{ \left[\log\left(\coth\left(\tilde{\beta}_{\rm T} \sin\theta \right) \right) \right]^2 - \left[\log\left(\coth\left(\tilde{\beta}_{\rm T} \sin\theta/2 \right) \right) \right]^2 \right\} \frac{d\theta}{2\pi}$$

which depends only on $\tilde{\beta}_{\rm T}$ and can be easily studied. This function is negative for every value of $\tilde{\beta}_{\rm T}$ and it vanishes when $\tilde{\beta}_{\rm T} \to \infty$, as expected. When $\tilde{\beta}_{\rm T} \to 0$ in (9.69), we find the following logarithmic divergence

$$a_{\rm TFD}(\tilde{\omega}_{\rm R} = 0, \tilde{\omega}_{\rm T} = 0, \tilde{\beta}_{\rm R} \to \infty, \tilde{\beta}_{\rm T}) \;=\; \log 2 \left(\log \tilde{\beta}_{\rm T} - \frac{3}{2} \log 2 \right) + \dots \,. \qquad (9.70)$$

In figure 8 we compare the mutual complexity for the TFD in (9.59) with its thermodynamic limit in (9.66) for various values of the parameters. In the left panel we show $\mathcal{M}_{\rm TFD}/L$ (dashed lines) as function of $\omega_{\rm T}$ for fixed $\omega_{\rm R} = 1$ and for two values of $\beta_{\rm R} = \beta_{\rm T} \equiv \beta$. As L increases, the dashed curves approach the solid curves representing $a_{\rm TFD}$ given in (9.67). When $\omega_{\rm T} \to 0$, $\mathcal{M}_{\rm TFD}/L$ evalueted for finite L diverges, while its thermodynamic limit is finite, as observed above. In the right panel we show $\mathcal{M}_{\rm TFD}/L$ as function of $\beta_{\rm T}$ when $\beta_{\rm R} \to \infty$ and $\omega_{\rm R} = \omega_{\rm T} \equiv \omega = 1$. Remarkably, the curves obtained for finite number of sites coincide with their thermodynamic limit already for $L = 5$. In the same panel we plot $a_{\rm TFD}(\omega_{\rm R} = 0, \omega_{\rm T} = 0, \beta_{\rm R} \to \infty, \beta_{\rm T})$ in (9.69) (red solid curve), checking also that its behaviour for $\beta_{\rm T} \ll 1$ is well reproduced by (9.70) (green dot-dashed curve).

We find it worth considering the mutual complexity for the thermofield double state in the continuum limit procedure where $\epsilon = \sqrt{m/\kappa} \to 0$ and $L \to \infty$, while $\tilde{L} \equiv \epsilon L$ is kept fixed, as done also in [23] for the purification complexity. In this limiting regime, the sum

JHEP12(2020)101

over dimensionless numbers k becomes an integral over the positive momenta p. Moreover, from (9.9), (9.4) and (9.36), we find that $\Omega_{\mathrm{S},k} \to \epsilon\sqrt{\omega_{\mathrm{S}}^2 + p^2} \equiv \epsilon E_{\mathrm{S},p}$ and $\tilde{\beta}_{\mathrm{S}}\Omega_{\mathrm{S},k} \to \beta_{\mathrm{S}} E_{\mathrm{S},p}$. Thus, (9.59) becomes

$$\begin{aligned}
&\mathcal{M}_{\mathrm{TFD}}(\omega_{\mathrm{R}}, \omega_{\mathrm{T}}, \beta_{\mathrm{R}}, \beta_{\mathrm{T}}) \qquad (9.71)\\
&\quad = \frac{\tilde{L}}{4\pi}\int_0^\infty \Bigg\{ \left[\log\left(\frac{E_{\mathrm{R},p}\coth\left(\beta_{\mathrm{R}}E_{\mathrm{R},p}/2\right)}{E_{\mathrm{T},p}\coth\left(\beta_{\mathrm{T}}E_{\mathrm{T},p}/2\right)}\right)\right]^2 - \left[\log\left(\frac{E_{\mathrm{R},p}\coth\left(\beta_{\mathrm{R}}E_{\mathrm{R},p}/4\right)}{E_{\mathrm{T},p}\coth\left(\beta_{\mathrm{T}}E_{\mathrm{T},p}/4\right)}\right)\right]^2\\
&\qquad + \left[\log\left(\frac{E_{\mathrm{R},p}\coth\left(\beta_{\mathrm{T}}E_{\mathrm{T},p}/2\right)}{E_{\mathrm{T},p}\coth\left(\beta_{\mathrm{R}}E_{\mathrm{R},p}/2\right)}\right)\right]^2 - \left[\log\left(\frac{E_{\mathrm{R},p}\coth\left(\beta_{\mathrm{T}}E_{\mathrm{T},p}/4\right)}{E_{\mathrm{T},p}\coth\left(\beta_{\mathrm{R}}E_{\mathrm{R},p}/4\right)}\right)\right]^2 \Bigg\} dp
\end{aligned}$$

Notice that, given $\mathrm{S} = \{\mathrm{R}, \mathrm{T}\}$, since $E_{\mathrm{S},p} \sim p$ when $p \gg \omega_{\mathrm{S}}$, all the four terms of the integrand vanish when $p \to \infty$ and the four resulting integrals in (9.71) are separately UV finite.

Instead, if we consider the mutual complexity of the TFD when the reference state is the unentangled product state given in (9.65) in this limiting regime, the UV finiteness is due to a non trivial cancellation among divergent contributions. In this case, from (9.10), we have $\sigma_{\mathrm{phys},\mathrm{S},k} \to \sqrt{\omega_{\mathrm{S}}^2 + p^2} \equiv E_{\mathrm{S},p}$ with $\mathrm{S} = \{\mathrm{R}, \mathrm{T}\}$; hence (9.65) becomes

$$\begin{aligned}
&\mathcal{M}_{\mathrm{TFD}}(\omega_{\mathrm{R}}, \omega_{\mathrm{T}}, \beta_{\mathrm{R}} \to \infty, \beta_{\mathrm{T}}) \qquad (9.72)\\
&\quad = \frac{\tilde{L}}{4\pi}\int_0^\infty \Bigg\{ \left[\log\left(\frac{\omega_{\mathrm{R}}}{E_{\mathrm{T},p}\coth\left(\beta_{\mathrm{T}}E_{\mathrm{T},p}/2\right)}\right)\right]^2 - \left[\log\left(\frac{\omega_{\mathrm{R}}}{E_{\mathrm{T},p}\coth\left(\beta_{\mathrm{T}}E_{\mathrm{T},p}/4\right)}\right)\right]^2\\
&\qquad + \left[\log\left(\frac{\omega_{\mathrm{R}}\coth\left(\beta_{\mathrm{T}}E_{\mathrm{T},p}/2\right)}{E_{\mathrm{T},p}}\right)\right]^2 - \left[\log\left(\frac{\omega_{\mathrm{R}}\coth\left(\beta_{\mathrm{T}}E_{\mathrm{T},p}/4\right)}{E_{\mathrm{T},p}}\right)\right]^2 \Bigg\} dp
\end{aligned}$$

Up to the global factor $\frac{\tilde{L}}{4\pi}$, both the terms of the integrand coming from $2\mathcal{C}_{\mathrm{th}}^2$ in (9.58), i.e. the first one and the third one, diverge as $2[\log(p/\omega_{\mathrm{R}})]^2$ when $p \to \infty$ while both the second term and the fourth term, which originate from $\mathcal{C}_{\mathrm{TFD}}^2$ in (9.58), diverge as $-2[\log(p/\omega_{\mathrm{R}})]^2$. Because of the relative factor 2 between $\mathcal{C}_{\mathrm{th}}^2$ and $\mathcal{C}_{\mathrm{TFD}}^2$ in the definition (9.58), these UV divergences cancel in (9.72). This feature has been first observed in [23] for the mutual complexity of the thermofield double state evaluated through the thermal purification complexity.

9.5 Reduced density matrices

Important mixed states to explore are the reduced density matrices of a subsystem A.

Consider the density matrix $\hat{\rho}_{\mathrm{R}}$ and $\hat{\rho}_{\mathrm{T}}$ of the reference and of the target states respectively and introduce a spatial bipartition $A \cup B$ of the system that induces a factorisation of the Hilbert space, as already discussed in section 6. For the Gaussian states that we are interested in, let us denote by $\gamma_{\mathrm{R},A}$ and $\gamma_{\mathrm{T},A}$ the reduced covariance matrices corresponding to the subsystem A, that characterise the reduced density matrices $\hat{\rho}_{\mathrm{R},A} \equiv \mathrm{Tr}_B\hat{\rho}_{\mathrm{R}}$ and $\hat{\rho}_{\mathrm{T},A} \equiv \mathrm{Tr}_B\hat{\rho}_{\mathrm{T}}$ respectively. We remark that, whenever $B \neq \emptyset$, the reduced density matrices $\hat{\rho}_{\mathrm{R},A}$ and $\hat{\rho}_{\mathrm{T},A}$ are mixed states, even when $\hat{\rho}_{\mathrm{R}}$ and $\hat{\rho}_{\mathrm{T}}$ are pure states. The reduced covariance matrix γ_A is obtained by just restricting the indices of the covariance matrix of the entire system to the ranges identifying the subsystem A.

JHEP12(2020)101

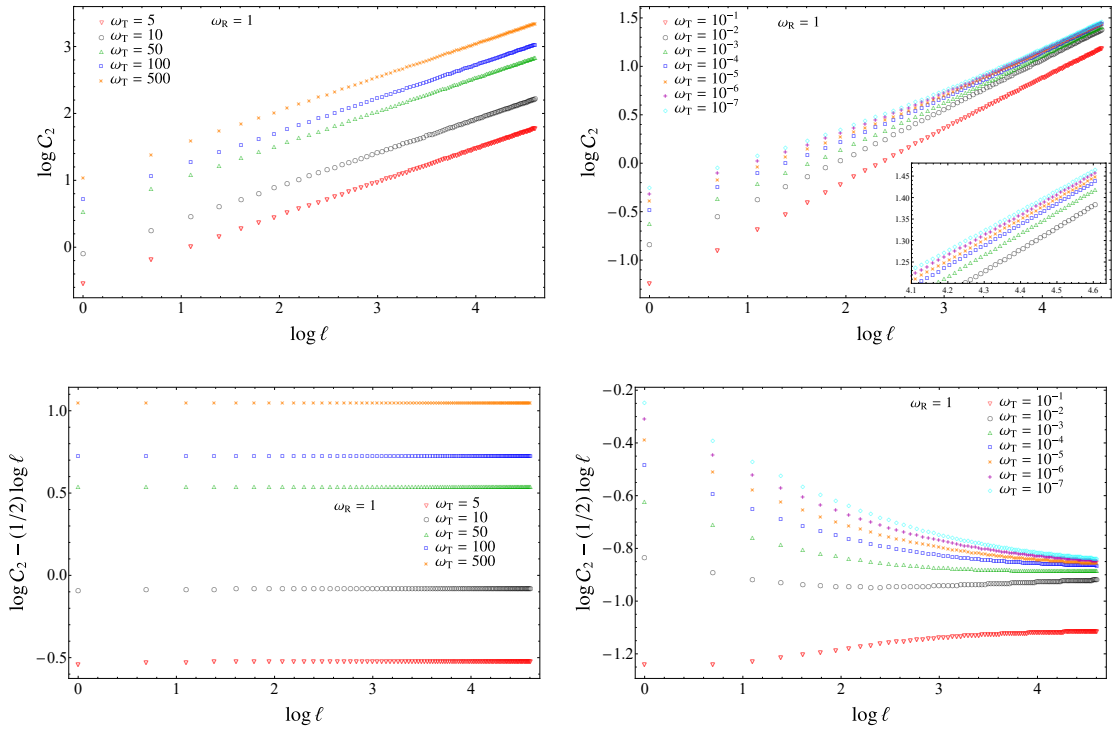

Figure 9. Subregion complexity $\mathcal{C}_2$ for an interval made by ℓ sites in an infinite harmonic chain as function of ℓ. The chain is in its ground state and $\omega_R \neq \omega_T$. Here $\kappa = m = 1$; hence $\tilde{\omega}_R = \omega_R$ and $\tilde{\omega}_T = \omega_T$. We fix $\omega_R = 1$, considering various values for ω_T: $\omega_T > \omega_R$ in the left panels and $\omega_T < \omega_R$ in the right panels. The subregion complexity $\mathcal{C}_2$ is reported in the top panels, while its subleading term is studied in the bottom panels.

By applying (2.33) to these mixed states, one obtains the subregion complexity

$$\mathcal{C}_2 = \frac{1}{2\sqrt{2}} \sqrt{\mathrm{Tr}\left\{ \left[\log(\gamma_{T,A}\, \gamma_{R,A}^{-1}) \right]^2 \right\}}. \tag{9.73}$$

In the context of the gauge/gravity correspondence, the subregion complexity has been studied e.g. in [10, 29, 141, 142].

In the following we provide numerical results of this complexity only for the simplest case where A is an interval in an infinite harmonic chain and for some convenient reference and target states. In order to construct the reduced covariance matrices, in this case we need the two-point correlators of the harmonic chain in the thermodynamic limit. For a thermal state, they can be found by taking the limit $L \to \infty$ of (9.34) and (9.35). The results can be written in terms of $\Omega_\theta = \sqrt{\tilde{\omega}^2 + 4\,(\sin\theta)^2}$ (see (9.29)) as follows

$$\langle \hat{q}_i \hat{q}_j \rangle_\beta = \frac{1}{2\pi} \int_0^\pi \frac{\coth[\Omega_\theta/(2\widetilde{T})]}{\Omega_\theta} \cos[2\theta\,(i-j)]\, d\theta \tag{9.74}$$

$$\langle \hat{p}_i \hat{p}_j \rangle_\beta = \frac{1}{2\pi} \int_0^\pi \Omega_\theta \coth[\Omega_\theta/(2\widetilde{T})] \cos[2\theta\,(i-j)]\, d\theta\,. \tag{9.75}$$

JHEP12(2020)101

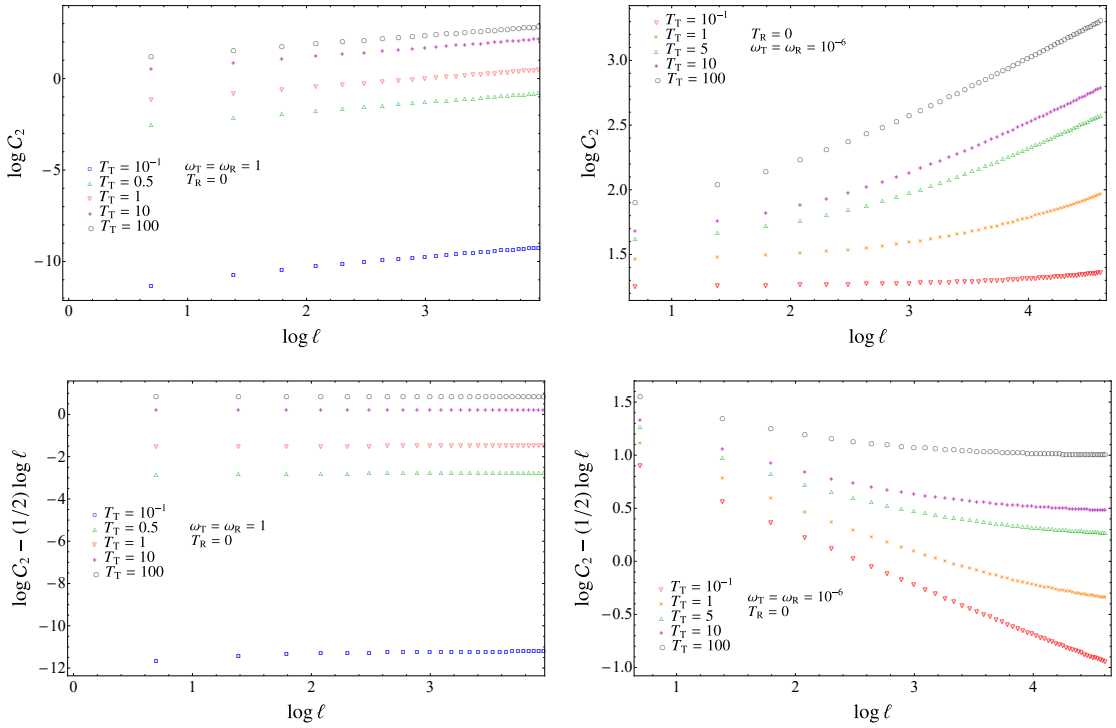

Figure 10. Subregion complexity $\mathcal{C}_2$ for an interval made by ℓ sites in an infinite harmonic chain as function of ℓ. The infinite harmonic chain is in a thermal state and $T_R \neq T_T$. Here $\kappa = m = 1$; hence $\tilde{\omega}_R = \omega_R$, $\tilde{\omega}_T = \omega_T$, $\tilde{T}_R = T_R$ and $\tilde{T}_T = T_T$. We fix $T_R = 0$, considering various values for T_T. We set $\omega_T = \omega_R = 1$ in the left panels and $\omega_T = \omega_R = 10^{-6}$ in the right panels. The subregion complexity $\mathcal{C}_2$ is reported in the top panels, while its subleading term is studied in the bottom panels.

The limit $\widetilde{T} \to 0$ of these expressions provides the two-point correlators in the ground state, namely

$$\langle \hat{q}_i \hat{q}_j \rangle = \frac{1}{2\pi} \int_0^\pi \frac{1}{\Omega_\theta} \cos[2\theta\,(i-j)] d\theta \tag{9.76}$$

$$\langle \hat{p}_i \hat{p}_j \rangle = \frac{1}{2\pi} \int_0^\pi \Omega_\theta \cos[2\theta\,(i-j)]\, d\theta \tag{9.77}$$

whose analytic expressions read [97]

$$\langle \hat{q}_i \hat{q}_j \rangle = \frac{\mu^{i-j+1/2}}{2} \binom{i-j-1/2}{i-j} {}_2F_1(1/2\,, i-j+1/2\,, i-j+1\,, \mu^2\,) \tag{9.78}$$

$$\langle \hat{p}_i \hat{p}_j \rangle = \frac{\mu^{i-j-1/2}}{2} \binom{i-j-3/2}{i-j} {}_2F_1(-1/2\,, i-j-1/2\,, i-j+1\,, \mu^2\,) \tag{9.79}$$

where the parameter μ depends only on $\tilde{\omega}$ as follows

$$\mu \equiv \frac{1}{4}\Big(\tilde{\omega} - \sqrt{\tilde{\omega}^2+4}\Big)^2 . \tag{9.80}$$

In figure 9 we consider the subregion complexity for a block made by ℓ consecutive sites in an infinite harmonic chain when the entire system is in its ground state and $\omega_R \neq \omega_T$.

JHEP12(2020)101

The data reported in figure 9, where we have fixed $\omega_{\rm R} = 1$, allow to conclude that

$$\log \mathcal{C}_2 = \frac{1}{2} \log \ell + O(1) \qquad\qquad \ell \to \infty \tag{9.81}$$

where the additive constant depends on $\omega_{\rm T}$. Comparing the left panels and the right panels, we observe that larger values for ℓ are needed to reach the behaviour (9.81) for these choices of $\omega_{\rm R} > \omega_{\rm T}$. We checked numerically that, when $\omega_{\rm R} \neq 1$, (9.81) holds with a subleading term that depends also on $\omega_{\rm R}$.

In figure 10 we have reported the subregion complexity for a block made by ℓ consecutive sites in an infinite harmonic chain when the entire system is in a thermal state and $\omega_{\rm R} = \omega_{\rm T}$. In particular, we have chosen $T_{\rm R} = 0$ and various values of $T_{\rm T} > 0$. In the left panels we have considered $\omega_{\rm T} = \omega_{\rm R} = 1$, finding a reasonable agreement with (9.81), where the subleading constant term depends on $T_{\rm T}$. In the right panels we have fixed $\omega_{\rm T} = \omega_{\rm R} = 10^{-6}$, finding that the behaviour (9.81) is more difficult to observe as $T_{\rm T} \to 0$ because larger values for ℓ are needed.

9.6 Mutual complexity of reduced density matrices

The complexity of the ground states and of the thermal states, considered in section 9.2 and section 9.3 respectively, grow like $\sqrt{L}$ as $L \to \infty$, where L is the number of sites composing the entire periodic chain. Furthermore, considering an interval made by ℓ sites in an infinite harmonic chain, the numerical results reported in section 9.5 tell us that the subregion complexity for this interval grows like $\sqrt{\ell}$ as $\ell \to \infty$.

Given a spatial subregion A and the density matrices $\hat{\rho}_{\rm R}$ and $\hat{\rho}_{\rm T}$, which can correspond to pure or mixed states, let us denote by $\mathcal{C}_{\rm R,T}(A)$ the subregion complexity between the reduced density matrices $\hat{\rho}_{{\rm R},A}$ and $\hat{\rho}_{{\rm T},A}$ introduced in section 9.5.

In this subsection we consider the cases where the spatial subregion A is bipartite into two complementary spatial subregions A_1 and A_2 such that $A = A_1 \cup A_2$. For this spatial configuration, various entanglement quantifiers like the entanglement entropies [143–148] (see e.g. [149–152] for related calculations in the gauge/gravity correspondence) and the entanglement negativity [100, 101, 153–157] have been studied.

The subregions A_1 and A_2 can be either disjoint or have a non vanishing intersection. Since $\mathcal{C}_{\rm R,T}(A)^2$ grows with the volume of A as the number of sites in A diverges, we are naturally led to introduce the mutual complexity for subregions as follows [23, 141]

$$\mathcal{M}_{\rm R,T}(A_1, A_2) \equiv \mathcal{C}_{\rm R,T}(A_1)^2 + \mathcal{C}_{\rm R,T}(A_2)^2 - \mathcal{C}_{\rm R,T}(A_1 \cup A_2)^2 - \mathcal{C}_{\rm R,T}(A_1 \cap A_2)^2 \tag{9.82}$$

which is finite as the number of sites in A_1 and A_2 diverges.

In an infinite chain, let us consider the mutual complexity when A_1 and A_2 are two equal and disjoint intervals made by ℓ sites and separated by d sites. In figure 11 we report the numerical results of the mutual complexity for this configuration as function of ℓ, while d/ℓ is kept fixed ($d/\ell = 1/2$ for the data in the figure).

In the top and middle panels of figure 11, the reference state and the target state are the ground states of the chains characterised by $\omega_{\rm R}$ and $\omega_{\rm T}$ respectively. The mutual complexity is shown as function of ℓ: for the data shown in each panel $\omega_{\rm R}$ is fixed and

JHEP12(2020)101

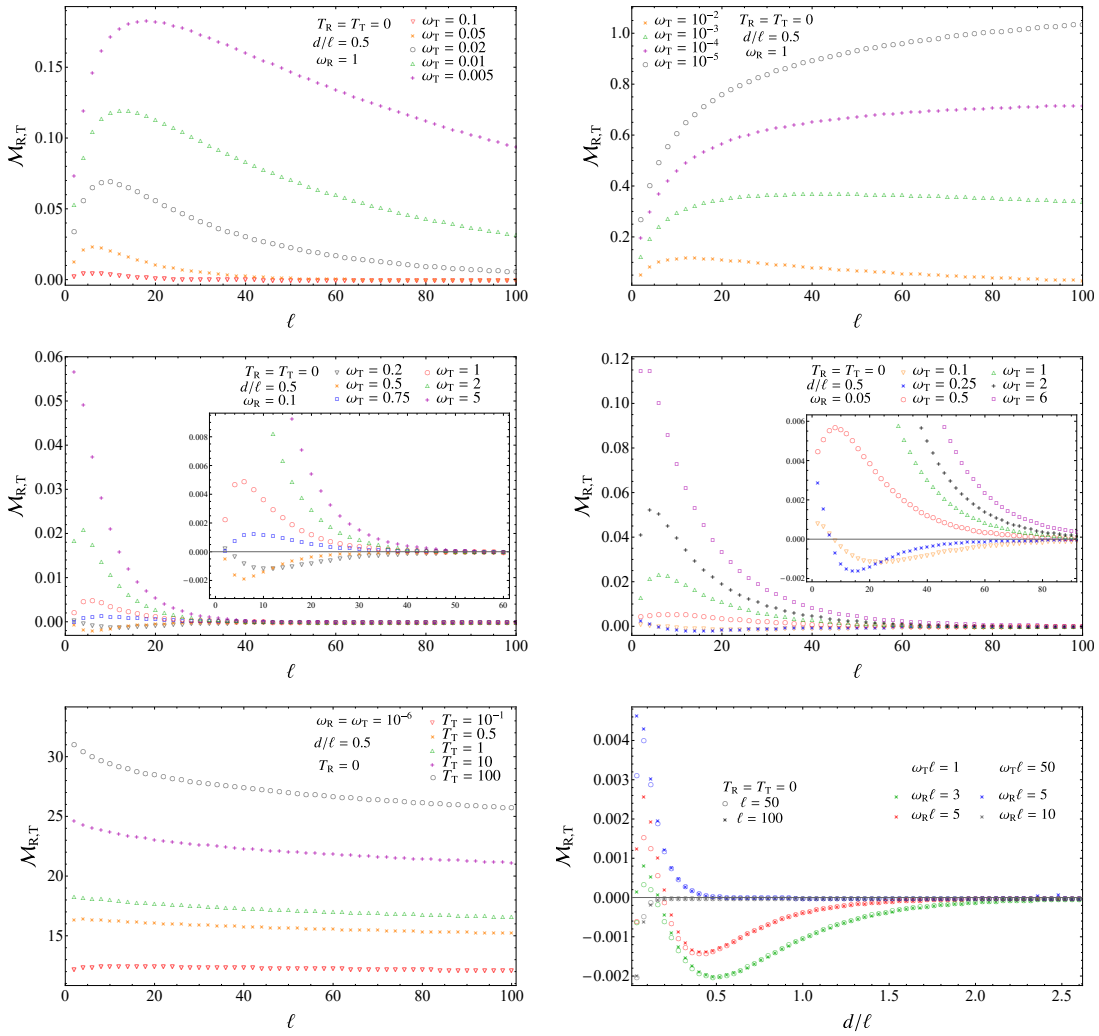

Figure 11. The mutual complexity $\mathcal{M}_{\mathrm{R,T}}$ for two disjoint equal intervals made by ℓ sites and separated by d sites in an infinite harmonic chain. Here $\kappa = m = 1$, hence $\tilde{\omega}_{\mathrm{R}} = \omega_{\mathrm{R}}$, $\tilde{\omega}_{\mathrm{T}} = \omega_{\mathrm{T}}$, $\widetilde{T}_{\mathrm{R}} = T_{\mathrm{R}}$ and $\widetilde{T}_{\mathrm{T}} = T_{\mathrm{T}}$. In the top panels, in the middle panels and in the bottom right panel the chain is in its ground state and $\omega_{\mathrm{R}} \neq \omega_{\mathrm{T}}$: both $\omega_{\mathrm{T}} < \omega_{\mathrm{R}}$ (top panels) and $\omega_{\mathrm{T}} > \omega_{\mathrm{R}}$ (middle panels) are considered. In the bottom left panel, a case involving thermal states with $T_{\mathrm{R}} = 0$ and various $T_{\mathrm{T}} > 0$ is explored. The ratio d/ℓ is kept fixed, except in the bottom right panel, where $\mathcal{M}_{\mathrm{R,T}}$ is shown as function of d/ℓ.

the different curves are associated to different values of ω_{T}. When $\omega_{\mathrm{T}} < \omega_{\mathrm{R}}$ (top panels) the numerical curves for small values of ℓ are increasing until they reach a maximum at a value of ℓ that depends on ω_{T} (top left panel). After the maximum, the mutual complexity decreases with ℓ, but for many values of ω_{T} we cannot appreciate the finite asymptotic limit as $\ell \to \infty$ because larger values of ℓ are needed. In the top right panel, for small enough values of ω_{T}, the values of ℓ that we consider are too small to appreciate the occurrence of a maximum.

When $\omega_{\mathrm{T}} > \omega_{\mathrm{R}}$ (middle panels) a similar behaviour is observed: also in these cases the position of the maximum of the curve depends on ω_{T}. In these cases we observe that, as

JHEP12(2020)101

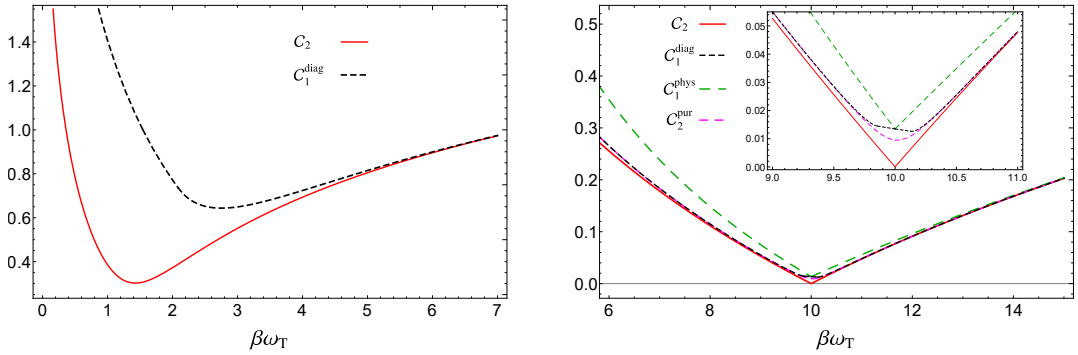

Figure 12. One-mode mixed states: The complexity $\mathcal{C}_2$ from (9.83) (red solid line) and the complexities $\mathcal{C}_1$ and $\mathcal{C}_2^{\rm pur}$ based on the purification complexity, as functions of $\beta\omega_{\rm T}$. The complexity $\mathcal{C}_1$ is evaluated for the diagonal basis from (9.84) (black dashed line) and for the physical basis from (9.85) (green dashed line). The complexity $\mathcal{C}_2^{\rm pur}$ from (9.86) is independent on the basis (magenta dashed line). In the left panel $\beta\omega_{\rm R} = 1$, while in the right panel $\beta\omega_{\rm R} = 10$, hence also $\mathcal{C}_1^{\rm phys}$ and $\mathcal{C}_2^{\rm pur}$ are shown.

$\ell \to \infty$, the mutual complexity decreases until the zero value is reached. By comparing the two panels in the middle, one observes that the value of ℓ where the data vanish increases when $\omega_{\rm R}$ decreases. Furthermore, from the middle panels we can appreciate also the fact that the sign of $\mathcal{M}_{\rm R,T}$ is not definite: it is mainly positive, but for some values of the parameters ($\omega_{\rm T}$ close to $\omega_{\rm R}$ and ℓ sufficiently small) the curve is negative.

In the bottom left panel of figure 11, the reference state is a ground state again, while $\hat{\rho}_{\rm T}$ is a thermal state at temperature $T_{\rm T} > 0$. The curves corresponding to different values of $T_{\rm T} > 0$ decrease with ℓ and the asymptotic value depends on $T_{\rm T}$.

In the bottom right panel of figure 11, the dependence of the mutual complexity on the ratio d/ℓ is considered, when the chain is in its ground state and $\omega_{\rm R} \neq \omega_{\rm T}$. We observe an interesting collapse for data corresponding to fixed values of $\omega_{\rm R}\ell$ and $\omega_{\rm T}\ell$, while ℓ changes. Furthermore, the resulting curve vanishes after a critical value of d/ℓ. This critical ratio increases as either $\omega_{\rm R}\ell$ or $\omega_{\rm T}\ell$ decreases.

9.7 A comparison with the approach based on the purification complexity

We find it worth comparing our results in section 9.3 for the complexity of thermal states with the corresponding ones obtained in [23] through the approach based on the purification complexity, that has been discussed in section 8.2.

The results from [23] that we consider have been obtained using the F_1 cost function (see appendix G for details), while the complexity (2.33) is based on the F_2 cost function. These different cost functions lead to a different scaling with the total size L of the chain. In particular, the F_1 cost function provides a complexity that diverges with L, while the F_2 cost function leads to the milder divergence given by $\sqrt{L}$. This feature, which has been observed already in [17] for pure states, holds also for thermal states, as remarked in [23] for the F_1 cost function and in (9.51) for our approach, that is based on the F_2 cost function. Because of this different scaling, a meaningful comparison between these two approaches can be done only for one-mode mixed states, where $L = 1$. When both the reference and

JHEP12(2020)101

the target states are pure and $L = 1$, both the F_1 cost function and the F_2 cost function provide the same complexity [17].

Let us consider the circuit made by one-mode mixed states where the reference state is the ground state with frequency $\omega_{\rm R}$ and the target state is a thermal state at inverse temperature β with frequency $\omega_{\rm T}$.

Specialising the complexity in (9.48) to this case and for $m = \kappa = 1$ we obtain

$$\mathcal{C}_2 = \frac{1}{2\sqrt{2}} \sqrt{\left[\log\left(\frac{\omega_{\rm R}}{\omega_{\rm T}} \coth\frac{\beta\omega_{\rm T}}{2}\right)\right]^2 + \left[\log\left(\frac{\omega_{\rm T}}{\omega_{\rm R}} \coth\frac{\beta\omega_{\rm T}}{2}\right)\right]^2} \,. \tag{9.83}$$

In this simple case, analytical results have been found in [23] also through the approach based on the purification complexity. The results for the $\mathcal{C}_1$ complexity, which is defined through the F_1 cost function, are basis dependent. In [23] two particular bases have been considered, which have been called physical basis and diagonal basis (see appendix G for their definitions). In the diagonal basis, the analytic result found in [23] for this case reads

$$\mathcal{C}_1^{\rm diag} = \begin{cases} \dfrac{1}{2}\log\left(\dfrac{\omega_{\rm R}}{\omega_{\rm T}}\right) + \dfrac{1}{2}\log\left(\dfrac{\frac{\omega_{\rm R}}{\omega_{\rm T}}\coth\left(\beta\omega_{\rm T}/2\right) - 1}{\frac{\omega_{\rm R}}{\omega_{\rm T}} - \coth\left(\beta\omega_{\rm T}/2\right)}\right) & \coth\left(\dfrac{\beta\omega_{\rm T}}{4}\right) \leqslant \dfrac{\omega_{\rm R}}{\omega_{\rm T}} \\ \log\left[\coth\left(\beta\omega_{\rm T}/4\right)\right] & \tanh\left(\dfrac{\beta\omega_{\rm T}}{4}\right) \leqslant \dfrac{\omega_{\rm R}}{\omega_{\rm T}} \leqslant \coth\left(\dfrac{\beta\omega_{\rm T}}{4}\right) \\ \dfrac{1}{2}\log\left(\dfrac{\omega_{\rm T}}{\omega_{\rm R}}\right) + \dfrac{1}{2}\log\left(\dfrac{\frac{\omega_{\rm T}}{\omega_{\rm R}}\coth\left(\beta\omega_{\rm T}/2\right) - 1}{\frac{\omega_{\rm T}}{\omega_{\rm R}} - \coth\left(\beta\omega_{\rm T}/2\right)}\right) & \tanh\left(\dfrac{\beta\omega_{\rm T}}{4}\right) \geqslant \dfrac{\omega_{\rm R}}{\omega_{\rm T}} \,. \end{cases} \tag{9.84}$$

For the physical basis analytic results are not available. In the regime $\beta\omega_{\rm T} \gg 1$, the following perturbative expansion has been found [23]

$$\mathcal{C}_1^{\rm phys} = \frac{1}{2}\left|\log(\omega_{\rm R}/\omega_{\rm T})\right| + \frac{\log\left[\coth\left(\beta\omega_{\rm T}/4\right)\right]\,\log(\omega_{\rm R}/\omega_{\rm T})}{\sqrt{\omega_{\rm R}/\omega_{\rm T}} - \sqrt{\omega_{\rm T}/\omega_{\rm R}}} + O(e^{-\beta\omega_{\rm T}}) \,. \tag{9.85}$$

As for the F_2 purification complexity, an analytic result valid in the entire range of the parameter is not available in the literature. However, in the regime where $\beta\omega_{\rm T} \gg 1$, it has been found [23]

$$\mathcal{C}_2^{\rm pur} = \frac{1}{2}\sqrt{\log\left(\omega_{\rm R}/\omega_{\rm T}\right)\left[\log\left(\omega_{\rm R}/\omega_{\rm T}\right) + \left[\log(\coth\left(\beta\omega_{\rm T}/4\right))\right]^2\left(\frac{\omega_{\rm R}/\omega_{\rm T}+1}{\omega_{\rm R}/\omega_{\rm T}-1}\right)\right]} + O(e^{-\beta\omega_{\rm T}}) \tag{9.86}$$

The expressions for the complexity in (9.83), (9.84), (9.85) and (9.86) depend only on $\beta\omega_{\rm T}$ and on the ratio $\omega_{\rm R}/\omega_{\rm T}$. As consistency check, we notice that in the limit $\beta\omega_{\rm T} \to \infty$, where the circuit is made by pure states, all the expressions in (9.83), (9.84), (9.85) and (9.86) become $\frac{1}{2}|\log(\omega_{\rm R}/\omega_{\rm T})|$, as expected from [17].

In figure 12 we show the expressions for the complexity in (9.83), (9.84), (9.85) and (9.86) in terms of $\beta\omega_{\rm T}$ for a fixed value of $\beta\omega_{\rm R}$ (we choose $\beta\omega_{\rm R} = 1$ in the left panel and $\beta\omega_{\rm R} = 10$ in the right panel). The curves for $\mathcal{C}_1^{\rm phys}$ ad $\mathcal{C}_2^{\rm pur}$ occur only in the right panel because they exist only in the regime of $\beta\omega_{\rm T} \gg 1$. We find it worth remarking that curves for $\mathcal{C}_2$ always lie below the curves corresponding to the complexity evaluated through the purification complexity. Furthermore, as $\beta\omega_{\rm T}$ growths, all the curves collapse on the same

JHEP12(2020)101

curve, as expected from the above observation, since $\beta\omega_{\rm T} \to \infty$ corresponds to the limit where the circuit is made by pure states. In the right panel one also notices that $\mathcal{C}_2^{\rm pur}$ is smaller than the complexity $\mathcal{C}_1$ in the diagonal basis, which in turn is smaller than $\mathcal{C}_1$ in the physical basis, as already remarked in [23].

9.8 A comparison with holography

In the context of the gauge/gravity correspondence, the procedures introduced for the gravitational dual of the circuit complexity are known as "complexity = volume" proposal (CV) [7, 8], "complexity = action" proposal (CA) [11, 12] and "complexity = spacetime volume" proposal (CV2.0) [15].

The subregion holographic complexity corresponding to these three proposals have been also explored [10, 16, 23]. Considering a subregion A in the constant time slice of the d-dimensional Conformal Field Theory (CFT) on the boundary of AdS_{d+1}, it has been found that the leading divergence of the holographic complexity is proportional to $V(A)/\epsilon^{d-1}$, where $V(A)$ is the volume of A and ϵ is the UV cutoff. This divergence suggests that the holographic results should be compared with the square of the complexity $\mathcal{C}_2$ mainly explored in this manuscript.

Denoting by $\mathcal{C}_{\rm AdS}$ the holographic complexity evaluated through one of the proposals mentioned above and by the $\mathcal{C}_{\rm AdS}(A)$ the corresponding subregion holographic complexity, $\mathcal{C}_{\rm AdS}$ is superadditive when, given two disjoint subregions A and B on the boundary of the AdS space, the following inequality holds [29]

$$\mathcal{C}_{\rm AdS}(A) + \mathcal{C}_{\rm AdS}(B) \leqslant \mathcal{C}_{\rm AdS}(A \cup B) \tag{9.87}$$

while $\mathcal{C}_{\rm AdS}$ is subadditive when the opposite inequality holds. Equivalently, in terms of the holographic mutual complexity [141]

$$\mathcal{M}_{\rm AdS}(A, B) = \mathcal{C}_{\rm AdS}(A) + \mathcal{C}_{\rm AdS}(B) - \mathcal{C}_{\rm AdS}(A \cup B) \tag{9.88}$$

which should be the gravitational dual of (9.82), the holographic complexity is superadditive when $\mathcal{M}_{\rm AdS}(A, B) \leqslant 0$ for any choice of the regions A and B.

When the gravitational background is the eternal black hole, which is the gravitational dual of the TFD state [158], and the subregions L and R are constant time-slices of the two disconnected boundaries where the two copies of the same CFT are defined, the definition of the holographic mutual complexity becomes [23]

$$\mathcal{M}_{\rm AdS}(\mathrm{TFD}) = \mathcal{C}_{\rm AdS}(\mathrm{L}) + \mathcal{C}_{\rm AdS}(\mathrm{R}) - \mathcal{C}_{\rm AdS}(\mathrm{TFD}) \tag{9.89}$$

It has been found that, while the CV and the CV2.0 proposals for the holographic complexity are superadditive, this property is not always satisfied for the CA proposal [29, 159].

It has been shown that the mutual complexity (9.89) is negative in any number of spacetime dimensions for all the three proposals for the holographic complexity [23, 29]. This qualitatively agrees with the results that we have obtained in section 9.4 for the mutual complexity given in (9.58) and (9.59).

JHEP12(2020)101

When the dual CFT is in its ground state (hence its gravitational dual is the empty AdS spacetime) and a spatial subregion is considered, for AdS_3 it has been shown that the holographic mutual complexity (9.88) is negative for all the three proposals [10, 16, 23]. This qualitatively disagrees with the results reported in section 9.6 because we do not observe a definite sign for the mutual complexity (9.82) (see e.g. figure 11).

10 Conclusions

In this manuscript we have studied the circuit complexity of the mixed bosonic Gaussian states occurring in the Hilbert space of harmonic lattices in any number of dimensions by employing the Fisher-Rao distance between Gaussian Wigner functions.

Considering mixed states with vanishing first moments, by applying a known result for the symmetric and positive definite matrices [64–68] to the covariance matrices of the model, we have provided the optimal circuit (2.28), which holds when the set of the allowed gates provides circuits made only by Gaussian states. The length (2.31) of this optimal circuit in the geometry determined by the Fisher information matrix is identified with the circuit complexity (2.33) to obtain a target state from a given reference state (the tolerance is zero for these circuits). In the special case of pure states, the known results of [17, 22] for the $\mathcal{C}_2$ complexity have been recovered. For thermal states originating from the same hamiltonian, the expression (2.80) has been obtained.

The Williamson's decomposition of the covariance matrix (see section 2.3) is the main tool employed throughout our analysis. This decomposition identifies the symplectic spectrum, that is invariant under changes of basis that preserve the canonical commutation relations. The role of the symplectic spectra and of the basis in the computation of the $\mathcal{C}_2$ complexity is made manifest in the expression (2.49). Furthermore, the Williamson's decomposition leads to natural ways to introduce the spectrum complexity and the basis complexity for mixed bosonic Gaussian states (see section 3.3 and section 3.4). This provides an explicit realisation of the proposal made in [29].

The optimal circuits described in this manuscript allow us to study the purification of mixed states without ancillae. Motivated by the first law of complexity, in section 4 we have mainly considered the purification of a given mixed state through the W path (4.5). Further future analyses could lead to find the optimal purification path.

The Gaussian mixed states that are not pure in harmonic lattices can be characterised also through their entanglement hamiltonian matrices. The optimal circuit and the corresponding complexity in terms of the entanglement hamiltonian matrices have been investigated in section 6.

It is important to understand how to construct the optimal circuits. A preliminary analysis has been carried out in section 7, where the possibility to express the optimal circuit in terms of Gaussian channels has been explored. We have not been able to find a general solution to this interesting problem, hence further future investigations are needed.

It is instructive to compare alternative quantitative approaches to the complexity of mixed states. The approach described in this manuscript holds only for the bosonic Gaussian states occurring in harmonic lattices and it provides computable expressions for a

JHEP12(2020)101

generic number of degrees of freedom. The method discussed in [23] (see section 8), that is based on the introduction of ancillary degrees of freedom, can be formulated for every model but it leads to expressions that are more difficult to evaluate.

A detailed analysis has been carried out in the simplest case of the harmonic chain either on the circle or on the infinite line (see section 9). Analytic or numerical results have been reported. For the thermal states we have explored the optimal path, the corresponding circuit complexity (see e.g. (9.43)) and the purification. Analytic and numerical results have been found for the mutual complexity of thermofield double states (see section 9.4). Finally, for the mixed states given by reduced density matrices, we have studied the circuit complexity for an interval in the infinite line and the mutual complexity of two disjoint intervals (see section 9.6). Interestingly, in figure 11 we observe that, for two disjoint and equal intervals of length ℓ separated by d sites, the mutual complexity vanishes as ℓ increases, while the ratio d/ℓ is kept fixed. Furthermore, considering this quantity as function of d/ℓ, we observe that data corresponding to given value of $\omega_{\mathrm{T}}\ell$ and $\omega_{\mathrm{R}}\ell$ collapse and the resulting curves vanish after a critical value of the ratio d/ℓ.

Our analysis mainly focusses on bosonic Gaussian states with vanishing first moments. It is very interesting to explore also the complexity of mixed Gaussian states whose first moments are non vanishing. The expression (2.33) for the circuit complexity holds also when the reference state and the target state have the same first moments, that can be non vanishing [70, 85, 89]. In section 2.7 we have provided results for the coherent states (pure states with non vanishing first moments) and the complexity (2.92) has been discussed [85, 91], finding agreement with [18]. We emphasise that an explicit expression of the Fisher-Rao distance in the most general case of mixed states with non vanishing first moments is not available in the literature [85, 89]. Upper and lower bounds for the complexity have been discussed in section 5.

The circuit complexity of mixed states is a challenging task deserving many future studies.

The analysis reported in this manuscript in the simple setup of bosonic Gaussian states can be extended in various directions. For instance, it is a straightforward application to study the $\mathcal{C}_2$ circuit complexity in harmonic lattices in the presence of boundary, defects [24, 37, 41] or in time dependent scenarios [36, 160–162].

One of the main motivations of our work is to provide some tools to study complexity in quantum field theories. Evaluating complexity of mixed states in quantum field theories remains an important challenge. The complexity of pure states in quantum field theories has been explored in various studies [21, 30–43] and it would be instructive to extend these analyses to mixed states. The tools of Information Geometry, that we have largely employed in our analysis, could provide further tools to handle this interesting problem [163].

Let us remark that our analysis has been performed by assuming that all the states of the quantum circuits are Gaussian. It is important to go beyond this limitation by exploring the complexity of circuits involving mixed states that are not Gaussian.

Finally, we remind that the results reported in this manuscript have been obtained in the ideal situation where the maximal freedom is allowed in the choice of the gates. Typically, only a limited number of gates can be employed in the construction of quantum

JHEP12(2020)101

circuits. It is worth trying to adapt our analysis to more realistic cases by introducing a tolerance and various kinds of restrictions in the set of the allowed gates [4, 5].

Acknowledgments

It is a pleasure to thank Juan Hernandez, Rob Myers and Shan-Ming Ruan for collaboration and important discussions throughout the development of this project. We are grateful to Leonardo Banchi, Fabio Benatti, Vittorio Giovannetti, Ro Jefferson and Domenico Seminara for useful discussions. We thank Rob Myers also for his comments on the draft. ET acknowledges the organisers of the following meetings and workshops, where parts of this work have been done, for the kind hospitality and the financial support: the program *The Dynamics of Quantum Information* at KITP in Santa Barbara (October 2018), the meeting *Qubits on the Horizon* in Aruba (January 2019), the long term workshop *Quantum Information in String Theory and Many-body Systems* at YITP in Kyoto (June 2019) and the IV annual meeting of the It from Qubit Simons collaboration in New York (December 2019). ET's research has been conducted within the framework of the Trieste Institute for Theoretical Quantum Technologies (TQT).

A Schrödinger representation

In this appendix we briefly discuss two aspects of the Gaussian mixed states described in section 2.1 in the Schrödinger representation. In section A.1 we report the kernel $\rho(\boldsymbol{q},\tilde{\boldsymbol{q}}) = \langle \boldsymbol{q}|\,\hat{\rho}\,|\tilde{\boldsymbol{q}}\rangle$ of the density matrix corresponding to the Gaussian Wigner function (2.10). In section A.2 we consider the spatial bipartition $A\cup B$ of a system in a pure state, writing the kernel $\rho_A(\boldsymbol{q}_A,\tilde{\boldsymbol{q}}_A)$ for the reduced density matrix of the spatial subsystem A in terms of the parameters occurring in the wave function of the pure state of the entire system.

A.1 Wigner-Weyl transform

The density matrix $\hat{\rho}$, that fully characterises a mixed state, is hermitean, positive definite and its trace is equal to one. Being a linear operator on the Hilbert space, $\hat{\rho}$ is completely determined by its kernel $\rho(\boldsymbol{q},\tilde{\boldsymbol{q}}) = \langle \boldsymbol{q}|\,\hat{\rho}\,|\tilde{\boldsymbol{q}}\rangle$ in the Schrödinger representation.

In this manuscript we are interested in the states whose kernel $\rho(\boldsymbol{q},\tilde{\boldsymbol{q}})$ is Gaussian [75]. This means that

$$\rho(\boldsymbol{q},\tilde{\boldsymbol{q}}) = \mathcal{N}_\rho^2 \, \exp\left\{ -\frac{1}{2}(\boldsymbol{q}^{\mathrm{t}},\tilde{\boldsymbol{q}}^{\mathrm{t}}) \begin{pmatrix} \Theta & -\Phi \\ -\Phi^* & \Theta^* \end{pmatrix} \begin{pmatrix} \boldsymbol{q} \\ \tilde{\boldsymbol{q}} \end{pmatrix} \right\} \tag{A.1}$$

where Θ are Φ are $N\times N$ complex matrices. Since the argument of the exponential in (A.1) must be invariant under transposition, we have $\Theta = \Theta^{\mathrm{t}}$ and $\Phi = \Phi^\dagger$. This implies that (A.1) is fixed by choosing $N(2N+1)$ real parameters: $N(N+1)$ real parameters in Θ and N^2 real parameters in Φ. The normalisation condition $\int_{\mathbb{R}^N} \rho(\boldsymbol{q},\boldsymbol{q})\, d\boldsymbol{q} = 1$ for (A.1) gives

$$\mathcal{N}_\rho^2 = \frac{1}{\pi^{N/2}} \sqrt{\det[\mathrm{Re}(\Theta) - \mathrm{Re}(\Phi)]} \tag{A.2}$$

JHEP12(2020)101

which is well defined when $\mathrm{Re}(\Theta) - \mathrm{Re}(\Phi)$ is strictly positive. We remark that $\hat{\rho} = \hat{\rho}^\dagger$ is equivalent to $\rho(\boldsymbol{q}, \tilde{\boldsymbol{q}})^* = \rho(\tilde{\boldsymbol{q}}, \boldsymbol{q})$ [75]. This condition is satisfied by (A.1).

The Wigner-Weyl transform (also called Moyal transform) of $\rho(\boldsymbol{q}, \tilde{\boldsymbol{q}})$ is defined as

$$w(\boldsymbol{q}, \boldsymbol{p}) = \frac{1}{(2\pi)^N} \int_{\mathbb{R}^N} \rho\Big(\boldsymbol{q} - \frac{1}{2}\,\tilde{\boldsymbol{q}}\,, \boldsymbol{q} + \frac{1}{2}\,\tilde{\boldsymbol{q}}\Big)\, e^{\mathrm{i}\,\tilde{\boldsymbol{q}}^{\mathrm{t}}\boldsymbol{p}}\, d\tilde{\boldsymbol{q}}\,. \tag{A.3}$$

By using (A.1) and (A.2) into (A.3) and performing a Gaussian integral,[21] one finds that the Wigner-Weyl transform of (A.1) is Gaussian as well. In particular, it reads

$$w_{\mathrm{G}}(\boldsymbol{q}, \boldsymbol{p}) = \frac{1}{\pi^N} \sqrt{\frac{\det(T)}{\det(T + C)}}\, \exp\Big\{ -\frac{1}{2}\Big[\, 4\, \boldsymbol{q}^{\mathrm{t}}\, T\, \boldsymbol{q} + (\boldsymbol{p} - I\boldsymbol{q})^{\mathrm{t}}\, (T + C)^{-1} (\boldsymbol{p} - I\boldsymbol{q})\Big]\Big\} \tag{A.5}$$

where

$$T + C = \frac{1}{2}\,\big[\,\mathrm{Re}(\Theta) + \mathrm{Re}(\Phi)\,\big] \qquad T = \frac{1}{2}\,\big[\,\mathrm{Re}(\Theta) - \mathrm{Re}(\Phi)\,\big] \qquad I \,=\, \mathrm{Im}(\Phi) - \mathrm{Im}(\Theta)\,. \tag{A.6}$$

Since $\mathrm{Re}(\Theta)$ and $\mathrm{Re}(\Phi)$ are symmetric, T and C are $N \times N$ real and symmetric matrices, while I is a generic $N \times N$ real matrix, given that $\mathrm{Im}(\Theta)$ is symmetric and $\mathrm{Im}(\Phi)$ is antisymmetric; hence (A.5) is determined by $N(2N+1)$ real parameters, as expected. The complex matrices Θ and Φ can be written in terms of the real matrices T, C and I by inverting (A.6). The result is

$$\Theta = 2\,T + C - \mathrm{i}\,\frac{I + I^{\mathrm{t}}}{2} \qquad \Phi = C + \mathrm{i}\,\frac{I - I^{\mathrm{t}}}{2}\,. \tag{A.7}$$

The expression (A.5) can be written in the form (2.10) with γ given by (8.2) with

$$Q = \frac{1}{4}\,T^{-1} \qquad P = T + C + \frac{1}{4}\,I^{\mathrm{t}}\,T^{-1} I^{\mathrm{t}} \qquad M = \frac{1}{4}\,T^{-1} I^{\mathrm{t}}\,. \tag{A.8}$$

This is obtained by noticing that

$$\det(\gamma) = \det(Q)\,\det(P - M^{\mathrm{t}}\,Q^{-1} M) = \frac{\det(T + C)}{4^N \det(T)}\,. \tag{A.9}$$

The matrices T, C and I can be expressed in terms of the blocks of γ in (8.2) by inverting (A.8). The result is

$$T = \frac{1}{4}\,Q^{-1} \qquad C = P - \frac{1}{4}\,Q^{-1} - M^{\mathrm{t}}\,Q^{-1}\,M \qquad I = M^{\mathrm{t}}\,Q^{-1}\,. \tag{A.10}$$

Thus, in terms of the blocks of γ in (8.2), the complex matrices in (A.1) and (A.7) read

$$\Theta \,=\, P - M^{\mathrm{t}}\,Q^{-1}\,M + \frac{1}{4}\,Q^{-1} - \mathrm{i}\,M^{\mathrm{t}}\,Q^{-1} \tag{A.11}$$

$$\Phi \,=\, P - M^{\mathrm{t}}\,Q^{-1}\,M - \frac{1}{4}\,Q^{-1} + \mathrm{i}\,M^{\mathrm{t}}\,Q^{-1} \tag{A.12}$$

These matrices are real when $\gamma = Q \oplus P$ in (8.2) is block diagonal.

[21] The following Gaussian integral

$$\int_{\mathbb{R}^n} e^{-\boldsymbol{x}^{\mathrm{t}} A\, \boldsymbol{x} + \boldsymbol{b}^{\mathrm{t}} \boldsymbol{x}}\, d\boldsymbol{x} \,=\, \sqrt{\frac{\pi^n}{\det(A)}}\; e^{\frac{1}{4}\boldsymbol{b}^{\mathrm{t}} A^{-1}\, \boldsymbol{b}} \tag{A.4}$$

has been employed, where $d\boldsymbol{x} \equiv \prod_{i=1}^n dx_i$.

JHEP12(2020)101

We remark that the Wigner characteristic function in (2.3) is related to the kernel $\rho(\boldsymbol{q},\tilde{\boldsymbol{q}})$ through the following relation

$$\rho\Big(\boldsymbol{q}-\frac{\tilde{\boldsymbol{q}}}{2},\boldsymbol{q}+\frac{\tilde{\boldsymbol{q}}}{2}\Big)=\int_{\mathbb{R}^N}\chi(\boldsymbol{\xi})\,e^{-\mathrm{i}\,\boldsymbol{q}^{\mathrm{t}}\tilde{\boldsymbol{p}}}\,d\tilde{\boldsymbol{p}}\qquad\qquad \boldsymbol{\xi}=\begin{pmatrix}\tilde{\boldsymbol{q}}\\ \tilde{\boldsymbol{p}}\end{pmatrix}. \tag{A.13}$$

Indeed, the Wigner function (2.5) is recovered by plugging (A.13) into (A.3).

A.2 Reduced density matrix

In the Schrödinger representation, the kernel $\rho_A(\boldsymbol{q}_A,\tilde{\boldsymbol{q}}_A)$ corresponding to the reduced density matrix $\hat{\rho}_A$ of the subsystem A of a bipartite harmonic lattice in a pure state can be computed as follows.

Considering the wavefunction (2.24) for the pure state of the entire system, the spatial bipartition $A\cup B$ of the harmonic lattice naturally leads to write the real and symmetric matrices E and F in (2.24) as the following block matrices

$$E\equiv\begin{pmatrix}E_A & E_{AB}\\ E_{AB}^{\mathrm{t}} & E_B\end{pmatrix}\qquad\qquad F\equiv\begin{pmatrix}F_A & F_{AB}\\ F_{AB}^{\mathrm{t}} & F_B\end{pmatrix}. \tag{A.14}$$

In terms of the blocks introduced in (A.14), the wave function (2.24) becomes

$$\psi(\boldsymbol{q}_A,\boldsymbol{q}_B)=\mathcal{N}_\psi\,\exp\Big\{-\frac{1}{2}\Big[\,\boldsymbol{q}_A^{\mathrm{t}}\,\Omega_A\,\boldsymbol{q}_A+\boldsymbol{q}_B^{\mathrm{t}}\,\Omega_B\,\boldsymbol{q}_B+2\,\boldsymbol{q}_A^{\mathrm{t}}\,\Omega_{AB}\,\boldsymbol{q}_B\,\Big]\Big\} \tag{A.15}$$

where

$$\Omega_A\equiv E_A+\mathrm{i}\,F_A\qquad\qquad \Omega_B\equiv E_B+\mathrm{i}\,F_B\qquad\qquad \Omega_{AB}\equiv E_{AB}+\mathrm{i}\,F_{AB} \tag{A.16}$$

and

$$\mathcal{N}_\psi=\Big(\frac{\det(E)}{\pi^N}\Big)^{1/4}=\frac{1}{\pi^{N/4}}\,\sqrt[4]{\det(E_B)\,\det\big(E_A-E_{AB}\,E_B^{-1}\,E_{AB}^{\mathrm{t}}\big)}\,. \tag{A.17}$$

The kernel $\rho_A(\boldsymbol{q}_A,\tilde{\boldsymbol{q}}_A)$ corresponding to the reduced density matrix $\hat{\rho}_A$ is obtained by tracing out the degrees of freedom corresponding to the part B of the harmonic lattice. By employing (A.15) and the Gaussian integral (A.4), one obtains

$$\begin{aligned}\rho_A(\boldsymbol{q}_A,\tilde{\boldsymbol{q}}_A)\;&=\;\int_{\mathbb{R}^{N_B}}\psi(\boldsymbol{q}_A,\boldsymbol{q}_B)\,\psi(\tilde{\boldsymbol{q}}_A,\boldsymbol{q}_B)^*\,d\boldsymbol{q}_B\\ &=\mathcal{N}_\rho^2\,\exp\Big\{-\frac{1}{2}(\boldsymbol{q}_A^{\mathrm{t}}\,,\,\tilde{\boldsymbol{q}}_A^{\mathrm{t}})\begin{pmatrix}\Theta_A & -\Phi_A\\ -\Phi_A^* & \Theta_A^*\end{pmatrix}\begin{pmatrix}\boldsymbol{q}_A\\ \tilde{\boldsymbol{q}}_A\end{pmatrix}\Big\}\end{aligned} \tag{A.18}$$

where

$$\Theta_A\;\equiv\;\Omega_A-\frac{1}{2}\,\Omega_{AB}\,E_B^{-1}\,\Omega_{AB}^{\mathrm{t}}\qquad\qquad \Phi_A\;\equiv\;\frac{1}{2}\,\Omega_{AB}\,E_B^{-1}\,\Omega_{AB}^{\dagger}\,. \tag{A.19}$$

Notice that Θ_A is symmetric and Φ_A is hermitean, as expected from the general expression in (A.1). We find it worth remarking that F_B does not occur in (A.19). The real and the imaginary parts of Θ_A read respectively

$$\mathrm{Re}(\Theta_A)\;=\;E_A-\frac{1}{2}\Big(E_{AB}\,E_B^{-1}E_{AB}^{\mathrm{t}}-F_{AB}\,E_B^{-1}F_{AB}^{\mathrm{t}}\Big) \tag{A.20}$$

$$\mathrm{Im}(\Theta_A)\;=\;F_A-\frac{1}{2}\Big(F_{AB}\,E_B^{-1}E_{AB}^{\mathrm{t}}+E_{AB}\,E_B^{-1}F_{AB}^{\mathrm{t}}\Big) \tag{A.21}$$

JHEP12(2020)101

and for Φ_A we have respectively

$$\mathrm{Re}(\Phi_A) = \frac{1}{2}\Big(E_{AB}\, E_B^{-1} E_{AB}^{\mathrm{t}} + F_{AB}\, E_B^{-1} F_{AB}^{\mathrm{t}}\Big) \tag{A.22}$$

$$\mathrm{Im}(\Phi_A) = \frac{1}{2}\Big(F_{AB}\, E_B^{-1} E_{AB}^{\mathrm{t}} - E_{AB}\, E_B^{-1} F_{AB}^{\mathrm{t}}\Big)\,. \tag{A.23}$$

Imposing that the trace of (A.19) is one leads to

$$\mathcal{N}_\rho^2 = \frac{1}{\pi^{N_A/2}} \sqrt{\det(E_A - E_{AB}\, E_B^{-1}\, E_{AB}^{\mathrm{t}})} \tag{A.24}$$

which is consistent with (A.2), once (A.20) and (A.22) have been employed.

If Ω_{AB} is left invertible i.e. the $N_B \times N_A$ matrix Ω_{AB}^{-1} exists such that $\Omega_{AB}^{-1}\,\Omega_{AB} = \mathbf{1}$, we have that $\Omega_{AB}^{\dagger}$ is right invertible with $(\Omega_{AB}^{\dagger})^{-1} = (\Omega_{AB}^{-1})^{\dagger}$. Assuming also that Φ_A is invertible, we can isolate Ω_A and E_B in (A.19), finding

$$\Omega_A \;=\; \Theta_A + \Omega_{AB}\,\Omega_{AB}^{-1}\,\Phi_A\,(\Omega_{AB}^{-1})^{\dagger}\,\Omega_{AB}^{\mathrm{t}} \qquad\qquad E_B \;=\; \frac{1}{2}\,\Omega_{AB}^{\dagger}\,\Phi_A^{-1}\,\Omega_{AB}\,. \tag{A.25}$$

Thus, for given Θ_A and Φ_A, we have the freedom to choose the $N_B \times N_B$ real symmetric matrix F_B and the $N_A \times N_B$ complex matrix Ω_{AB}, namely $\frac{N_B(N_B+1)}{2} + 2N_AN_B$ real parameters.

In the special case $F = \mathbf{0}$, that has been considered e.g. in [23, 136], the matrices in (A.16) are real. Furthermore, from (A.21) and (A.23), we have that also Θ_A and Φ_A are real.

In section 8 we have discussed the purification of a mixed state with N sites through the introduction of an auxiliary lattice with N_{anc} sites. The results reported in this appendix can be employed in section 8 by setting $N = N_A$ and $N_{\mathrm{anc}} = N_B$. In particular, in the simplest case, which is given by $N_A = N_B = 1$, the above counting tells us that we have three parameters to choose. This result has been found also in section 8.1.1 by using (8.17).

The above results provide a lower bound for the number N_B of ancillary degrees of freedom that must be introduced to purify a mixed state. A theorem of matrix algebra [164] guarantees that, given two matrices M and N, the rank of their product is bounded by $\mathrm{rank}(MN) \leqslant \min[\mathrm{rank}(M), \mathrm{rank}(N)]$. Applying this result to the second equation in (A.19), we have that $\mathrm{rank}(\Phi_A) \leqslant \min[\mathrm{rank}(E_B^{-1}), \mathrm{rank}(\Omega_{AB})]$, where the fact that $\mathrm{rank}(\Omega_{AB}) = \mathrm{rank}(\Omega_{AB}^{\dagger})$ has been used. Then, since $\mathrm{rank}(E_B^{-1}) = N_B$ (given that E_B^{-1} is invertible) and the rank of the $N_A \times N_B$ rectangular matrix Ω_{AB} is bounded by $\mathrm{rank}(\Omega_{AB}) \leqslant \min[N_A, N_B] \leqslant N_B$, we can conclude that $N_B \geqslant \mathrm{rank}(\Phi_A)$. In [23] this argument has been applied for real matrices.

B On the Fisher-Rao distance between Gaussian PDF's

In this appendix we report some known results about the Fisher-Rao distance between Gaussian probability distribution functions [62, 69, 70, 84–90] in order to apply them to the analysis of the complexity of mixed bosonic Gaussian states.

JHEP12(2020)101

A Gaussian probability distribution function (PDF) in one variable (also called univariate PDF) reads

$$p(x;\boldsymbol{\theta}) \equiv \frac{e^{-\frac{1}{2}(x-\mu)^2/v^2}}{\sqrt{2\pi}\,v} \qquad \boldsymbol{\theta} \equiv (\mu, v) \tag{B.1}$$

where $\mu \in \mathbb{R}$ is the mean and $v > 0$ is the standard deviation.

These Gaussian PDF's provide a manifold $\mathcal{M}_1$ once the metric is introduced through the *Fisher information matrix* [62, 69, 84]

$$g_{i,j}(\boldsymbol{\theta}) \equiv \int_{\mathbb{R}} \frac{\partial \log[p(x;\boldsymbol{\theta})]}{\partial \theta_i} \, \frac{\partial \log[p(x;\boldsymbol{\theta})]}{\partial \theta_j} \, p(x;\boldsymbol{\theta}) \, dx \tag{B.2}$$

where $i, j \in \{1, 2\}$. Plugging (B.1) into (B.2), one obtains the diagonal matrix $\mathrm{diag}(1/v^2, 2/v^2)$, that provides the following infinitesimal distance [69, 70]

$$ds^2 = \frac{d\mu^2 + 2\, dv^2}{v^2} \tag{B.3}$$

which characterises the hyperbolic upper half plane $\mathbb{H}_2$ after the rescaling $\mu \to \sqrt{2}\,\mu$. Thus, by equipping the space of the univariate Gaussian PDF's parameterised by the pair (μ, v) with the metric characterised by the Fisher information matrix (B.2), the geodesics are either the lines with constant μ or the half-ellipses with eccentricity $1/\sqrt{2}$ ending on the axis $v = 0$. By evaluating the length of these geodesics, one finds that the Fisher-Rao distance between two univariate Gaussian PDF's associated to the parameters $\boldsymbol{\theta}_1 = (\mu_1, v_1)$ and $\boldsymbol{\theta}_2 = (\mu_2, v_2)$ is [69, 70]

$$d^{(1)}_{\mathrm{FR}}(\boldsymbol{\theta}_1, \boldsymbol{\theta}_2) \equiv 2\,\mathrm{arccosh}\left(1 + \frac{1}{2v_1v_2}\left[\frac{(\mu_1-\mu_2)^2}{2} + (v_1-v_2)^2\right]\right). \tag{B.4}$$

When $\mu_1 = \mu_2 = \mu$, by using the relation $\mathrm{arccosh}(x) = \log(x + \sqrt{x^2-1}\,)$, one finds that (B.4) becomes $2\log(|v_2/v_1|)$, which is the distance (2.31) specialised to Gaussian PDF's in one variable.[22]

We are interested in the manifold $\mathcal{M}_n$ made by the Gaussian PDF's in n variables $\boldsymbol{x}^{\mathrm{t}} \in \mathbb{R}^n$, which are (see (2.6) with $n = 2N$)

$$p(\boldsymbol{x};\boldsymbol{\theta}) \equiv \frac{e^{-\frac{1}{2}(\boldsymbol{x}-\boldsymbol{\mu})^{\mathrm{t}}\,\Sigma^{-1}(\boldsymbol{x}-\boldsymbol{\mu})}}{(2\pi)^{n/2}\sqrt{\det(\Sigma)}} \qquad \boldsymbol{\theta} \equiv (\boldsymbol{\mu}, \Sigma) \tag{B.5}$$

where $\boldsymbol{\mu}^{\mathrm{t}} \in \mathbb{R}^n$ is the mean vector and Σ is a $n \times n$ positive definite symmetric matrix called covariance matrix. The parameter space for $\boldsymbol{\theta}$ has $n + n(n+1)/2$ real dimensions: n parameters for $\boldsymbol{\mu}$ and $n(n+1)/2$ for Σ. In this space, it would be interesting to have a closed form for the Fisher-Rao distance that generalises (B.4) to $n \geqslant 1$. Nonetheless, important explicit results have been obtained for some interesting submanifolds of $\mathcal{M}_n$.

In 1976, S. T. Jensen [70] found that the $n(n+1)/2$ dimensional submanifold $\mathcal{M}_{\boldsymbol{\mu}_0}$ defined by the Gaussian PDF's with the same $\boldsymbol{\mu} = \boldsymbol{\mu}_0$ is totally geodesic[23] and that the

[22] The normalisation of (B.4) is different from the one used in [85].

[23] A submanifold $\widetilde{\mathcal{M}} \subset \mathcal{M}$ is totally geodesics if any geodesics in $\widetilde{\mathcal{M}}$ is also geodesics in $\mathcal{M}$ [165].

JHEP12(2020)101

Fisher-Rao distance in this case becomes

$$d_{\boldsymbol{\mu}_0}(\boldsymbol{\theta}_1,\boldsymbol{\theta}_2) \equiv \left[\sum_{i=1}^{n} \left(\log(\lambda_i)\right)^2\right]^{1/2} \qquad \boldsymbol{\theta}_j \equiv (\boldsymbol{\mu}_0, \Sigma_j) \tag{B.6}$$

where λ_i are the eigenvalues of $\Sigma_1^{-1/2}\,\Sigma_2\,\Sigma_1^{-1/2}$. The distance (B.6) is employed throughout this manuscript to evaluate the complexity of mixed bosonic Gaussian states (see (2.31)).

Another interesting submanifold $\mathcal{M}_{\Sigma_0}$ to consider is given by the Gaussian PDF's with the same covariance matrix $\Sigma = \Sigma_0$. The Fisher-Rao distance on this submanifold becomes the Mahalanobis distance [85, 87]

$$d_{\Sigma_0}(\boldsymbol{\theta}_1,\boldsymbol{\theta}_2) \equiv \sqrt{2}\left[(\boldsymbol{\mu}_1-\boldsymbol{\mu}_2)^{\mathrm{t}}\,\Sigma_0^{-1}(\boldsymbol{\mu}_1-\boldsymbol{\mu}_2)\right]^{1/2} \qquad \boldsymbol{\theta}_j \equiv (\boldsymbol{\mu}_j, \Sigma_0)\,. \tag{B.7}$$

We remark that $\mathcal{M}_{\Sigma_0}$ is not a totally geodesic submanifold of $\mathcal{M}_n$ [85, 90].

It is worth considering also the submanifold $\mathcal{M}_{\text{diag}}$ made by the Gaussian PDF's whose covariance matrix is diagonal, namely $\Sigma = \text{diag}(v_1^2,\dots,v_n^2)$, with $v_i > 0$. In this submanifold the infinitesimal distance becomes [90, 166]

$$ds^2 = \sum_{i=1}^{n} \frac{d\mu_i^2 + 2\,dv_i^2}{v_i^2} \tag{B.8}$$

which suggests that it is convenient to arrange the parameters as $\boldsymbol{\theta} = (\boldsymbol{\theta}_1^{(1)},\dots,\boldsymbol{\theta}_n^{(1)})$, with $\boldsymbol{\theta}_i^{(1)} \equiv (\mu_i, v_i)$ in this case. The infinitesimal distance (B.8) leads to write the distance between two PDF's in $\mathcal{M}_{\text{diag}}$ in terms of (B.4) as follows

$$d_{\text{diag}}(\boldsymbol{\theta}_1,\boldsymbol{\theta}_2) \equiv \left[\sum_{i=1}^{n} d_{\text{FR}}^{(1)}(\boldsymbol{\theta}_{i,1}^{(1)},\boldsymbol{\theta}_{i,2}^{(1)})^2\right]^{1/2}. \tag{B.9}$$

From (B.8) one concludes that the geodesics in $\mathcal{M}_{\text{diag}}$ are the curves $\boldsymbol{\theta}(s)$ such that $\boldsymbol{\theta}_i^{(1)}(s)$ is a geodesic in hyperbolic upper half plane equipped with the metric (B.3), for all $1 \leqslant i \leqslant n$. Notice that we are not guaranteed that a geodesic in $\mathcal{M}_{\text{diag}}$ is also a geodesic in $\mathcal{M}_n$ because $\mathcal{M}_{\text{diag}}$ is not a totally geodesic submanifold of $\mathcal{M}_n$. Instead, a totally geodesics submanifold of $\mathcal{M}_n$ is $\widetilde{\mathcal{M}}_{\text{diag}} \subset \mathcal{M}_{\text{diag}}$, which is made by the elements of $\mathcal{M}_{\text{diag}}$ such that $\boldsymbol{\mu}$ is a given eigenvector of Σ (see e.g. Proposition II.1 in [91][24]). For instance, the Gaussian PDF's whose covariance matrices are proportional to the identity are contained in $\widetilde{\mathcal{M}}_{\text{diag}}$ and in this case $\boldsymbol{\mu}$ is the generic element of $\mathbb{R}^n$.

Consider a diagonal Σ and the eigenvector $\boldsymbol{\mu}^{\mathrm{t}} = (\mu, 0, \dots, 0)$ [91]. In this case the metric (B.8) becomes

$$ds^2 = \frac{d\mu^2 + 2\,dv_1^2}{v_1^2} + 2\sum_{i=2}^{n} \frac{dv_i^2}{v_i^2} \tag{B.10}$$

and the corresponding geodesics can be found as discussed above [90, 91]. By specialising (B.9) to this case and employing (B.4), one obtains

$$d_{\text{diag}}(\boldsymbol{\theta}_1,\boldsymbol{\theta}_2) = \sqrt{\left[2\,\text{arccosh}\left(1 + \frac{(\mu_1-\mu_2)^2/2 + (v_{1,1}-v_{2,1})^2}{2\,v_{1,1}v_{2,1}}\right)\right]^2 + \sum_{i=2}^{n}\left[2\log\left(\frac{v_{2,i}}{v_{1,i}}\right)\right]^2}\,. \tag{B.11}$$

[24] In [85] the submanifold $\widetilde{\mathcal{M}}_{\text{diag}}$ is denoted by $\mathcal{M}_{D\mu}$.

JHEP12(2020)101

Notice that, when Σ has a degenerate spectrum, its eigenvectors can have more than one non vanishing components.

The Mahalanobis distance (B.7) can be applied on the submanifold $\mathcal{M}_{\Sigma_0}$, which is not totally geodesic. Very recently, a closed form for the distance $d_{\rm FR}(\boldsymbol{\theta}_1, \boldsymbol{\theta}_2)$ between PDF's in $\mathcal{M}_n$ having the same covariance matrix Σ_0 has been found [89]. Since $\mathcal{M}_{\Sigma_0}$ is not a totally geodesic submanifold of $\mathcal{M}_n$, the Mahalanobis distance (B.7) does not necessarily correspond to the length of a geodesic connecting two PDF's with the same covariance matrix in $\mathcal{M}_n$. Instead, the distance $d_{\rm FR}(\boldsymbol{\theta}_1, \boldsymbol{\theta}_2)$ provides the length of the shortest path in $\mathcal{M}_n$ between two PDF's with the same Σ_0. Since we are not restricting to a submanifold of $\mathcal{M}_n$, this is the proper Fisher-Rao distance in $\mathcal{M}_n$ between two PDF's with the same covariance matrix. Thus, given two Gaussians PDF's with the same covariance matrix Σ_0, we have that $d_{\rm FR}(\boldsymbol{\theta}_1, \boldsymbol{\theta}_2) \leqslant d_{\Sigma_0}(\boldsymbol{\theta}_1, \boldsymbol{\theta}_2)$.

Given two Gaussian PDF's in $\mathcal{M}_n$ parametrised by $\boldsymbol{\theta}_1 \equiv (\boldsymbol{\mu}_1, \Sigma_0)$ and $\boldsymbol{\theta}_2 \equiv (\boldsymbol{\mu}_2, \Sigma_0)$, let us consider the orthogonal matrix Π such that $\Pi(\boldsymbol{\mu}_2 - \boldsymbol{\mu}_1) = (|\boldsymbol{\mu}_2 - \boldsymbol{\mu}_1|, 0, \dots, 0) \equiv |\boldsymbol{\mu}_2 - \boldsymbol{\mu}_1| \boldsymbol{e}_1$. Since Σ_0 is symmetric and positive definite and Π orthogonal, also the matrix $\Pi\, \Sigma_0\, \Pi^{\rm t}$ is symmetric and positive definite, hence it can be decomposed as [89]

$$\Pi\, \Sigma_0\, \Pi^{\rm t} = U\, \mathcal{S}_{\Sigma_0}\, U^{\rm t} \tag{B.12}$$

where U is an upper triangular matrix with all the diagonal entries equal to one and $\mathcal{S}_{\Sigma_0}$ is a diagonal matrix with positive entries. The Fisher-Rao distance between $\boldsymbol{\theta}_1 = (\boldsymbol{\mu}_1, \Sigma_0)$ and $\boldsymbol{\theta}_2 = (\boldsymbol{\mu}_2, \Sigma_0)$ in $\mathcal{M}_n$ found in [89] reads

$$d_{\rm FR}(\boldsymbol{\theta}_1, \boldsymbol{\theta}_2) = d_{\rm diag}(\boldsymbol{\theta}_0, \boldsymbol{\theta}_\mu) \qquad \boldsymbol{\theta}_0 \equiv (\boldsymbol{0}, \mathcal{S}_{\Sigma_0}) \qquad \boldsymbol{\theta}_\mu \equiv (|\boldsymbol{\mu}_2 - \boldsymbol{\mu}_1| \boldsymbol{e}_1, \mathcal{S}_{\Sigma_0}) \tag{B.13}$$

where $d_{\rm diag}$ is defined in (B.11).

In order to construct the matrices Π and $\mathcal{S}_{\Sigma_0}$, let us introduce the unit vector $\boldsymbol{m} \equiv (\boldsymbol{\mu}_2 - \boldsymbol{\mu}_1)/|\boldsymbol{\mu}_2 - \boldsymbol{\mu}_1|$, observing that the orthogonal matrix Π satsfies $\Pi\, \boldsymbol{m} = \boldsymbol{e}_1$. This matrix can be constructed by considering the basis of $\mathbb{R}^n$ given by $\mathfrak{B} = \{\boldsymbol{m}, \boldsymbol{e}_1, \dots, \boldsymbol{e}_{k-1}, \boldsymbol{e}_{k+1}, \dots, \boldsymbol{e}_n\}$, where $m_k \neq 0$ is a non vanishing component of $\boldsymbol{m}$ and $\boldsymbol{e}_i$ is the unit vector having only the i-th component equal to one. The standard Gram-Schmidt procedure [164] allows to construct an orthonormal basis $\bar{\mathfrak{B}} = \{\boldsymbol{m}, \boldsymbol{u}_1, \dots, \boldsymbol{u}_{n-1}\}$ from $\mathfrak{B}$. Then, the orthogonal matrix Π in (B.12) is the matrix whose columns are the vectors of $\bar{\mathfrak{B}}$.

The Cholesky decomposition [167] allows to write a symmetric and positive definite matrix M in a unique way as $M = L_c\, L_c^{\rm t}$, where L_c is a lower triangular matrix. This result can be related to (B.12) by considering the matrix $\mathcal{I}$ having 1 on the antidiagonal and 0 elsewhere, which satisfies $\mathcal{I} = \mathcal{I}^{\rm t} = \mathcal{I}^{-1}$. The matrix $\mathcal{I}\, \Pi\, \Sigma_0\, \Pi^{\rm t}\, \mathcal{I}$ is symmetric and positive definite, hence its Cholesky decomposition tells us that it can be written as $\mathcal{I}\, \Pi\, \Sigma_0\, \Pi^{\rm t}\, \mathcal{I} = L_c\, L_c^{\rm t}$ in term of a lower triangular matrix L_c. This gives $\Pi\, \Sigma_0\, \Pi^{\rm t} = \mathcal{I}\, L_c\, L_c^{\rm t}\, \mathcal{I} = \mathcal{I}\, L_c\, \mathcal{I}\, (\mathcal{I}\, L_c\, \mathcal{I})^{\rm t}$. Since L_c is a lower triangular matrix, we have that $U_c \equiv \mathcal{I}\, L_c\, \mathcal{I}$ is an upper triangular matrix and it satisfies

$$\Pi\, \Sigma_0\, \Pi^{\rm t} = U_c\, U_c^{\rm t}\,. \tag{B.14}$$

This decomposition agrees with (B.12), provided that $U_c = U \mathcal{S}_{\Sigma_0}^{1/2}$.

JHEP12(2020)101

For any upper triangle matrix U, we have that[25]

$$U = \widetilde{U}\,\mathrm{diag}(U) \tag{B.15}$$

where $\widetilde{U}$ has 1 along the diagonal. Applying this to U_c gives $\mathcal{S}_{\Sigma_0}^{1/2} = \mathrm{diag}(U_c)$ and $U = \widetilde{U}_c$.

When $n = 1$, the distance $d_{\mathrm{FR}}(\boldsymbol{\theta}_1, \boldsymbol{\theta}_2)$ in (B.13) becomes $d^{(1)}_{\mathrm{FR}}(\boldsymbol{\theta}_1, \boldsymbol{\theta}_2)$ in (B.4).

The above discussion can be employed to define the complexity for coherent states, which are pure states described by Gaussian Wigner functions with non vanishing first moments (see section 2.1 and section 2.7) [48]. Let us restrict to the coherent states with diagonal covariance matrices and first moments with a single non vanishing component. Since the coherent states are pure states, their covariance matrices are constrained by (2.23) [48, 103]. Applying the constraints to (B.10), one obtains the metric (2.90). This metric and the distance (B.11) lead to the expression (2.92) for the complexity for coherent states. This is consistent with the results found in [18], as discussed in section 2.7 in a more detailed way. In section 2.7 we have also exploited the distance (B.13) to compute the complexity (2.93) between two coherent states defined by (2.84) from the same ground state. These states have the same covariance matrix, but different first moments.

C Bures distance and Hilbert-Schmidt distance

In the literature of quantum information, different distances have been constructed for mixed states, even in the simple case of the bosonic Gaussian states. In this appendix we discuss the Bures distance and the Hilbert-Schmidt distance [59], that have been introduced in section 2.2. In particular, we report their expressions in terms of the covariance matrices and then consider the special case of thermal states. An application of the Bures metric in the context of the complexity is discussed in [168].

The Bures distance between quantum states (defined in (2.16) from the fidelity) is Riemannian and contractive [93] (see section 2.2). An explicit expression for the fidelity between two bosonic Gaussian states in terms of the corresponding covariance matrices γ_1 and γ_2 has been found in [117]. For vanishing first moments, it reads[26]

$$\mathcal{F}(\gamma_1, \gamma_2) = \frac{F_{\mathrm{tot}}}{\sqrt[4]{\det\left(\gamma_1 + \gamma_2\right)}} \tag{C.1}$$

where F_{tot} is defined as

$$F^4_{\mathrm{tot}} \;=\; \det\!\left[2\left(\sqrt{\mathbf{1} + \frac{(\gamma_{\mathrm{aux}}\, J)^{-2}}{4}} + \mathbf{1}\right)\gamma_{\mathrm{aux}}\right] \qquad \gamma_{\mathrm{aux}} = J^{\mathrm{t}}(\gamma_1 + \gamma_2)^{-1}\left(\frac{J}{4} + \gamma_2\, J\, \gamma_1\right) . \tag{C.2}$$

The Bures distance in terms of the covariance matrices can be easily obtained by plugging (C.1) into (2.16). A canonical transformation characterised by the symplectic matrix

[25] Writing (B.15) in components we have $U_{j,k} = \sum_l \widetilde{U}_{j,l}\delta_{l,k}U_{k,k} = \widetilde{U}_{j,k}U_{k,k}$. When $j = k$, the identity is verified because $\widetilde{U}_{j,j} = 1$. When $j > k$, we have that $U_{j,k} = 0$ implies $\widetilde{U}_{j,k} = 0$, given that $U_{k,k} > 0$ (which comes from the Cholesky decomposition).

[26] In [117] the fidelity (C.1) between two Gaussian states with non vanishing first moments is also provided.

JHEP12(2020)101

S induces the change $\gamma_i \to S\gamma_i S^{\rm t}$ for the covariance matrices γ_i, with $i = 1, 2$. Simple matrix algebra based on the property of the symplectic matrices leads to conclude that the auxiliary covariance matrix $\gamma_{\rm aux}$ in (C.2) changes as $\gamma_{\rm aux} \to S\gamma_{\rm aux}S^{\rm t}$ and also that $\gamma_{\rm aux}J \to S(\gamma_{\rm aux}J)S^{-1}$. Thus, both $F^4_{\rm tot}$ in (C.1) and $\mathcal{F}(\gamma_1, \gamma_2)$ in (C.2) are left invariant by a canonical transformation. We refer to [117, 169, 170] for the Bures distance between two density matrices that are infinitesimally close.

Let us focus on γ_1 and γ_2 corresponding to thermal states having temperatures T_i in harmonic chains with frequencies ω_i, elastic constants κ_i and masses m_i, where $i = 1, 2$.

By using (9.41) and exploiting the fact that V depends only on the size of the chain, we can easily diagonalise $\gamma_1 + \gamma_2$ as follows

$$\gamma_1 + \gamma_2 = V\left[(\mathcal{Q}_1 + \mathcal{Q}_2) \oplus (\mathcal{P}_1 + \mathcal{P}_2)\right] V^{-1} \tag{C.3}$$

where the elements of $\mathcal{Q}_i$ and $\mathcal{P}_i$ with $i = 1, 2$ are defined in (9.38) and the matrix V has been introduced in section 9.1. By employing (9.20) and the fact that V is orthogonal and symplectic, we observe that for $\gamma_{\rm aux}$ in (C.2) we have

$$\gamma_{\rm aux} \;=\; V\,\mathcal{M}_{1,2}\,V^{-1} \qquad\qquad \gamma_{\rm aux}\,J \;=\; V\,\mathcal{M}_{1,2}\,J\,V^{-1} \tag{C.4}$$

where

$$\mathcal{M}_{1,2} \equiv \Big[(\mathcal{Q}_1 + \mathcal{Q}_2)^{-1} \oplus (\mathcal{P}_1 + \mathcal{P}_2)^{-1}\Big] \left(\frac{J}{4} + (\mathcal{Q}_2 \oplus \mathcal{P}_2)\, J\, (\mathcal{Q}_1 \oplus \mathcal{P}_1)\right). \tag{C.5}$$

Notice that $\mathcal{M}_{1,2}$ is not diagonal, while $\mathcal{M}_{1,2}\,J$ is diagonal. From (C.3) and (C.4) one realises that V cancels in (C.1) and (C.2), leaving the diagonal matrices $\mathcal{Q}_i$ and $\mathcal{P}_i$. After some algebra, we find that the fidelity (C.1) for the thermal states γ_i with $i = 1, 2$ becomes

$$\mathcal{F}(\gamma_1, \gamma_2) \;=\; \frac{1}{2^{L/2}} \prod_{k=1}^{L} \left[\frac{\Omega_{1,k}\,\Omega_{2,k}\,(1 + \sqrt{1 - 4B_k})^2}{(\sigma_{1,k}\Omega_{1,k} + \sigma_{2,k}\Omega_{2,k})(\sigma_{2,k}\Omega_{1,k} + \sigma_{1,k}\Omega_{2,k})\,B_k}\right]^{1/4} \tag{C.6}$$

where

$$B_k \equiv \frac{(\sigma_{1,k}\Omega_{1,k} + \sigma_{2,k}\Omega_{2,k})(\sigma_{2,k}\Omega_{1,k} + \sigma_{1,k}\Omega_{2,k})}{(4\sigma_{1,k}\sigma_{2,k}\Omega_{1,k} + \Omega_{2,k})(4\sigma_{1,k}\sigma_{2,k}\Omega_{2,k} + \Omega_{1,k})} \qquad \sigma_{i,k} = \frac{1}{2}\coth(\Omega_{i,k}/(2\widetilde{T}_i))\,. \tag{C.7}$$

The Bures distance is easily obtained by substituting (C.6) into (2.16). The result reads

$$d_{\rm B} \;=\; \sqrt{2}\,\sqrt{1 - \frac{1}{2^{L/2}} \prod_{k=1}^{L} \left[\frac{\Omega_{1,k}\,\Omega_{2,k}\,(1 + \sqrt{1 - 4B_k})^2}{(\sigma_{1,k}\Omega_{1,k} + \sigma_{2,k}\Omega_{2,k})(\sigma_{2,k}\Omega_{1,k} + \sigma_{1,k}\Omega_{2,k})\,B_k}\right]^{1/4}}\,. \tag{C.8}$$

As consistency check of this expression, we can consider the limit $\widetilde{T}_i \to 0$, which provides the Bures distance between pure states. In this limit all the symplectic eigenvalues are $\frac{1}{2}$; hence, from (C.7) we get $B_k = \frac{1}{4}$. Then, the fidelity (C.6) simplifies to

$$\mathcal{F}(\gamma_1, \gamma_2) \;=\; \prod_{k=1}^{L} \left[\frac{(\Omega_{1,k} + \Omega_{2,k})^2}{4\,\Omega_{1,k}\Omega_{2,k}}\right]^{-1/4} = \prod_{k=1}^{L} \left[\cosh\left(\frac{1}{2}\log\left(\frac{\Omega_{2,k}}{\Omega_{1,k}}\right)\right)\right]^{-1/2} \tag{C.9}$$

JHEP12(2020)101

and the Bures distance (C.8) becomes

$$d_{\rm B}(\gamma_1,\gamma_2) = \sqrt{2}\sqrt{1-\prod_{k=1}^{L}\left[\frac{1}{4}\frac{(\Omega_{1,k}+\Omega_{2,k})^2}{\Omega_{1,k}\Omega_{2,k}}\right]^{-1/4}}$$
$$= \sqrt{2}\sqrt{1-\prod_{k=1}^{L}\left[\cosh\left(\frac{1}{2}\log\left(\frac{\Omega_{2,k}}{\Omega_{1,k}}\right)\right)\right]^{-1/2}} \tag{C.10}$$

which is equal to the Fubini-Study distance between the two states, as expected.

The other distance that we consider is the Hilbert-Schmidt distance, which has been defined in (2.19) for two generic density operators. When the two density matrices are infinitesimally close to each other (i.e. $\hat\rho' = \hat\rho + d\hat\rho$), this definition gives

$$ds^2_{\rm HS} = {\rm Tr}(d\rho)^2\,. \tag{C.11}$$

Focussing on Gaussian states, the Hilbert-Schmidt distance (2.19) between two mixed states can be written in terms of their covariance matrices as follows [60]

$$d_{\rm HS}(\gamma_1,\gamma_2) = \sqrt{\frac{1}{\sqrt{\det(2\gamma_1)}}+\frac{1}{\sqrt{\det(2\gamma_2)}}-\frac{2}{\sqrt{\det[\gamma_1+\gamma_2]}}}\,. \tag{C.12}$$

Since a canonical transformation characterised by the symplectic matrix S induces the transformation $\gamma_i \to \gamma_i' = S\,\gamma_i\,S^{\rm t}$ on the covariance matrices and $\det(S)=1$, it is straightforward to check that $d_{\rm HS}$ is invariant under canonical transformations. The infinitesimal distance for (C.12) reads [60]

$$ds^2_{\rm HS} = \frac{1}{16\sqrt{\det(2\gamma)}}\left\{\left[{\rm Tr}(\gamma^{-1}d\gamma)\right]^2 + 2\,{\rm Tr}\left[(\gamma^{-1}d\gamma)^2\right]\right\}. \tag{C.13}$$

The Hilbert-Schmidt distance (C.12) between the thermal states introduced in the text above (C.3) can be evaluated by employing (9.41) and (C.3), where the diagonal matrices are given by (9.38). Thus, for the determinants involved in (C.12), one finds

$$\det(2\gamma_i) = \prod_{k=1}^{L}\coth^2(\Omega_{i,k}/(2\widetilde{T}_i)) \tag{C.14}$$

where $i=1,2$ and

$$\det[(\gamma_1+\gamma_2)] = \prod_{k=1}^{L}\left\{\frac{1}{4}\left[\coth^2\left(\frac{\Omega_{1,k}}{2\widetilde{T}_1}\right)+\coth^2\left(\frac{\Omega_{2,k}}{2\widetilde{T}_2}\right)\right.\right.$$
$$\left.\left.+\left(\frac{\Omega_{2,k}}{\Omega_{1,k}}+\frac{\Omega_{1,k}}{\Omega_{2,k}}\right)\coth\left(\frac{\Omega_{1,k}}{2\widetilde{T}_1}\right)\coth\left(\frac{\Omega_{2,k}}{2\widetilde{T}_2}\right)\right]\right\}. \tag{C.15}$$

Plugging (C.14) and (C.15) into (C.12), in terms of the notation in (C.7) we get[27]

$$d_{\rm HS}(\gamma_1,\gamma_2) \tag{C.16}$$
$$= \frac{1}{2^{L/2}}\sqrt{\prod_{k=1}^{L}\sigma_{1,k}^{-1}+\prod_{k=1}^{L}\sigma_{2,k}^{-1}-2^{L+1}\prod_{k=1}^{L}\left\{\left[\sigma_{1,k}^2+\sigma_{2,k}^2+\left(\frac{\Omega_{2,k}}{\Omega_{1,k}}+\frac{\Omega_{1,k}}{\Omega_{2,k}}\right)\sigma_{1,k}\sigma_{2,k}\right]^{-1/2}\right\}}\,.$$

[27] Our definition of covariance matrix differs from the one adopted in [60] by a factor of 2.

JHEP12(2020)101

In the special case of pure states, all the symplectic eigenvalues are equal to $\frac{1}{2}$; hence (C.16) simplifies to

$$d_{\rm HS}(\gamma_1,\gamma_2) \;=\; \sqrt{2\left\{1-\prod_{k=1}^{L}\left[\frac{(\Omega_{1,k}+\Omega_{2,k})^2}{4\,\Omega_{1,k}\,\Omega_{2,k}}\right]^{-1/2}\right\}}$$
$$\;=\; \sqrt{2\left\{1-\prod_{k=1}^{L}\left[\cosh\left(\frac{1}{2}\log\left(\frac{\Omega_{2,k}}{\Omega_{1,k}}\right)\right)\right]^{-1}\right\}}\,. \tag{C.17}$$

It is worth comparing the Bures and the Hilbert-Schmidt distances in the case of pure states. From (C.10) and (C.17), one obtains

$$d_{\rm HS} \;=\; \sqrt{2}\,d_{\rm B}\,\sqrt{1-(d_{\rm B}/2)^2}\,. \tag{C.18}$$

The occurrence of this relation should be related to the fact that the Fubini-Study distance is the natural distance between pure states [59, 93].

D Comments on some matrix identities

In this appendix we discuss some matrix identities employed throughout this manuscript.

In many matrix computations we have used the following property

$$f(MN) \;=\; N^{-1}f(NM)\,N = M\,f(NM)\,M^{-1}\,. \tag{D.1}$$

It is straightforward to prove these matrix identities when $f(x)=x^n$ and n is an integer number. Nonetheless, (D.1) has been often employed for $f(x)=\log x$ or for $f(x)=x^s$ with $0\leqslant s\leqslant 1$; hence in the following we show that (D.1) holds also for these functions.

The logarithm of a matrix M is defined through the series expansion [127]

$$\log M = \sum_{k=1}^{\infty}\frac{(-1)^{k+1}}{k}\,(M-\mathbf{1})^k\;. \tag{D.2}$$

This definition gives

$$N^{-1}\big[\log(NM)\big]N = \sum_{k=1}^{\infty}\frac{(-1)^{k+1}}{k}\;N^{-1}(NM-\mathbf{1})^k N\,. \tag{D.3}$$

Since for the k-th term of this series we have $N^{-1}\,(NM-\mathbf{1})^k\,N \;=\; (MN-\mathbf{1})^k$, (D.3) becomes

$$N^{-1}\left[\log\left(NM\right)\right]N = \sum_{k=1}^{\infty}\frac{(-1)^{k+1}}{k}\,(MN-\mathbf{1})^k = \log\left(MN\right) \tag{D.4}$$

which provides the first equality in (D.1) for $f(x)=\log x$. The second equality in (D.1) can be obtained by repeating the steps in (D.3) and (D.4) for $M\big[\log(NM)\big]M^{-1}$ in (D.3).

In order to check that (D.1) holds also when $f(x)=x^s$, let us observe that

$$(NM)^s = e^{s\log(NM)} = \sum_{k=0}^{\infty}\frac{s^k}{k!}\big[\log\left(NM\right)\big]^k\,. \tag{D.5}$$

JHEP12(2020)101

This leads to

$$N^{-1}\,(NM)^s\,N = \sum_{k=0}^{\infty} \frac{s^k}{k!}\, N^{-1}\big[\log(NM)\big]^k N \tag{D.6}$$

whose k-th term can be written as $N^{-1}\big[\log(NM)\big]^k N = \big[\log(MN)\big]^k$, once (D.4) has been employed. Thus, (D.6) becomes

$$N^{-1}\,(NM)^s\,N = \sum_{k=0}^{\infty} \frac{s^k}{k!}\,\big[\log(MN)\big]^k = (MN)^s \tag{D.7}$$

which corresponds to the first equality in (D.1) for $f(x) = x^s$. The second equality in (D.1) for $f(x) = x^s$ can be found by repeating the steps in (D.6) and (D.7) for $M(NM)^s M^{-1}$.

Another remark deserving more detailed comments concerns (2.31), where we introduced the Fisher-Rao distance $d(\gamma_{\rm R}, \gamma_{\rm T})$ as $\|\log(\gamma_{\rm R}^{-1/2}\,\gamma_{\rm T}\,\gamma_{\rm R}^{-1/2})\|_2$, pointing out that this expression is not equal to $\|\log(\gamma_{\rm T}\,\gamma_{\rm R}^{-1})\|_2$. Indeed, since $\|M\|_2 \equiv \sqrt{{\rm Tr}\,(M^\dagger M)}$ [67], we can exploit that $\log(\gamma_{\rm R}^{-1/2}\,\gamma_{\rm T}\,\gamma_{\rm R}^{-1/2})$ is real and symmetric to write

$$\|\log(\gamma_{\rm R}^{-1/2}\,\gamma_{\rm T}\,\gamma_{\rm R}^{-1/2})\|_2 = \sqrt{{\rm Tr}\big[\log(\gamma_{\rm R}^{-1/2}\,\gamma_{\rm T}\,\gamma_{\rm R}^{-1/2})\big]^2} = \sqrt{{\rm Tr}\big[\log(\gamma_{\rm T}\,\gamma_{\rm R}^{-1})\big]^2} \tag{D.8}$$

where in the last equality the cyclic property of the trace has been used. On the other hand, since $[\log(\gamma_{\rm T}\,\gamma_{\rm R}^{-1})]^{\rm t} = \log(\gamma_{\rm R}^{-1}\,\gamma_{\rm T})$, the matrix $\log(\gamma_{\rm T}\,\gamma_{\rm R}^{-1})$ is not symmetric, we have

$$\|\log(\gamma_{\rm T}\,\gamma_{\rm R}^{-1})\|_2 = \sqrt{{\rm Tr}\left[\log(\gamma_{\rm R}^{-1}\,\gamma_{\rm T})\log(\gamma_{\rm T}\,\gamma_{\rm R}^{-1})\right]} \neq \sqrt{{\rm Tr}\left[\log(\gamma_{\rm T}\,\gamma_{\rm R}^{-1})\right]^2} \tag{D.9}$$

which tells us that $d(\gamma_{\rm R}, \gamma_{\rm T})$ cannot be written as $\|\log(\gamma_{\rm T}\,\gamma_{\rm R}^{-1})\|_2$.

We find it worth providing further details about the construction of the symplectic matrices occurring in the Williamson's decompositions of $\widehat{H}^{\rm phys}$ and of some covariance matrices in section 9.

Let us consider two symmetric and positive definite $N \times N$ real matrices A and B that are diagonalised by the same orthogonal real matrix $\widetilde{O}$. It is straightforward to write $A \oplus B = O^{\rm t}(\mathcal{A} \oplus \mathcal{B})O$, where $O \equiv \widetilde{O} \oplus \widetilde{O}$ is orthogonal and symplectic, while the diagonal matrices $\mathcal{A} = {\rm diag}(\alpha_1, \ldots, \alpha_N)$ and $\mathcal{B} = {\rm diag}(\beta_1, \ldots, \beta_N)$ collect the eigenvalues of A and B respectively. The Williamson's decomposition of $A \oplus B$ reads $A \oplus B = W^{\rm t}(\mathcal{D} \oplus \mathcal{D})W$, where $\mathcal{D} = {\rm diag}(\sqrt{\alpha_1\beta_1}, \ldots, \sqrt{\alpha_N\beta_N}\,)$ and the symplectic matrix W is given by

$$W \equiv \chi\, O \qquad \chi \equiv {\rm diag}\big((\alpha_1/\beta_1)^{1/4}, \ldots, (\alpha_N/\beta_N)^{1/4}, (\alpha_1/\beta_1)^{-1/4}, \ldots, (\alpha_N/\beta_N)^{-1/4}\big) \tag{D.10}$$

where χ is a diagonal symplectic matrix. We remark that (D.10) provides the Euler decomposition (2.21) with $\mathcal{X} = \chi$, $R = O$ and $L = \mathbf{1}$.

E Details on the first law of complexity

In this appendix we report some technical details concerning the first law of complexity and the derivations of the results reported in section 3.

JHEP12(2020)101

The variation of the square of the distance (2.31) under the independent variations $\gamma_{\rm T} \to \gamma_{\rm T} + \delta\gamma_{\rm T}$ and $\gamma_{\rm R} \to \gamma_{\rm R} + \delta\gamma_{\rm R}$ of the covariance matrices of the reference and of the target state reads

$$\delta d^2 \,=\, 2\,\mathrm{Tr}\Big\{\log\Delta_{\rm TR}\,\delta\big[\log\Delta_{\rm TR}\big]\Big\} = 2\,\mathrm{Tr}\Big\{\big(\log\Delta_{\rm TR}\big)\,\Delta_{\rm TR}^{-1}\,\delta\Delta_{\rm TR}\Big\}\,. \tag{E.1}$$

The last expression can be found by first observing that, since M and δM do not commute in general, we can exploit the following formula [171]

$$\delta\log M \,=\, \int_0^1 \big[(1-b)M + b\,\mathbf{1}\big]^{-1}\delta M\,\big[(1-b)M + b\,\mathbf{1}\big]^{-1} db \tag{E.2}$$

When M and δM commute, by employing the matrix that diagonalises them simultaneously, one can easily check that (E.2) becomes $M^{-1}\delta M \,=\, \delta M\, M^{-1}$. In the general situation where M and δM do not necessarily commute, from the cyclic property of the trace and the fact that different functions of the same matrix commute we find that the first expression in (E.1) becomes

$$\begin{aligned}\delta d^2 \,&=\, 2\int_0^1 \mathrm{Tr}\Big\{\log\Delta_{\rm TR}\,\big[(1-b)\Delta_{\rm TR} + b\,\mathbf{1}\big]^{-2}\,\delta\Delta_{\rm TR}\Big\}\,db \\ &=\, 2\,\mathrm{Tr}\Big\{\log\Delta_{\rm TR}\Big(\int_0^1 \big[(1-b)\Delta_{\rm TR} + b\,\mathbf{1}\big]^{-2} db\Big)\,\delta\Delta_{\rm TR}\Big\}\,.\end{aligned} \tag{E.3}$$

Notice that $\log\Delta_{\rm TR}$ and $\delta\Delta_{\rm TR}$ do not commute in general. The last expression in (E.1) is obtained from (E.3) and

$$\int_0^1 \big[(1-b)\Delta_{\rm TR} + b\,\mathbf{1}\big]^{-2} db \,=\, \Delta_{\rm TR}^{-1}\,. \tag{E.4}$$

Straightforward matrix manipulations and the identity $\delta M^{-1} = -M^{-1}\,\delta M\,M^{-1}$ lead to write (E.1) as

$$\delta d^2 \,=\, 2\,\mathrm{Tr}\Big\{\big(\log\Delta_{\rm TR}\big)\,\gamma_{\rm R}\,\gamma_{\rm T}^{-1}\big(\delta\gamma_{\rm T}\,\gamma_{\rm R}^{-1} - \gamma_{\rm T}\,\gamma_{\rm R}^{-1}\,\delta\gamma_{\rm R}\gamma_{\rm R}^{-1}\big)\Big\} \tag{E.5}$$

$$= 2\,\mathrm{Tr}\Big\{\big(\log\Delta_{\rm TR}\big)\,\Big(\Delta_{\rm TR}^{-1}\,\delta\gamma_{\rm T} - \delta\gamma_{\rm R}\Big)\gamma_{\rm R}^{-1}\Big\}\,. \tag{E.6}$$

Finally, $\delta d^2 = 2d\,\delta d$ and (D.1) with $f(x) = \log x$ provide the expression (3.6).

In the following we compute separately the two sides of (3.4). Considering the r.h.s. of (3.4) first, from (3.3) one obtains

$$\sum_{ij}\frac{\partial F}{\partial\dot\gamma_{ij}}\,\delta\gamma_{ij} \,=\, \frac{\mathrm{Tr}\big[\gamma^{-1}\,\dot\gamma\,\gamma^{-1}\,\delta\gamma\big]}{\sqrt{\mathrm{Tr}\big[\,(\gamma^{-1}\dot\gamma)^2\,\big]}}\,. \tag{E.7}$$

From the expression (2.28) for the geodesic, it is not difficult to find that

$$G_s^{-1} \,=\, \gamma_{\rm R}^{-1/2}\Big(\gamma_{\rm R}^{-1/2}\,\gamma_{\rm T}\,\gamma_{\rm R}^{-1/2}\Big)^{-s}\gamma_{\rm R}^{-1/2} \tag{E.8}$$

$$\partial_s G_s \,=\, \gamma_{\rm R}^{1/2}\Big[\log\Big(\gamma_{\rm R}^{-1/2}\,\gamma_{\rm T}\,\gamma_{\rm R}^{-1/2}\Big)\Big]\Big(\gamma_{\rm R}^{-1/2}\,\gamma_{\rm T}\,\gamma_{\rm R}^{-1/2}\Big)^{s}\gamma_{\rm R}^{1/2} \tag{E.9}$$

$$\partial_s\, G_s^{-1} \,=\, -\,\gamma_{\rm R}^{-1/2}\Big[\log\Big(\gamma_{\rm R}^{-1/2}\,\gamma_{\rm T}\,\gamma_{\rm R}^{-1/2}\Big)\Big]\Big(\gamma_{\rm R}^{-1/2}\,\gamma_{\rm T}\,\gamma_{\rm R}^{-1/2}\Big)^{-s}\gamma_{\rm R}^{-1/2}\,. \tag{E.10}$$

JHEP12(2020)101

For the subsequent discussion, let us remark that, by specifying (E.10) to $s = 0$ and $s = 1$, and using (D.1), we find

$$\partial_s G_s^{-1}\big|_{s=1} = -\,\gamma_{\rm T}^{-1}\log(\Delta_{\rm TR}) = \log\left(\gamma_{\rm T}^{-1}\gamma_{\rm R}\right)\gamma_{\rm T}^{-1} \tag{E.11}$$

$$\partial_s G_s^{-1}\big|_{s=0} = -\,\gamma_{\rm R}^{-1}\log(\Delta_{\rm TR}) = \log\left(\gamma_{\rm T}^{-1}\gamma_{\rm R}\right)\gamma_{\rm R}^{-1}\,. \tag{E.12}$$

The denominator in the r.h.s. of (E.7) along the geodesic (2.28) reads

$$\sqrt{\mathrm{Tr}\left[\left(G_s^{-1}\,\partial_s G_s\right)^2\right]} \tag{E.13}$$

Combining (E.8) and (E.9), we observe that, for any $0 \leqslant s \leqslant 1$, this expression is equal to d defined in (2.31). Furthermore, the numerator in the r.h.s. of (E.7) at the endpoints of the geodesics can be expressed by using (E.8), (E.9) and (E.10). Thus, from (E.7) we get

$$\sum_{ij}\frac{\partial F}{\partial\dot\gamma_{ij}}\,\delta\gamma_{ij}\bigg|_0^1 = \frac{1}{d}\Big(\mathrm{Tr}\Big\{\partial_s G_s^{-1}\big|_{s=0}\,\delta\gamma_{\rm R}\Big\} - \mathrm{Tr}\Big\{\partial_s G_s^{-1}\big|_{s=1}\,\delta\gamma_{\rm T}\Big\}\Big)\,. \tag{E.14}$$

As for the l.h.s. of (3.4), let us consider d^2 from (2.31). First, one notices that (D.1) gives

$$\gamma_{\rm R}^{-1} f(\gamma_{\rm T}\gamma_{\rm R}^{-1}) = \gamma_{\rm R}^{-1/2}\, f(\gamma_{\rm R}^{-1/2}\,\gamma_{\rm T}\,\gamma_{\rm R}^{-1/2})\,\gamma_{\rm R}^{-1/2}\,. \tag{E.15}$$

The expressions obtained by specialising this result to $f(x) = \log x$ and $(\log x)\,x^{-1}$ allow to write (E.6) as follows

$$\begin{aligned}\delta d^2 \;=\; & 2\,\mathrm{Tr}\Big\{\gamma_{\rm R}^{-1/2}\left[\log\left(\gamma_{\rm R}^{-1/2}\,\gamma_{\rm T}\,\gamma_{\rm R}^{-1/2}\right)\right]\left(\gamma_{\rm R}^{-1/2}\,\gamma_{\rm T}\,\gamma_{\rm R}^{-1/2}\right)^{-1}\gamma_{\rm R}^{-1/2}\,\delta\gamma_{\rm T}\Big\} \\ & -2\,\mathrm{Tr}\Big\{\gamma_{\rm R}^{-1/2}\left[\log\left(\gamma_{\rm R}^{-1/2}\,\gamma_{\rm T}\,\gamma_{\rm R}^{-1/2}\right)\right]\gamma_{\rm R}^{-1/2}\,\delta\gamma_{\rm R}\Big\}\,.\end{aligned} \tag{E.16}$$

Then, by using (E.10) in (E.16), we obtain that $\delta d = (2d)^{-1}\delta d^2$ can be written as

$$\delta d = \frac{1}{d}\Big(\mathrm{Tr}\Big\{\partial_s G_s^{-1}\big|_{s=0}\,\delta\gamma_{\rm R}\Big\} - \mathrm{Tr}\Big\{\partial_s G_s^{-1}\big|_{s=1}\,\delta\gamma_{\rm T}\Big\}\Big) \tag{E.17}$$

whose r.h.s. coincides with the r.h.s. of (E.14); hence (3.4) is satisfied. Furthermore, by plugging (E.11) and (E.12) into (E.17), the expression (3.6) is obtained.

It is worth verifying that the Fisher-Rao cost function F defined in (3.3) evaluated along the path (2.28) satisfies the Euler-Lagrange equations, namely

$$\left[\,\frac{\partial F}{\partial\gamma_{ij}} - \frac{d}{ds}\left(\frac{\partial F}{\partial\dot\gamma_{ij}}\right)\right]\Big|_{\gamma\,=\,G_s} = 0\,. \tag{E.18}$$

This consistency check can be performed first by observing that from (3.3) we have

$$\frac{\partial F}{\partial\gamma} = -\,\frac{\gamma^{-1}\,\dot\gamma\,\gamma^{-1}\,\dot\gamma\,\gamma^{-1}}{\sqrt{\mathrm{Tr}\left[(\gamma^{-1}\dot\gamma)^2\right]}} \tag{E.19}$$

while $\frac{\partial F}{\partial\dot\gamma}$ can be read from (E.7). The expression (E.19) and $\frac{\partial F}{\partial\dot\gamma}$ along the geodesics (2.28) can be found by using (E.8), (E.9) and (E.10). Then, some algebra leads to (E.18).

JHEP12(2020)101

We find it instructive specialising the above results to pure states. Considering the geodesic given by (2.63), whose initial and final covariance matrices are given in (2.62), we have that both $\Delta_{\rm TR}$ and $\Delta_{\rm TR}+\delta\Delta_{\rm TR}$ are diagonal, hence they commute. This implies that (E.6) can be obtained directly from (E.1). Indeed, since in this basis $\Delta_{\rm TR}=\mathcal{X}^2_{\rm TR}$, we have that (E.1) becomes

$$\delta d^2 \,=\, 2\,\mathrm{Tr}\big[\,(\log\mathcal{X}^2_{\rm TR})\,\mathcal{X}^{-2}_{\rm TR}\,\delta\mathcal{X}^2_{\rm TR}\,\big]\,. \tag{E.20}$$

From (2.62) we find $\delta\gamma'_{\rm R}=0$ and $\delta\gamma'_{\rm T}=\frac{1}{2}\delta\mathcal{X}^2_{\rm TR}$. Thus, (E.20) and (E.6) are equivalent in the case of pure states.

In order to write (E.20) in terms of the geodesics (2.28), let us consider the a-th power (with $a\neq 0$) of the geodesic (2.63) and compute the derivative of the resulting matrix w.r.t. to the parameter s along the geodesic. The result reads

$$(\log\mathcal{X}^2_{\rm TR})\,\left(\mathcal{X}^2_{\rm TR}\right)^{s\,a}=\frac{2^a}{a}\,\partial_s(G_s)^a\,. \tag{E.21}$$

Setting $sa=-1$ in this expression, one finds

$$(\log\mathcal{X}^2_{\rm TR})\,\left(\mathcal{X}^2_{\rm TR}\right)^{-1}=-\frac{1}{2}\,\partial_s G_s^{-1}\big|_{s=1}\,. \tag{E.22}$$

This leads to write (E.6) for pure states as follows

$$\delta d^2 \;=\; -\,\mathrm{Tr}\Big\{\,\partial_s G_s^{-1}\big|_{s=1}\,\delta\gamma_{\rm T}\Big\} \tag{E.23}$$

where we have also used that $\delta\gamma'_{\rm T}=\frac{1}{2}\delta\mathcal{X}^2_{\rm TR}$ in the basis that we are considering. Since $\delta\gamma'_{\rm R}=0$, one immediately realises that (E.23) corresponds to (E.17) for pure states.

Another natural value for s to choose in (E.21) is $s=1/2$, that corresponds to the middle point of the geodesic. Comparing (E.21) with (E.20), it is natural to consider $s\,a=-1$, i.e. $a=-2$, finding that (E.20) can be written as

$$\delta d^2=-\frac{1}{4}\,\mathrm{Tr}\Big\{\partial_s G_s^{-2}\big|_{s=1/2}\,\delta(\mathcal{X}^2_{\rm TR})\Big\}\,. \tag{E.24}$$

We remark that $\mathcal{X}_{\rm TR}$ is the diagonal matrix providing the complexity in the case of pure states.

Another useful expression for δd comes from the Williamson's decompositions (2.41). Considering variations $\delta\gamma$ such that $\gamma+\delta\gamma$ is also a covariance matrix (in particular, $\delta\gamma$ is symmetric). Given the Williamson's decomposition (2.20) for γ, let us express $\delta\gamma$ in terms of the variations $\delta\mathcal{D}$ and δW of the symplectic spectrum and of the symplectic matrix W respectively. By using $\delta W^{\rm t}=(\delta W)^{\rm t}$, $\mathrm{Tr}(MN^{\rm t})=\mathrm{Tr}(M^{\rm t}N)$ and the fact that $\partial_s G_s^{-1}$ is symmetric,[28] we can write (E.17) as

$$\begin{aligned}\delta d=\frac{1}{d}\Big(&\mathrm{Tr}\Big\{\partial_s G_s^{-1}\big|_{s=0}\,\big[\,2\,W_{\rm R}^{\rm t}\,\mathcal{D}_{\rm R}\,\delta W_{\rm R}+W_{\rm R}^{\rm t}\,\delta\mathcal{D}_{\rm R}\,W_{\rm R}\,\big]\Big\}\\&-\mathrm{Tr}\Big\{\partial_s G_s^{-1}\big|_{s=1}\,\big[\,2\,W_{\rm T}^{\rm t}\,\mathcal{D}_{\rm T}\,\delta W_{\rm T}+W_{\rm T}^{\rm t}\,\delta\mathcal{D}_{\rm T}\,W_{\rm T}\,\big]\Big\}\Big)\end{aligned} \tag{E.25}$$

[28] This property can be proved by first transposing (E.10) and then using $f(M)^{\rm t}=f(M^{\rm t})$ and $[f(M),g(M)]=0$, that hold for generic functions of the same matrix.

JHEP12(2020)101

in terms of the four contributions coming from the basis variations $\delta W_{\rm R}$ and $\delta W_{\rm T}$ and from the spectra variations $\delta\mathcal{D}_{\rm R}$ and $\delta\mathcal{D}_{\rm T}$. The expression (3.7) for δd can be easily obtained by plugging (E.11) and (E.12) into (E.25).

F Thermofield double states

In this appendix we consider the thermofield double states (TFD's) for the harmonic lattices [172], whose circuit complexity has been explored in various studies over the last few years [22, 25, 26].

The TFD's are pure states constructed by entangling two equal copies of the harmonic lattice in such a way that a thermal state of the original system is obtained by tracing out one of the two copies. In section F.1 we provide the Williamson's decomposition of these pure states, showing also that they are special cases of the analysis reported in section 8. In section F.2 the circuit complexity for TFD's is discussed.

Consider two harmonic lattices (that will be denoted as "left" and "right" in the following) made by the same number N of sites. These two systems can be combined creating a system made by $2N$ sites (denoted as "doubled" system) whose hamiltonian reads

$$\widehat{H}_{\rm d} \equiv \frac{1}{2}\,\hat{\boldsymbol{r}}_{\rm d}^{\rm t}\,H_{\rm d}^{\rm phys}\,\hat{\boldsymbol{r}}_{\rm d} = \frac{1}{2}\,\hat{\boldsymbol{r}}_{\rm d}^{\rm t}\Big(Q_{\rm d}^{\rm phys} \oplus \frac{1}{m}\,\mathbf{1}\Big)\,\hat{\boldsymbol{r}}_{\rm d} \qquad Q_{\rm d}^{\rm phys} = Q^{\rm phys} \oplus Q^{\rm phys} \tag{F.1}$$

where $\hat{\boldsymbol{r}}_{\rm d}^{\rm t} \equiv (\hat{\boldsymbol{q}}_{\rm l}^{\rm t}, \hat{\boldsymbol{q}}_{\rm r}^{\rm t}, \hat{\boldsymbol{p}}_{\rm l}^{\rm t}, \hat{\boldsymbol{p}}_{\rm r}^{\rm t})$, where the subiindices refer to the left and right part of the doubled system, and $Q^{\rm phys}$ has been introduced in (2.64). For the periodic chain the matrix $Q^{\rm phys}$ has been written explicitly in (9.3).

It is not difficult to adapt the diagonalisation procedure described in section 2.6 to (F.1). This leads to construct the $4N \times 4N$ matrix $H_{\rm d}^{\rm phys}$ defined in (F.1) as follows (see (2.66))

$$H_{\rm d}^{\rm phys} = V_{\rm d}\,\mathcal{X}_{\rm d}\,\mathcal{D}_{\rm d}\,\mathcal{X}_{\rm d}\,V_{\rm d}^{\rm t} \tag{F.2}$$

where we have introduced the diagonal matrix $\mathcal{D}_{\rm d} \equiv \mathcal{D}_{\rm phys} \oplus \mathcal{D}_{\rm phys}$, the symplectic and orthogonal matrix $V_{\rm d} \equiv V \oplus V$ and the symplectic diagonal matrix

$$\mathcal{X}_{\rm d} = S \oplus S^{-1} \qquad S \equiv \mathcal{S} \oplus \mathcal{S} \tag{F.3}$$

where

$$\mathcal{S} \equiv \sqrt{m}\,\mathrm{diag}\Big(\sqrt{\Omega_1}, \dots, \sqrt{\Omega_N}\Big) \tag{F.4}$$

with Ω_k the dispersion relation introduced through (2.65). These matrices are defined in terms of the $2N \times 2N$ matrices V and $\mathcal{D}_{\rm phys}$ in (2.65) and (2.68) respectively.

Since $V_{\rm d}$ and $\mathcal{X}_{\rm d}$ are symplectic matrices, the expression (F.2) leads us to write the Williamson's decomposition of $H_{\rm d}^{\rm phys}$ as follows

$$H_{\rm d}^{\rm phys} = W_{\rm d}^{\rm t}\,\mathcal{D}_{\rm d}\,W_{\rm d} \qquad W_{\rm d} = \mathcal{X}_{\rm d}\,V_{\rm d}^{\rm t}\,. \tag{F.5}$$

This decomposition suggests to introduce the following set of canonical conjugated variables (see section 2.6)

$$\hat{\boldsymbol{s}}_{\rm d} \equiv W_{\rm d}\,\hat{\boldsymbol{r}}_{\rm d} \qquad \hat{\boldsymbol{s}}_{\rm d}^{\rm t} \equiv (\hat{\mathrm{q}}_{{\rm l},1}, \dots, \hat{\mathrm{q}}_{{\rm l},N}, \hat{\mathrm{q}}_{{\rm r},1}, \dots, \hat{\mathrm{q}}_{{\rm r},N}, \hat{\mathrm{p}}_{{\rm l},1}, \dots, \hat{\mathrm{p}}_{{\rm l},N}, \hat{\mathrm{p}}_{{\rm r},1}, \dots, \hat{\mathrm{p}}_{{\rm r},N})\,. \tag{F.6}$$

JHEP12(2020)101

Defining the annihilation operators and the creation operators for the two parts of the system as in (2.71), one obtains a vector $\hat{\boldsymbol{b}}_{\rm d}^{\rm t} \equiv (\hat{\boldsymbol{b}}_{\rm l}^{\rm t}, \hat{\boldsymbol{b}}_{\rm r}^{\rm t}, (\hat{\boldsymbol{b}}_{\rm l}^{\dagger})^{\rm t}, (\hat{\boldsymbol{b}}_{\rm r}^{\dagger})^{\rm t})$, where $\hat{\mathfrak{b}}_{l,k}$ and $\hat{\mathfrak{b}}_{r,k}$ are the k-th element of $\hat{\boldsymbol{b}}_{\rm l}$ and $\hat{\boldsymbol{b}}_{\rm r}$ respectively. In terms of the components of $\hat{\boldsymbol{b}}_{\rm d}$, the hamiltonian (F.1) becomes

$$\widehat{H}_{\rm d} = \sum_{k=1}^{N} \Omega_k \Big(\hat{\mathfrak{b}}_{l,k}^{\dagger} \, \hat{\mathfrak{b}}_{l,k} + \hat{\mathfrak{b}}_{r,k}^{\dagger} \, \hat{\mathfrak{b}}_{r,k} + 1 \Big) \,. \tag{F.7}$$

The standard quantisation procedure leads to introduce the eigenstates $|\boldsymbol{n}_{\rm r}, \boldsymbol{n}_{\rm l}\rangle \equiv |\boldsymbol{n}_{\rm l}\rangle_{\rm l} \, |\boldsymbol{n}_{\rm r}\rangle_{\rm r}$ of the number operator, that can be factorised through the eigenstates $|\boldsymbol{n}_{\rm l}\rangle_{\rm l}$ and $|\boldsymbol{n}_{\rm r}\rangle_{\rm r}$ of the number operators corresponding to the two parts. The eigenstates with $\boldsymbol{n}_{\rm r} = \boldsymbol{n}_{\rm l} \equiv \boldsymbol{n}$ allow to define the thermofield double state (TFD) as follows [172]

$$|{\rm TFD}\rangle = \prod_{k=1}^{N} \sqrt{1 - e^{-\beta\Omega_k}} \sum_{\boldsymbol{n}} e^{-\frac{\beta}{2} \sum_{k=1}^{N} \Omega_k n_k} |\boldsymbol{n}\rangle_{\rm l} \, |\boldsymbol{n}\rangle_{\rm r} \,. \tag{F.8}$$

When $\beta \to \infty$, the TFD becomes the product state of the two ground states $|\boldsymbol{0}\rangle_{\rm l} \, |\boldsymbol{0}\rangle_{\rm r}$.

Tracing out the degrees of freedom corresponding to one of the two parts, e.g. the right part, in (F.8) one obtains

$${\rm Tr}_{\mathcal{H}_{\rm r}} \big(|{\rm TFD}\rangle\langle{\rm TFD}| \big) = \prod_{k=1}^{N} \big(1 - e^{-\beta\Omega_k} \big) \sum_{\boldsymbol{n}} e^{-\beta \sum_{k=1}^{N} \Omega_k n_k} \, |\boldsymbol{n}\rangle_{\rm l} \, {}_{\rm l}\langle \boldsymbol{n}| \tag{F.9}$$

which is the thermal density matrix for the left half system at temperature $1/\beta$.

F.1 Covariance matrix

The covariance matrix of the TFD can be found through a slight generalisation of the procedure described in section 2.6 for the thermal states. From (2.9) and (F.6), the covariance matrix of this pure state can be written as

$$\gamma_{\rm TFD} = {\rm Re}\langle {\rm TFD}| \, \hat{\boldsymbol{r}}_{\rm d} \, \hat{\boldsymbol{r}}_{\rm d}^{\rm t} \, |{\rm TFD}\rangle = W_{\rm d}^{-1} \, {\rm Re}\big[\langle {\rm TFD}| \, \hat{\boldsymbol{s}}_{\rm d} \hat{\boldsymbol{s}}_{\rm d}^{\rm t} \, |{\rm TFD}\rangle \big] \, W_{\rm d}^{-{\rm t}} \,. \tag{F.10}$$

In order to compute the matrix ${\rm Re}\langle{\rm TFD}|\hat{\boldsymbol{s}}_{\rm d}\hat{\boldsymbol{s}}_{\rm d}^{\rm t}|{\rm TFD}\rangle$, one first expresses the operators in $\hat{\boldsymbol{s}}_{\rm d}$ in terms of the creation and annihilation operators in $\hat{\boldsymbol{b}}_{\rm d}$ and then exploits their action on (F.8). The non vanishing elements of ${\rm Re}\langle{\rm TFD}|\hat{\boldsymbol{s}}_{\rm d}\hat{\boldsymbol{s}}_{\rm d}^{\rm t}|{\rm TFD}\rangle$, are

$$\begin{aligned}
&{\rm Re}\langle \hat{\mathfrak{q}}_{l,k} \hat{\mathfrak{q}}_{l,k} \rangle = {\rm Re}\langle \hat{\mathfrak{q}}_{r,k} \hat{\mathfrak{q}}_{r,k} \rangle = {\rm Re}\langle \hat{\mathfrak{p}}_{l,k} \hat{\mathfrak{p}}_{l,k} \rangle = {\rm Re}\langle \hat{\mathfrak{p}}_{r,k} \hat{\mathfrak{p}}_{r,k} \rangle = \frac{1}{2} \coth(\beta\Omega_k/2) \\
&{\rm Re}\langle \hat{\mathfrak{q}}_{r,k} \hat{\mathfrak{q}}_{l,k} \rangle = {\rm Re}\langle \hat{\mathfrak{q}}_{l,k} \hat{\mathfrak{q}}_{r,k} \rangle = -{\rm Re}\langle \hat{\mathfrak{p}}_{r,k} \hat{\mathfrak{p}}_{l,k} \rangle = -{\rm Re}\langle \hat{\mathfrak{p}}_{l,k} \hat{\mathfrak{p}}_{r,k} \rangle = \frac{1}{2} \, \frac{1}{\sinh(\beta\Omega_k/2)}
\end{aligned} \tag{F.11}$$

where the notation $\langle \widehat{O} \rangle \equiv \langle {\rm TFD}| \, \widehat{O} \, |{\rm TFD}\rangle$ has been adopted. By using (F.11), the covariance matrix ${\rm Re}\langle{\rm TFD}|\hat{\boldsymbol{s}}_{\rm d}\hat{\boldsymbol{s}}_{\rm d}^{\rm t}|{\rm TFD}\rangle$ in (F.10) can be written as

$${\rm Re}\langle \hat{\boldsymbol{s}}_{\rm d} \, \hat{\boldsymbol{s}}_{\rm d}^{\rm t} \rangle = \Upsilon_{\rm TFD}^{(+)} \oplus \Upsilon_{\rm TFD}^{(-)} \qquad \Upsilon_{\rm TFD}^{(\pm)} \equiv \begin{pmatrix} \Lambda_{\rm TFD} & \pm\tilde{\Lambda}_{\rm TFD} \\ \pm\tilde{\Lambda}_{\rm TFD} & \Lambda_{\rm TFD} \end{pmatrix} \tag{F.12}$$

JHEP12(2020)101

where we have introduced the following $N \times N$ diagonal matrices

$$\begin{aligned} \Lambda_{\text{TFD}} &\equiv \frac{1}{2}\,\text{diag}\Big(\,\coth(\beta\Omega_1/2),\ldots,\coth(\beta\Omega_N/2)\Big) \\ \tilde{\Lambda}_{\text{TFD}} &\equiv \frac{1}{2}\,\text{diag}\Big(\frac{1}{\sinh(\beta\Omega_1/2)},\ldots,\frac{1}{\sinh(\beta\Omega_N/2)}\Big) \end{aligned} \tag{F.13}$$

which satisfy

$$\Lambda^2_{\text{TFD}} - \tilde{\Lambda}^2_{\text{TFD}} = \frac{1}{4}\,\mathbf{1} \tag{F.14}$$

and

$$(\Lambda_{\text{TFD}} + \tilde{\Lambda}_{\text{TFD}})\,(\Lambda_{\text{TFD}} - \tilde{\Lambda}_{\text{TFD}})^{-1} = \text{diag}(\,\coth^2(\beta\Omega_1/4),\ldots,\coth^2(\beta\Omega_N/4))\,. \tag{F.15}$$

Plugging (F.12) into (F.10) and employing the definition of W_{d} in (F.5), for the covariance matrix of the TFD we find

$$\gamma_{\text{TFD}} = V_{\text{d}}\,\mathcal{X}_{\text{d}}^{-1}\Big(\Upsilon^{(+)}_{\text{TFD}} \oplus \Upsilon^{(-)}_{\text{TFD}}\Big)\mathcal{X}_{\text{d}}^{-1}\,V_{\text{d}}^{\text{t}} = Q_{\text{TFD}} \oplus P_{\text{TFD}} \tag{F.16}$$

where (F.3) and $V_{\text{d}} \equiv V \oplus V$ have been employed to write the last expression, which is given in terms of the following $2N \times 2N$ symmetric matrices

$$Q_{\text{TFD}} = V S^{-1}\,\Upsilon^{(+)}_{\text{TFD}}\,S^{-1}\,V^{\text{t}} \qquad P_{\text{TFD}} = V S\,\Upsilon^{(-)}_{\text{TFD}}\,S\,V^{\text{t}}\,. \tag{F.17}$$

By using that V is an orthogonal matrix and that

$$\Upsilon^{(+)}_{\text{TFD}}\,\Upsilon^{(-)}_{\text{TFD}} = \frac{1}{4}\,\mathbf{1} \tag{F.18}$$

which can be obtained from (F.12) and (F.14), one finds

$$Q_{\text{TFD}}\,P_{\text{TFD}} = \frac{1}{4}\,\mathbf{1} \tag{F.19}$$

as expected, since the TFD is a pure state whose covariance matrix has non vanishing blocks only along the diagonal.

In order to write the Williamson's decompositions of γ_{TFD}, let us observe that the matrices $\Upsilon^{(\pm)}_{\text{TFD}}$ can be diagonalised by the $2N \times 2N$ symplectic and orthogonal matrix O as follows

$$\Upsilon^{(\pm)}_{\text{TFD}} = O^{\text{t}}\Big((\Lambda_{\text{TFD}} \pm \tilde{\Lambda}_{\text{TFD}}) \oplus (\Lambda_{\text{TFD}} \mp \tilde{\Lambda}_{\text{TFD}})\Big)O \qquad O = \frac{1}{\sqrt{2}}\begin{pmatrix} \mathbf{1} & \mathbf{1} \\ -\mathbf{1} & \mathbf{1} \end{pmatrix}. \tag{F.20}$$

By using (D.10), (F.14) and (F.15), these matrices can be written as

$$\Upsilon^{(\pm)}_{\text{TFD}} = \frac{1}{2}\,O^{\text{t}}\mathcal{X}^{\pm 2}_{\text{TFD}}\,O \tag{F.21}$$

where

$$\begin{aligned} \mathcal{X}_{\text{TFD}} = \text{diag}\Big(&\sqrt{\coth(\beta\Omega_1/4)},\ldots,\sqrt{\coth(\beta\Omega_N/4)}\,, \\ &\sqrt{\tanh(\beta\Omega_1/4)},\ldots,\sqrt{\tanh(\beta\Omega_N/4)}\,\Big). \end{aligned} \tag{F.22}$$

JHEP12(2020)101

Plugging (F.3) and (F.21) into (F.16), one gets the Williamson's decompositions of γ_{TFD} as

$$\gamma_{\text{TFD}} = \frac{1}{2}\, W_{\text{TFD}}^{\text{t}}\, W_{\text{TFD}} \tag{F.23}$$

where the $4N \times 4N$ symplectic matrix W_{TFD} is

$$W_{\text{TFD}} = (\mathcal{X}_{\text{TFD}}\, O\, S^{-1} V^{\text{t}}) \oplus (\mathcal{X}_{\text{TFD}}^{-1}\, O\, S\, V^{\text{t}})\,. \tag{F.24}$$

It is instructive to express the fact that the TFD is a particular purification of a thermal state (see (F.9)) by identifying it within the analysis reported in section 8. This can be done by setting $N_{\text{anc}} = N$ and by rewriting the covariance matrix of the TFD in terms of the matrices occurring in (8.10).

Comparing (F.16) with (8.3), we easily conclude that in this case Q_{TFD} and P_{TFD} correspond to Q_{ext} and P_{ext} respectively, while $M_{\text{ext}} = \mathbf{0}$. Then, by employing the block diagonal matrices (F.3), (F.12) and $V = \widetilde{V} \oplus \widetilde{V}$, where $\widetilde{V}$ is the $N \times N$ orthogonal matrix (see (2.65) and (9.6)–(9.7) for the periodic harmonic chain), we can write Q_{TFD} and P_{TFD} as the partitioned matrices in (8.10) with

$$Q = Q_{\text{anc}} = \widetilde{V}\, \mathcal{S}^{-1} \Lambda_{\text{TFD}}\, \mathcal{S}^{-1}\, \widetilde{V}^{\text{t}} \qquad P = P_{\text{anc}} = \widetilde{V}\, \mathcal{S}\, \Lambda_{\text{TFD}}\, \mathcal{S}\, \widetilde{V}^{\text{t}} \tag{F.25}$$

and

$$\Gamma_Q \;=\; \widetilde{V}\, \mathcal{S}^{-1} \tilde{\Lambda}_{\text{TFD}}\, \mathcal{S}^{-1}\, \widetilde{V}^{\text{t}} \qquad \Gamma_P \;=\; -\,\widetilde{V}\, \mathcal{S}\, \tilde{\Lambda}_{\text{TFD}}\, \mathcal{S}\, \widetilde{V}^{\text{t}}\,. \tag{F.26}$$

We remark that (F.25) and (F.26) satisfy the conditions in (8.20). Furthermore, $Q \oplus P = Q_{\text{anc}} \oplus P_{\text{anc}}$ constructed from (F.25) provides the covariance matrix of a thermal state given in (2.76), as expected. Thus, the TFD is a purification of the thermal state and its covariance matrix satisfies (8.19).

F.2 Complexity

The TFD are pure states; hence the complexity of a target TFD with respect to a reference TFD can be computed by employing (2.58). In the most general case where the target TFD and the reference TFD originate from different hamiltonians, complicated expressions occur because W_{TFD} depends on the physical hamiltonian through S and V in a non trivial way.

For the sake of simplicity, let us focus on the special case where the same hamiltonian underlies both the target TFD and the reference TFD, which are only distinguished by their inverse temperatures β_{R} and β_{T}. In this case both the reference state and the target state have the same S and V. Moreover, since (F.20) tells us that O does not contain parameters, the reference and target states that we are considering can be distinguished only through their matrices $\mathcal{X}_{\text{TFD,R}}$ and $\mathcal{X}_{\text{TFD,T}}$. In this case, by employing (F.24) we find that the matrix defined in (2.45) crucially simplifies to the following diagonal matrix

$$W_{\text{TFD,TR}} = (\mathcal{X}_{\text{TFD,T}}\, \mathcal{X}_{\text{TFD,R}}^{-1}) \oplus (\mathcal{X}_{\text{TFD,T}}^{-1}\, \mathcal{X}_{\text{TFD,R}})\,. \tag{F.27}$$

The circuit complexity corresponding to this choice of TFD's can be obtained by plugging (F.27) into (2.58). The result reads

$$\mathcal{C}_2 = \frac{1}{2\sqrt{2}} \sqrt{\text{Tr}\left\{ \left[\log(\mathcal{X}_{\text{TFD,T}}^2 \mathcal{X}_{\text{TFD,R}}^{-2})\right]^2 \oplus \left[\log(\mathcal{X}_{\text{TFD,T}}^{-2} \mathcal{X}_{\text{TFD,R}}^2)\right]^2 \right\}} \tag{F.28}$$

JHEP12(2020)101

which can be written more explicitly by employing (F.22) for these TFD's, finding

$$\mathcal{C}_2 = \frac{1}{\sqrt{2}} \sqrt{\sum_{k=1}^{N} \left[\log\left(\frac{\coth\left(\beta_{\mathrm{T}}\Omega_k/4\right)}{\coth\left(\beta_{\mathrm{R}}\Omega_k/4\right)} \right) \right]^2} \,. \tag{F.29}$$

An interesting regime to consider corresponds to $\beta_{\mathrm{R}}\Omega_k \gg 1$. In this limit the reference state is the product of the ground states of the two parts because only $\boldsymbol{n} = \boldsymbol{0}$ contributes in (F.8). In this regime the complexity (F.29) simplifies to

$$\mathcal{C}_2 = \frac{1}{\sqrt{2}} \sqrt{\sum_{k=1}^{N} \left[\log(\coth\left(\beta_{\mathrm{T}}\Omega_k/4\right)) \right]^2} \tag{F.30}$$

which is consistent with the results reported in [22].

We find it worth generalising (F.29) by considering a circuit where the reference state and the target state correspond to different hamiltonians that have the same matrix V_{d} in their decompositions (F.2). This is the case e.g. for the periodic harmonic chain explored in section 9.1, where $\widetilde{V}$ defined in (9.6) and (9.7) depends only on the number of sites of the chain, hence it is independent of the parameters occurring in the hamiltonian of the chain. From (F.16) and (F.19), we have that $\gamma_{\mathrm{TFD}} = Q_{\mathrm{TFD}} \oplus 4Q_{\mathrm{TFD}}^{-1}$, which implies

$$\gamma_{\mathrm{TFD,T}}\, \gamma_{\mathrm{TFD,R}}^{-1} = Q_{\mathrm{TFD,T}}\, Q_{\mathrm{TFD,R}}^{-1} \oplus Q_{\mathrm{TFD,T}}^{-1}\, Q_{\mathrm{TFD,R}} \,. \tag{F.31}$$

This allows to write the complexity (2.33) as follows

$$\begin{aligned} \mathcal{C}_2 &= \frac{1}{2\sqrt{2}} \sqrt{\mathrm{Tr}\Big\{ \big[\log(Q_{\mathrm{TFD,T}}\, Q_{\mathrm{TFD,R}}^{-1} \oplus Q_{\mathrm{TFD,T}}^{-1}\, Q_{\mathrm{TFD,R}}) \big]^2 \Big\}} \\ &= \frac{1}{2} \sqrt{\mathrm{Tr}\Big\{ \big[\log(Q_{\mathrm{TFD,T}}\, Q_{\mathrm{TFD,R}}^{-1}) \big]^2 \Big\}} \,. \end{aligned} \tag{F.32}$$

By applying (F.17) to this case, where the reference and target states have the same matrix V, the argument of the logarithm in (F.32) becomes

$$Q_{\mathrm{TFD,T}}\, Q_{\mathrm{TFD,R}}^{-1} \;=\; V\, S_{\mathrm{T}}^{-1}\, \Upsilon_{\mathrm{TFD,T}}^{(+)}\, S_{\mathrm{T}}^{-1}\, S_{\mathrm{R}}\, (4\Upsilon_{\mathrm{TFD,R}}^{(-)})\, S_{\mathrm{R}} V^{\mathrm{t}} \tag{F.33}$$

where we have used that $\big(\Upsilon_{\mathrm{TFD,R}}^{(+)}\big)^{-1} = 4\Upsilon_{\mathrm{TFD,R}}^{(-)}$ (see (F.18)). The relations in (F.3), (F.4), (F.12) and (F.13) lead to write (F.33) as follows

$$Q_{\mathrm{TFD,T}}\, Q_{\mathrm{TFD,R}}^{-1} = V \begin{pmatrix} \Lambda_{\mathrm{TR}} & \tilde{\Lambda}_{\mathrm{TR}} \\ \tilde{\Lambda}_{\mathrm{TR}} & \Lambda_{\mathrm{TR}} \end{pmatrix} V^{\mathrm{t}} \tag{F.34}$$

where Λ_{TR} and $\tilde{\Lambda}_{\mathrm{TR}}$ are $N \times N$ diagonal matrices whose entries read

$$\begin{aligned} (\Lambda_{\mathrm{TR}})_{k,k} &= \frac{\Omega_{\mathrm{R},k}}{\Omega_{\mathrm{T},k}} \left[\coth\left(\beta_{\mathrm{R}}\Omega_{\mathrm{R},k}/2\right) \coth\left(\beta_{\mathrm{T}}\Omega_{\mathrm{T},k}/2\right) - \frac{1}{\sinh\left(\beta_{\mathrm{R}}\Omega_{\mathrm{R},k}/2\right) \sinh\left(\beta_{\mathrm{T}}\Omega_{\mathrm{T},k}/2\right)} \right] \\ (\tilde{\Lambda}_{\mathrm{TR}})_{k,k} &= \frac{\Omega_{\mathrm{R},k}}{\Omega_{\mathrm{T},k}} \left[\frac{\coth\left(\beta_{\mathrm{R}}\Omega_{\mathrm{R},k}/2\right)}{\sinh\left(\beta_{\mathrm{T}}\Omega_{\mathrm{T},k}/2\right)} - \frac{\coth\left(\beta_{\mathrm{T}}\Omega_{\mathrm{T},k}/2\right)}{\sinh\left(\beta_{\mathrm{R}}\Omega_{\mathrm{R},k}/2\right)} \right] \qquad 1 \leqslant k \leqslant N \,. \end{aligned} \tag{F.35}$$

JHEP12(2020)101

By adapting the result given in (F.20) for $\Upsilon^{(+)}_{\text{TFD}}$, we can diagonalise the matrix containing Λ_{TR} and $\tilde{\Lambda}_{\text{TR}}$ in the r.h.s. of (F.34) through the orthogonal matrix O. This leads to write (F.34) as follows

$$Q_{\text{TFD,T}} Q^{-1}_{\text{TFD,R}} = V O^{\text{t}} \Big[(\Lambda_{\text{TR}} + \tilde{\Lambda}_{\text{TR}}) \oplus (\Lambda_{\text{TR}} - \tilde{\Lambda}_{\text{TR}}) \Big] O V^{\text{t}} \tag{F.36}$$

where the entries of the diagonal matrices within the square brackets are given by

$$(\Lambda_{\text{TR}} + \tilde{\Lambda}_{\text{TR}})_{k,k} = \frac{\Omega_{\text{R},k} \coth\left(\beta_{\text{T}} \Omega_{\text{T},k}/4\right)}{\Omega_{\text{T},k} \coth\left(\beta_{\text{R}} \Omega_{\text{R},k}/4\right)} \qquad (\Lambda_{\text{TR}} - \tilde{\Lambda}_{\text{TR}})_{k,k} = \frac{\Omega_{\text{R},k} \coth\left(\beta_{\text{R}} \Omega_{\text{R},k}/4\right)}{\Omega_{\text{T},k} \coth\left(\beta_{\text{T}} \Omega_{\text{T},k}/4\right)} \,. \tag{F.37}$$

Plugging (F.36) into (F.32), we find that the orthogonal matrices V and O do not contribute to the complexity. By employing also (F.37), one obtains

$$\mathcal{C}_2 = \frac{1}{2} \sqrt{\sum_{k=1}^{N} \left\{ \left[\log\left(\frac{\Omega_{\text{R},k} \coth\left(\beta_{\text{R}} \Omega_{\text{R},k}/4\right)}{\Omega_{\text{T},k} \coth\left(\beta_{\text{T}} \Omega_{\text{T},k}/4\right)} \right) \right]^2 + \left[\log\left(\frac{\Omega_{\text{R},k} \coth\left(\beta_{\text{T}} \Omega_{\text{T},k}/4\right)}{\Omega_{\text{T},k} \coth\left(\beta_{\text{R}} \Omega_{\text{R},k}/4\right)} \right) \right]^2 \right\}} \,. \tag{F.38}$$

In the regime $\beta_{\text{R}} \Omega_{\text{R},k} \gg 1$ this expression simplifies to

$$\mathcal{C}_2 = \frac{1}{2} \sqrt{\sum_{k=1}^{N} \left\{ \left[\log\left(\frac{\Omega_{\text{T},k} \coth\left(\beta_{\text{T}} \Omega_{\text{T},k}/4\right)}{\Omega_{\text{R},k}} \right) \right]^2 + \left[\log\left(\frac{\Omega_{\text{R},k} \coth\left(\beta_{\text{T}} \Omega_{\text{T},k}/4\right)}{\Omega_{\text{T},k}} \right) \right]^2 \right\}} \tag{F.39}$$

which is consistent with the results reported in [22].[29]

G Diagonal and physical bases for the $\mathcal{C}_1$ complexity

In this appendix we briefly discuss the definition of the $\mathcal{C}_1$ complexity, which is based on the F_1 cost function, hence it is a base dependent quantity. We also introduce the diagonal basis and the physical basis, slightly extending the definition given in [23]. Some results reported in section 9.7 have been obtained by employing these bases.

In the Nielsen's geometric approach to complexity between pure states [1–3], the circuit connecting the reference and the target states is made by the unitary matrices $\widehat{U}_{\text{N}}(s)$, with $s \in [0,1]$, which are written as follows

$$\widehat{U}_{\text{N}}(s) = \overleftarrow{\mathcal{P}}\, e^{-\text{i} \int_0^s H_{\text{N}}(\sigma)\, d\sigma} \qquad H_{\text{N}}(\sigma) = \sum_I Y^I(\sigma)\, \widehat{K}_I \tag{G.1}$$

where $\overleftarrow{\mathcal{P}}$ is the path-ordered exponential indicating that the circuit is constructed from right to left as s increases, $\widehat{K}_I$ are the hermitian generators of the unitary transformation and the functions $Y^I(\sigma)$, that are called control functions, characterise the gates at a given point of the circuit. The circuit depth is defined through cost function F as follows

$$D(\widehat{U}_{\text{N}}) = \int_0^1 F(\widehat{U}_{\text{N}}(s), Y^I(s))\, ds \,. \tag{G.2}$$

[29] See eq. (192) of [22] at $t = 0$.

JHEP12(2020)101

The complexity corresponds to the minimal circuit depth, obtained by comparing all the possible unitary circuits connecting the reference state to the target state. The allowed cost functions must satisfy some properties that have been discussed e.g. in [17].

In this manuscript we consider only the F_1 cost function and the F_2 cost function. These cost functions are defined respectively as

$$F_1 = \sum_I |Y^I| \qquad F_2 = \left[\sum_I (Y^I)^2 \right]^{1/2} \tag{G.3}$$

and, through (G.2), they provide the $\mathcal{C}_1$ complexity and the $\mathcal{C}_2$ complexity respectively.

Consider the harmonic lattice and the corresponding covariance matrix introduced in section 2.

In [22], the complexity of pure states has been studied by employing the fact that, since a unitary circuit can be represented as a circuit in $\mathrm{Sp}(2N,\mathbb{R})$, instead of (G.1), for this model we can equivalently consider

$$U(s) = \mathcal{P}\, e^{\int_0^s K(\sigma)\, d\sigma} \qquad K(\sigma) = \sum_I \mathcal{Y}^I(\sigma)\, K_I \tag{G.4}$$

where K_I are the generators of $\mathrm{Sp}(2N,\mathbb{R})$, hence the index $1 \leqslant I \leqslant N(2N+1)$.

The symplectic matrix $U(s)$ in (G.4) has been discussed also in section 2.5. In particular, from (2.61) and eq. (57) in [22], we have

$$G_s = U(s)\, \gamma_{\mathrm{R}}\, U(s)^{\mathrm{t}} = \frac{1}{2}\, W_s^{\mathrm{t}}\, W_s \qquad G_1 = \gamma_{\mathrm{T}} \tag{G.5}$$

where γ_{R} and γ_{T} are the covariance matrices of the reference pure state and the target pure state respectively. In [22] the symplectic matrix $U(s)$ has been written in terms of the matrix Δ_{TR} defined in (2.32) as

$$U(s) = e^{sK} = e^{\frac{s}{2}\log \Delta_{\mathrm{TR}}} \qquad K = \frac{1}{2}\log \Delta_{\mathrm{TR}}\,. \tag{G.6}$$

By setting $U(s) = U_s$ defined in (2.38), one observes that $U(s)$ in (G.6) coincides with (2.61). Comparing (G.6) with (G.4), one observes that both K and $\mathcal{Y}^I$ (obtained by expanding K as in (G.4)) are independent of σ. Because of this feature, the integral in (G.2) is trivial to perform. For the cost functions in (G.3), the results read respectively

$$\mathcal{C}_1 = \sum_I |\mathcal{Y}^I| \qquad \mathcal{C}_2 = \left[\sum_I (\mathcal{Y}^I)^2 \right]^{1/2}. \tag{G.7}$$

After a change of basis, the generators K_I and the control functions in (G.4) change respectively as follows [17, 22]

$$K_I = \sum_J O_{IJ}\, \widetilde{K}_J \qquad \mathcal{Y}^I = \sum_J O_{JI}\, \widetilde{\mathcal{Y}}^J \tag{G.8}$$

where O_{IJ} are the entries of an orthogonal $N(2N+1) \times N(2N+1)$ real matrix O. Given that O is orthogonal, in (G.7) the $\mathcal{C}_2$ complexity is invariant while the $\mathcal{C}_1$ complexity is not.

JHEP12(2020)101

In [23] the complexity of mixed states based on the purification complexity (see section 8) is mainly studied by employing the F_1 cost function. In particular, this $\mathcal{C}_1$ complexity is investigated in two different bases: the diagonal basis and the physical basis.

The diagonal basis in the extended system, which is in a pure state, is defined by the change of basis corresponding to the symplectic and orthogonal matrix R introduced in (2.22).

In order to introduce the physical basis, let us consider the wave function (2.24) of the pure state characterising the extended system. This wave function is completely described by $N_{\rm ext} \times N_{\rm ext}$ complex symmetric matrix $E_{\rm ext} + \mathrm{i}F_{\rm ext}$, that can be written as follows

$$E_{\rm ext} + \mathrm{i}F_{\rm ext} \equiv \begin{pmatrix} E + \mathrm{i}F & \Gamma_E + \mathrm{i}\Gamma_F \\ \Gamma_E^{\rm t} + \mathrm{i}\Gamma_F^{\rm t} & E_{\rm anc} + \mathrm{i}F_{\rm anc} \end{pmatrix} \tag{G.9}$$

where E and F are $N \times N$ real symmetric matrices, $E_{\rm anc}$ and $F_{\rm anc}$ are $N_{\rm anc} \times N_{\rm anc}$ real symmetric matrices, while Γ_E and Γ_F are $N \times N_{\rm anc}$ real matrices.

In the physical basis both $E+\mathrm{i}F$ and $E_{\rm anc}+\mathrm{i}F_{\rm anc}$ are diagonal matrices. By employing a result of matrix algebra (see Corollary 4.4.4 of [173]), the complex and symmetric matrices $E + \mathrm{i}F$ and $E_{\rm anc} + \mathrm{i}F_{\rm anc}$ can be diagonalised as follows

$$D = X(E + \mathrm{i}F)X^{\rm t} \qquad D_{\rm anc} = X_{\rm anc}(E_{\rm anc} + \mathrm{i}F_{\rm anc})X_{\rm anc}^{\rm t} \tag{G.10}$$

where D and $D_{\rm anc}$ are real diagonal matrices with non negative entries and the matrices X and $X_{\rm anc}$ are unitary. The physical basis is defined through the change of basis characterised by the matrix $X^{\rm phys} \equiv X \oplus X_{\rm anc}$, that brings the blocks on the diagonal of $E_{\rm ext}+\mathrm{i}F_{\rm ext}$ in (G.9) in their diagonal forms. In the special case of $F_{\rm ext} = \mathbf{0}$, the definition of physical basis given in [23] is recovered.

Open Access. This article is distributed under the terms of the Creative Commons Attribution License (CC-BY 4.0), which permits any use, distribution and reproduction in any medium, provided the original author(s) and source are credited.

References

[1] M.A. Nielsen, *A geometric approach to quantum circuit lower bounds*, *Quantum Info. Comput.* **6** (2006) 213 [quant-ph/0502070].

[2] M. A. Nielsen, M. R. Dowling, M. Gu and A. Doherty, *Quantum computation as geometry*, *Science* **311** (2006) 1133 [quant-ph/0603161].

[3] M.R. Dowling and M.A. Nielsen, *The geometry of quantum computation*, *Quantum Info. Comput.* **8** (2008) 861 [quant-ph/0701004].

[4] J. Watrous, *Quantum computational complexity*, *Encycl. Compl. Syst. Sci.* **7174** (2009) [arXiv:0804.3401].

[5] S. Aaronson, *The complexity of quantum states and transformations: from quantum money to black holes*, arXiv:1607.05256 [INSPIRE].

[6] D. Aharonov, A. Kitaev and N. Nisan, *Quantum circuits with mixed states*, quant-ph/9806029.

JHEP12(2020)101

[7] L. Susskind, *Computational complexity and black hole horizons*, *Fortsch. Phys.* **64** (2016) 24 [*Addendum ibid.* **64** (2016) 44] [arXiv:1403.5695] [INSPIRE].

[8] D. Stanford and L. Susskind, *Complexity and shock wave geometries*, *Phys. Rev. D* **90** (2014) 126007 [arXiv:1406.2678] [INSPIRE].

[9] L. Susskind, *Entanglement is not enough*, *Fortsch. Phys.* **64** (2016) 49 [arXiv:1411.0690] [INSPIRE].

[10] M. Alishahiha, *Holographic complexity*, *Phys. Rev. D* **92** (2015) 126009 [arXiv:1509.06614] [INSPIRE].

[11] A.R. Brown, D.A. Roberts, L. Susskind, B. Swingle and Y. Zhao, *Holographic complexity equals bulk action?*, *Phys. Rev. Lett.* **116** (2016) 191301 [arXiv:1509.07876] [INSPIRE].

[12] A.R. Brown, D.A. Roberts, L. Susskind, B. Swingle and Y. Zhao, *Complexity, action, and black holes*, *Phys. Rev. D* **93** (2016) 086006 [arXiv:1512.04993] [INSPIRE].

[13] J.L.F. Barbón and E. Rabinovici, *Holographic complexity and spacetime singularities*, *JHEP* **01** (2016) 084 [arXiv:1509.09291] [INSPIRE].

[14] J.L.F. Barbón and J. Martin-Garcia, *Holographic complexity of cold hyperbolic black holes*, *JHEP* **11** (2015) 181 [arXiv:1510.00349] [INSPIRE].

[15] J. Couch, W. Fischler and P.H. Nguyen, *Noether charge, black hole volume, and complexity*, *JHEP* **03** (2017) 119 [arXiv:1610.02038] [INSPIRE].

[16] D. Carmi, R.C. Myers and P. Rath, *Comments on holographic complexity*, *JHEP* **03** (2017) 118 [arXiv:1612.00433] [INSPIRE].

[17] R. Jefferson and R.C. Myers, *Circuit complexity in quantum field theory*, *JHEP* **10** (2017) 107 [arXiv:1707.08570] [INSPIRE].

[18] M. Guo, J. Hernandez, R.C. Myers and S.-M. Ruan, *Circuit complexity for coherent states*, *JHEP* **10** (2018) 011 [arXiv:1807.07677] [INSPIRE].

[19] R. Khan, C. Krishnan and S. Sharma, *Circuit complexity in fermionic field theory*, *Phys. Rev. D* **98** (2018) 126001 [arXiv:1801.07620] [INSPIRE].

[20] L. Hackl and R.C. Myers, *Circuit complexity for free fermions*, *JHEP* **07** (2018) 139 [arXiv:1803.10638] [INSPIRE].

[21] A. Bhattacharyya, A. Shekar and A. Sinha, *Circuit complexity in interacting QFTs and RG flows*, *JHEP* **10** (2018) 140 [arXiv:1808.03105] [INSPIRE].

[22] S. Chapman et al., *Complexity and entanglement for thermofield double states*, *SciPost Phys.* **6** (2019) 034 [arXiv:1810.05151] [INSPIRE].

[23] E. Caceres, S. Chapman, J.D. Couch, J.P. Hernández, R.C. Myers and S.-M. Ruan, *Complexity of mixed states in QFT and holography*, *JHEP* **03** (2020) 012 [arXiv:1909.10557] [INSPIRE].

[24] P. Braccia, A.L. Cotrone and E. Tonni, *Complexity in the presence of a boundary*, *JHEP* **02** (2020) 051 [arXiv:1910.03489] [INSPIRE].

[25] S. Chapman and H.Z. Chen, *Complexity for charged thermofield double states*, arXiv:1910.07508 [INSPIRE].

[26] M. Doroudiani, A. Naseh and R. Pirmoradian, *Complexity for charged thermofield double states*, *JHEP* **01** (2020) 120 [arXiv:1910.08806] [INSPIRE].

JHEP12(2020)101

[27] M. Guo, Z.-Y. Fan, J. Jiang, X. Liu and B. Chen, *Circuit complexity for generalized coherent states in thermal field dynamics*, *Phys. Rev. D* **101** (2020) 126007 [arXiv:2004.00344] [INSPIRE].

[28] N. Jaiswal, M. Gautam and T. Sarkar, *Complexity and information geometry in spin chains*, arXiv:2005.03532 [INSPIRE].

[29] C.A. Agón, M. Headrick and B. Swingle, *Subsystem complexity and holography*, *JHEP* **02** (2019) 145 [arXiv:1804.01561] [INSPIRE].

[30] P. Caputa, N. Kundu, M. Miyaji, T. Takayanagi and K. Watanabe, *Anti-de Sitter space from optimization of path integrals in conformal field theories*, *Phys. Rev. Lett.* **119** (2017) 071602 [arXiv:1703.00456] [INSPIRE].

[31] B. Czech, *Einstein equations from varying complexity*, *Phys. Rev. Lett.* **120** (2018) 031601 [arXiv:1706.00965] [INSPIRE].

[32] P. Caputa, N. Kundu, M. Miyaji, T. Takayanagi and K. Watanabe, *Liouville action as path-integral complexity: from continuous tensor networks to AdS/CFT*, *JHEP* **11** (2017) 097 [arXiv:1706.07056] [INSPIRE].

[33] S. Chapman, M.P. Heller, H. Marrochio and F. Pastawski, *Toward a definition of complexity for quantum field theory states*, *Phys. Rev. Lett.* **120** (2018) 121602 [arXiv:1707.08582] [INSPIRE].

[34] A. Bhattacharyya, P. Caputa, S.R. Das, N. Kundu, M. Miyaji and T. Takayanagi, *Path-integral complexity for perturbed CFTs*, *JHEP* **07** (2018) 086 [arXiv:1804.01999] [INSPIRE].

[35] P. Caputa and J.M. Magan, *Quantum computation as gravity*, *Phys. Rev. Lett.* **122** (2019) 231302 [arXiv:1807.04422] [INSPIRE].

[36] H.A. Camargo, P. Caputa, D. Das, M.P. Heller and R. Jefferson, *Complexity as a novel probe of quantum quenches: universal scalings and purifications*, *Phys. Rev. Lett.* **122** (2019) 081601 [arXiv:1807.07075] [INSPIRE].

[37] S. Chapman, D. Ge and G. Policastro, *Holographic complexity for defects distinguishes action from volume*, *JHEP* **05** (2019) 049 [arXiv:1811.12549] [INSPIRE].

[38] H.A. Camargo, M.P. Heller, R. Jefferson and J. Knaute, *Path integral optimization as circuit complexity*, *Phys. Rev. Lett.* **123** (2019) 011601 [arXiv:1904.02713] [INSPIRE].

[39] D. Ge and G. Policastro, *Circuit complexity and 2D bosonisation*, *JHEP* **10** (2019) 276 [arXiv:1904.03003] [INSPIRE].

[40] P. Bueno, J.M. Magan and C.S. Shahbazi, *Complexity measures in QFT and constrained geometric actions*, arXiv:1908.03577 [INSPIRE].

[41] Y. Sato and K. Watanabe, *Does boundary distinguish complexities?*, *JHEP* **11** (2019) 132 [arXiv:1908.11094] [INSPIRE].

[42] J. Erdmenger, M. Gerbershagen and A.-L. Weigel, *Complexity measures from geometric actions on Virasoro and Kac-Moody orbits*, *JHEP* **11** (2020) 003 [arXiv:2004.03619] [INSPIRE].

[43] M. Flory and M.P. Heller, *Complexity and conformal field theory*, arXiv:2005.02415 [INSPIRE].

[44] A. Ferraro, S. Olivares and M.G.A. Paris, *Gaussian states in continuous variable quantum information*, quant-ph/0503237.

JHEP12(2020)101

[45] A. Holevo, *Probabilistic and statistical aspects of quantum theory*, Edizioni della Normale, Italy (2011).

[46] C. Weedbrook et al., *Gaussian quantum information*, *Rev. Mod. Phys.* **84** (2012) 621 [arXiv:1110.3234].

[47] G. Adesso, S. Ragy and A.R. Lee, *Continuous variable quantum information: gaussian states and beyond*, *Open Syst. Inf. Dynam.* **21** (2014) 1440001 [arXiv:1401.4679].

[48] A. Serafini, *Quantum continuous variables: a primer of theoretical methods*, CRC press, U.S.A. (2017).

[49] J. Eisert, M. Cramer and M.B. Plenio, *Area laws for the entanglement entropy - a review*, *Rev. Mod. Phys.* **82** (2010) 277 [arXiv:0808.3773] [INSPIRE].

[50] H. Casini and M. Huerta, *Entanglement entropy in free quantum field theory*, *J. Phys. A* **42** (2009) 504007 [arXiv:0905.2562] [INSPIRE].

[51] P. Calabrese and J. Cardy, *Entanglement entropy and conformal field theory*, *J. Phys. A* **42** (2009) 504005 [arXiv:0905.4013] [INSPIRE].

[52] I. Peschel and V. Eisler, *Reduced density matrices and entanglement entropy in free lattice models*, *J. Phys. A* **42** (2009) 504003 [arXiv:0906.1663].

[53] S. Ryu and T. Takayanagi, *Holographic derivation of entanglement entropy from AdS/CFT*, *Phys. Rev. Lett.* **96** (2006) 181602 [hep-th/0603001] [INSPIRE].

[54] S. Ryu and T. Takayanagi, *Aspects of holographic entanglement entropy*, *JHEP* **08** (2006) 045 [hep-th/0605073] [INSPIRE].

[55] V.E. Hubeny, M. Rangamani and T. Takayanagi, *A covariant holographic entanglement entropy proposal*, *JHEP* **07** (2007) 062 [arXiv:0705.0016] [INSPIRE].

[56] M. Rangamani and T. Takayanagi, *Holographic entanglement entropy*, Springer, Germany (2017).

[57] M. Headrick, *Lectures on entanglement entropy in field theory and holography*, arXiv:1907.08126 [INSPIRE].

[58] E. Tonni, *An introduction to entanglement measures in conformal field theories and AdS/CFT*, *Springer Proc. Phys.* **239** (2020) 69 [INSPIRE].

[59] I. Bengtsson and K. Życzkowski, *Geometry of quantum states: an introduction to quantum entanglement*, Cambridge University Press, Cambridge U.K. (2017).

[60] V. Link and W. Strunz, *Geometry of Gaussian quantum states*, *J. Phys. A* **48** (2015) 275301 [arXiv:1503.02471].

[61] N. Chentsov, *Statistical decision rules and optimal inference*, Translations of Mathematical Monographs volume 53, American Mathematical Society, U.S.A. (1982).

[62] S. Amari, *Information geometry and its applications*, Springer, Germany (2016).

[63] F. Nielsen, *An elementary introduction to information geometry*, arXiv:1808.08271.

[64] D. Petz, *Monotone metrics on matrix spaces*, *Linear Alg. Appl.* **244** (1996) 81.

[65] J. Lawson and Y. Lim, *The geometric mean, matrices, metrics, and more*, *Amer. Math. Mon.* **108** (2001) 797.

[66] W. Förstner and B. Moonen, *A metric for covariance matrices*, in *Geodesy-the challenge of the* 3rd *Millennium*, E.W. Grafarend ed., Springer, Germany (2003).

[67] R. Bhatia, *Positive definite matrices*, Princeton University Press, Princeton U.S.A. (2007).

JHEP12(2020)101

[68] R. Bhatia and T. Jain, *On symplectic eigenvalues of positive definite matrices*, *J. Math. Phys.* **56** (2015) 112201 [arXiv:1803.04647]

[69] C. Rao, *Information and the accuracy attainable in the estimation of statistical parameters*, *Bull. Calcutta Math. Soc.* **37** (1945) 81.

[70] C. Atkinson and A. Mitchell, *Rao's Distance Measure*, *Sankhyā* **43** (1981) 345.

[71] D. Felice, M.H. Quang and S. Mancini, *The volume of Gaussian states by information geometry*, *J. Math. Phys.* **58** (2017) 012201 [arXiv:1509.01049].

[72] J. Williamson, *On the algebraic problem concerning the normal forms of linear dynamical systems*, *Amer. J. Math.* **58** (1936) 141.

[73] A. Bernamonti, F. Galli, J. Hernandez, R.C. Myers, S.-M. Ruan and J. Simón, *First law of holographic complexity*, *Phys. Rev. Lett.* **123** (2019) 081601 [arXiv:1903.04511] [INSPIRE].

[74] A. Bernamonti, F. Galli, J. Hernandez, R.C. Myers, S.-M. Ruan and J. Simón, *Aspects of the first law of complexity*, arXiv:2002.05779 [INSPIRE].

[75] N. Mukunda, R. Simon and G. Sudarshan, *Gaussian Wigner distributions in quantum mechanics and optics*, *Phys. Rev. A* **36** (1987) 3868 [INSPIRE].

[76] R. Simon, N. Mukunda and B. Dutta, *Quantum-noise matrix for multimode systems:* U(n) *invariance, squeezing, and normal forms*, *Phys. Rev. A* **49** (1994) 1567.

[77] Arvind, B. Dutta, N. Mukunda and R. Simon, *The real symplectic groups in quantum mechanics and optics*, *Pramana* **45** (1995) 471 [quant-ph/9509002] [INSPIRE].

[78] R. Simn, S. Chaturvedi and V. Srinivasan, *Congruences and canonical forms for a positive matrix: application to the Schweinler–Wigner extremum principle*, *J. Math. Phys.* **40** (1999) 3632 [math-ph/9811003].

[79] M. de Gosson, *Symplectic geometry and quantum mechanics*, Birkhäuser, Switzerland (2006).

[80] K. Audenaert, J. Eisert, M.B. Plenio and R.F. Werner, *Entanglement properties of the harmonic chain*, *Phys. Rev. A* **66** (2002) 042327 [quant-ph/0205025] [INSPIRE].

[81] M.B. Plenio, J. Eisert, J. Dreissig and M. Cramer, *Entropy, entanglement, and area: analytical results for harmonic lattice systems*, *Phys. Rev. Lett.* **94** (2005) 060503 [quant-ph/0405142] [INSPIRE].

[82] M. Cramer, J. Eisert, M.B. Plenio and J. Dreissig, *An entanglement-area law for general bosonic harmonic lattice systems*, *Phys. Rev. A* **73** (2006) 012309 [quant-ph/0505092] [INSPIRE].

[83] A. Holevo, *Some statistical problems for quantum Gaussian states*, *IEEE Trans. Inf. Theor.* **21** (1975) 533.

[84] R. Fisher, *On the mathematical foundations of theoretical statistics*, *Phil. Trans. Roy. Soc. London* **222** (1921) 309.

[85] J. Pinele, S.I.R. Costa and J.E. Strapasson, *On the Fisher-Rao information metric in the space of normal distributions*, *Lect. Notes Comp. Sci.* **11712** (2019) 676.

[86] H. Hotelling, *Spaces of statistical parameters*, *Bull. Am. Math. Soc.* **36** (1930) 191.

[87] P. Mahalanobis, *On the generalized distance in statistics*, *Proc. Natl. Inst. Sci. India* **2** (1936) 49.

[88] A. Bhattacharyya, *On a measure of divergence between two statistical populations defined by their probability distributions*, *Bull. Calcutta Math. Soc.* **35** (1943) 99.

JHEP12(2020)101

[89] J. Pinele, J.E. Strapasson and S.I.R. Costa, *The Fisher-Rao distance between multivariate normal distributions: special cases, boundsand applications*, *Entropy* **22** (2020) 404.

[90] S.I. Costa, S.A. Santos and J.E. Strapasson, *Fisher information distance: A geometrical reading*, *Discrete Appl. Math.* **197** (2015) 59 [arXiv:1210.2354].

[91] J. Strapasson, J. Pinele and S. Costa, *A totally geodesic submanifold of the multivariate normal distributions and bounds for the Fisher-Rao distance*, in the proceedings of the *2016 IEEE Information Theory Workshop (ITW)*, September 11–14, Cambridge U.K. (2016).

[92] M. Nielsen and I. Chuang, *Quantum computation and quantum information*, Cambridge University Press, Cambridge U.K. (2000).

[93] D. Spehner, F. Illuminati, M. Orszag and W. Roga, *Geometric measures of quantum correlations with Bures and Hellinger distances*, arXiv:1611.03449.

[94] I. Peschel and M.C. Chung, *Density matrices for a chain of oscillators*, *J. Phys. A* **32** (1999) 8419 [cond-mat/9906224].

[95] I. Peschel, *Calculation of reduced density matrices from correlation functions*, *J. Phys. A* **36** (2003) L205 [cond-mat/0212631].

[96] A. Coser, C. De Nobili and E. Tonni, *A contour for the entanglement entropies in harmonic lattices*, *J. Phys. A* **50** (2017) 314001 [arXiv:1701.08427] [INSPIRE].

[97] A. Botero and B. Reznik, *Spatial structures and localization of vacuum entanglement in the linear harmonic chain*, *Phys. Rev. A* **70** (2004) 052329 [quant-ph/0403233].

[98] Y. Chen and G. Vidal, *Entanglement contour*, *J. Stat. Mech.* **10** (2014) P10011 [arXiv:1406.1471]

[99] G. Vidal and R.F. Werner, *Computable measure of entanglement*, *Phys. Rev. A* **65** (2002) 032314 [quant-ph/0102117] [INSPIRE].

[100] P. Calabrese, J. Cardy and E. Tonni, *Entanglement negativity in quantum field theory*, *Phys. Rev. Lett.* **109** (2012) 130502 [arXiv:1206.3092] [INSPIRE].

[101] P. Calabrese, J. Cardy and E. Tonni, *Entanglement negativity in extended systems: a field theoretical approach*, *J. Stat. Mech.* **1302** (2013) P02008 [arXiv:1210.5359] [INSPIRE].

[102] P. Calabrese, J. Cardy and E. Tonni, *Finite temperature entanglement negativity in conformal field theory*, *J. Phys. A* **48** (2015) 015006 [arXiv:1408.3043] [INSPIRE].

[103] A. Holevo and R.F. Werner, *Evaluating capacities of Bosonic Gaussian channels*, *Phys. Rev. A* **63** (2001) 032312 [quant-ph/9912067].

[104] P. Sohr, V. Link, K. Luoma and W. T. Strunz, *Typical Gaussian quantum information*, *J. Phys. A* **52** (2018) 035301 [arXiv:1808.10153].

[105] M. Calvo and J.M. Oller, *A distance between multivariate normal distributions based in an embedding into the Siegel group*, *J. Multivar. Anal.* **35** (1990) 223.

[106] J. Strapasson, J. Porto and S. Costa, *On bounds for the Fisher-Rao distance between multivariate normal distributions*, *AIP Conf. Proc.* **1641** (2015) 313.

[107] J. Bisognano and E.H. Wichmann, *On the duality condition for a Hermitian scalar field*, *J. Math. Phys.* **16** (1975) 985 [INSPIRE].

[108] H. Casini, M. Huerta and R.C. Myers, *Towards a derivation of holographic entanglement entropy*, *JHEP* **05** (2011) 036 [arXiv:1102.0440] [INSPIRE].

JHEP12(2020)101

[109] G. Wong, I. Klich, L.A. Pando Zayas and D. Vaman, *Entanglement temperature and entanglement entropy of excited states*, *JHEP* **12** (2013) 020 [arXiv:1305.3291] [INSPIRE].

[110] J. Cardy and E. Tonni, *Entanglement Hamiltonians in two-dimensional conformal field theory*, *J. Stat. Mech.* **1612** (2016) 123103 [arXiv:1608.01283] [INSPIRE].

[111] R. Arias, D. Blanco, H. Casini and M. Huerta, *Local temperatures and local terms in modular Hamiltonians*, *Phys. Rev. D* **95** (2017) 065005 [arXiv:1611.08517] [INSPIRE].

[112] R. Arias, H. Casini, M. Huerta and D. Pontello, *Anisotropic Unruh temperatures*, *Phys. Rev. D* **96** (2017) 105019 [arXiv:1707.05375] [INSPIRE].

[113] E. Tonni, J. Rodríguez-Laguna and G. Sierra, *Entanglement hamiltonian and entanglement contour in inhomogeneous* 1*D critical systems*, *J. Stat. Mech.* **1804** (2018) 043105 [arXiv:1712.03557] [INSPIRE].

[114] A. Roy, F. Pollmann and H. Saleur, *Entanglement Hamiltonian of the* $1+1$*-dimensional free, compactified boson conformal field theory*, *J. Stat. Mech.* **2008** (2020) 083104 [arXiv:2004.14370] [INSPIRE].

[115] M.C. Chung and I. Peschel, *Density-matrix spectra for two-dimensional quantum systems*, *Phys. Rev. B* **62** (2000) 4191 [cond-mat/0004222].

[116] I. Peschel, *On the reduced density matrix for a chain of free electrons*, *J. Stat. Mech.* **06** (2004) P06004 [cond-mat/0403048].

[117] L. Banchi, S.L. Braunstein and S. Pirandola, *Quantum fidelity for arbitrary Gaussian states*, *Phys. Rev. Lett.* **115** (2015) 260501 [arXiv:1507.01941].

[118] V. Eisler and I. Peschel, *Analytical results for the entanglement Hamiltonian of a free-fermion chain*, *J. Phys. A* **50** (2017) 284003 [arXiv:1703.08126] [INSPIRE].

[119] V. Eisler, E. Tonni and I. Peschel, *On the continuum limit of the entanglement Hamiltonian*, *J. Stat. Mech.* **1907** (2019) 073101 [arXiv:1902.04474] [INSPIRE].

[120] G. Di Giulio, R. Arias and E. Tonni, *Entanglement Hamiltonians in* 1*D free lattice models after a global quantum quench*, *J. Stat. Mech.* **1912** (2019) 123103 [arXiv:1905.01144] [INSPIRE].

[121] G. Di Giulio and E. Tonni, *On entanglement hamiltonians of an interval in massless harmonic chains*, *J. Stat. Mech.* **2003** (2020) 033102 [arXiv:1911.07188] [INSPIRE].

[122] H. Li and F. Haldane, *Entanglement spectrum as a generalization of entanglement entropy: identification of topological order in non-Abelian fractional quantum Hall effect states*, *Phys. Rev. Lett.* **101** (2008) 010504 [arXiv:0805.0332] [INSPIRE].

[123] P. Calabrese and A. Lefevre, *Entanglement spectrum in one-dimensional systems*, *Phys. Rev. A* **78** (2008) 032329 [arXiv:0806.3059].

[124] A.M. Läuchli, *Operator content of real-space entanglement spectra at conformal critical points*, arXiv:1303.0741 [INSPIRE].

[125] V. Alba, P. Calabrese and E. Tonni, *Entanglement spectrum degeneracy and the Cardy formula in 1+1 dimensional conformal field theories*, *J. Phys. A* **51** (2018) 024001 [arXiv:1707.07532] [INSPIRE].

[126] J. Surace, L. Tagliacozzo and E. Tonni, *Operator content of entanglement spectra in the transverse field Ising chain after global quenches*, *Phys. Rev. B* **101** (2020) 241107(R) [arXiv:1909.07381] [INSPIRE].

JHEP12(2020)101

[127] B. Hall, *Lie groups, Lie algebras and representations: an elementary introduction*, Springer, Germany (2015).

[128] F. Benatti and R. Floreanini, *Open quantum dynamics: complete positivity and entanglement*, *Int. J. Mod. Phys. B* **19** (2005) 3063 [quant-ph/0507271] [INSPIRE].

[129] K. Audenaert, J. Eisert, M.B. Plenio and R.F. Werner, *Entanglement Properties of the Harmonic Chain*, *Phys. Rev. A* **66** (2002) 042327 [quant-ph/0205025] [INSPIRE].

[130] F.W. Stinespring, *Positive functions on C^*-algebras*, *Proc. Amer. Math. Soc.* **6** (1955) 211.

[131] F. Caruso, J. Eisert, V. Giovannetti and A. Holevo, *Multi-mode bosonic Gaussian channels*, *New J. Phys.* **10** (2008) 083030 [arXiv:0804.0511].

[132] G. Lindblad, *Cloning the quantum oscillator*, *J. Phys. A* **33** (2000) 5059.

[133] B.M. Terhal, M. Horodecki, D.W. Leung and D.P. DiVincenzo, *The entanglement of purification*, *J. Math. Phys.* **43** (2002) 4286 [quant-ph/0202044].

[134] T. Takayanagi and K. Umemoto, *Entanglement of purification through holographic duality*, *Nature Phys.* **14** (2018) 573 [arXiv:1708.09393] [INSPIRE].

[135] P. Nguyen, T. Devakul, M.G. Halbasch, M.P. Zaletel and B. Swingle, *Entanglement of purification: from spin chains to holography*, *JHEP* **01** (2018) 098 [arXiv:1709.07424] [INSPIRE].

[136] A. Bhattacharyya, T. Takayanagi and K. Umemoto, *Entanglement of purification in free scalar field theories*, *JHEP* **04** (2018) 132 [arXiv:1802.09545] [INSPIRE].

[137] V. Eisler and Z. Zimborás, *Entanglement negativity in the harmonic chain out of equilibrium*, *New J. Phys.* **16** (2014) 123020 [arXiv:1406.5474].

[138] A. Coser, E. Tonni and P. Calabrese, *Entanglement negativity after a global quantum quench*, *J. Stat. Mech.* **1412** (2014) P12017 [arXiv:1410.0900] [INSPIRE].

[139] J.S. Cotler, M.P. Hertzberg, M. Mezei and M.T. Mueller, *Entanglement growth after a global quench in free scalar field theory*, *JHEP* **11** (2016) 166 [arXiv:1609.00872] [INSPIRE].

[140] A. Altland and B. Simons, *Condensed matter field theory*, Cambridge University Press Cambridge, U.K. (2010).

[141] M. Alishahiha, K. Babaei Velni and M.R. Mohammadi Mozaffar, *Black hole subregion action and complexity*, *Phys. Rev. D* **99** (2019) 126016 [arXiv:1809.06031] [INSPIRE].

[142] R. Auzzi, S. Baiguera, A. Legramandi, G. Nardelli, P. Roy and N. Zenoni, *On subregion action complexity in AdS_3 and in the BTZ black hole*, *JHEP* **01** (2020) 066 [arXiv:1910.00526] [INSPIRE].

[143] P. Calabrese, J. Cardy and E. Tonni, *Entanglement entropy of two disjoint intervals in conformal field theory*, *J. Stat. Mech.* **0911** (2009) P11001 [arXiv:0905.2069] [INSPIRE].

[144] P. Calabrese, J. Cardy and E. Tonni, *Entanglement entropy of two disjoint intervals in conformal field theory II*, *J. Stat. Mech.* **1101** (2011) P01021 [arXiv:1011.5482] [INSPIRE].

[145] J. Cardy, *Some results on the mutual information of disjoint regions in higher dimensions*, *J. Phys. A* **46** (2013) 285402 [arXiv:1304.7985] [INSPIRE].

[146] A. Coser, L. Tagliacozzo and E. Tonni, *On Rényi entropies of disjoint intervals in conformal field theory*, *J. Stat. Mech.* **1401** (2014) P01008 [arXiv:1309.2189] [INSPIRE].

[147] C. De Nobili, A. Coser and E. Tonni, *Entanglement entropy and negativity of disjoint intervals in CFT: some numerical extrapolations*, *J. Stat. Mech.* **1506** (2015) P06021 [arXiv:1501.04311] [INSPIRE].

JHEP12(2020)101

[148] A. Coser, E. Tonni and P. Calabrese, *Spin structures and entanglement of two disjoint intervals in conformal field theories*, *J. Stat. Mech.* **1605** (2016) 053109 [arXiv:1511.08328] [INSPIRE].

[149] V.E. Hubeny and M. Rangamani, *Holographic entanglement entropy for disconnected regions*, *JHEP* **03** (2008) 006 [arXiv:0711.4118] [INSPIRE].

[150] M. Headrick, *Entanglement Rényi entropies in holographic theories*, *Phys. Rev. D* **82** (2010) 126010 [arXiv:1006.0047] [INSPIRE].

[151] E. Tonni, *Holographic entanglement entropy: near horizon geometry and disconnected regions*, *JHEP* **05** (2011) 004 [arXiv:1011.0166] [INSPIRE].

[152] P. Fonda, L. Giomi, A. Salvio and E. Tonni, *On shape dependence of holographic mutual information in AdS_4*, *JHEP* **02** (2015) 005 [arXiv:1411.3608] [INSPIRE].

[153] P. Calabrese, L. Tagliacozzo and E. Tonni, *Entanglement negativity in the critical Ising chain*, *J. Stat. Mech.* **1305** (2013) P05002 [arXiv:1302.1113] [INSPIRE].

[154] V. Eisler and Z. Zimborás, *On the partial transpose of fermionic Gaussian states*, *New J. Phys.* **17** (2015) 053048.

[155] A. Coser, E. Tonni and P. Calabrese, *Partial transpose of two disjoint blocks in XY spin chains*, *J. Stat. Mech.* **1508** (2015) P08005 [arXiv:1503.09114] [INSPIRE].

[156] V. Eisler and Z. Zimborás, *Entanglement negativity in two-dimensional free lattice models*, *Phys. Rev. B* **93** (2016) 115148 [arXiv:1511.08819].

[157] C. De Nobili, A. Coser and E. Tonni, *Entanglement negativity in a two dimensional harmonic lattice: Area law and corner contributions*, *J. Stat. Mech.* **1608** (2016) 083102 [arXiv:1604.02609] [INSPIRE].

[158] J.M. Maldacena, *Eternal black holes in Anti-de Sitter*, *JHEP* **04** (2003) 021 [hep-th/0106112] [INSPIRE].

[159] E. Cáceres, J. Couch, S. Eccles and W. Fischler, *Holographic purification complexity*, *Phys. Rev. D* **99** (2019) 086016 [arXiv:1811.10650] [INSPIRE].

[160] S. Chapman, H. Marrochio and R.C. Myers, *Holographic complexity in Vaidya spacetimes. Part I*, *JHEP* **06** (2018) 046 [arXiv:1804.07410] [INSPIRE].

[161] S. Chapman, H. Marrochio and R.C. Myers, *Holographic complexity in Vaidya spacetimes. Part II*, *JHEP* **06** (2018) 114 [arXiv:1805.07262] [INSPIRE].

[162] R. Auzzi, G. Nardelli, F.I. Schaposnik Massolo, G. Tallarita and N. Zenoni, *On volume subregion complexity in Vaidya spacetime*, *JHEP* **11** (2019) 098 [arXiv:1908.10832] [INSPIRE].

[163] J. Erdmenger, K.T. Grosvenor and R. Jefferson, *Information geometry in quantum field theory: lessons from simple examples*, *SciPost Phys.* **8** (2020) 073 [arXiv:2001.02683] [INSPIRE].

[164] S. Lang, *Linear algebra*, Springer, Germany (2004).

[165] S. Helgason, *Differential geometry, Lie groups, and symmetric spaces*, Academic Press, U.S.A. (1978).

[166] L. Skovgaard, *A Riemannian geometry of the multivariate normal model*, *Scand. J. Stat.* **11** (1984) 211.

[167] D. Watkins, *Fundamentals of matrix computations*, Wiley, U.S.A. (2002).

JHEP12(2020)101

[168] S.-M. Ruan, *Purification complexity without purifications*, arXiv:2006.01088 [INSPIRE].

[169] A. Monras and F. Illuminati, *Information geometry of Gaussian channels*, *Phys. Rev. A* **81** (2010) 062326.

[170] A. Monras, *Phase space formalism for quantum estimation of Gaussian states*, arXiv:1303.3682.

[171] S. Adler, *Taylor expansion and derivative formulas for matrix logarithms.*

[172] F. Khanna, A. Malbouisson, J. Malbouisson and A. Santana, *Thermal quantum field theory — Algebraic aspects and applications*, World Scientific, Singapore (2009).

[173] R. Horn and C. Johnson, *Matrix analysis*, Cambridge University Press (2013).

JHEP12(2020)101